Functional Role of Glycogen synthase Kinase-3β on Glucocorticoid-mediated signaling

Camila Rubio Patiño

BIOMEDICINE DOCTORAL PROGRAM

FUNCTIONAL ROLE OF GLYCOGEN SYNTHASE KINASE-3β ON GLUCOCORTICOID-MEDIATED SIGNALING

This thesis has been conducted under the guidance of Dr. Gabriel Pons Irazazábal and Dr. Daniel Iglesias i Serret at the Biochemistry Unit of the Departament de Ciències Fisiològiques II at the Universitat de Barcelona

Thesis directors

Camila Rubio Patiño Gabriel Pons Irazazábal Daniel Iglesias i Serret

Doctoral thesis submitted by Camila Rubio Patiño to obtain the PhD Degree by the Universitat de Barcelona

"Only one who devotes himself to a cause with his whole strength and soul can be a true master. For this reason mastery demands all of a person."

-Albert Einstein

Table of contents

I. Introduction

1. Apoptosis and Cancer

Tissue homeostasis is the maintenance of normal tissue morphology and function. Homeostasis is determined by a complex balance between the rate of cell proliferation, differentiation, quiescence and cell death, including apoptosis. This balance is possible through the integration of a variety of signals of intracellular and extracellular origin, that when broken lead to uncontrolled cell growth and cancer. Recently, it has been described by Hanahan and Weinberg that there are 10 known hallmarks of cancer with distinctive and complementary capabilities that enable tumor growth and metastatic dissemination (Fig. 1). These cancer hallmarks have provided a useful and conceptual framework for understanding the complex biology of cancer. They include: deregulating cellular energetics, sustaining proliferative signaling, evading growth suppressors, avoiding immune destruction, enabling replicative immortality, tumor-promoting inflammation, activating invasion and metastasis, inducing angiogenesis, genome instability and mutation and resisting cell death (Hanahan and Weinberg, 2011).

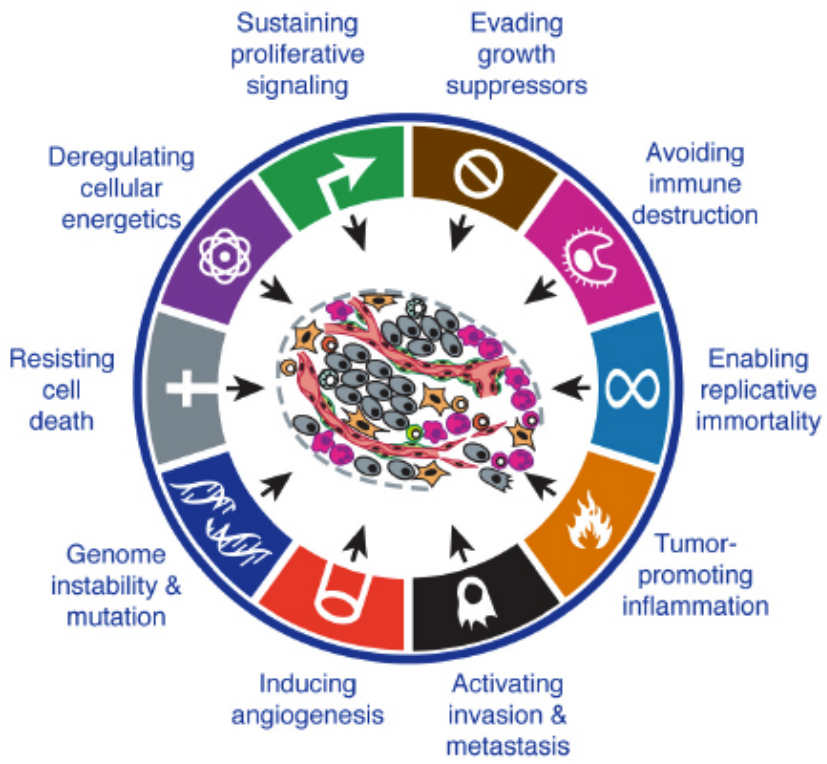

Figure 1. The hallmarks of cancer. Ten biological capabilities acquired during the multistep development of human tumors (modified from Hanahan and Weinberg, 2011).

The concept that programmed cell death by apoptosis serves as a natural barrier to cancer development has been established through functional studies conducted over the last decades (Hanahan and Weinberg, 2011). Elucidation of the signaling pathways regulating the apoptotic program has revealed how apoptosis is triggered in response to various physiologic stresses that cancer cells experience during tumorigenesis or as a result of anticancer therapy. Therefore, apoptosis plays a crucial role in the carcinogenic process and is critical for the cell response to anticancer drugs. Besides apoptosis, tumor cells can also die through non-apoptotic mechanisms, including autophagy, mitotic catastrophe, and necrosis (Vangestel et al., 2009).

Apoptosis is the major type of programmed cell death in animals. This is a process that is highly conserved throughout evolution and is essential for normal tissue development and homeostasis (Kerr et al., 1972). Apoptosis is a highly controlled and energy-dependent process that enables normal development and elimination of damaged and potentially dangerous cells like cancer cells, cells infected with a virus or cells with highly damaged DNA.

Apoptotic cells can be recognized by characteristic morphological changes (Fig. 2). Cells shrink, become rounded, and retract from neighboring cells while chromatin condensation and nuclear fragmentation take place. The Golgi apparatus, endoplasmic reticulum and mitochondrial networks also undergo pronounced fragmentation during apoptosis, and numerous proteins are released from the mitochondrial intermembrane space. This is accompanied by a prolonged period of plasma membrane blebbing. During apoptosis membrane integrity is maintained, thus preventing the release of cellular contents, which ensures a process without inflammation. In the final stages of apoptosis, cell is fragmented in compact corpuscles surrounded by membrane, called apoptotic bodies that contain condensed chromatin and organelles and cytosol. The apoptotic process culminates with phagocytosis of the apoptotic bodies by macrophages (Taylor et al., 2008).

Apoptosis is in contrast to the necrotic mode of cell-death in which case the cells suffer a major insult, resulting in a loss of membrane integrity, swelling and rupture of the cells. During necrosis, the cellular contents are released in an uncontrolled manner into the cells

environment, which results in damage of surrounding cells and a strong inflammatory response in the corresponding tissue (Leist and Jaattela, 2001).

Deregulation of apoptosis leads to pathological conditions such as autoimmune and degenerative diseases, and cancer (Burz et al., 2009). Moreover, the anti-apoptotic mechanisms regulating cell death have also been implicated in conferring drug resistance to tumor cells (Fulda and Debatin, 2006). In mammalian cells, apoptosis occurs through two distinct molecular pathways. The extrinsic apoptosis pathway receives signals through the binding of extracellular protein death ligands to pro-apoptotic death receptors (DRs) with subsequent activation of caspases, which are proteolytic enzymes that are closely involved in the induction and execution phases of apoptosis. By contrast, the intrinsic or mitochondrial pathway is activated by intracellular events and depends on the release of pro-apoptotic factors from the mitochondria. Anti-apoptotic BCL-2 family members preserve the integrity of the outer mitochondrial membrane whereas pro-apoptotic members promote its permeabilization. Mitochondrial outer membrane permeabilization (MOMP) allows the release into the cytosol of mitochondrial proteins like cytochrome c, leading to caspase activation, which is essential in the execution of apoptosis. Other pro-apoptotic proteins released by the mitochondria are EndoG, AIF, Omi/HtrA2, and Smac/DIABLO (Fulda and Debatin, 2006) (Burz et al., 2009) (Pradelli et al., 2010) (Tait and Green, 2010).

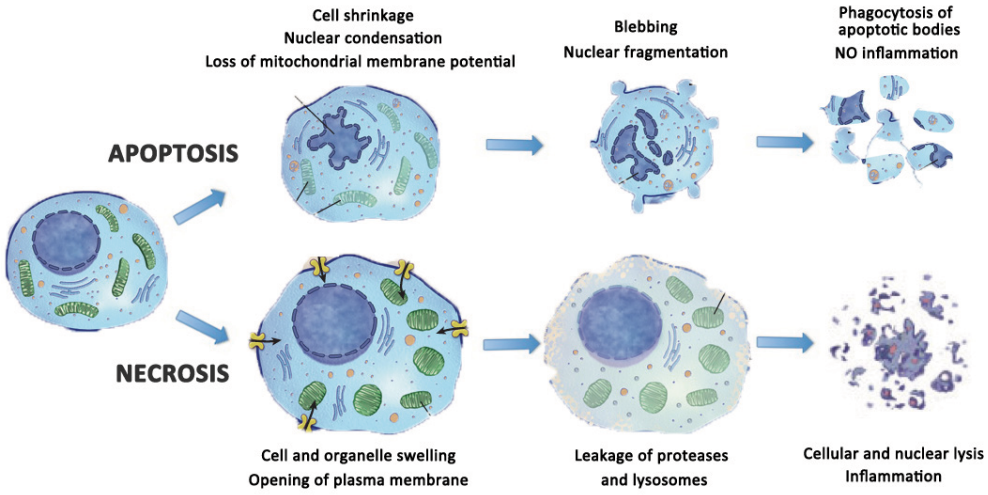

Figure 2. Typical features of apoptosis and necrosis. A particular mode of cell death may predominate, dependingon the injury and the type of cell (modified from Van Cruchten and Van Den Broeck, 2002; Hotchkiss et al., 2009).

1.1 Apoptotic phases

Apoptosis is blocked in viable cells, but when they receive physiological and external apoptotic signals, the apoptotic machinery is activated. The apoptotic process can be divided in three stages (Vaux and Strasser, 1996):

1) Initiator phase: Includes a great variety of signaling pathways that mediate signals from outside the cell, as well as others that originate inside the cell. There are three main mechanisms for apoptosis activation, mainly through DRs, cell damage like stress and radiation and through the action of T cytotoxic cells and natural killers.

2) Effector phase: Once signal transduction pathways have sent the apoptotic message to the cell death effector machinery, this process is irreversible. At this point caspases are activated.

3) Destruction phase: The activation of the cell death effector machinery leads to the loss of cell integrity through biochemical and physiological changes that includes chromatin condensation and DNA degradation.

1.2. Caspases: The executioners of apoptosis

The cell death effector machinery is constituted of a family of cysteine-dependent aspartate-directed proteases (caspases). These enzymes proteolyse vital proteins to the cell, as well as proteins that will contribute to the destruction of the cell, leading to the morphological and biochemical changes that typically occur in apoptosis (Thornberry and Lazebnik, 1998) (Danial and Korsmeyer, 2004). It is estimated that caspases have over 400 substrates, including protein kinases of the cytoskeleton, DNA repair enzymes, and proteins involved in the processing of the mRNA (Meier and Vousden, 2007) (The Caspase Substrate database http://bioinf.gen.tcd.ie/casbah/). These proteases share similar domain structure including an N-terminal peptide or prodomain, and two subunits, one large and one short, sometimes separated by a linker peptide (Fig. 3). There are three groups of caspases (Fuentes-Prior and Salvesen, 2004) :

1. Initiator caspases: These include caspases-2, -8, -9 and -10. They are the first to be activated after the apoptotic stimulus. Initiator caspases are characterized by the

presence of a CARD (caspase-recruitment domain) or DED (death effector domain) interaction domains at their N-terminus. These domains favor the proximity of caspases with their regulating proteins (APAF-1 or DRs).

2. Effector caspases: These include caspases-3, -6 and -7. They are activated by the initiator caspases and are responsible of the proteolytic events that combine to induce apoptosis.

3. Inflammatory caspases: These include caspases-1, -4, -5 and -12 and they are not implicated in apoptosis.

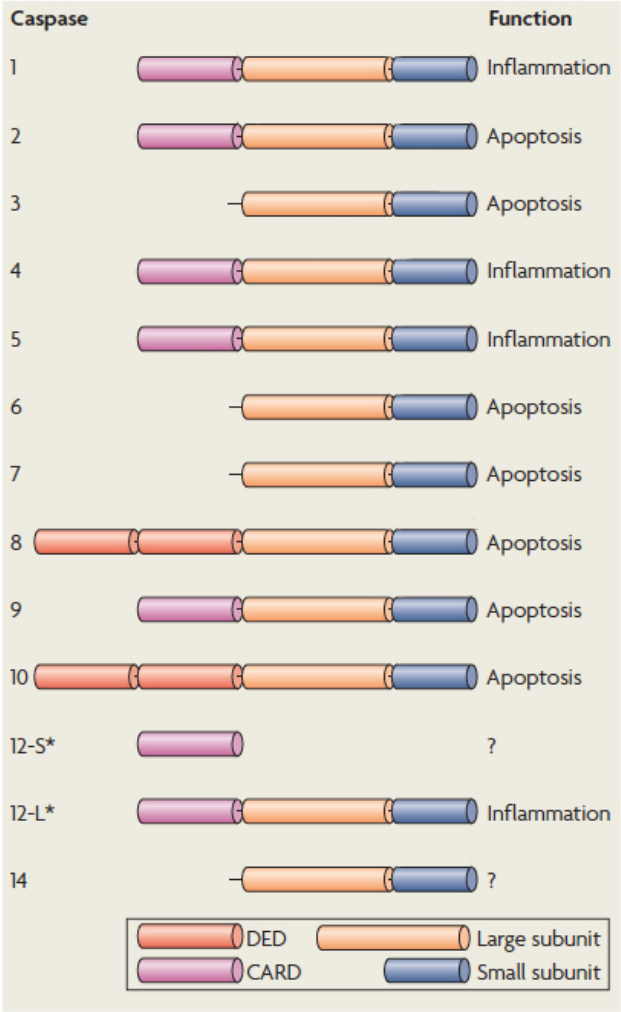

Figure 3. The caspases. Structure of the different caspases involved in apoptosis and inflammation (taken from Taylor et al, 2008).

Perhaps the most important characteristic of the initiator caspases is their substrate specificity, with an unusual requirement for cleavage after aspartic acid. Recognition of at least four amino acids N-terminal to the cleavage site is also a necessary requirement for efficient catalysis. The tetrapeptide recognition motif differs significantly among caspases and explains the diversity of their biological functions (Thornberry and Lazebnik, 1998). Caspase activation is a highly regulated process, in order to avoid non-specific apoptosis induction. For this reason caspases are synthesized as precursors that have little or no catalytic activity (pro-caspases). Caspase activation is usually initiated through proteolytic processing of the caspase between the large and small subunits to form a heterodimer (Taylor et al., 2008).

Caspases are activated through cascades of proteolysis, in order to amplify the apoptotic signal. In this way, two heterodimers of caspases associate to form a tetramer. In the case of caspase-9, it is activated by the formation of the protein complex known as the apoptosome. In the cytosol, cytochrome c binds the apoptotic protease-activating factor-1 (APAF-1), triggering its oligomerization into a complex that binds pro-caspase-9, forming the apoptosome, which induces the dimerization of caspase-9 (Pop et al., 2006). The apoptosome facilitates the auto-activation of caspase-9 and the consequent initiation of the proteolytic cascade, where caspase-9 cleaves and activates downstream effector caspases-3 and -7, followed by chromatin condensation, DNA fragmentation and apoptotic bodies formation (Pop et al., 2006) (Bratton and Salvesen, 2010).

Caspases cleave their substrates without altering the target protein's structure, causing gain- or loss-of-function (Timmer and Salvesen, 2007). The known caspase substrates include the anti-apoptotic proteins BCL-2, BCL-XL and MCL-1; the pro-apoptotic proteins BAX, BAD, or BID; and other apoptosis-related proteins like Akt, cFLIP or RAS (Fischer et al., 2003), essential regulators of the apoptotic program, as we will see later.

Not all caspases are involved in apoptosis. The caspases that have been well described are caspases-3, -6, -7, -8, and -9. The intrinsic and extrinsic apoptotic pathways converge to caspase-3. The upstream caspases that converge to caspase-3 are caspases-9 and -8 in the intrinsic and extrinsic pathways, respectively. The downstream caspases induce cleavage of apoptosis regulators, protein kinases, phosphatases, cytoskeletal proteins, DNA repair

proteins, inhibitory subunits of endonucleaes, etc. Caspases also affect cytoskeletal structure, cell cycle regulation, and signaling pathways, ultimately leading to the morphologic manifestations of apoptosis, such as DNA condensation and fragmentation, and membrane blebbing (Fulda and Debatin, 2006) (Tait and Green, 2010). In addition to regulation by human IAPs (HIAPs), which are caspase inhibitors, this apoptotic signaling pathway may be antagonized by the cFLIP family of proteins (FLICE inhibitory protein) having structural homology and sequence of caspases-8 and -10 (Deveraux et al., 1997) (Krueger et al., 2001).

1.3. The HIAP family: endogenous caspase inhibitors

The human IAPs (inhibitors of apoptosis) are a family of proteins containing one or more characteristic BIR (baculoviral IAP repeat) domains each consisting of approximately 70 amino acid residues (Fig. 4). This family of proteins is well conserved through evolution. Among the HIAPs, HIAP1, HIAP2, and XIAP have three BIRs in the N-terminal portion of the molecule and a RING (Really Interesting New Gene) finger at the C-terminus, NAIP contains three BIRs without RING, and SURVIVIN and BRUCE each has just one BIR (Hinds et al., 1999) (Sun et al., 1999). There are other domains that may be present in some of these proteins, but all family members do not share them. These are the CARD, UBC (ubiquitin-conjugating), NOD (Nucleotide-binding and oligomerization domain), LRR (leucine repeats), and CC (coiled-coil). HIAPs are not only capable of regulating apoptosis but they are also implicated in cell signaling of MAPK and NF-κB pathways, mitosis, morfogenesis, and protein tagging for proteasome degradation (Srinivasula and Ashwell, 2008). Through the BIR domain, HIAPs can bind and inhibit caspases. XIAP is the most anti-apoptotic HIAP and is now known to be the only one able to directly inhibit caspases, while the rest of HIAPs bind but do not inhibit them (Eckelman and Salvesen, 2006). The BIR domain mediates protein-protein interactions with proteins like caspases and is necessary for the anti-apoptotic activity of HIAPs. The RING domain has E3 ubiquitin ligase activity and autoubiquitination of HIAPs may play an important role in their own degradation, allowing cells to commit to apoptosis.

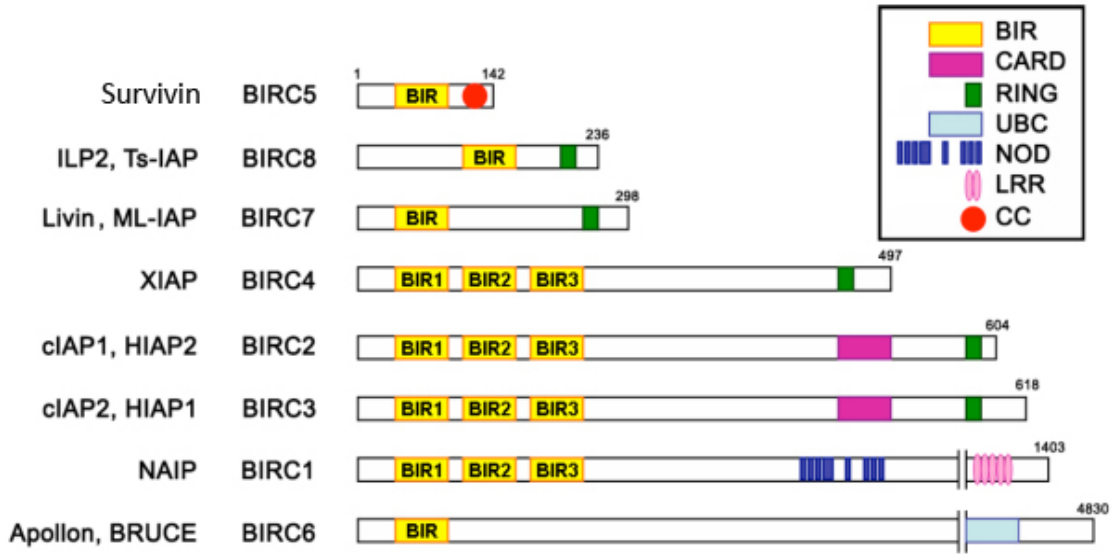

Figure 4. Structure of human IAPs. Schematic representation of the eight human IAPs with their functional domains. The common name and oficial name in BIRC nomenclature (baculoviral IAP repeat-containing) are shown (modified from Graaf et al., 2004; Srinivasula and Ashwell, 2008).

HIAP1 and HIAP2 are part of the cytoplasmic complex of TNFα where they interact through the BIR1 domain with the adaptor protein TRAF2 (Rothe et al., 1995) (Shu et al., 1996) and they activate the canonical NF-κB pathway (Chu et al., 1997) (Wang et al., 1998) (Santoro et al., 2007) (Bertrand et al., 2008) (Mahoney et al., 2008), while they negatively regulate the noncanonical pathway and spontaneous NF-κB activation (Varfolomeev et al., 2007) (Vince et al., 2007).

1.4. Apoptotic pathways

1.4.1. Extrinsic apoptotic pathway

The extrinsic apoptotic pathway is initiated with the binding of specific ligands to cell surface receptors or DRs, including TNFR, FasR/CD95, and TNF-related apoptosis-inducing ligand (TRAIL) receptors and leading to the formation of the death-inducing signaling complex that will end up in caspase activation (Fig.5) (Danial and Korsmeyer, 2004) (Tait and Green, 2010). These trans-membrane receptors share a common feature, the presence of a cytoplasmic domain termed Death Domain. This domain mediates protein-protein interactions by binding to homologous domains (Fulda and Debatin, 2006).

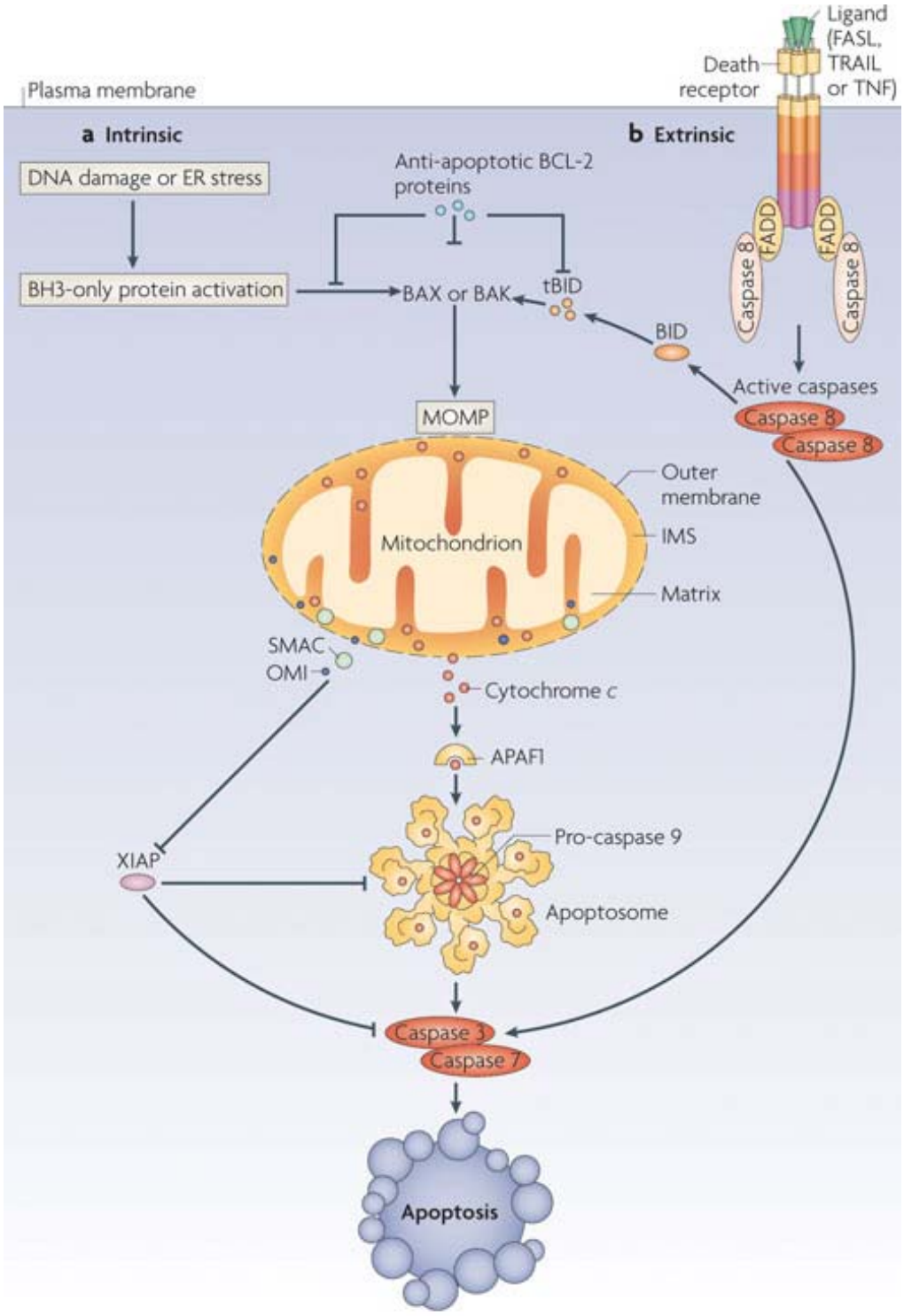

Figure 5. Intrinsic and extrinsic apoptotic pathways. (a) Intrinsic pathway of apoptosis. The main organelle in the intrinsic pathway is the mitochondria. **(b)** Extrinsic pathway of apoptosis. Schematic representation of the extrinsic pathway of apoptosis with binding of death ligands to death receptors, subsequent activation of caspase-8, which results in the activation of caspases-3/-7 and commitment to apoptosis (taken from Tait and Green, 2010).

In the case of the FasR/CD95, when it binds to its ligand it induces the trimerization of the receptor, which in turn recruits the adaptor protein FADD through Death Domain-Death Domain contact. FADD recruites pro-caspases-8 and results in the assembly of the Death-Inducing Signaling Complex (DISC), which is the platform for capsase-8 activation. Caspase-8 can activate the downstream caspases: caspase-3, -6 and -7. In some cases, the activation of caspase-8 may be sufficient to execute cell death. In other cases, caspase-8 interacts with the intrinsic apoptotic pathway by cleaving BID (a pro-apoptotic member of the BCL-2 family) and generating truncated BID (tBID), leading to the subsequent release of cytochrome c (Fulda and Debatin, 2006).

1.4.2. Intrinsic apoptotic pathway

The intrinsic apoptotic pathway is the main route of caspase activation, where the mitochondria play a central role. The intrinsic apoptotic pathway is triggered by various external or internal stimuli, such as activation of oncogenes, infection by viruses or bacteria, the deprivation of cytokines and growth factors, DNA damage, ER stress, and chemotherapy, among others (Fig. 5). The intrinsic or mitochondrial pathway depends on the release of pro-apoptotic factors from the mitochondria (Danial and Korsmeyer, 2004) (Tait and Green, 2010). MOMP allows the release into the cytosol of mitochondrial proteins like cytochrome c, leading to caspase activation and apoptotic cell death. Other pro-apoptotic proteins released by the mitochondria are Smac/DIABLO, EndoG, AIF and Omi/HtrA2 (Pradelli et al., 2010).

Besides being a key component of electron transport during oxidative phosphorylation, cytochrome c is absolutely necessary for the activation of caspases following MOMP (Liu et al., 1996). In the cytosol, cytochrome c binds to APAF-1, activating it in an ATP-dependent manner, inducing its conformational change and oligomerization, which leads to the formation of a complex called the apoptosome, which provides a platform for caspases activation. The apoptosome activates an initiator caspase, caspase-9, which in turn activates the executing caspases-3 and -7 (Pop et al., 2006) (Bratton and Salvesen, 2010). Cytochrome c knockout causes embryonic lethality and cells deficient in cytochrome c (Li et al., 2000) APAF-1 (Yoshida et al., 1998) or caspase-9 (Kuida et al., 1998) are resistant to apoptosis through the intrinsic pathway. Mitochondrial release of Smac/DIABLO and OMI neutralizes the caspase inhibitory function of XIAP (Tait and Green, 2010).

Mitochondrial integrity and the intrinsic pathway are controlled mainly by the evolutionarily conserved BCL-2 family of proteins, which contains both pro-apoptotic and anti-apoptotic members, which are able to respond to a variety of stimuli and stress stimuli (Youle and Strasser, 2008) (Chipuk et al., 2010). Anti-apoptotic BCL-2 family members preserve the integrity of the outer mitochondrial membrane whereas pro-apoptotic members promote its permeabilization.

1.5. BCL-2 family members

Members of the BCL-2 (B-cell lymphoma-2) family can be classified into three groups according to their structure and function (Fig. 6):

Anti-apoptotic members (BCL-2-like)

This subfamily includes proteins that contain all four BH domains (BH1-4). A1 (BCL2A1 gene, or BFL-1), BCL-2, BCL-XL (BCL-2-related gene, long isoform), BCL-W, MCL-1 (myeloid cell leukemia 1), and BCL-B are the members of this subgroup and preserve the integrity of the outer mitochondrial membrane to inhibit other pro-apoptotic proteins of the family. The domains BH1, BH2 and BH3 are folded to form a hydrophobic pocket that allows interaction with other pro-apoptotic members (Muchmore et al., 1996) (Sattler et al., 1997). When overexpressed, each of these proteins protects cells in culture against a variety of apoptotic stimuli. Some of these proteins are required for the survival of certain cell types, such as BCL-2 and MCL-1, which are necessary to extend the life of mature B and T lymphocytes (Veis et al., 1993) (Danial and Korsmeyer, 2004) (Strasser, 2005).

Pro-apoptotic multidomain members (BAX-like)

This group includes the effector members of apoptosis BAX (BCL-2-associated X protein) and BAK (BCL-2-antagonist/killer-1). The members of this subfamily contain the homology domains BH1-3 and induce apoptosis when overexpressed (Danial and Korsmeyer, 2004). When activated, these proteins are supposed to promote apoptosis by forming pores in the outer mitochondrial membrane and subsequent MOMP and mitochondrial apoptogenic factors output. The protein BOK (BCL-2-related ovarian killer) is also a potential effector protein, however, there is no biochemical evidence of a role similar to that of BAX or BAK.

Members with only the pro-apoptotic BH3 domain (BH3-only)

This subfamily is structurally diverse. Classically, the BH3-only proteins have been identified to possess only the BH3 homology domain, which seems essential for its pro-apoptotic function. However, recent sequence analysis indicate that, except BID, the members of this subfamily differ in structure from the core members of the BCL-2 family and is postulated to have acquired the BH3 motif by convergent evolution (Aouacheria et al., 2005). These proteins interact with other family members to promote and regulate apoptosis. The BH3 domain mediates these interactions. This group includes BAD, BIM, BIK, BID/BOD, HRK/DP5, BMF, NOXA and PUMA although, it could include other members as NIP3, BNIP3/NIX or MOAP-1.

There are other proteins homologous to BCL-2 like BCL-RAMBO, BCL-B/BOO/DIVA or BCL-G that have not been deeply studied and that, nowadays, we cannot categorize. There are other pro-apoptotic multidomain proteins identified as BFK (BCL-2-family kin) and BCL-XS, which only have two BH domains, and whose role in apoptotic signaling is unclear (Youle and Strasser, 2008). Furthermore, various forms of alternative splicing of many of the family proteins have been described. For example, anti-apoptotic proteins whose splicing variants are pro-apoptotic: BCL-XS or MCL-1S. Or conversely, BID-S, an alternative splicing of BID-EL and BID-L, has an anti-apoptotic role since it has no BH3 domain (Renshaw et al., 2004). Interestingly, the BIM gene has 19 splicing variants (Akgul et al., 2004). Many studies have achieved the knockout or overexpression mouse model of the BCL-2 family members that allow the analysis of their physiological role, redundancy and interactions *in vivo* and their contribution to the formation and progression of tumors and resistance to therapy (Chipuk et al., 2010) (Youle and Strasser, 2008).

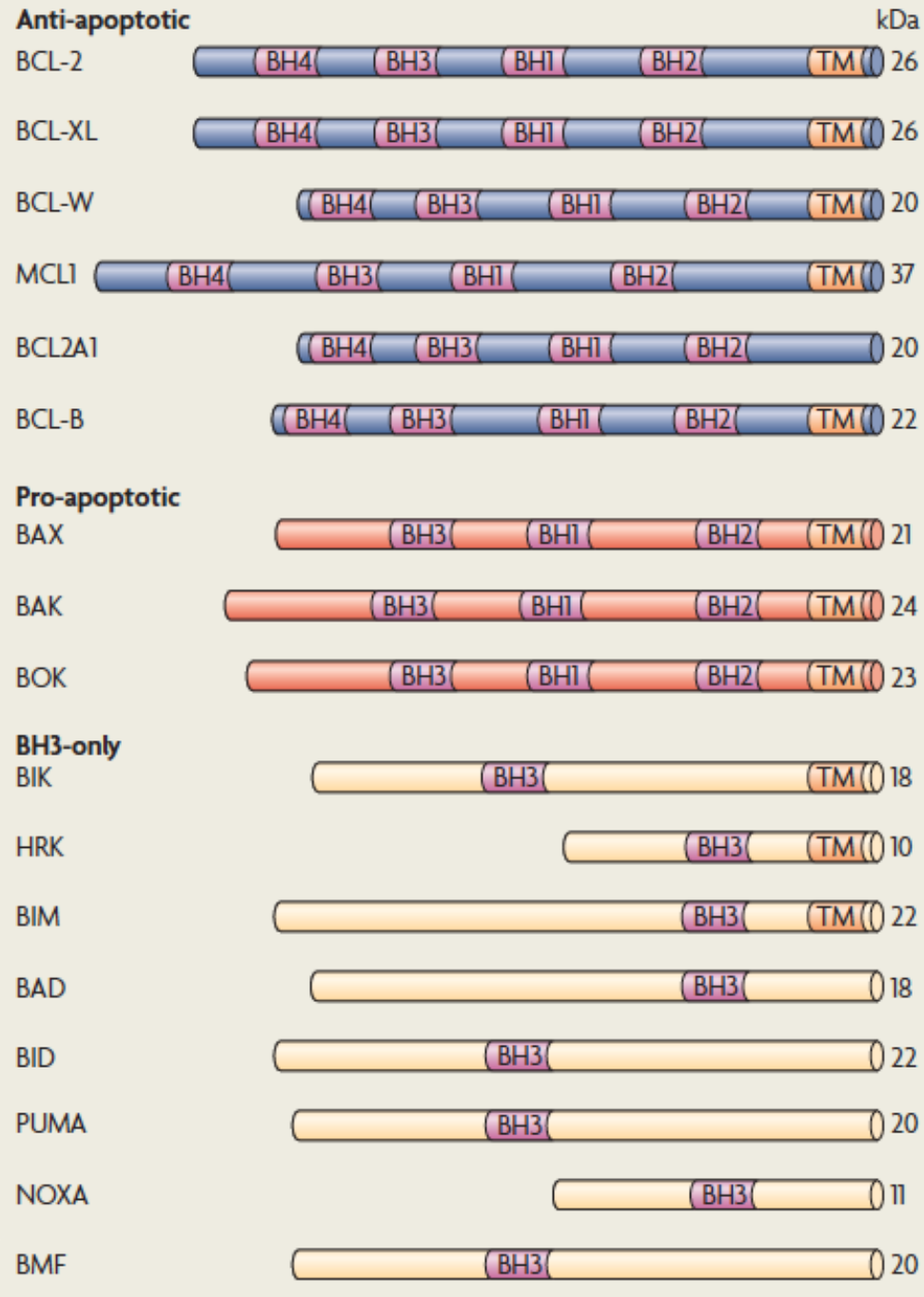

Figure 6. BCL-2 family members. This family of proteins is divided into three groups based on their BCL-2 homology (BH) domain organization. TM: transmembrane domain. Molecular weight is shown in kDa (taken from Taylor et al, 2008).

1.5.1. Interaction between the BCL-2 family members

The BCL-2 family proteins are associated temporarily with each other through their BH domains to form homo and/or heterocomplexes, which play different roles in the process of MOMP and cytochrome c release. Although in the past it was thought that BH3-only

proteins could join anti-apoptotic counterparts indiscriminately, currently the quantitative assessment of the binding of BH3 peptides to BCL-2-like proteins revealed that the affinities between different pairs varies up to 10,000 times (Chen et al., 2005) (Kuwana et al., 2005) (Certo et al., 2006) (Kim et al., 2006). While BIM, PUMA and BID bind to all anti-apoptotic family members, other BH3-only proteins bind only to a few. For example, NOXA interacts only with MCL-1 and A1, and BAD only interacts with BCL-2, BCL-XL and BCL-W (Fig. 7A). In addition, promiscuous members are much more potent as inducers of apoptosis that members with restricted interactions. BH3-only proteins act over BAX and BAK, which promote the activation of caspases through their effect on mitochondrion. However, it is unknown how BH3-only proteins activate BAX and BAK.

1.5.2. Interaction models of BCL-2 family members

Two models have been proposed to explain this mechanism (Fig. 7B):

Indirect activation model (or neutralization). BAX and BAK are united in a constitutively active state to the anti-apoptotic proteins of the family. Competitive interactions of BH3-only proteins with anti-apoptotic proteins are sufficient to displace and liberate activated BAX and BAK (Chen et al., 2005) (Willis and Adams, 2005) (Willis et al., 2007).

Direct activation (or derepression) model. BAX and BAK are activated following the interaction with a subset of proteins called BH3-only activators. Anti-apoptotic proteins of the BCL-2 family prevent MOMP by abducting these activating proteins or inhibiting activated BAX and BAK. A second subset of BH3-only proteins called sensitizers, bind to anti-apoptotic proteins displacing and freeing BH3-only proteins that activate BAX and BAK (Letai et al., 2002) (Cartron et al., 2004) (Kuwana et al., 2005) (Certo et al., 2006).

Although different, both models agree on the fundamental basis: BH3-only proteins are essential activators of apoptosis, among them BIM, BID, and PUMA are especially powerful because they can join all anti-apoptotic proteins (indirect model), or they can bind directly to BAX and BAK (direct model) (Meier and Vousden, 2007).

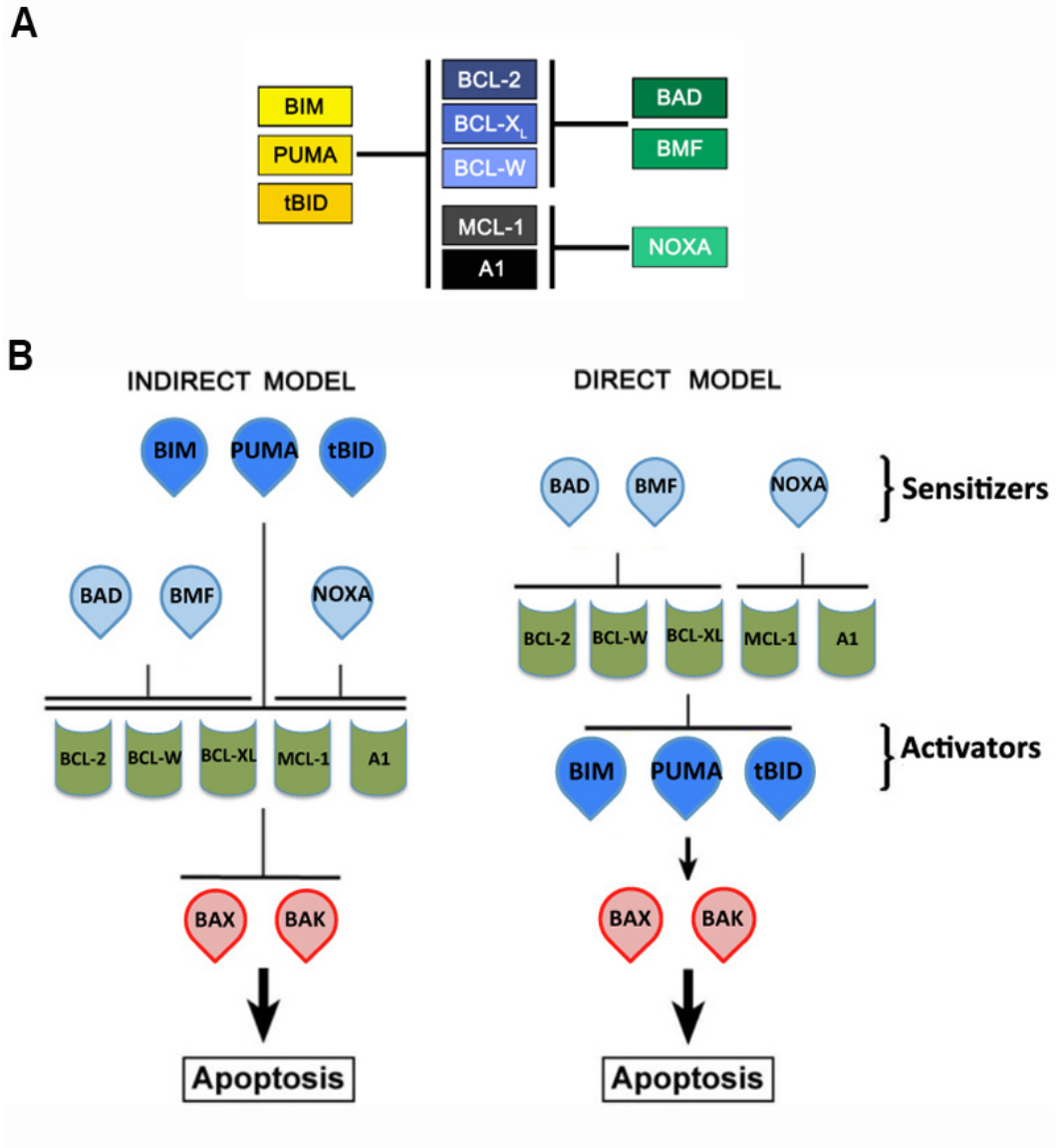

Figure 7. Models of interaction between the BCL-2 family members. (A) BH3-only proteins interact with anti-apoptotic proteins in a selective manner (modified from Adams and Cory, 2007). **(B)** Representation of the two proposed models for BH3-only activity in apoptosis (modified from Meier and Vousden, 2007).

1.5.3. Activation of BH3-only proteins by different stimuli

BH3-only proteins monitor the status of the cell and mediate cell death induced by both physiological stimuli such as deprivation of cytokines, signaling receptors or loss of adhesion to the matrix cells (a type of cell death called anoikis) as signals induced by activated oncogenes, DNA damage, chemotherapeutic agents, UV or γ radiation (Fig. 8). Although at times their physiological functions are partially redundant, and although BIM

and PUMA have a dominant role, each of the BH3-only members respond to a specific type of aggression (Adams and Cory, 2007) (Kelly and Strasser, 2011). BIM, PUMA, and BMF are glucocorticoid induced proteins. The balance between the pro and anti-apoptotic members of the family and the interactions among them dictate the integrity of the mitochondrial outer membrane and determine cell death or survival.

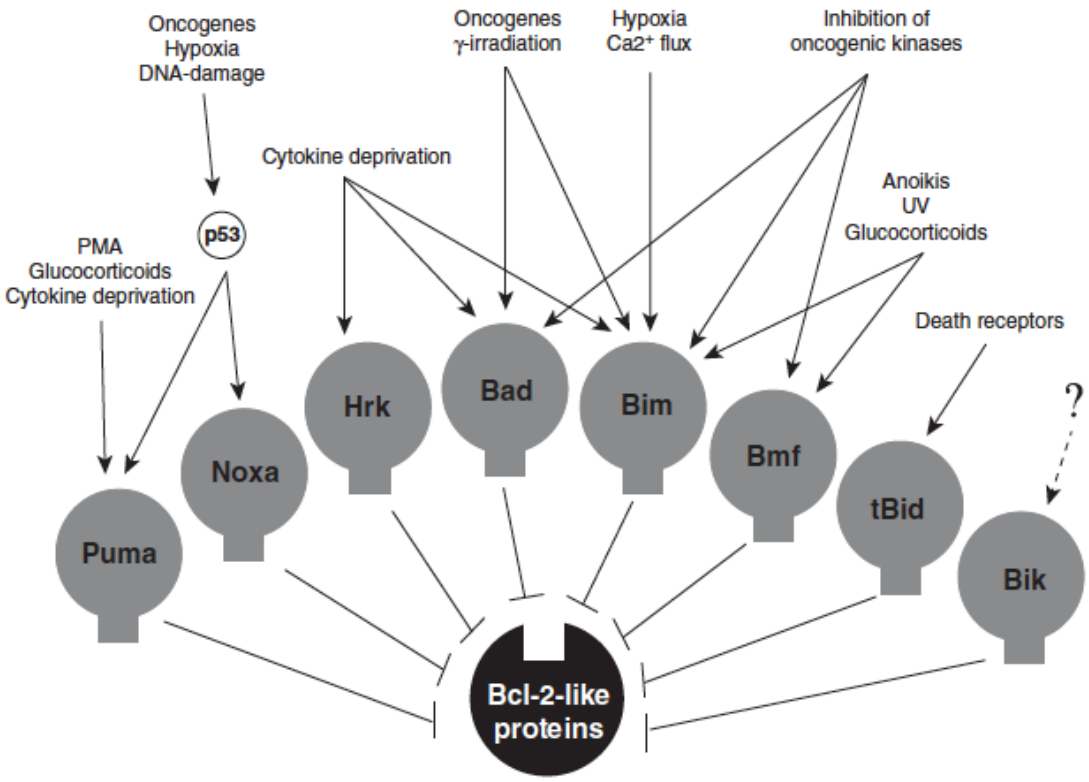

Figure 8. Activation of BH3-only proteins by different apoptotic stimuli including those elicited by oncogene activation (taken from Kelly and Strasser, 2011).

2. Mechanisms of glucocorticoid signaling

Glucocorticoids (GCs) are steroid hormones that regulate essential biological processes, including growth, development, metabolism, survival, differentiation, proliferation and apoptosis in a large variety of cell types and are commonly used in the treatment of various inflammatory diseases and cancer. Specifically, GCs are currently being used in the treatment of hematopoietic malignancies such as chronic lymphocytic leukemia (CLL), T-acute lymphoblastic leukemia, multiple myeloma, and non-Hodgkin lymphoma, due to

their ability to induce intrinsic caspase-dependent apoptosis in these cell types (Kfir-Erenfeld et al., 2010). These properties have made GCs one of the most frequently prescribed drugs.

Steroid hormone research began in the late 1800s. In the early 1960s it was demonstrated that a hormone can be taken up and retained by specific tissues, thus leading to the identification of the estrogen receptor. It was not until 1966 that the glucocorticoid receptor (GR) was first identified on rat thymic lymphocytes. The GR was cloned in 1985 (Hollenberg et al., 1985), starting an explosion of molecular studies on the GR and its related family members, the steroid receptors. Members of this superfamily include the GR, mineralocorticoid receptor (MR), progesterone receptor (PR), estrogen receptor (ER), and androgen receptor (AR) (Heitzer et al., 2007).

GCs induce apoptosis in cells of the hematopoietic lineage, but also in non-hematologic cells as described for osteoblasts (Herr et al., 2007). On the other hand, GCs support survival in several non-hematologic tissues such as fibroblasts, liver, and ovary, among others (Beck et al., 2011). Correspondingly, it seems that GCs acutely induce therapy resistance in normal and transformed cells of epithelial origin, including the majority of human solid malignant tumor cells like ovary, pancreas, brain, cervix and bladder. The diverse steroid-mediated effects generate an unfavorable side-effect profile in chronic GC-based therapy. These side effects result from overstimulation of normal physiological GC-induced GR actions (Beck et al., 2011).

2.1. GR isoforms

Most of the actions of GCs are mediated through the GR. Ever since the cloning of the GR (Hollenberg et al., 1985) much progress has been made in understanding the mechanism of action of GCs (Beck et al., 2011). The GR is a member of the steroid receptor superfamily (Zhou and Cidlowski, 2005) that is a class of transcription factors regulated by small lipophilic ligands such as steroids, thyroid hormone retinoids, and vitamin D3. Nuclear receptors are known for their ability to form homodimers (McKenna and O'Malley, 2001) (McKenna and O'Malley, 2002). These receptors share a common structural organization consisting of several modulatory domains very conserved throughout evolution (Heitzer et al., 2007).

The GR gene (NR3C1) is located at chromosome 5q31-32 and consists of nine exons highly conserved among species. The full length GR consists of an N-Terminal transactivation domain (NTD) containing an activation function-1 (AF-1; aa 77-262). The function of this region in transcriptional regulation can be ligand independent. Close to the AF-1 region is the DNA-binding domain (DBD; aa 418-488) with two zinc fingers, a hinge region, and a C-terminal ligand-binding domain (LBD; aa 526-777). The LBD is important for receptor dimerization and contains sequences for protein-protein interactions with proteins such as Hsp90. This interaction allows the folding of the receptor and prevents the receptor to bind DNA in the absence of hormone. A second activation function (AF-2) is embedded in the LBD and interacts with coregulators in a ligand-dependent manner, facilitating the interaction of additional factors known as coactivators and corepressors. AF-2 and AF-1 can act synergistically to mediate transcriptional activity (Heitzer et al., 2007) (Oakley and Cidlowski, 2011).

Alternative splicing of the primary transcript generates several receptor isoforms (Fig. 9). GRα and GRβ differ at their C-terminus. GRα (777 amino acid residues; 94 kDa) is currently the main research isoform and results from the end of exon 8 being joined to the beginning of exon 9. On the other hand, GRβ (742 amino acid residues; 90kDa), uses and alternative splice acceptor site resulting in the union of the end of exon 8 to the downstream sequences of exon 9. GRβ is unable to bind to GCs or activate GC-responsive genes. It resides constitutively in the nucleus of cells and is not ubiquitously expressed.

Several additional GR isoforms (GRϒ, GR-A, GR-P) arise from alternative splicing and can affect GC signaling. GRϒ binds GCs and DNA in a similar way to GRα, but cannot activate GC-responsive reporter constructs and exhibits a transcriptional profile distinct from GRα on a subset of commonly regulated genes. GR-A and GR-P are non-hormone binding variants due to the fact that they miss large regions of the LBD. GR-P appears to be the predominant isoform in several GC-resistant cells (Oakley and Cidlowski, 2011).

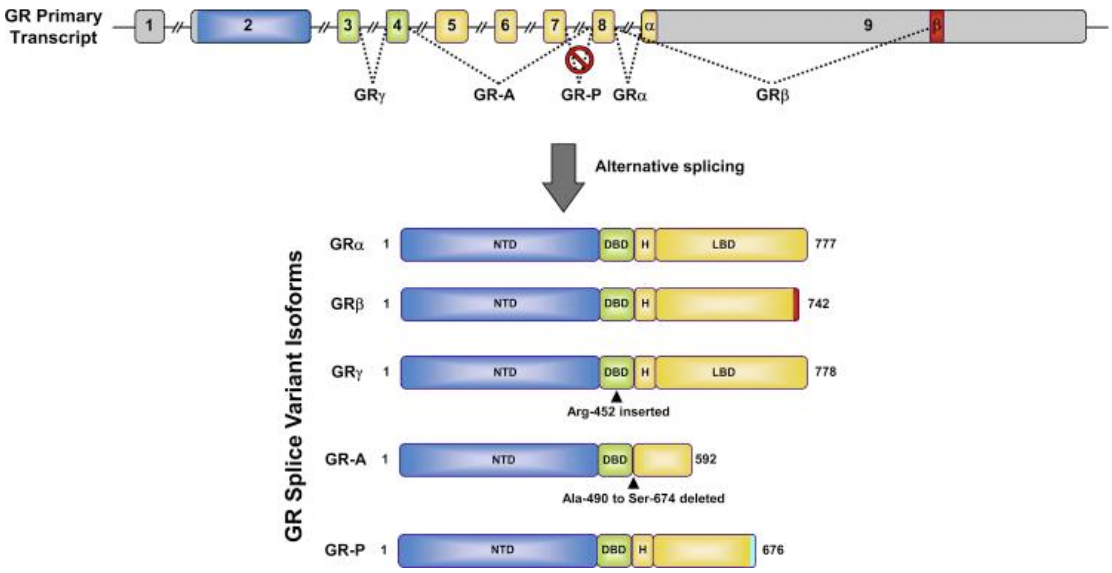

Figure 9. GR isoforms generated by alternative splicing. The human GR primary transcript is composed of nine exons, with exon 2 encoding most of the NTD, exons 3 and 4 encoding the DBD, and exons 5–9 encoding the hinge region (H) and LBD. The classic GRα protein results from splicing of exon 8 to the beginning of exon 9. GRβ is produced from an alternative splice acceptor site that links the end of exon 8 to downstream sequences in exon 9, encoding a variant with a unique 15-amino acid C terminus (positions 728–742). GRγ is generated by an alternative splice donor site in the intronic sequence separating exons 3 and 4, resulting in a protein with an arginine insertion (Arg452) between the two zinc fingers of the DBD. GR-A is produced from alternative splicing that joins exon 4 to exon 8, deleting the proximal 185 amino acids of the LBD (Ala490 –Ser674) encoded by exons 5–7. GR-P is formed by a failure to splice exon 7 to exon 8. The retained intronic sequence introduces a stop codon, resulting in a truncated receptor mutant missing the distal half of the LBD (taken from Oakley and Cidlowski, 2011).

It was also recently demonstrated that additional receptor proteins are generated by alternative translation initiation from a single GR mRNA (Fig. 10). There are two well-conserved AUG start codons derived from exon 2 and they produce eight GRα isoforms with truncated N-terminus. They show no difference in their affinity for their ligand or their capacity to bind GRE's after GC exposure. Nevertheless, the GRα-D isoform resides primarily in the nucleus and is constitutively binding to certain GRE-containing promoters. GRα-C is the most active isoform and GRα-D is the less capable of enhancing GC-dependent gene induction. Each of the other GR splice variants (GRβ, GRϒ, GR-A, GR-P) are expected to give rise to similar translation variants (Oakley and Cidlowski, 2011). Due to the fact that GRα is the most predominant isoform and our prime focus of attention, it will be referred to as GR throughout this thesis.

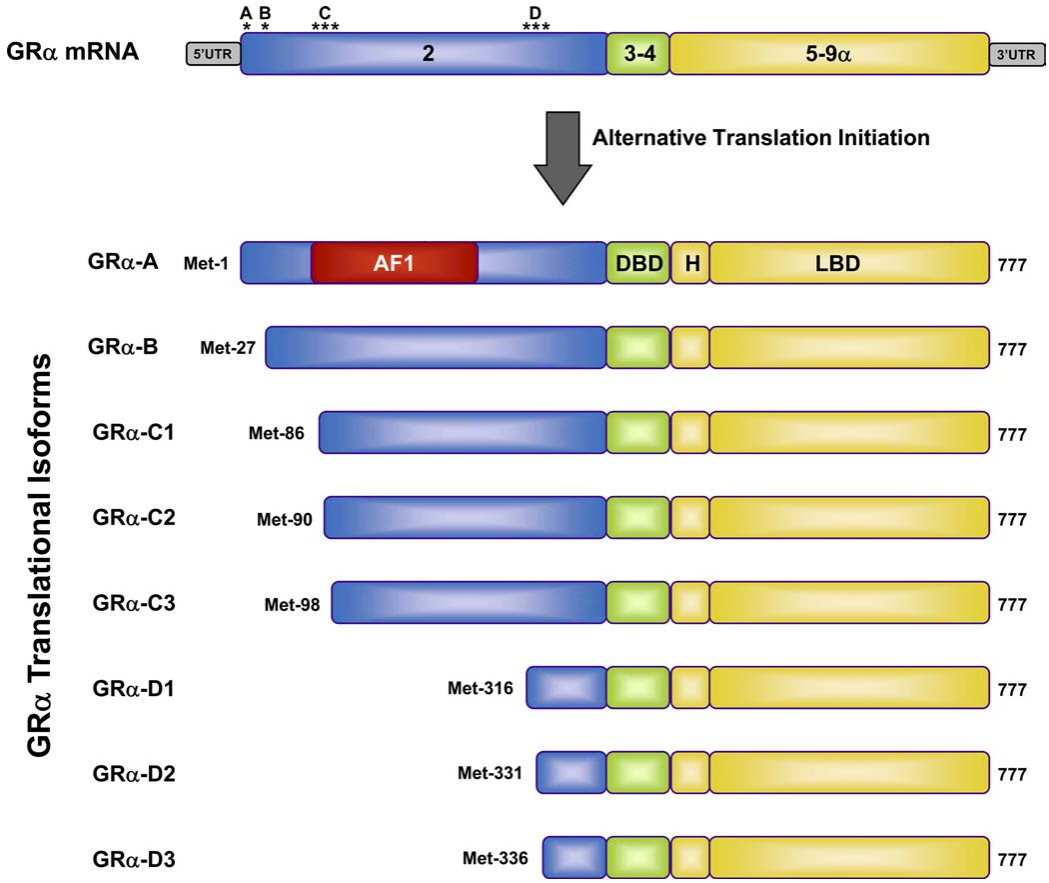

Figure 10. GRα isoforms that are generated by alternative translation initiation and sites of post-translational modification. Initiation of translation from eight different AUG start codons in a single GR mRNA generates receptor isoforms with progressively shorter N-terminal transactivation domains (NTDs). Asterisks designate approximate locations of the AUG start codons in the exon 2 sequences of the GR mRNA. Hinge region (H) (modified from Oakley and Cidlowski, 2011).

2.2. GC signaling through the GR

The unliganded GR resides mostly in the cytoplasm in an inactive state as part of a large heat shock protein heterocomplex that includes various chaperone proteins, such as Hsp90, Hsp70, Hsp40, and cochaperones Hsp90 binding protein p23 and Hoc among others (Oakley and Cidlowski, 2011). Upon GC binding, the GR undergoes a conformational change that results in its dissociation from the cytoplasmic chaperone multiprotein complex and unmasking of the nuclear localization signal, leading to its translocation to the nucleus. Nuclear translocation of the GR complex occurs within minutes of cell exposure to GCs (Stahn and Buttgereit, 2008). Once in the nucleus, the dimerized GR binds glucocorticoid response elements (GREs), usually located in the promoter of GR-regulated genes (Beck et al., 2011).

2.3. GR translocation

Even though the GR is thought to always reside in the cytoplasm in the absence of a ligand, the GR continuously shuttles between the cytoplasm and the nucleus. Thus, the subcellular localization of the GR is the result of the import and export rates of the receptor through the nuclear pore complex (NPC) (Beck et al., 2011) (Vandevyver et al., 2011). Previous studies suggest that GR dissociation form the chaperone complex does not precede nuclear translocation. It has been observed that the Hsp90 chaperone multiprotein complex is involved in GR fast and efficient trafficking (Vandevyver et al., 2011).

There are two distinct nuclear localization signals (NLS) in the GR protein: NLS1 and NLS2 (Fig. 11). The NLS1 is situated near the DBD-hinge region boundary and has been reported to mediate rapid nuclear import (4-6 minutes). The NLS2 resides in the LBD and mediates a slower incomplete nuclear import (45-60 minutes). NLSs are recognized by large proteins (90-130kDa) called importins. These proteins, in collaboration with the RanGTPase system, are known to mediate nuclear import of substrate proteins through the NPC. Importins bind to the NLS of cargo proteins and translocate to the nucleus, where the importin is recycled to the cytoplasm. Among the importins known to interact with the GR we find importins 7 and 8, which bind NLS1 and NLS2 and importin α/β heterodimer, which only binds NLS1(Vandevyver et al., 2011).

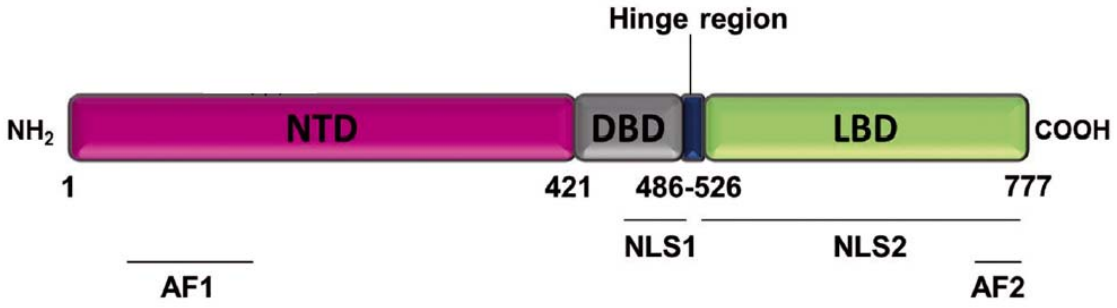

Figure 11. GR domains and nuclear localization signals (NLS) (modified from Vandevyver et al, 2012).

The nuclear export of proteins is mostly mediated by exportins, which bind to the nuclear export signal (NES) of proteins. The most characterized exportin is chromosome-region maintenance 1 (CRM1). However, GR nuclear export after hormone withdrawal seems to

be independent of CRM1-mediated transport as export appears not to be sensitive to the CRM1 inhibitor leptomycin B (LMB) (Liu and DeFranco, 2000) (Holaska et al., 2001). In this type of export it appears that there is a role for calreticulin (CRT), a calcium binding protein localized to the lumen of the endoplasmic reticulum (Holaska et al., 2001). CRT binds to the receptor's DBD between the two zinc fingers, at a sequence that function as NES. In fact, the redistribution of GR to the cytoplasm after hormone withdrawal is compromised in CRT-deficient cells. Finally, GR shuttling between the cytoplasm and the nucleus can influence GR nuclear signaling by altering the receptor's turnover (Heitzer et al., 2007).

2.4. Transactivation and transrepression

In transactivation the GR binds the major DNA groove via their zinc finger DBD targeting consensus glucocorticoid response elements (GREs) (Fig. 12A). When bound to the GRE, conformational changes of the GR lead to the recruitment of coregulators and chromatin-remodeling complexes that influence the activity of RNA polymerase II and modulate gene transcription (Jenkins et al., 2001) (Lonard and O'Malley, 2005). However, many known GC-induced genes do not contain consensus GREs and do not require binding of the GR. Some of these promoters contain composite elements where transcription is enhanced in a cooperative manner by the direct binding of the GR to DNA-bound transcription factors (tethering) (Fig. 12B). There are also composite GREs in which the DNA-bound GR combines forces with another DNA-bound transcription factor to enhance gene transcription (Fig. 12C).

The receptor briefly interacts with target promoters, rapidly cycling on and off the GRE, allowing the GR to bind a large number of sites and interacting proteins (McNally et al., 2000) (Stavreva et al., 2004). A common feature of GREs is the half-site sequence TGTTCT. A consensus GRE is composed of two hexamer half-sites separated by three nonspecific nucleotides, which may be palindromic (AGAACAnnnTGTTCT where n is any nucleotide) (Freedman and Luisi, 1993) (Truss and Beato, 1993), or partial palindromic (GGTACAnnnTGTTCT) (Garlatti et al., 1994) (Nogami et al., 2002).

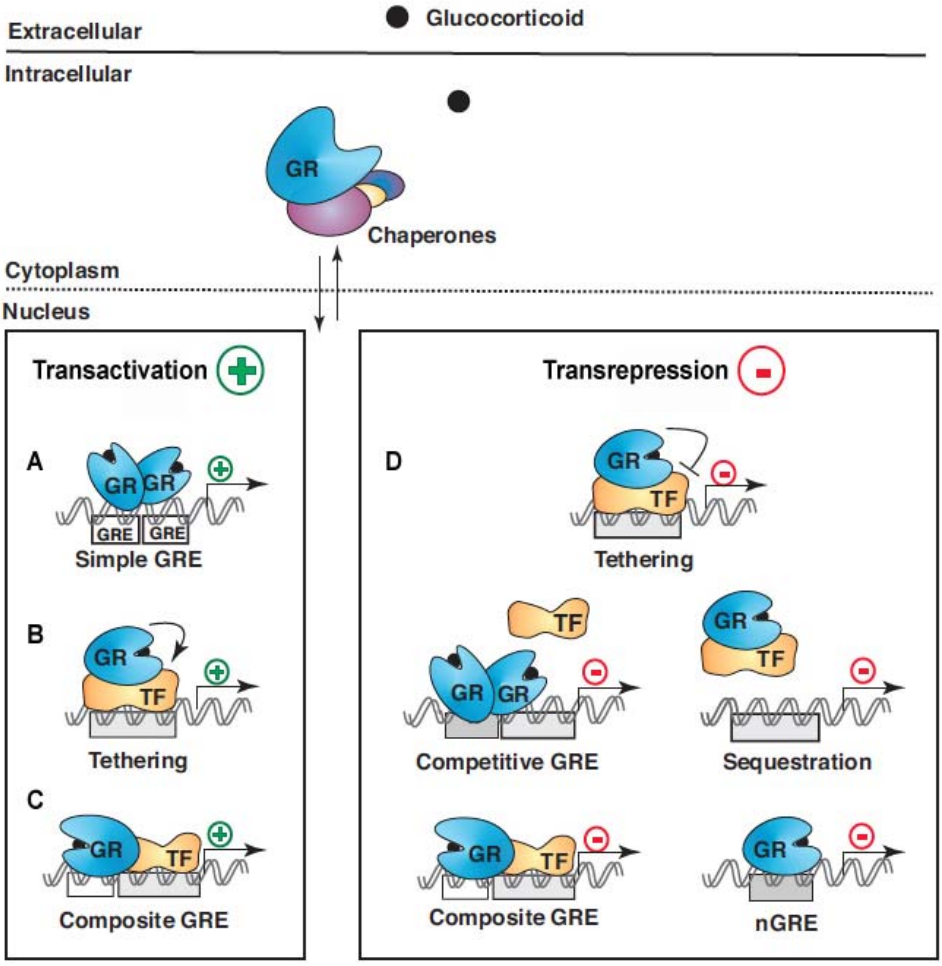

Figure 12. GR-mediated transcriptional regulation (modified from Beck et al, 2011).

GR-mediated transrepression (Fig. 12D) most commonly occurs through a tethering mechanism in which non DNA-bound GR associates with and thus inhibits the function of a DNA-bound transcription factor, such as AP-1 and NF-κB. The anti-inflammatory actions of GCs are mainly attributed to the interaction of the GR with AP-1 and NF-κB at the promoters of transcriptionally active pro-inflammatory genes (Heitzer et al., 2007). The GR can act as a monomer to repress NF-κB and AP-1, evidenced by GR dimerization-deficient mutants that still transrepress, modulating the transcription of genes regulated by these proteins (Beck et al., 2011). Nevertheless, the GR can also activate and repress gene promoters via other mechanisms like GR binding to competitive GREs or sequestration of transcription factors. Transrepression is also achieved through GR binding to atypical response elements called negative GREs (nGREs). nGREs have been described in several promoters, such as the POMC (Drouin et al., 1993), CRF (Malkoski and Dorin, 1999) and

osteocalcin (Meyer et al., 1997). Even though consequences of GR action may take hours, some effects are observed within minutes. These are called non-genomic effects of GCs and have been shown to involve protein kinases, phosphatases, and G-protein coupled receptors (Heitzer et al., 2007).

2.5. GR coactivators and corepressors

The liganded GR can interact with components of the transcriptional machinery, chromatin remodeling proteins, as well as RNA polymerase II and components of the basal transcriptional machinery (Kumar and Thompson, 2005). The transcriptional complex formed by the GR also includes the coactivators CREB-binding protein (CBP) or its close homolog p300 (Chakravarti et al., 1996) and p160 family members known as steroid receptor coactivators (SRCs) (Leo and Chen, 2000). Most coactivators bind to the LBD of the GR and they enhance GR-dependent gene expression. Coactivator complexes assemble to GR-bound promoters and stimulate GR transcriptional activation either through direct interaction with the basal trancription machinery or by chromatin remodeling through histone acetylation or methylation (Heitzer et al., 2007).

Besides coactivators, other GR interacting proteins have been identified and termed corepressors. These corepressors include both nuclear receptor corepressor (NCoR) and silencing mediator or retinoid and thyroid receptors (SMRT) (Szapary et al., 1999) (Schulz et al., 2002). These corepressors repress transcription through the interaction with histone deacetylases (HDACs) that are able to modify chromatin leading to a closed chromatin structure (Watson et al., 2012).

2.6. GR phosphorylation

GR regulation is achieved by a combination of mechanisms involving ligand accessibility, GR concentration, subcellular localization, and post-translational modifications of the GR (Oakley and Cidlowski, 2011). Phosphorylation was the first identified modification of the GR (Beck et al., 2009) and previous studies have highlighted the involvement of different protein kinases in GC-mediated effects (Fig. 13) (Galliher-Beckley et al., 2008). It has been shown that the modulation of GR phosphorylation cycle by phosphatases maintains steady-state receptor phosphorylation at a low basal level in the absence of ligand, and GC-

dependent GR phosphorylation ultimately affects transactivating and transrepressing capacities of the GR (Wang et al., 2007).

Eight phosphorylated residues of the murine GR have been mapped: Ser122, 150, 212, 220, 234, 315, 412 and Thr159. Furthermore, Ser122, 150, 212, 220, 234, and 412 and the surrounding sequences are conserved in the rat and human GR. Only Thr159 and Ser315 lacked homology to the human GR. Interestingly, all sites with the exception of Ser315 were constrained to the N-terminal transactivation domain of the GR, suggesting that phosphorylation of the GR may function to modulate the transcription of target genes. With the exception of Ser150 and Thr159, the majority of data suggest that the phosphorylation of GR is induced by ligand binding to the receptor. Altogether, results suggest that the GR can be phosphorylated at one or more residues and phosphorylation is a dynamic process involving the dephosphorylation and phosphorylation of several serine/threonine residues. Therefore, different patterns of GR phosphorylation could lead to the alteration of the transcriptional activity of the GR (Galliher-Beckley and Cidlowski, 2009).

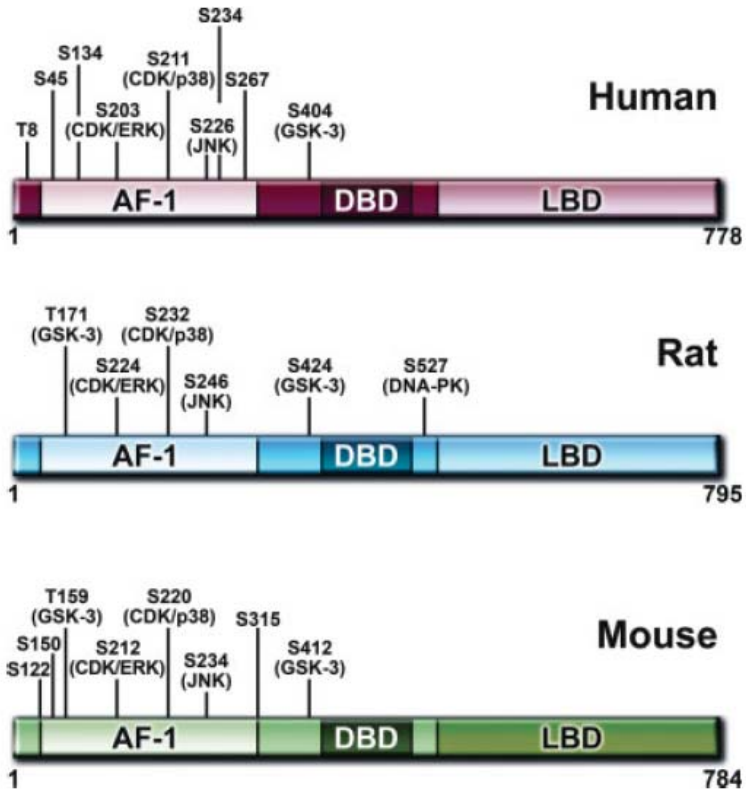

Figure 13. The known GR phosphorylation sites. Phosphorylation sites on the human, rat, and mouse receptor and the kinases implicated are shown (taken from Galliher-Beckley and Cidlowski, 2009).

The protein kinases involved in GR phosphorylation after GR exposure are still being studied. The protein kinases that have been shown to phosphorylate the GR and modulate its transcriptional activity include mitogen-activated protein kinases (MAPKs), glycogen synthase kinase-3 (GSK3), and cyclin–dependent kinases (CDKs) (Fig. 13). The GR is also a susbtrate for ubquitination, sumoylation and acetylation (Kfir-Erenfeld et al., 2010) (Oakley and Cidlowski, 2011).

2.7. GSK3

GSK3 is one of the kinases known to phosphorylate and modulate the GR (Galliher-Beckley and Cidlowski, 2009). GSK3 is a Serine/Threonine protein kinase highly conserved from yeast to mammals (Beurel and Jope, 2006) (Forde and Dale, 2007) (Rayasam et al., 2009). It was initially identified as a key regulator of insulin-dependent glycogen synthesis, but it has been demonstrated that GSK3 is a multifunctional kinase involved in cellular metabolism, signaling transduction, growth, differentiation, and cell fate determination (Forde and Dale, 2007). There are two homologous mammalian GSK3 isoforms encoded by different genes, GSK3α and GSK3β. They share 98% identity within their catalytic domain, but N- and C-terminal sequences diverge, making them structurally similar but not functionally identical (Woodgett, 1990) (Forde and Dale, 2007).

GSK3α (483 amino acid residues; 52kDa) is larger than GSK3β (433 aminoacod residues; 47 kDa) due to a glycine-rich extension at the N-terminus (Woodgett, 1990) (Fig. 14). The GSK3β mRNA undergoes alternative splicing, producing at least two protein products GSK3β1 and GSK3β2, the later being a brain specific isoform. GSK3α and GSK3β are ubiquitously expressed, but GSK3β is the most predominant form in the brain (Sutherland, 2011). While GSK3α deficient mice are born fertile; GSK3β knockout causes embryonic lethality due to severe liver degeneration and defects in embryonic cardiomyocyte proliferation and differentiation resulting in heart failure and death (Force and Woodgett, 2009). The differential phenotypes between isoform deletions suggest nonredundant functions of the GSK3 isoforms. Due to the fact that GSK3 inhibitors do not discriminate between the two isoforms, many functions attributed in the literature to GSK3β are likely shared by GSK3α.

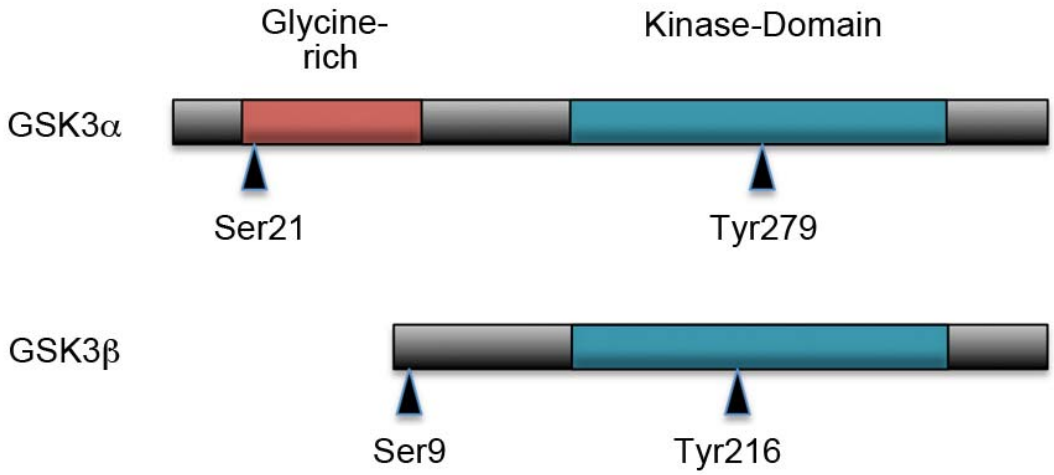

Figure 14. GSK3 α and GSK3 β isoforms. Inhibitory serine phosphorylation sites (Ser9 and Ser21) and activating tyrosine sites (Tyr216 and Tyr279) are shown.

GSK3 demonstrates a preference for pre-phosphorylated (primed) substrates by different priming kinases (Beurel and Jope, 2006) (Forde and Dale, 2007) (Rayasam et al., 2009). GSK3β phosphorylates different substrates, including glycogen synthase, and transcription factors such as c-myc, β-Catenin and Tau microtubule-associated protein, cyclin D1, and the BCL-2 family member MCL-1 (Maurer et al., 2006). Phosphorylation by GSK3 usually has inhibitory effects on its substrates, making this kinase a suppressor of many signaling pathways.

Basal activity of GSK3 is relatively high in resting cells and is an important component of the Wnt and phosphatydilinositol-3-kinase (PI3K) signaling pathways (Beurel and Jope, 2006). In the Wnt pathway, GSK3 is associated with Axin and APC in a complex that phosphorylates β-Catenin, leading to its degradation. Wnt signaling disrupts this complex, leading to β-Catenin/TCF transcriptional activation of target genes. In the PI3K pathway GSK3 is constitutively active in the absence of growth factors and its inhibition is achieved through phosphorylation by Akt on Ser21 in GSK3α and Ser9 in GSK3β (Beurel and Jope, 2006). Phosphorylation of these residues results in the interaction of the N-terminal domain of GSK3 with the phosphate-binding pocket, preventing recognition of primed substrates. On the other hand, direct tyrosine phosphorylation (Tyr279 in GSK3α and Tyr216 in GSK3β) is associated with increased kinase activity (Fig. 14) (Hughes et al., 1993) (Pearl and Barford, 2002). Phosphorylation of these residues is crucial for the proper folding of the catalytic domain of the kinase, and occurs through autophosphorylation

during the synthesis of the GSK3 peptide. It appears that different pools of the kinase function in Wnt and PI3-Kinase signaling, as regulation of GSK3 in Wnt signaling pathway do not involve N-terminal or tyrosine phosphorylation. In this way, compartmentalization of GSK3 allows differential upstream and downstream substrate phosphorylation. Aditionally, ERK may phosphorylate Thr43 and p38 can phosphorylate Ser389 and Thr390 of GSK3β reducing its activity. Thr43 and Thr390 are not conserved among GSK3 α and β isoforms, suggesting an isoform specific regulation. In both cases this phosphorylation may favor Ser9 phosphorylation rather than promoting direct inhibition (Sutherland, 2011) (Medina and Wandosell, 2011).

Additional mechanisms besides phosphorylation are employed to regulate GSK3 like the control of its subcellular localization. GSK3β locates between the cytoplasm and nucleus in a steady-state and GSK3α is mostly cytoplasmic. GSK3α accumulates in the nucleus via activation of the calcium/calpain pathway or upon serum starvation. Additionally, the N-terminal domain of GSK3α is responsible for GSK3α nuclear exclusion (Azoulay-Alfaguter et al., 2011).

GSK3β is primarily cytoplasmic during G1 phase of the cell cycle and triggers the proteolysis of some proteins that promote G1 to S transition. On the other hand, nuclear levels of GSK3β are higher in the S phase were it phosphorylates cyclin D1 which is subsequently degraded (Diehl et al., 1998). Additionally, GSK3β has been implicated in regulating interphase microtubule dynamics and GSK3 inhibitors induce a delay in mitotic entry and exit, mitotic spindle defects, and chromosome misalignment (Tighe et al., 2007).

2.7.1. Regulation of apoptotic pathways by GSK3

A) GSK3 facilitates the intrinsic apoptotic pathway

There is a well-established relationship between GSK3 activity and apoptosis. GSK3 seems to prompt the intrinsic apoptosis-signaling pathway under a broad range of stimuli including growth factor deprivation or inhibition of the PI3K/Akt signaling pathway, DNA damage, hypoxia, ER-stress, and staurosporine treatment (Beurel and Jope, 2006). These conditions that activate the intrinsic apoptotic signaling pathway cause the disruption of mitochondrion, leading to cell destruction.

Although direct intramitochondrial substrates of GSK3 involved in intrinsic apoptosis pathway have not yet been identified, GSK3 targets several key proteins that regulate signals leading to the disruption of mitochondrion. GSK3 can directly phosphorylate BAX on Ser163, stimulating BAX translocation to the mitochondria, which leads to MOMP and mitochondrial proteins release during apoptosis (Linseman et al., 2004). GSK3 is also required for the stress-induced expression of BIM in cerebellar neurons (Hongisto et al., 2003) and is able to target MCL-1 for ubiquitin-dependent degradation (Maurer et al., 2006). Altogether, GSK3 regulates the expression of proteins that are key mitochondrial components of the intrinsic apoptotic-signaling pathway and oppositely regulates anti-apoptotic protein expression levels.

Importantly, GSK3 can modulate the activity of a great number of transcription factors that encode apoptosis-regulating proteins that control gene expression. These proteins include p53, β-Catenin, Myc, NFκB, cyclic AMP response element binding protein (CREB) and Heat shock factor-1 (HSF-1). HSF-1 inhibition by GSK3 reduces the expression of heat shock proteins, contributing to cell death. Besides regulating gene expression, GSK3 also regulates translation, and it was described that inhibition of protein synthesis, which GSK3 achieves by phosphorylating and inhibiting eIF2B, contributes to GSK3-induced apoptosis (Pap and Cooper, 2002). Thus, the role of GSK3 in intrinsic apoptotic signaling is not that of an initiator but of a facilitator, promoting the signaling responses to insults that initiate this pathway.

B) GSK3 inhibits the extrinsic apoptotic pathway

The involvement of GSK3 in the extrinsic apoptotic signaling pathway was first described in mouse embryonic fibroblasts (MEFs), where knocking out GSK3β caused mouse embryonic lethality due to TNF hypersensitivity in the liver (Hoeflich et al., 2000). This provided the key insight that GSK3β inhibits TNF-induced apoptosis. This was supported by the fact that lithium, a widely used GSK3 inhibitor, was shown to potentiate TNF-induced cytotoxicity in MEFs from WT mice. The inhibitory effect of GSK3 on TNF-induced apoptosis has been extended to other DRs. It is now clear that GSK3 inhibits TNF-, TRAIL- or FAS-mediated apoptosis, demonstrating that this is a generalized action regulating the extrinsic apoptotic pathway (Liao et al., 2003) (Song et al., 2004).

2.8. GR regulation by GSK3

Different interactions between GSK3 and the GR have been previously described. There is a hormone-dependent GR phosphorylation of human Ser404 by GSK3β, which targets the GR for nuclear export. This phosphorylation seems to play a role in GR protein stability and turnover as an un-phosphorylatable mutant had an increase in half-life in the absence of a ligand and when exposed to dexamethasone (Galliher-Beckley et al., 2008). Moreover, a mutant that mimics both the size and negative charge of a phosphorylation serine residue showed a decrease in half-life in the absence and presence of hormone. Additionally, GSK3β mediated phosphorylation of rat GR Thr171 has been described (Rogatsky et al., 1998).

Recently, a protein kinase screening in lymphoid cells showed that GSK3 has a role in GC-induced apoptosis (Spokoini et al., 2010). In the absence of a ligand, GSK3α is bound to the GR and exposure to GCs leads to its dissociation from the GR (Spokoini et al., 2010) and then GSK3α and GSK3β interact with BIM, a BH3-only protein induced by GCs in leukemia cells (Wang et al., 2003) (Zhang and Insel, 2004) (Iglesias-Serret et al., 2007). Moreover, it has been described that the GR associates with GSK3β in the presence of dexamethasone but not with GSK3α (Galliher-Beckley et al., 2008). Pharmacological inhibition of GSK3 blocked GC-induced apoptosis in different hematopoietic cell lines (Spokoini et al., 2010), and attenuated GC-induced upregulation of BIM (Nuutinen et al., 2009). Thus, it seems that GSK3 isoforms regulate GR cellular response by using different mechanisms.

2.9. Crosstalk between kinases and the GR

Some GC signaling events occur much faster and are of shorter duration than would be expected on the basis of genomic signaling. It has been suggested that besides the genomic mechanism, GCs could also act on diverse downstream targets, bypassing nuclear signaling. This could be achieved by positively or negatively regulating kinase signaling. Several of these target kinases have been identified, among which are intracellular proteins such as kinases, including MAPKs, CDKs, PI3K/Akt, IKKs and protein kinase C (PKC) (Herr et al., 2007) (Beck et al., 2009).

MAPKs

Activated GR forms a complex regulatory loop with the MAPK signaling pathway. GC induce DUSP1-mediated phosphorylation of JNK. The GR can also directly interact with JNK, interfering with its activity (Bruna et al., 2003). JNK has been shown to phosphorylate the rat GR at Ser246 and this phosphorylation attenuates GR transcriptional activity. Additionally, homologous phosphorylation of human GR (Ser226) has a negative effect on hormone signaling by enhancing nuclear export of the GR (Galliher-Beckley and Cidlowski, 2009).

On the other hand, ERK can phosphorylate the rat GR on Ser224 and Ser232 and the human GR on Ser203 and these phosphorylations attenuate the transcriptional activity of the GR. GCs are known to inhibit ERK MAPK activation by inhibiting the interaction of Raf-1 with its cochaperone Hsp90. In the case of p38 MAPK, there seems to be cell-specific effects. GC exposure in lymphoid cells seems to activate p38 but in many cell lines it seems to decrease its phosphorylation and activity. The phosphorylation of Ser134 of the GR by p38 significantly increases the association of the GR with the 14-3-3 class of signaling proteins on chromatin promoter regions, resulting in a blunted hormone-dependent transcriptional response of specific genes (Galliher-Beckley et al., 2011). In lymphoid cells, p38 MAPK-induced Ser211 phosphorylation of GR promoting GC sensitivity while ERK/JNK activity decreased the amount of Ser211 phosphorylation resulting in enhanced GC resistance.

CDKs

GCs can cell dependently repress gene expression of CDK4, CDK6 and their associating cyclin D3. GCs can also induce the expression of the CDK inhibitor p21. CDK2 and CDK4 activity are also inhibited by GCs. CDK1 and CDK2 were also described to be activated by Cyclin O during GC-induced apoptosis in lymphoid cells (Roig et al., 2009). On the other hand, several cyclin–CDK complexes (cyclin A-CDK2, cyclin A-CDC2, cyclin B-CDK2, cyclin B-CDC2, and cyclin E-CDK2) can phosphorylate the rat GR on Ser224 and Ser232 and this phosphorylation of GR by cyclin-CDKs is required for full GR-mediated transcriptional activity. Additionally, CDK5 activity blunts GC signaling and phosphorylates the GR at Ser226. However, it seems that Ser226 phosphorylated receptor may still be transcriptionally active, and further research is required to determine the

precise role of human Ser226 phosphorylation of GR in modulating GC signaling. Unlike most CDKs, CDK5 activity is restricted to cells of the nervous system. The data also show that multiple serines within the human GR (Ser45, Ser203, Ser211, Ser226, Ser395) become phosphorylated by CDK5 (Galliher-Beckley and Cidlowski, 2009).

PI3K/Akt

The PI3K/Akt signaling regulates important cellular functions such as proliferation and survival. This pathway is activated in a wide variety of cancers, which results in apoptosis resistance. Akt also known as protein kinase B (PKB) is rapidly activated upon GC treatment through PI3K. PI3K is a heterodimer composed of a regulatory unit (p58) and two catalytic α and β subunits. Although the activation of PI3K by GC requires the GR, no GRE-mediated gene transcription is necessary for PI3K activation. Instead, the GR can interact with the p85α subunit of PI3K under high doses of GC. PI3K/Akt signaling seems to play a role in NF-κB mediated GC resistance. Additionally, transcriptional and protein induction of serum and GC-regulated kinase-1 (SGK-1), a downstream effector of PI3K signaling, is required for survival signaling induced upon GR activation (Beck et al., 2009). Akt inhibition has been shown to enhance dexamethasone-induced apoptosis, as PI3K/Akt protects and delays dexamethasone-induced apoptosis. Importantly, PI3K/Akt signaling inhibits BIM expression by phosphorylating the FOXO3 transcription factor (Nuutinen et al., 2006).

IKKα

IKKα and IKKβ can phosphorylate IκB leading to its proteosomal degradation. This leads to NF-κB to translocate to the nucleus. GCs can induce IKKα in some cell lines mediating apoptosis protection. This apoptosis protection is lost when the dominant negative form of IκB is expressed. Thus, GC-induced resistance may require NF-κB activation (Beck et al., 2009).

PKC

PKC regulates both positive and negative signal transduction pathways essential for the initiation and homeostasis of immune responses. PKC isoforms constitute a family of

serine/threonine kinases that depending on the cellular context regulate a wide variety of cell responses including MAPKs (Spitaler and Cantrell, 2004). Glucocorticoids can both increase (Kajita et al., 2001) (Maddali et al., 2005) (Cote-Velez et al., 2008) and decrease (Jun et al., 1994) (Nguyen and Watts, 2006) PKC activity in several tissues or cells affecting gene transcription.

3. Mediators of glucocorticoid action

3.1. Glucocorticoid-induced leucine zipper (GILZ)

GILZ was initially isolated as a dexamethasone-responsive gene from a thymus subtraction DNA library (D'Adamio et al., 1997). Ever since, GILZ has been identified as a GC-transactivated gene in various cell types. Most of the research done on GILZ has been made in T cells. In T cells GILZ has been reported to inhibit transcription factors such as NF-κB and AP-1 and the kinases RAF-1 and ERK (Beaulieu and Morand, 2011).

GILZ is a protein of 137 amino acids in humans and consists of three major domains: the N-terminal, leucine zipper (LZ), and C-terminal domains. GILZ, also known as TSC22 domain family protein 3, also contains a tuberous sclerosis complex (TSC) domain (Beaulieu and Morand, 2011). The LZ motif of GILZ is located in the central part of the protein and mediates the homodimerization of GILZ required for many of its functions (D'Adamio et al., 1997), while the other domains are responsible for protein-protein interactions between GILZ and transcriptional and signaling molecules. The promoter of GILZ contains 6 GREs and two functional forkhead-responsive elements. FOXO3 binding to these binding sites is necessary for maximal dexamethasone-induced expression of GILZ in T lymphocytes (Asselin-Labat et al., 2004). The GILZ promoter also harbors binding sites for signal transducer and activator of transcription 6 (STAT 6), nuclear factor of activated T cells (NFAT), Octamer, and c-myc (Beaulieu and Morand, 2011). Activation of Akt leads to the phosphorylation of transcription factors belonging to the FOXO family, which results in the nuclear exclusion of the FOXO proteins and thus leads to the inhibition of their cognate transcriptional targets. Thus, the inhibition of the PI3K/Akt pathway results in the upregulation of GILZ expression (Grugan et al., 2008). In addition, GILZ negatively feeds back to regulate the nuclear exclusion of FOXO3 in a CRM1 dependent manner (Latre de Late et al., 2010) (Fig. 15). Thus, GILZ not only inhibits its own expression but also limits the effects of nuclear FOXO3.

GILZ can also participate in the GC-mediated inhibition of AP-1 by directly binding to its components c-Jun and c-Fos and by binding RAF-1, inhibiting its phosphorylation. The resulting impairment of RAF-1 activation decreases ERK activity, which is important for transcriptional activity of AP-1 (Beaulieu and Morand, 2011). Increased expression of GILZ inhibits the activation, nuclear translocation and DNA binding activity of NF-κB (Ayroldi et al., 2001). This inhibition of NF-κB is the result of direct association between GILZ and both the p65 and p52 subunits of NF-κB, while the phosphorylation or degradation of proteins belonging to the IκB family are not affected, which suggests that GILZ acts directly as a glucocorticoid-induced corepressor of NF-κB. Altogether, it appears that GILZ is an important mediator of GC signaling.

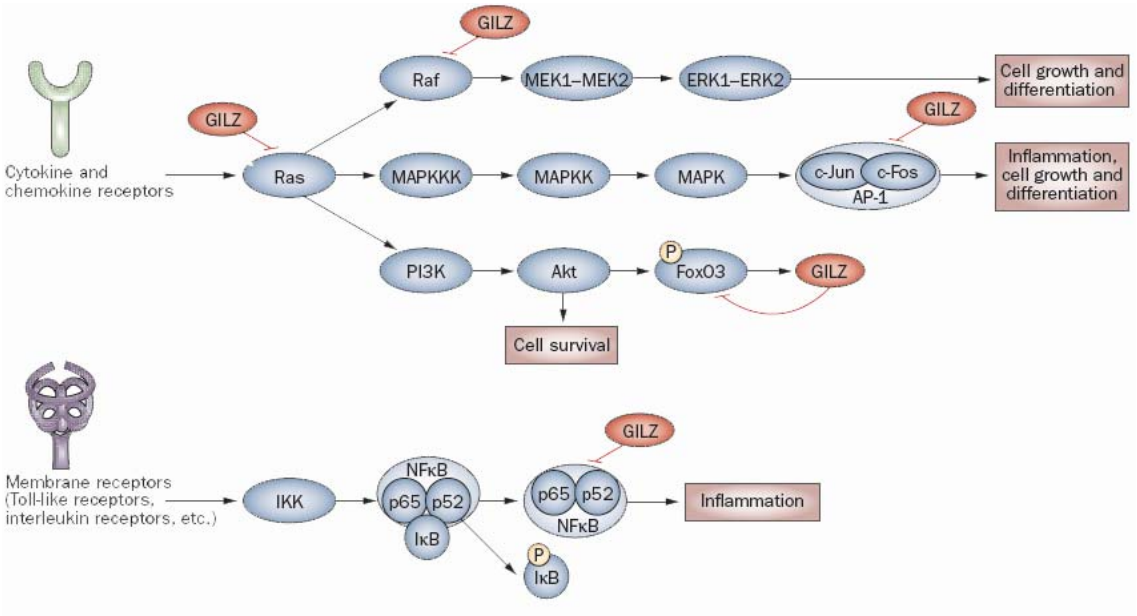

Figure 15. Interactions of GILZ with key signaling pathways. GILZ affects several major cell signaling pathways involved in cell growth, cell differentiation, cell survival and inflammation (taken from Beaulieu et al., 2011).

3.2. BIM

Among the GC responsive genes that have been described that can be involved in GC-induced apoptosis is the pro-apoptotic BH3-only BCL-2 family protein BIM (Wang et al., 2003) (Zhang and Insel, 2004). The role of BIM in GC-induced cell death was confirmed

in BIM knockout thymocytes, which showed partial resistance to GCs (Bouillet et al., 1999). Additionally, BIM down-regulation in malignant lymphoid cells confers resistance to dexamethasone (Abrams et al., 2004) (Lu et al., 2006) (Rambal et al., 2009) (Lopez-Royuela et al., 2010).

The three major isoforms BIM-EL, BIM-L, and BIM-S can all induce apoptosis, the latter being the most potent inducer (Kfir-Erenfeld et al., 2010). Previous studies demonstrated that the promoter of *BIM* does not contain GREs (Wang et al., 2003), suggesting a mechanism of *BIM* regulation not mediated directly by the GR in response to GCs. In accordance to this, it was recently demonstrated that GCs repress the expression of miR-17-92, which results in elevated BIM protein expression (Molitoris et al., 2011). During the writing of this thesis it was described that dexamethasone treatment induces transcription factor RUNX2 and c-Jun in parallel with *BIM* induction. c-Jun binds to and activates the AP-1-binding site at about 2.7 kb from the transcription start site of the *BIM* promoter (Heidari et al., 2012).

4. GCs and Chronic Lymphocytic Leukemia (CLL)

Chronic lymphocytic leukemia (CLL) was first defined in 1966 as a disease characterized for the monoclonal expansion of B lymphocytes with poor capacity to proliferate and long lifespan (Galton, 1966) (Dameshek, 1967). These lymphocytes are small, with mature appearance but functionally immature (immunoincompetents) due to deficient production of antibodies, which favours the appearance of infectious diseases (Chiorazzi et al., 2005). CLL is a disorder that is manifested by progressive accumulation of these resting cells in the blood, bone marrow, lymphatic tissues and that ultimately becomes lethal (Dighiero and Hamblin, 2008). In this lymphoid neoplasm, lymphocyte counts in the blood are usually greater than or equal to $5x10^9$/L with a characteristic immunophenotype of CD5- and CD23-positive B cells (Hallek et al., 2008) (Shanafelt et al., 2009).

CLL is a malignancy that results in failed apoptosis, as blood circulating CLL cells are non-proliferating and are arrested in the G0/G1 phase of the cell cycle (Decker et al., 2003). Cell division occurs in 'proliferation centers' in tissue microenvironments, accounting for the rise in white blood cell counts in some patients. However, lack of apoptosis is considered the prime cause for the loss of balance in B-cell homeostasis in this malignancy.

Thus, clinically used chemotherapeutic agents act by inducing apoptosis in CLL lymphocytes (Packham and Stevenson, 2005).

CLL is considered a clinically and biologically heterogeneous disease originated from stimulated mature B cells and expressing in its surface the above mentioned markers and low levels of IgM, IgD, and CD79. CLL cells may differ in activation, maturation state, or cellular subgroup (Chiorazzi et al., 2005). CLL is the most common leukemia in western countries (Europe and USA), where it represents approximately 30% of leukemias, 90% of chronic lymphoid leukemia and 7% of non-Hodgkin lymphomas (Montserrat and Rozman, 1995). Each year 180,000 new cases are diagnosed in the world (Chen and McMillan, 2008) (Gribben, 2010) (Pekarsky et al., 2010). The global incidence rate is 3 new cases per 100,000 inhabitants per year (Oscier et al., 2004). CLL is a disease of the elderly, with a median age at diagnosis of 72 years and median age at death from CLL of 79 years. Almost 70% of CLL patients are older than 65 years at the time of diagnosis; less than 2%, younger than 45; and the incidence increases gradually with age (Chen and McMillan, 2008) (Gribben, 2008) (Gribben, 2010). The clinical course of CLL is heterogeneous as some patients, have an aggressive disease and require treatment, most commonly with cytotoxic therapy. On the other hand, there are patients that have a stable, non-progressive disease that often requires no treatment. Relapses are common and CLL remains incurable (Packham and Stevenson, 2005).

CLL is usually detected in routine medical check-ups or in response to a slight discomfort of the patient, such as fatigue or respiratory problems during exercise. CLL cells are monomorphic, small, round B lymphocytes, apparently mature, with condensed nuclear chromatin, absence of nucleoli and poor cytoplasm (Fig. 16), characterized by a peculiar fragility of the cell membrane that leads to frequent rupture of the leukemic cells while preparing the blood film, creating the so-called "Gumprecht nuclear shadows" or "smudge cells". In addition, there are two morphologically atypical CLL forms: CLL/PL, containing 10-55% of prolymphocytes, and atypical or mixed CLL, containing >15% of population with lymphoplasmocitoid features. These morphological variants have typical immunophenotypic features of CLL (Gentile et al., 2005).

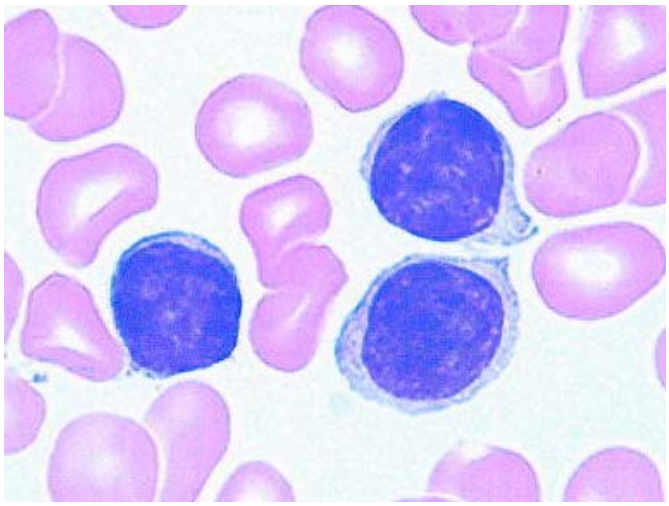

Figure 16. Typical morphology of CLL cells in peripheral blood. The cells are small with condensed nuclear chromatin and scant pale cytoplasm (May Grumwald Giemsa staining taken from Schlette et al., 2003).

It is still unknown if the apoptotic resistance of CLL cells is due to genetic or epigenetic alterations of apoptosis regulators within the cell, or are driven by environmental signals that are received by cells *in vivo* (Malavasi et al., 2011). The microenvironment play and important role in this apoptosis resistance, as there is propensity of CLL cells to undergo apoptosis when cultured *ex vivo* (Collins et al., 1989). On the other hand, intrinsic cellular alterations could also contribute to cell death evasion. Furthermore, there is considerable patient-to-patient heterogeneity in CLL cell apoptosis induction *ex vivo*, suggesting that intrinsic susceptibility to apoptosis may differ (Packham and Stevenson, 2005).

Current therapeutic options are varied and include treatment with antineoplastic drugs (mainly analogues of purine and alkylating agents), monoclonal antibodies and bone marrow transplantation (Table 1). The most important advances have been the demonstration of improvement in the outcome in CLL with combination chemotherapy and then further marked improvement with chemo-immunotherapy. One of the most preferred treatments of choice (for patients with good performance status) is the combination of fludarabine, cyclophosphamide and rituximab (FCR) (Gribben, 2010). In addition, there are other combinations using all types of drugs summarized in Table 1.

Type of treatment	Drug
Glucocorticoids	Prednisone
Alkylating agents	Chlorambucil
	Cyclophosphamide
Purine analogues	Fludarabine
	2-clorodeoxyadenosine (2-Cda, cladribine)
	Pentostatin
Topoisomerase II inhibitors	Doxorrubicin (adriamycin)
	Mitoxantrone
Mitotic spindle inhibitors	Vincristine
Monoclonal antibodies	Rituximab
	Alemtuzumab

Table 1. Drugs used in CLL therapy (modified from Coll-Mulet, 2007).

Even though the apoptotic effects of GCs in CLL cells have been known for many years, their use is often confined to their immunosuppressive activity in order to control autoimmune phenomena (Thornton et al., 2003). Due to their p53-independent mechanism of action, GCs, either alone or in combination with other agents, have emerged as a useful and important treatment option for patients with chemoresistant or *TP53*-defective CLL (Melarangi et al., 2012). GCs are potent inducers of apoptosis in CLL cells, through a caspase-dependent mechanism (McConkey et al., 1991) (Chandra et al., 1997) (Bellosillo et al., 1997). Furthermore, the inhibition of PKC or the PI3K/Akt pathways increases glucocorticoid-induced apoptosis in the presence of survival factors (Barragan et al., 2002). It is also known that glucocorticoids upregulate BIM at mRNA and protein levels in CLL cells (Iglesias-Serret et al., 2007). However, the mechanism of glucocorticoid induced apoptosis in CLL remains largely unknown.

II. Materials and methods

1. Samples collection from CLL patients.

Clinicians from the hospital diagnose all patients following clinical, morphological, molecular and immunophenotypic criteria, as proposed by the World Health Organization. Peripheral blood samples of CLL patients were collected in the Servei d'Hematologia of Hospital Universitari de Bellvitge in tubes with anticoagulant EDTA. The information of the sample was collected in an internal database which scored diagnosis, date of sample removal, lymphocyte count and percentage of lymphocytes, as well as any information of interest, such as genetic anomalies, aggressive disease, treatment or chemoresistance. Each sample and each patient was assigned with an identification number, which was linked to the clinical history number given by Institut Català de la Salut. Thus, in order to give identification to each sample, we first refer to the patient number and then the sample number; for instance, 143_17/12 corresponds to the patient 143 and the sample 17 of the year 2012. In addition, the database informs whether there are cryopreserved samples and allows obtaining historical plots. We do not include any personal patient information as it is established by Universitat de Barcelona and Hospital de Bellvitge Ethical Committees. Written informed consent was obtained from all patients in accordance with Hospital de Bellvitge Ethical Committee.

2. Mononuclear cell isolation from peripheral blood of CLL patients

Mononuclear cells from peripheral blood samples were isolated by centrifugation on a Ficoll-Hypaque (Seromed, Berlin, Germany) gradient (Fig. 17). Blood was diluted in phosphate buffer saline (PBS) to a final volume of 8 mL. This mixture was added above 4 mL of Ficoll solution (density = 1,077 g/mL) with care to maintain the interface. The preparation was centrifuged for 20 minutes at 850 g at room temperature. The centrifuge stop was conducted without brake to avoid disrupting the gradient. In the resulting separation, erythrocytes and polimorphonucleated leukocytes are at the bottom of the tube due to their higher density. Above Ficoll solution and forming a ring are the mononuclear cells and at the top are plasma and platelets diluted in PBS. We picked up the ring with a glass Pasteur pipette. Mononuclear cells were deposited on 40 mL of PBS and a wash centrifugation was performed 10 minutes to 480 g at room temperature and cell count was performed. Pellets were resuspended with complete culture media when needed for experiments or the sample was cryopreserved in liquid nitrogen in the presence of 10% dimethyl sulfoxide (DMSO) (Sigma-Aldrich, Steinheim, Germany). Purified mononuclear

leukocytes contain B cells, T cells and monocytes in various proportions according to the patient and the stage of the disease. If the percentage of B cells is higher than 80%, samples were used to perform RNA and protein extractions or for cell viability analyses. Cells were used right after the purification or cells were cryopreserved for later use.

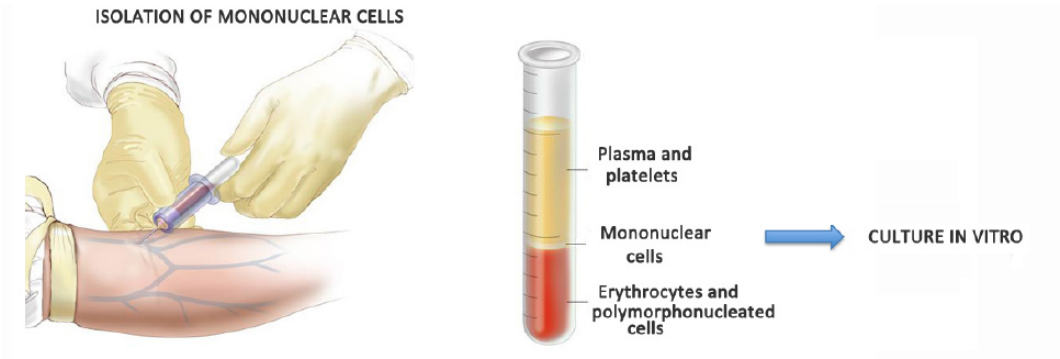

Figure 17. Purification of mononuclear cells from peripheral blood (modified from http://www.cancer.gov).

3. Cell culture and cell lines

Jurkat cells: Jurkat cell lines were derived from a parental cell line of Jurkat T-acute lymphoblastic leukemia cells harboring a nonfunctional GR (Riml et al., 2004). Jurkat GR wt cells were generated by expressing the rat wt GR under the control of the β-actin promoter (Helmberg et al., 1995). Jurkat LS7 cells were generated by expressing the GR LS7 mutant under the control of the β-actin promoter. These cells were kindly provided by Dr. Carme Caelles (Institute for Research in Biomedicine, Universitat de Barcelona, Barcelona, Spain).

HeLa cells: Epithelial cell line derived from human cervix adenocarcinoma. HeLa cells were purchased at the American Type Culture Collection (ATCC, www.atcc.org).

BxPC-3 cells: Human pancreatic adenocarcinoma cell line was kindly given by Dr. Pilar Navarro (Institut Hospital del Mar d'Investigacions Mèdiques, Barcelona).

MCF-7 cells: Human breast adenocarcinoma cell line was kindly given by Dr. Ana Manzano (Universitat de Barcelona, Barcelona).

MC3T3 cells: Mouse preosteoblast cell line was kindly given by Dr. Francesc Ventura (Universitat de Barcelon, Barcelona).

MEF cells: Mouse embryonic fibroblast cells. WT, GSK3α-/-, and GSK3β-/- MEF cells were kindly given by Dr. J. Woodgett (Samuel Lunenfeld Research Institute, Toronto, Canada).

Parental Jurkat, Jurkat GR WT, and BxPC-3 cells were grown in RPMI 1640 medium (Biological Industries) containing 10% inactivated fetal bovine serum (FBS) (Biological Industries), 2 mM L-glutamine, 100 μg/mL penicillin, and 100 mg/mL streptomycin at 37ºC in a humidified atmosphere at 5% carbon dioxide. HeLa, MC3T3, MCF-7 cells and WT, GSK3α -/-, and GSK3β -/- MEF cells were maintained in DMEM (Biological Industries) containing 10% FBS.

4. Freezing and thawing of cells.

Cryopreservation of CLL allows storage for later use. When CLL cells are thawed, they maintain their characteristics and viability after years of cryopreservation. Regarding cell lines, it is not recommended to keep them cycling for more than 1-3 months since many lines easily mutate in culture, being genetically unstable and changing characteristics after several passages. On the other hand, it is recommended to freeze cell lines right after thawing a tube and expanding the line. The cryopreservation procedure is performed in cold DMSO as a membrane stabilizer. Keep tubes at -80ºC for 12-24 hours in an isopropanol freezer or in polystyrene so that temperature decreases gradually. At 12-24 hours, move the tubes into a liquid nitrogen tank.

Protocol of cryopreservation of primary CLL cells:

Resuspend the pellet of mononuclear cells in cold FBS (previously inactivated by heat for 30 minutes at 56°C) so that there are 20-30x10^6 cells/0.75 mL FBS/tube. Maintain the suspension of cells in cold ice. Add slowly the previous suspension on an equal volume of cryopreservation solution, prepared with RPMI 1640, inactivated FBS and DMSO in ratio 3:1:1, also cold. Finally, there will be 20-30x10^6 cells/1.5 mL/ tube and 10% DMSO. Aliquote the sample in 2 mL cryopreservation tubes and cryopreserve in liquid nitrogen.

Protocol of cryopreservation of Jurkat and BxPC-3 cell lines:

Collect cells in exponential growth phase. Wash by centrifugation for 5 minutes at 480 g. The protocol is identical to CLL cells except that here we freeze $10x10^6$ cells/tube.

Protocol of cryopreservation of MEF, HeLa, MCF7 and MC3T3 cells:

Collect cells in exponential growth phase. Wash by centrifugation for 5 minutes at 480 g. On the basis of a 60 cm^2 confluent plate we obtain 4 tubes. Resuspend the pellet of mononuclear cells in cold FBS so that cells are in 0.75 mL FBS/tube. Maintain the suspension of cells in cold ice. Slowly add the previous suspension on an equal volume of cryopreservation solution, newly prepared in DMEM with 20% DMSO, also cold. Finally, there will be 1.5 mL/tube. Aliquote the sample in 2 mL cryopreservation tubes and cryopreserve in liquid nitrogen.

Protocol for thawing of primary CLL cells, Jurkat and BxPC-3 cell lines:

Place the cryopreserved tube in a bath at 37ºC unless its content is partially unfrozen. Pour the tube content on 40 mL of RPMI 1640 medium supplemented with 20% of inactivated FBS, previously heated at 37ºC, so that frozen cells thaw in a volume at least 10 times higher. Clean cells from DMSO by centrifugation to 480 g for 5 minutes in the case of leukemic cell lines or 10 minutes for CLL cells. Resuspend the pellet of cells in culture medium.

Protocol for thawing of MEF, HeLa, MCF7 and MC3T3 cells:

Place the cryopreserved tube in a bath at 37ºC unless its content is partially unfrozen. Pour the tube content on 40 mL of DMEM medium supplemented with 20% of inactivated FBS, previously heated at 37ºC, so that frozen cells thaw in a volume at least 10 times higher. Clean cells from DMSO by centrifugation to 480 g for 5 minutes. Resuspend the pellet of cells in culture medium.

5. Reagents

Dexamethasone, actinomycin D, cycloheximide, lovastatin, wortmannin and SB216763 were purchased from Sigma- Aldrich (St. Louis, MO). Akt inhibitor VIII (Akti), SB203580, U0126, LY294002, bisindolylmaleimide I (Bis I), and rapamycin were purchased from Calbiochem (La Jolla, CA). SP600125, GSK650394, and KU0063794 were from Tocris

Bioscience (Bristol, UK). Lithium chloride (LiCl), PP242, and MG-132 were from Sigma-Aldrich, and LY333531 from Enzo Life Sciences. ABT-737 was purchased from Selleck Chemicals LLC (Houston, TX). Roscovitine was kindly provided by Dr. Jacint Boix (Universitat de Lleida, Lleida, Spain). Suberoylanilide hydroxamic acid (SAHA; vorinostat, Zolinza) was obtained from Cayman Chemical (Ann Arbor, MI) and Kendine-92 (5-diaryl-1H-pyrrole- 2-carboxamide derivates) was generously provided by Dr. Fernando Cossío (Universidad del Pais Vasco, Bilbao, Spain). Annexin V allophycocyanin was purchased from eBiosciences (San Diego, CA).

6. Analysis of apoptosis and cell viability by flow cytometry

In general, cell viability analysis was performed using FACSCalibur flow cytometer (Becton Dickinson). The program used for the data acquisition and analysis was CellQuest Pro (Becton Dickinson).

The foundation of the technique is very simple. The cell membrane is composed of a lipid bilayer of asymmetrical distribution. Phosphatidylserine is a phospholipid entirely located on the inner monolayer surface of the plasma membrane. When a cell undergoes apoptosis, phosphatidylserine is no longer restricted to the cytosolic part of the membrane, but becomes exposed on the surface of the cell, which plays an important role in the recognition and removal of apoptotic cells by macrophages. The translocation of phosphatidylserine to the outer layer is considered an initial event in the apoptotic process and it has become a marker of apoptosis in mammalian cells. The protein annexin V binds with great affinity to the lipid in a calcium-dependent manner (Fig. 18).

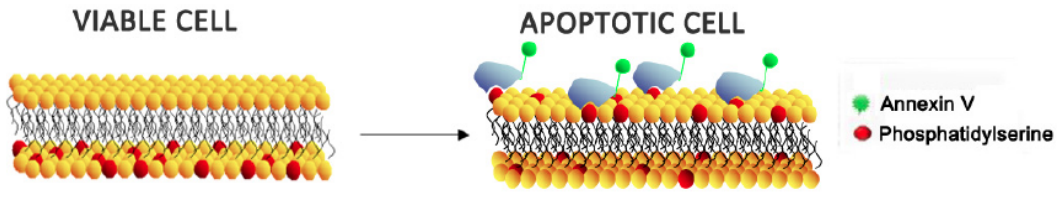

Figure 18. Staining of apoptotic cells with annexin V (modified from Coll-Mulet, 2007).

In this way, cell viability was determined by measuring phosphatidylserine exposure and membrane integrity. This was determined by annexin V-FITC staining and PI. Cell viability

was measured as the percentage of annexin V-FITC/PI-negative cell population, and it is expressed as the percentage of nonapoptotic cells. In cases where cells were pre-incubated with the GSK3 inhibitor SB216763, we used annexin V-APC to avoid interference. In this case cell viability was measured as the percentage of annexin V-APC negative cell population, and it is expressed as the percentage of nonapoptotic cells. In total, 2.5 x 10^5 cells were incubated for 24 hours with the indicated factors. Cells were washed and incubated with 150 μL annexin-binding buffer and 1.5 μL annexin V-FITC or -APC for 15 min in the dark. Cells were then analyzed by flow cytometry.

To analyze apoptosis in T cells and B cells from CLL patient samples, 0.5 x 106 cells were washed in annexin V-binding buffer, and incubated in 50 μL annexin V-binding buffer with 2 μL allophycocyanin (APC)-conjugated anti-CD3 and 2 μL phycoerythrin (PE)-conjugated anti-CD19, for 10 min in the dark. Cells were then diluted with annexin V-binding buffer to a volume of 150 μL and incubated with 1 μL annexin V-FITC for 15 min in the dark. Cells were then analyzed by flow cytometry.

7. Western blot analysis and antibodies

Lysing cells with reducing Laemmli sample buffer is quick, simple and reduces concerns that the protein of interest has not been solubilized. The presence of 2% SDS ensures total lysis of the nucleus, and results in the extraction of genomic DNA. This lysis procedure is denaturing. Cells were incubated with the indicated factors for a specific period of time that depends on each experiment. Cells were collected and washed with PBS. After centrifugation the pellet was resuspended in 50-100 μL of Laemmli (Sample Buffer). Depending on the cell number, samples were heated to 95°C for 10 minutes and the pellet was vortexed. Efficiency of lysis was checked by various cycles of heating, vortex and centrifugation to dissolve the pellets. Quantification of proteins was conducted with the kit Micro BCA Protein Assay Reagent (Thermo Scientific), using a plate reader of 550 mm. This kit is based on a colorimetric quantitative determination with bicinchoninic acid (BCA) to detect Cu reduction due to the basic pH of the proteins. Equal amounts of protein lysate were subjected to SDS-page-electrophoresis and electrophoretically transferred to PVDF membranes Immobilon-P (Millipore, Bedford, MA). The membranes were then blocked with 5% non-fat milk solution in TBS-T 0,1% for 1 hour at room temperature and immunoblotted. Both incubations with primary and secondary antibodies

(Table 2) were performed in 5% non-fat milk TBS-T solution for 90 minutes each. Some antibodies were incubated in BSA. The membrane was placed in a cassette with ECL solution (Amersham Biosciences) and a photographic film to detect the light emitted by the membrane in the area where the secondary antibody is attached to the primary antibody and detects the protein of interest. Finally, we developed the film by the traditional methods of developer and fixer.

Antibody	**Source**	**Application and dilution**	**Company**
MCL-1	Rabbit	WB (1:1000)	Santa Cruz Biotechnology (S-19): sc-819
BIM	Mouse	WB (1:1000)	Cell Signaling
GILZ	Rabbit	WB (1:200)	Santa Cruz Biotechnology (FL-134): sc-819
Cleaved Caspase-9	Rabbit	WB (1:1000)	Cell Signaling
Pro-Caspase-3	Mouse	WB (1:1000)	BD Biosciences
β-Catenin	Mouse	WB (1:1000)	BD Biosciences
GR	Rabbit	WB (1:1000) IP (1:1000)	Santa Cruz Biotechnology (H-300): sc-8992
GSK3α/β	Mouse	WB (1:1000)	StressGen Biotechnologies
GSK3α	Rabbit	WB (1:1000)	Cell Signaling
GSK3β	Mouse	WB (1:1000)	Cell Signaling (27C10)
Cytochrome oxidase subunit II	Mouse	WB (1:1000)	Molecular Probes, Inc.
Lamin A/C	Mouse	WB (1:1000)	Cell Signaling
α-TUBULIN	Rabbit	WB (1:1000)	Oncogene Research Products
ERK2	Mouse	WB (1:500)	Upstate Biotechnology
BCL-2	Mouse	WB (1:1000)	Dako (M0887)
RNA polymerase II	Mouse	IP (1:1000)	Upstate Biotechnology
IgGs	Rabbit	IP (1:1000)	Upstate Biotechnology
Anti-rabbit IgG, HRP linked whole antibody (from donkey)		WB (1:5000)	GE Healthcare
Anti-mouse IgG, HRP linked whole antibody (from sheep)		WB (1:5000)	GE Healthcare

Table 2. Sources, dilutions and companies of the antibodies used in this work. Western Blot (WB) and Immunoprecipitation (IP).

8. RNA extraction.

Total RNA was extracted from cells by using the RNeasy Micro Kit (QIAGEN, Germany). 2-5 x 10^6 cells were collected for each condition. Cells were centrifuged for 10 minutes at 480 g and we proceeded according to the manufacturer's instructions while maintaining the samples at room temperature (as opposed to other methods of RNA purification). Total RNA samples were quantified in the Nanodrop® spectrophotometer. To obtain and work with RNA solutions, all material used was RNAse free.

9. Reverse Transcriptase Multiplex Ligation-dependent Probe Amplification (RT-MLPA)

RNA content was analyzed by RT-MLPA using SALSA MLPA KIT R011-C1 Apoptosis mRNA from MRC-Holland for the simultaneous detection of 38 messenger RNA molecules (Eldering et al., 2003). In brief, RNA samples (200 ng total RNA) were first reverse transcribed using a gene-specific probe mix (Fig. 19). The resulting cDNA was annealed overnight at 60°C to the MLPA probe mix. Annealed oligonucleotides were ligated by adding Ligase-65 (MRC-Holland) and incubated at 54°C for 15 minutes. Ligation products were amplified by PCR (35 cycles; 30 seconds at 95°C, 30 seconds at 60°C, and 1 minute at 72°C) with one unlabeled and one FAM-labeled primer. The final PCR fragments amplified were separated by capillary electrophoresis on a 48-capillary ABI-Prism 3730 Genetic Analyzer (Applied Biosystems). Peak area and height were measured using GeneScan v3.0 analysis software (Applied Biosystems). The sum of all peak data was set at 100% to normalize for fluctuations in total signal among samples, and individual peaks were calculated relative to the 100% value. The mRNA levels of all the genes were standardized to those of *β-glucoronidase (GUS)* for Jurkat cells and *PARN* for HeLa cells. RNA content of wt, GSK3α-/- or GSK3β-/- MEF cells were analyzed by RT-MLPA using SALSA KIT RM002-B1 Mouse Apoptosis mRNA from MRC-Holland. The mRNA levels of all the genes were standardized to those of *TATA box-binding protein* (TBP).

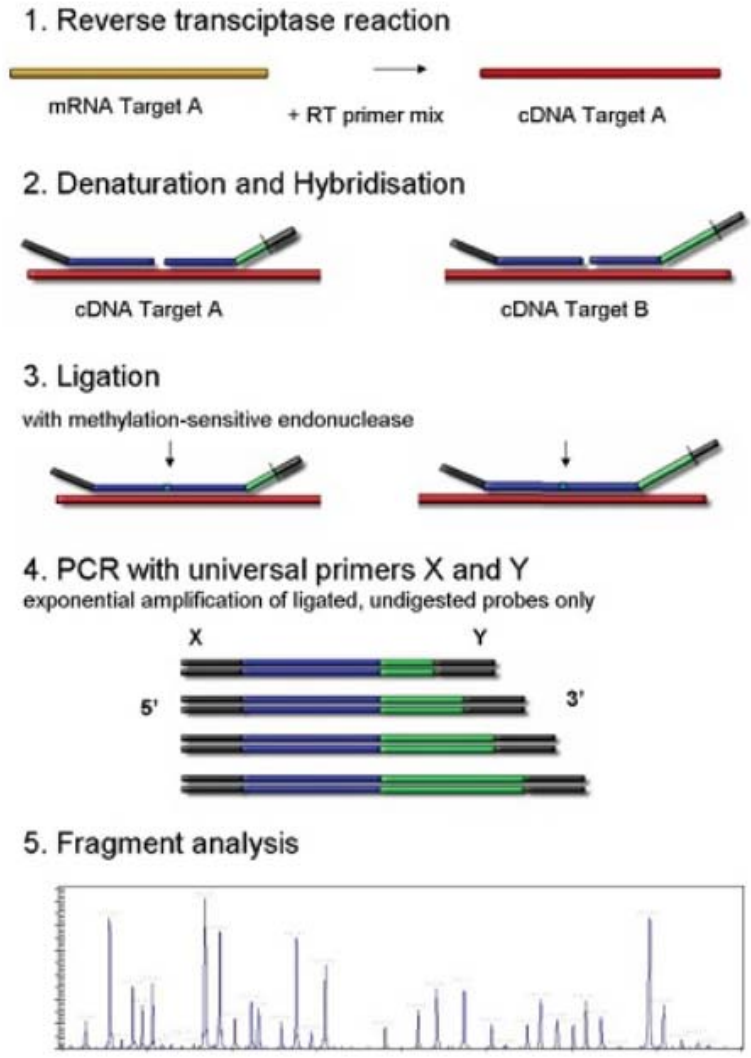

Figure 19. RT-MLPA steps (modified from www.mlpa.com).

10. Quantitative PCR (RT-qPCR) analysis

2 µg of total RNA were reverse-transcribed using a Ready-To-Go You-Prime First-Strand Beads Kit (GE Healthcare) and Random Hexamers (Applied Biosystems). Quantitative PCRs were carried out using ABI Prism 7900 HT Fast Real-Time PCR System and Designed human TaqMan assays (Applied Biosystems) were used to quantify gene expression of *BIM* (Hs00197982_m1), *GILZ* (Hs00608272_m1), *GILZ* (Mm00726417_s1), *HIAP1* (HS00154109_m1), BCL-3 (Hs00180403_m1), and MYC (Hs00153408_m1) according to the manufacturer's guidelines. The housekeeping gene *GUS* (Hs99999908_m1) or *GAPDH* (Mm99999915_g1) were used as a control for RNA quality, and used for normalization. PCR data were captured and analyzed using the Sequence

Detector Software (SDS version 2.2.2, Applied Biosystems). Each reaction was prepared as follows (Table 3):

RT-qPCR 384 wells reaction mix	
Sterile MilliQ Water	8,2µL
Taqman Universal Master Mix	10µL
cDNA	0,8µL
Gene Expression Assay	1µL

Table 3. RT-qPCR reaction mix composition.

11. Bacterial cultures

The bacteria used to amplify plasmids corresponded to the bacteria *E. coli* strain DH5α. The glass material and culture media (liquid LB (Luria Bertani) medium or LB-agar) (Table 4) were sterilized in an autoclave and the manipulation of bacteria was performed under sterile conditions.

Liquid bacterial culture

In the case of liquid cultures, cells are grown in agitation (220 rpm) in LB medium (Table 4) at 37°C over night. The volume of the culture medium occupies one third of the total volume of the container to ensure the oxygen required for the exponential growth of the culture. Generally 15 mL tubes have been employed with one half volume of 3-5 mL. In the case of cells transformed with a plasmid, as is usually the case, the antibiotic for which the plasmid has resistance (selection antibiotic) is added to the culture medium, the selective pressure thus allows only the growth of bacteria that have incorporated the plasmid.

Solid bacterial culture

The solid culture is carried out on solid LB-agar plates (Table 4), which include the selection antibiotic. The culture is allowed to grow at 37°C over night. Inverting the plates during their incubation to prevent water vapor to condense over the agar. Antibiotic stocks were prepared in water, filtered and aliquoted for storing at -20 ° C.

Liquid LB	LB-Agar
NaCl 10 g/L	NaCl 10 g/L
Bacto-Tryptone 10 g/L	Bacto-Tryptone 10 g/L
Bacto-Yeast Extract 5 g/L	Bacto-Yeast Extract 5 g/L
	Bacto-Agar 7,5 g/L

Table 4. Composition of Liquid LB medium and solid LB-Agar used for bacterial culture.

12. Preparation of thermocompetent bacteria

Preculture of bacteria was performed over night in 3 mL LB without antibiotic. The stock of bacteria is kept at -80 °C and we inoculated with the bacteria directly without thawing ice. We diluted the preculture (1:50) in 50 mL of LB and incubated at 37°C in agitation until an OD600 (optical density at λ = 600 nm) of 0.4-0.5. This confirms that the culture is in exponential growth. Bacteria were incubated on ice for 30 min and centrifuge for 15 min at 2500 rpm and 4°C. From this step on the entire process is performed in cold, this improves cell survival to shock treatment. The supernatant was discarded and the bacterial pellet resuspended in 1 mL of 0.1 M $CaCl^2$, take up to 3 mL of solution and then to a final volume of 20 mL. Bacteria were incubated on ice for 30 min and centrifuged for 15 min at 2500 rpm and 4°C. The supernatant was discarded and the bacterial pellet resuspended in 1 mL of 0.1 M CaCl2 and taken to a final volume of 5 mL. Bacteria can remain at 4°C for one week. For later use they must be frozen at -80°C. For the freezing of the 5 mL of competent bacteria 140 µL of DMSO were added, and after mixing and incubating 15 minutes on ice another 140 µL of DMSO are added. The bacteria are then aliquoted into 100 µL fractions and frozen at -80°C.

13. Transformation of competent bacteria and glycerol stock

The plasmids were introduced into competent cells of *E. coli* according to the following protocol. We thawed on ice, an aliquot of 100 µL of thermocompetent bacteria. The DNA mixture volume must correspond to 10-100ng of DNA. We incubate the mixture on ice for 40 minutes on ice, 2 minutes of heat shock at 42 ° C and subsequently cooled rapidly on ice for at least 5 minutes. We then added 1 mL of LB medium and incubated the bacteria at 37 ° C for 1 hour in agitation. Bacteria were grown on plates with solid LB media in the presence of the appropriate antibiotic selection and incubated at 37°C over

night. During the transformation negative controls were performed. Untransformed Bacteria were grown to detect possible contamination. Control positive bacteria: in the case of transforming a plasmid of unknown origin bacteria transformed with a known stock plasmid were grown.

To verify that the clones contain the correct plasmid construct, we inoculated a mini culture with 3 mL of LB culture and let it grow at 37°C in agitation over night. Subsequently was extracted and analyzed the plasmid DNA by digestion and subsequent agarose gel electrophoresis banding pattern. We kept a stock of the correct constructs for further amplifications.

The stock of transformed bacteria was done by mixing glycerol to a final concentration of 15% with bacteria grown in LB medium, after which they were frozen at -80°C.

14. Plasmid obtention

During the course of this work, we used different plasmids, both for protein expression, as in the case of plasmids used to normalize the number of transfected cells, and plasmids carrying different promoters binding to the luciferase gene. Some of these plasmids have been synthesized in our laboratory, while others have been kindly given by groups with which we have collaborated (Table 5).

For DNA purification in a small-scale we started from a culture of 3 mL of liquid LB previously inoculated and grown over night, following the kit instructions Wizard® Plus Minipreps (Promega). These small-scale cultures were performed to confirm the transformed plasmids by digestion and subsequent electrophoresis. To obtain large amounts of plasmid DNA for its use in *in vitro* transfection experiments, we started from a culture of 250 mL of liquid LB previously inoculated and grown over night and the kit used Qiafilter Plasmid Maxi Kit (Qiagen) following the manufacturer's instructions. This purification provides performance of up to 500µg DNA. Quantification of the concentration and purity of the plasmids were measured with the Nanodrop, and further analysis on gels 1% agarose.

Plasmids and their source	
Reporter plasmids	
BIM#1	Dr. Toshiba Inaba (Research Institute for Radiation Biology and Medicine, Hiroshima University, Barcelona) (Matsui et al., 2005).
BIM#2	
BIM#3	Dr. Yoshiaki Ito (Institute of Molecular Cell Biology, Singapore) (Yano et al., 2006).
BIM#4	Dr. Jonathan Ham (Molecular Haematology and Cancer Biology, Institute of Child Health, University College London, London) (Gilley et al., 2003).
MMTV-Luc	Dr. Carme Caelles (Institute for Research in Biomedicine, Universitat de Barcelona)
p-1940Luc	Dr. Marc Pallardy (Institut National de la Santé et de la Recherche Médicale Unité 461, Université de Paris, Paris) (Asselin-Labat et al., 2005).
Expression plasmids	
CMV-βGal	Dr. Francesc Ventura (Universitat de Barcelona)
pSGF-GR wt*	In collaboration with Dr. José M. López (Institut de Neurociències, Universitat Autònoma de Barcelona, Barcelona) (Rubio-Patino et al., 2012).
pSGF-T171A*	
pSGF-S424A*	
Double mutant*	

Table 5. Plasmids used in this work and their source. *Plasmid generation is detailed in next section.

15. Reporter plasmids pSGF-T171A, pSGF-S424A, and Double mutant

The mutants pSGF-T171A (with Thr171 mutated to Ala), pSGF-S424A (with Ser424 mutated to Ala), and Double mutant (with Thr171 and Ser404 mutated to Ala) were generated by PCR using the rat GR DNA as a template and the QuikChange site-directed mutagenesis kit (Stratagene) according to the manufacturer's instructions (Table 6). All plasmids and mutagenesis products were verified by DNA sequencing.

Primer ID	Primer (5'-3')
Thr171	Froward: GCAACTGGGTGTGCTGCCCCGACAGAGAA
	Reverse: TTCTCTGTCGGGGCAGCACACCCAGTTGC
Ser424	Froward: CCAGATGTAAGCGCTCCTCCATCCAGCTC
	Reverse: GAGCTGGATGGAGGAGCGCTTACATCTGG
Sequencing	Forward: CCTACAGCTCCTGGGCAACGTGCTGGTTA
	Reverse: CGAGTCAGTGAGCGAGGAAGCGGAAGAGT
	Forward: TCTCAGCAGCAGGATCAGAA
	Reverse: GCTGGATGGAGGAGAGCTTA

Table 6. Primers used for site-directed mutagenesis of Thr171 and Ser424 of the rat GR and for DNA sequencing. The mutated nucleotide is underlined.

16. Transient transfection and reporter assays

Jurkat GR wt were transiently transfected using Neon transfection system (Invitrogen). 1 x 10^6 Jurkat GR wt cells were resuspended in 100 µL of Neon Resuspension Buffer R. For each electroporation, cells and 10 µg of plasmid DNA were aliquoted into a sterile microcentrifuge tube. A Neon Tip was inserted into the Neon Pipette and the cell-DNA mixture was aspirated into the tip avoiding air bubbles. The Neon Pipette was then inserted into the Neon Tube containing 3 mL of Neon Electrolytic Buffer E in the Neon Pipette Station. Cells were pulsed 3 times with a voltage of 1,350 V and a width of 10 ms. After the pulse, cells were quickly transferred into a culture plate containing complete medium. After 24 hours, cells were split before reaching confluence and pre-incubated or not for 1 hour with SB216763 and treated with dexamethasone for 4 hours. HeLa cells were transiently transfected with 2 µg of plasmid DNA using Lipofectamine 2000 (Invitrogen). Luciferase activity was quantified using the Luciferase Assay System (Promega). Luciferase values were normalized by protein quantification for Jurkat GR wt and Jurkat parental cells and using Luminescent β-Galactosidase Kit II for HeLa cells.

17. Chromatin immunoprecipitation (ChIP)

20 x 10^6 Jurkat GR wt cells were untreated or treated with 10 µM SB216763 and/or 10 nM dexamethasone for 2 hours. The chromatin immunoprecipitation assays were performed using the Chromatin Immunoprecipitation Assay kit (Upstate) following the manufacturer's instructions. ChIP assays were performed using an antibody against rabbit IgG (Upstate) as

a negative control. Promoter recruitment was analyzed using GR (H-300) (Santa Cruz) and RNA pol II (Upstate). ChIP experiments were performed using the EZ ChIP kit (Upstate) adapting the protocol with modifications as detailed below:

Each immunoprecipitation (IP) was made from $2x10^6$ cells. The sonication conditions were optimized in a Branson Sonifier 250 sonicator using a total volume of 1 mL at a concentration of $2x10^6$ cells per 100 μL. Sonicator conditions (samples always in ice) were: output intensity of 6, 80% duty cycle, and 10 cycles of sonication of 10 sec/cycle. Sonication gives rise to genomic DNA fragments with a length between 200 and 1000bp. We used these parameters for all experiments. Three washes were performed to chromatin bound to protein A agarose with each of the buffers indicated, instead of one as suggested by the manufacturer. The chromatin final purification was performed with Qiaquick Gel Extraction Kit (Qiagen) according to the instructions.

We used previously described *GILZ* specific primers (Chen et al., 2006), which amplify a portion containing a GRE and other containing the transcription starting site (TSS) (Table 7).

Targeting Positions	**Forward Primer (5'-3')**	**Reverse Primer (5'-3')**
TSS +48-166	AGTTGGTACAAGAAAGTGC	CTCGTATGTCACAAACTCC
GRE -1716-1895	GATACCAGTTAAGCTCCTGA	AGGTGGGAGACAATAATGAT

Table 7. ChIP Assay Primer Pairs. These primers were previously used by Chen *et al*, 2006.

DNA amplification was performed for each condition by conventional PCR using the following mixture to a final volume of 50 μL:

2 μL of template DNA
1 mM of each oligonucleotide
1.5 mM MgCl2
0.2 mM dNTPs

Polymerase Buffer
0.5 µL of 5 U/µL EcoTaq (Ecogene)

To reduce the appearance of non-specific bands we performed a hot start for 5 min at 94 ° C before adding the EcoTaq. This ensures that all DNA strands are denatured before amplification.

Thermocycler programming:
Initial dehybridization for 5 min at 94°C (hot start).
35 amplification cycles: 45 sec at 94°C, 45 seconds at 61,5ºC (annealing temperature of the ChIP oligonucleotides), and the required elongation time at 72 ° C, assuming an average elongation rate of 1 Kb EcoTaq per min.
Final elongation of 7 min at 72°C.
Maintaining the mixture at 4°C.

The PCR product was analyzed in a 1%-1,5% agarose gel. Densitometric scanning and quantification of the intensities of PCR bands were carried out using Image J 1.44o software based analysis (National Institute of Health).

18. siRNA transfection

HeLa cells were transfected with commercially available scramble siRNA, anti-GSK3α, anti-GSK3β or both siRNAs (Invitrogen) (Table 8) at a concentration of 200 nM using Lipofectamine 2000 transfection reagent (Invitrogen), following the formation of lipid-DNA complexes for 20 minutes at room temperature in OptiMEM I medium (Gibco). After 48 hours, cell populations at a density of 50-60% in 6-well plates were transfected with 1-2 µg of MMTV-Luc plasmid DNA. Complexes were added directly to growing cells in DMEM and incubated for 4-6 hours followed by washing with PBS buffer and addition of fresh DMEM. Cells were used in experiments 72 hours following siRNA transfection.

Gene/oligo ID	Sequence
GSK3A (VHS50705)	GGAGUUCAAGUUCCCUCAGAUUAAA
	UUUAAUCUGAGGGAACUUGAACUCC
GSK3B (VHS40271)	GCUCCAGAUCAUGAGAAAGCUAGAU
	AUCUAGCUUUCUCAUGAUCUGGAGC

Table 8. anti-GSK3α and anti-GSK3β siRNAs (Invitrogen) used for GSK3 silencing.

19. Cellular Fractionation

Jurkat GR wt cells (5 x 10^6) were harvested, washed once with ice-cold PBS and gently lysed for 30 seconds in 80 μL ice-cold lysis buffer (250 mM sucrose, 1 mM EDTA, 0.05% digitonin, 25 mM Tris, pH 6.8, 1 mM dithiothreitol, 1 μg/mL leupeptin, 1 μg/mL pepstatin, 1 μg/mL aprotinin, 1 mM benzamidine, and 0.1 mM phenylmethylsulfonyl fluoride). Lysates were centrifuged at 12,000 x g for 3 minutes to obtain the supernatants (cytosolic extracts free of mitochondrion) and the pellets (membrane fraction that contains nuclei and mitochondrion), as described previously (Pique et al., 2000). Supernatants (50 μg) and pellets lysates (40 μg) were separated by SDS-PAGE.

HeLa cells were trypsinized and collected. Total cell extracts were prepared by resuspending cells directly in Laemmli buffer (3% SDS, 5% 2-mercaptoethanol, 10% glycerol, 50 mM Tris) followed by vortex. For fractionation experiments, cells were resuspended in buffer A (10 mM Hepes pH 7.9, 10 mM KCl, 1.5 mM $MgCl_2$, 0.34 M sucrose, 10% glycerol, 5 mM NaF, 1 mM Na_3VO_4, 1 mM dithiothreitol (DTT), and protease cocktails) containing 0.1% Triton X-100, and incubated on ice for 5 min for permeabilization. Cells were then centrifuged at 4000 rpm for 5 min at 4 °C, and supernatants were collected for preparation of cytoplasmic proteins, while pellets were further processed for nuclear proteins. The supernatants were further centrifuged at 16,000 rpm for 15 min at 4 °C to remove cell debris and insoluble aggregates and the supernatants (cytoplasmic proteins) were collected. Supernatants (30 μg) and pellets lysates (30 μg) were separated by SDS-PAGE.

20. Confocal Laser Scanning Microscopy

Jurkat GR wt cells were collected after treatment with 10 μM SB216763 and/or 10 nM dexamethasone for 2 hours, resuspended in PBS and incubated at room temperature for 30–60 minutes over poly-L-lysine coated coverslips (0.01% solution, Sigma-Aldrich). HeLa cells were grown on sterilized glass coverslips and then treated with 100 nM dexamethasone for 3 hours. Coverslips containing attached cells were fixed with 4% paraformaldehyde, permeabilized with 0.25% Triton X-100 in PBS and incubated for 1 hour in 5% PBS-BSA to block nonspecific binding. Slides were incubated overnight at 4ºC in a humidified chamber with rabbit polyclonal anti-GR (H-300) (1/100) primary antibody (Santa Cruz). Afterwards, the slides were washed three times with PBS and further incubated with Alexa Fluor 647 anti-rabbit secondary antibody (1/500; Invitrogen) for 1 hour. Nuclei were stained with Yoyo-1 iodide (Invitrogen). To validate the specificity of the immunostaining, controls were performed by applying the same protocol but replacing primary antibody with 5% PBS-BSA. Images were then obtained with a Spectral Confocal Microscope (TCS-SL, Leica Microsystems) using a Plan-Apochromat 63×/1.4 N.A. immersion oil objective (Leica Microsystems). We used HeNe Laser at 633 nm (Lasos Inc) and pinhole of 114.54 μm for Alexa Fluor 647 GR staining and Argon Laser at 488 nm and pinhole of 114.54 μm for Yoyo-1 nuclear staining. Images were captured using the accompanying image processing software from Cytovision.

21. Statistical analysis

Results are shown as the mean ± standard error of the mean (SEM) of values obtained in three or more independent experiments. Data were analyzed using SPSS 11.0 software package. The paired Student t-test was used to compare the differences between paired samples. ANOVA-Tukey was used to compare the differences between treatments. Differences were considered significant at p values <0.05: $*p<0.05$, $**p<0.01$, and $***p<0.001$ of dexamethasone treated cells compared to untreated cells and **+** $p<0.05$ compared to treated cells, as indicated in the figure legends.

22. Main Buffers and solutions. (Summarized in Table 9.)

Buffer	Composition	Final Concentration
PBS (phosphate buffered saline)	NaCl	140 mM
(1X)	KCl	0.27 mM
pH=7.4	Na2HPO4	0.81 mM
	KH2PO4	0.18 mM
Annexin Binding Buffer (1X)	HEPES-NaOH	10 mM
pH=7.4	NaCl	140 mM
	CaCl2	2.5 mM
Sample buffer; Laemmli (1X)	Tris-HCl pH 6.8	80 mM
	SDS	2 %
	Glycerol	10 %
	DTT	0.1 M
Upper buffer for electrophoresis	Tris	0,5 M
pH=6.8	SDS	0.4 %
Lower buffer for electrophoresis	Tris	1.5 M
pH=8.8	SDS	0.4 %
Electrophoresis buffer (1X)	Tris	25 mM
pH=8.3	Glycine	192 mM
	SDS	0.1%
Transfer buffer (1X)	Tris	25 mM
pH=8.3	Glycine	192 mM
	Methanol	10% for proteins of MW >30kDa
		20% for proteins of MW <30 kDa
TBS (Tris Buffered Saline) (1X)	Tris-HCl	20 mM
pH=7.4	NaCl	137 mM
TBS-T	TBS 1x	TBS 1x
pH=7.4	Tween-20	Tween-20
Blocking solution	TBS-T	1X
	Non-fat dry milk	5%
Loading buffer (6X)	Glycerol	30%
	Bromophenol blue	0.25%
TAE (1X)	Tris	40 mM
pH=8	EDTA	1 mM
	Glacial acetic acid	20 mM

Table 9. Buffers and solutions used in this work. All buffers are prepared with milliQ H2O, unless mentioned differently.

III. Objectives

GCs are steroid hormones that regulate important biological processes, including growth, development, metabolism, survival, differentiation, proliferation, and apoptosis. GCs induce cell cycle arrest and apoptosis in different cell types and therefore are widely used to treat a variety of diseases including autoimmune disorders and cancer. The effect of GCs is mediated by the GR, a member of the steroid receptor superfamily and a ligand-activated transcription factor that translocates into the nucleus where it modulates transcription of target genes in a promoter-specific manner. Previous studies have described the role of different protein kinases in GC-mediated effects and one of them is Glycogen synthase kinase-3 (GSK3). The aim of this thesis has been to study the mechanism of regulation of GC-induced apoptosis by GSK3. The specific objectives of this thesis are:

1. Analyze the effect of GCs in Jurkat Parental, GR wt and LS7 cells.

2. Analyze the role of GSK3 on GC-mediated signaling.

3. Study of the role of GSK3 in GC-induced apoptosis in CLL cells.

IV. Results

1. Analysis of the effect of glucocorticoids in Jurkat Parental, GR wt and LS7 cells

1.1. Dexamethasone induces apoptosis in Jurkat GR wt and LS7 cells

Our group is focused on the regulation of BCL-2 family members in the apoptosis induced by several drugs, like GCs, in Chronic Lymphocytic Leukemia (CLL) cells. Several studies in different cell models have demonstrated that BIM plays and important role in GC-induced apoptosis (Kfir-Erenfeld et al., 2010). Previous results from our group showed that BIM protein and mRNA levels are induced during dexamethasone-induced apoptosis in CLL cells (Iglesias-Serret et al., 2007). Unfortunately, we have been unable to successfully transfect CLL cells and maintain cell viability after transfection. For this reason, we searched for an alternative cell type that would allow us to continue studying GC-induced apoptosis at the molecular level.

To further elucidate the mechanism of GC-induced apoptosis, we used the T-acute lymphoblastic leukemia Jurkat parental cell line, which harbor a function-impairing point mutation (R477H) in one of their GR alleles that causes GC resistance (Riml et al., 2004). These cells were either stably transfected with a rat GR expression vector under the control of the β-actin promoter, to ensure constant GR protein expression (Jurkat GR wt) or with the LS7 mutant (Jurkat LS7) (Helmberg et al., 1995). The later contains two adjacent amino acid substitutions in the Hinge Region adjacent to the DBD of the GR, replacing Proline 493 and Alanine 494 by Arginine and Serine, respectively (Fig. 20). The LS7 mutant was reported to have little or no transactivating potential, while retaining transrepression activity.

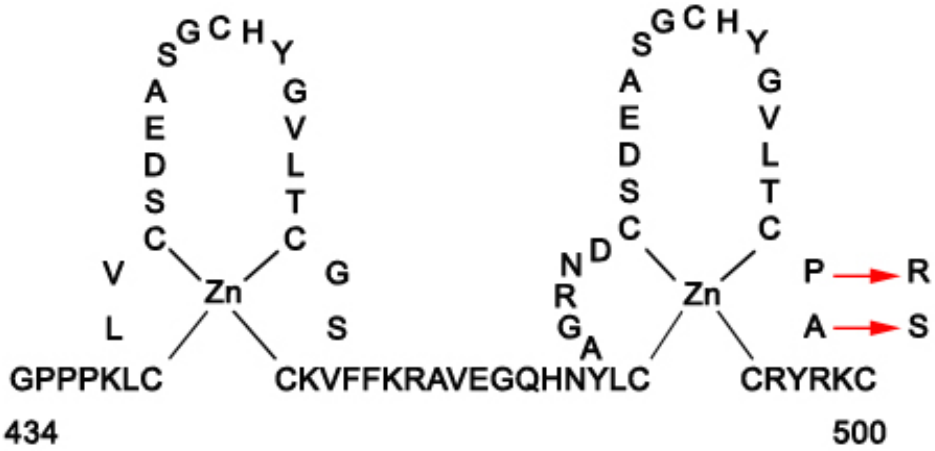

Figure 20. Primary structure of the Zn-finger region of wt and LS7 GR. Numbers represent the amino acid sequence. (Modified from Helmberg et al., 1995).

In order to analyze the effect of GCs over the cell viability of Jurkat cell lines, these were treated for 24 hours in the presence or absence of dexamethasone and then analyzed by flow cytometry. As expected, the parental Jurkat cell line was resistant to dexamethasone treatment. Exposure to dexamethasone resulted in a loss of cell viability of Jurkat GR wt (66±6%) and LS7 (44±9%) cells at 24 hours (Fig. 21), the first being more sensitive to GC-induced apoptosis, probably due to its GR ability to transactivate target genes.

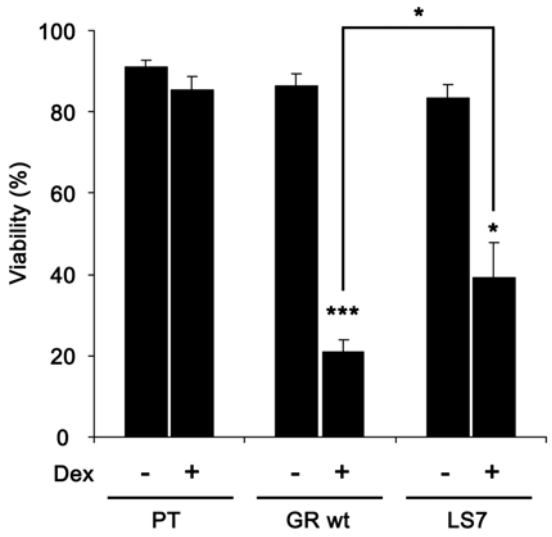

Figure 21. Effect of dexamethasone over Jurkat cell lines. Jurkat parental (PT), GR wt and LS7 cells were untreated or treated with 10 nM dexamethasone (Dex) for 24 hours. Cell viability was analyzed by phosphatidylserine exposure and PI uptake. Data corresponds to the mean ± SEM of at least three experiments. *p<0.05 ***p<0.001 versus untreated cells.

1.2. Dexamethasone's effect over gene expression in Jurkat parental, GR wt and LS7 cells

The GR is a transcription factor that remains inactive in the cytoplasm in the absence of its ligand. It becomes rapidly activated after the addition of dexamethasone, which induces the translocation of the GR to the nucleus, therefore activating GR-target gene expression. As an experimental system, these Jurkat cell lines appropriately allow the differentiation between direct and non-direct mediated effects of the GR as a transcription factor.

In order to confirm the specificity of our model, GR activity was measured by using an MMTV-Luc reporter construct in Jurkat GR wt and LS7 cell lines. Due to the fact that this reporter contains two consensus GREs (Drouin et al., 1993), the GR can directly induce MMTV-Luc reporter activity. Consistent with previous results (Helmberg et al., 1995),

Jurkat GR wt cells exhibited GC-induced transcriptional activation of the MMTV-Luc reporter construct, whereas the LS7 mutant exhibited minimal transactivating potential (Fig. 22).

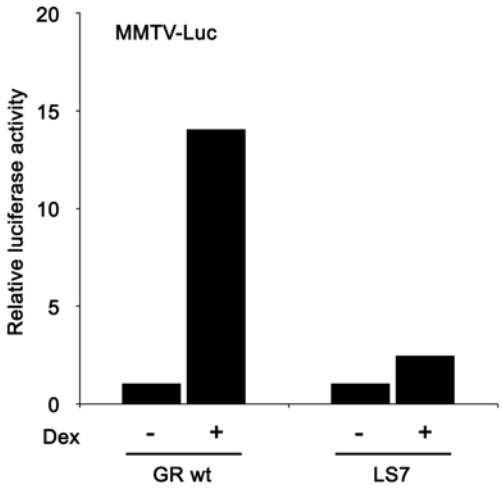

Figure 22. Transcriptional activation by GR in Jurkat GR wt and LS7 cells. Jurkat GR wt and LS7 cells were transfected with MMTV-Luc vector and untreated or treated with 10 nM dexamethasone (Dex) for 24 hours. Luciferase activity was measured and expressed relative to untreated cells basal activity.

Taking advantage of these cell specific characteristics, these cell lines were then used to analyze the effect of GC treatment over the expression of the pro-apoptotic protein BIM. As shown in Figure 23, Western Blot analysis showed that dexamethasone induced the expression of BIM-EL, BIM-L and BIM-S isoforms in a dose-dependent manner in Jurkat GR wt and LS7 cells. Jurkat LS7 cells were equally capable of inducing BIM protein levels. These results demonstrate that BIM regulation by GCs is independent of GR transactivation, as the LS7 GR mutant has no transactivation potential.

We also analyzed the effect of GCs over the expression of the anti-apoptotic BCL-2 family member protein, MCL-1. It has been described that MCL-1 is a sensor of protein synthesis inhibition and that the decrease of MCL-1 protein is necessary to induce apoptosis (Nijhawan et al., 2003). We observed that MCL-1 protein levels were downregulated in both Jurkat GR wt and LS7 cell lines in response to dexamethasone, therefore facilitating cell death (Fig. 23). As expected, the levels of BIM and MCL-1 were not affected by GC treatment in Jurkat parental cells, as they harbor a non-functional GR.

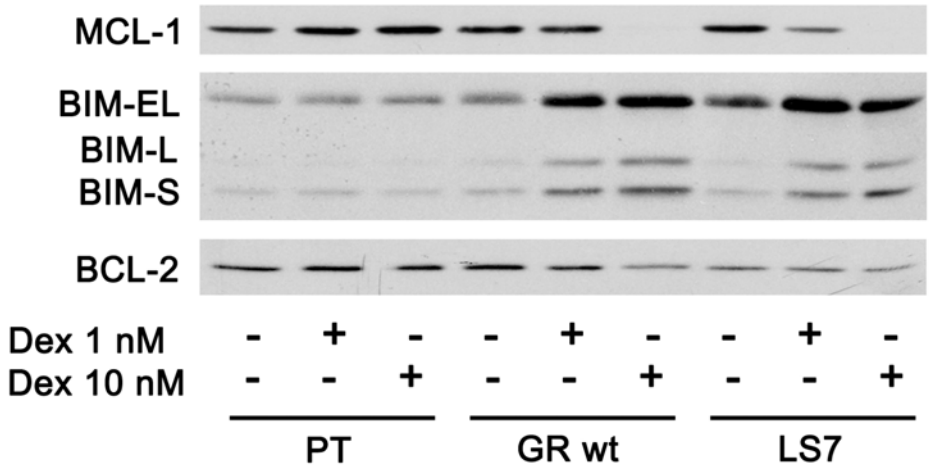

Figure 23. **BIM and MCL-1 protein levels are modulated by GCs in Jurkat GR wt and LS7 cells.** Jurkat GR wt and LS7 cells were untreated or treated with 10 nM dexamethasone (Dex) and harvested at 24 hours. MCL-1, BIM-EL, BIM-L and BIM-S protein levels were analyzed by Western Blot. BCL-2 was used to standardize protein levels. This is a representative experiment of 2 that were performed.

To further investigate BIM induction by glucocorticoids in Jurkat cell lines, we analyzed the mRNA expression of BCL-2 family members and other genes involved in the control of apoptosis by performing Reverse Trancriptase Multiplex Ligation-dependent Probe Amplification (RT-MLPA) (Fig. 24). As expected, there were no changes in response to dexamethasone treatment in the mRNA expression profile of the Jurkat parental cell line (Fig. 24A). Jurkat GR wt (Fig. 24B) and LS7 cells (Fig. 24C) showed very similar expression profiles. In both cell lines *BIM* was induced and *HIAP1*, a member of the human IAP family and a known GC induced gene (Webster et al., 2002), was also induced by dexamethasone in the two cell lines. These results suggest that *BIM* and *HIAP1* are induced in response to GC treatment through a mechanism that is independent of GR transactivation activity, as the LS7 mutant GR is unable to transactivate target genes (Fig. 22).

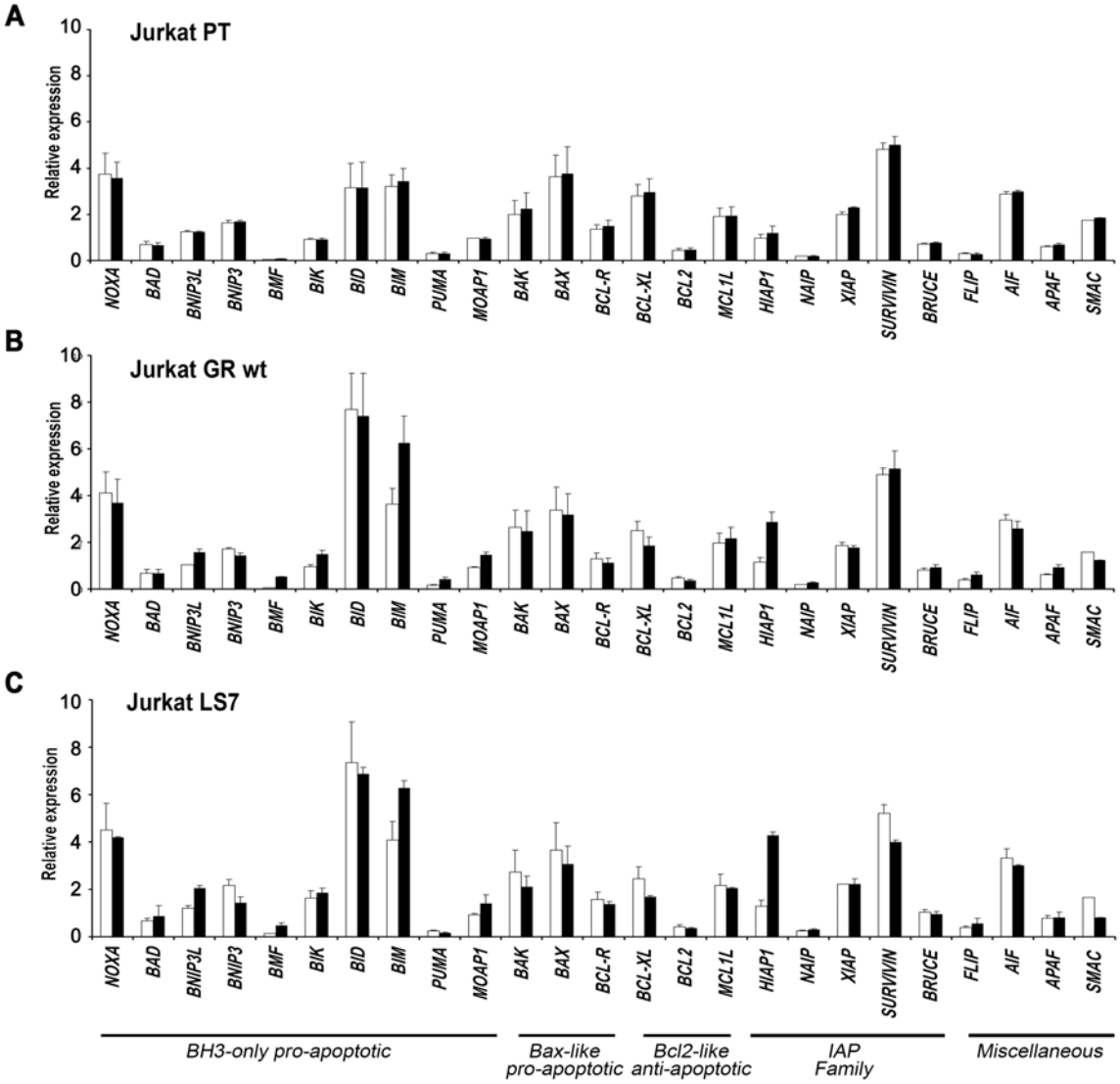

Figure 24. Dexamethasone affects gene expression profiles of Jurkat GR wt and LS7 cells. RT-MLPA gene expression profile induced by GCs. Jurkat parental (PT) **(A)**, GR wt **(B)** and LS7 cells **(C)** were untreated (white bars) or treated (black bars) with 10 nM dexamethasone (Dex) for 24 hours. Cells were lysed and the expression of apoptotic-related genes was analyzed by RT-MLPA as described in Materials and methods. The mRNA levels of all genes were normalized with respect to those of *β-glucoronidase (GUS)*. The results are shown as the mean ± SD of two representative experiments.

1.3. *BIM* and *GILZ* are GC-induced early genes

To further study dexamethasone-mediated gene induction we decided to choose genes whose induction is dependent or independent of GR transcriptional activity in Jurkat cell lines. We used *GILZ*, a well-known GC-induced gene, as a direct target of the GR and *BIM* as a gene that does not have GREs in its promoter. Jurkat GR wt cells were treated for 1 hour with dexamethasone and *BIM* and *GILZ* mRNA levels were analyzed by RT-qPCR.

As expected, *BIM* and *GILZ* mRNA levels were significantly induced in Jurkat GR wt cells (Fig. 25A and B).

We wanted to confirm that GC-induced genes *GILZ* and *BIM* were early genes in our model, as opposed to those regulated by another glucocorticoid-inducible factor that would require *de novo* protein synthesis. For this reason we used the protein synthesis inhibitor cycloheximide (CHX) in Jurkat GR wt cells (Fig. 25). The accumulation of both mRNAs was independent of protein synthesis but dependent on transcription, because pretreatment of cells with DNA transcription suppressor actinomycin D (Act D), abolished the transcriptional hormonal response.

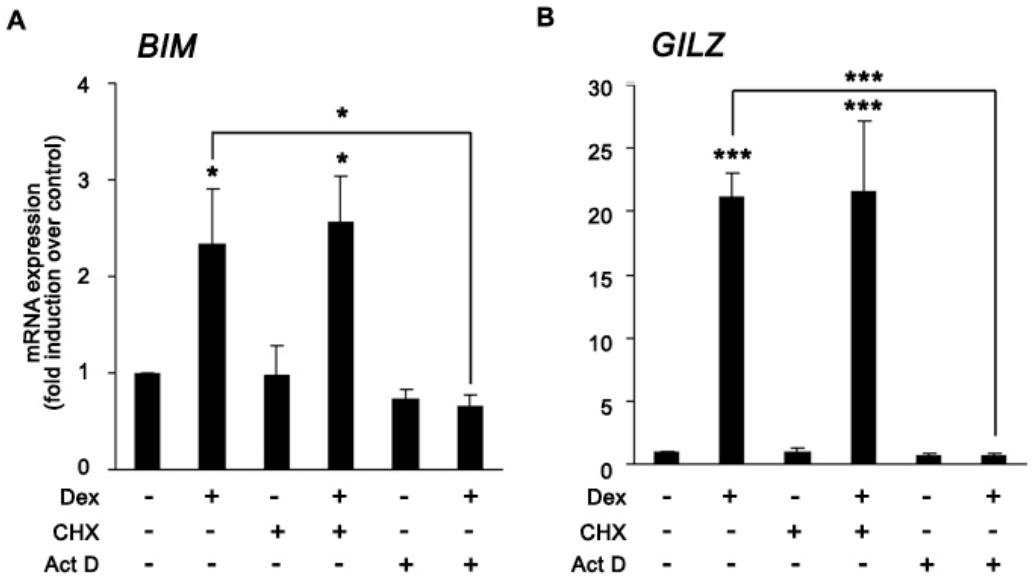

Figure 25. Transcription but not translation is required for the induction of GR targets. Jurkat GR wt cells were untreated or pretreated for 30 minutes with either 1 μg/mL cyclohexamide or 5 μg/mL actinomycin D, after which 10 nM dexamethasone (Dex) was added as indicated and incubation continued for 1 hour. **(A)** *BIM* and **(B)** *GILZ* mRNAs were measured by RT-qPCR. The mRNA levels were normalized with respect to those of *GUS*. Mean ± SEM of at least three independent experiments. *$p<0.05$, ***$p<0.001$ versus untreated cells.

1.4. Analysis of *BIM* promoter constructs transcriptional activities in response to GCs

We saw that BIM is induced at protein and mRNA levels in response to dexamethasone in Jurkat cell lines, apparently through a GR DNA-binding-independent mechanism. To examine *BIM* transcriptional induction in response to GCs, we used four different *BIM*

promoter constructs (Fig. 26). BIM#1 contains 874-bp upstream of the transcription initiation site and BIM#2 contains intron 1 inserted between the promoter/exon1 sequence and the luciferase gene (Matsui et al., 2005).

Jurkat GR wt cells were transfected with BIM #1 and #2 human promoter constructs and 24 hours later were treated with 10 nM dexamethasone for 24 hours. Basal luciferase activity was detected with both constructs, but the expected *BIM* induction in response to GC treatment was not observed (Fig. 27A). We thought this could mean that these plasmids did not have the necessary sequences for GC-dependent response of *BIM* gene. For this reason we used BIM#3 plasmid, which has 3.3 kb of the human *BIM* promoter region located upstream of the transcription start site (Fig. 26) (Yano et al., 2006). We transfected Jurkat GR wt cells with the BIM#3 plasmid from human origin and evaluated its response to dexamethasone treatment. Once again, there was no luciferase activity in response to GCs (Fig. 27B).

In previous studies, phosphorylation of FOXO1 was remarkably reduced and *BIM* increased after treatment with wortmannin in Jurkat cell lines (Qiong et al., 2010). On the other hand, induction of *BIM* appears to be a key event in cAMP-promoted apoptosis in both murine and human T-cell lymphoma and leukemia cells (Zhang and Insel, 2004) (Zambon et al., 2011). We used both stimuli to evaluate BIM#3 luciferase activity. No induction in luciferase activity was observed either (Fig. 27C).

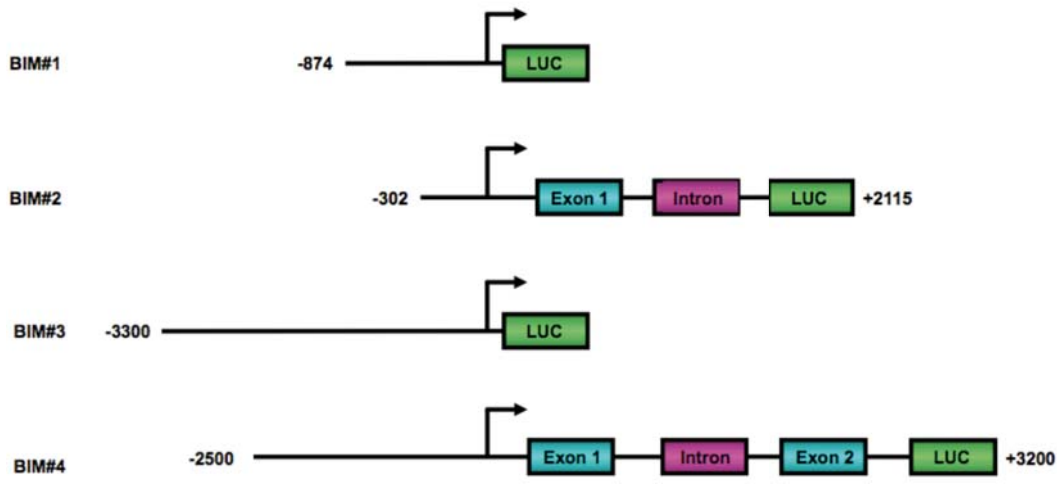

Figure 26. Luciferase *BIM* promoter constructs #1, #2, #3 and #4. These reporter constructs were used to analyze the transcriptional regulation of *BIM* by GCs.

Finally we used BIM#4, which contains a 2.5 kb region upstream of the major transcription start site, the noncoding exon 1, the 2.4 kb first intron, and the noncoding region of exon 2 of the rat *BIM* promoter (Fig. 26) (Gilley et al., 2003). This construct is a double mutant for FOXO binding sites, one at position -204 relative to the transcription start site and one at the boundary between exon 1 and the first intron. We observed no induction in response to dexamethasone treatment in Jurkat GR wt cells transfected with BIM#4 (Fig. 27D). Previous studies have described that lovastatin-induced death occurs in correlation with significantly increased levels of the BH3-only protein, BIM (Jiang et al., 2004). In this case, lovastatin was able to induce BIM#4 luciferase activity, but not that of BIM#3 in Jurkat GR wt cells (Fig. 27D).

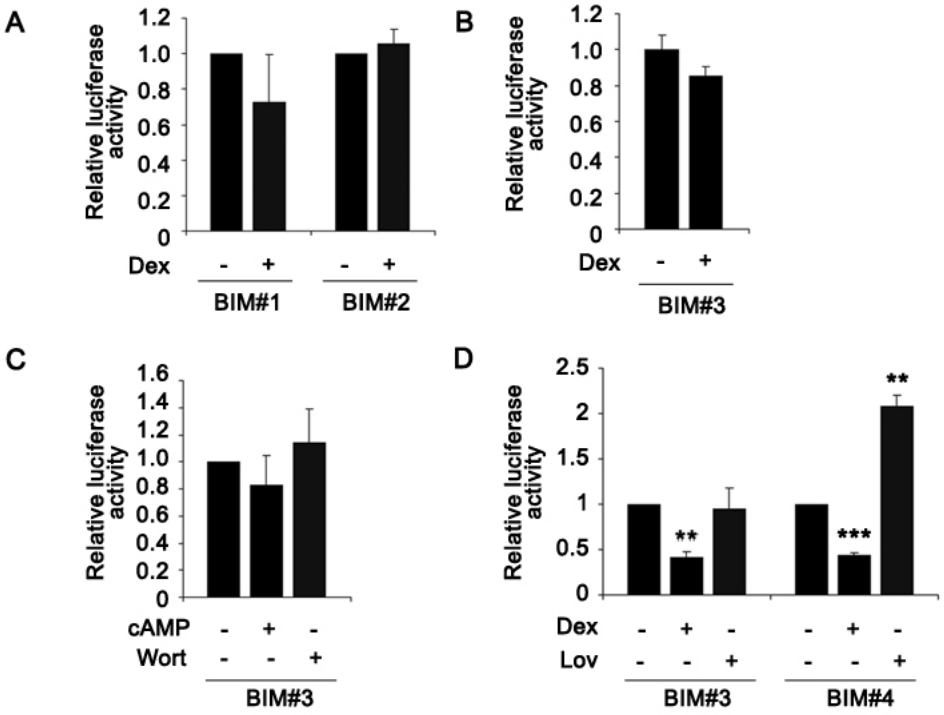

Figure 27. Luciferase *BIM* promoter constructs used to analyze transcriptional regulation by GCs. Jurkat GR wt transfected with **(A)** BIM #1, BIM#2 (n=2) **(B)** BIM#3 and treated with or without 10 nM dexamethasone (Dex) (n=2), **(C)** cAMP and wortmannin (Wort) for 24 hours (n=2). **(D)** Jurkat GR wt cells transfected with BIM#3 (n=4) and #4 (n=5) and treated with or without 10 nM dexamethasone (Dex) or lovastatin for 24 hours. Luciferase activity was measured and expressed relative to untreated cells basal activity. **p<0.01,***p<0.001 versus untreated cells.

All the promoter constructs used for the analysis of GC-dependent *BIM* induction did not respond to GCs, making them unsuitable for this study.

2. Analysis of the role of GSK3 on glucocorticoid-mediated signaling

2.1. Dexamethasone-induced apoptosis is reverted by GSK3 inhibition

The GR is known to be rapidly phosphorylated after exposure to GCs (Ismaili and Garabedian, 2004) and there is growing evidence that GCs can affect the cell's kinome (Kfir-Erenfeld et al., 2010). GCs are also known to regulate kinases such as MAPKs, CDKs and Akt (Kfir-Erenfeld et al., 2010).

In order to study the possible signaling pathways involved in GC-induced apoptosis, we examined cell viability upon treatment with dexamethasone in combination with different protein kinases inhibitors, as well as HDAC inhibitors, BCL-2 inhibitor and proteasome inhibitor (Table 10). Exposure to dexamethasone resulted in a significant loss of cell viability in Jurkat GR wt cells after 24 hours of treatment (Fig. 28). Dexamethasone decreased cell viability from 90% to 28%. These results are in agreement with previous reports that showed increased cell death upon GC stimulation in primary CLL cells (Bellosillo et al., 1997) (Iglesias-Serret et al., 2007) and other leukemic cells (Spokoini et al., 2010). Pre-incubation with the selective GSK3 inhibitor SB216763 significantly decreased this effect, in agreement with a previous observation where the pharmacological inhibition of GSK3 reduced GC-induced apoptosis in hematopoietic cell lines (Spokoini et al., 2010). Other inhibitors did not show inhibition of dexamethasone-induced apoptosis, included the less specific inhibitor of GSK3 lithium chloride (LiCl) (Fig. 28). This suggests that GSK3 plays an important role in GC-mediated apoptotic signaling pathways in leukemic cells. Additionally, both the Akt inhibitor Akti and the proteasome inhibitor MG-132 alone induced apoptotic cell death in these cells at the doses used.

We next evaluated the effect of SB216763 treatment on the expression of GC-induced proteins BIM and GILZ. The expression of these proteins was induced by dexamethasone treatment, and pre-incubation with SB216763 reduced this upregulation, as shown by Western Blot analysis (Fig. 29A-B). These data establish for the first time that GILZ, a GR direct target gene, requires GSK3 activity for its GC-dependent protein induction.

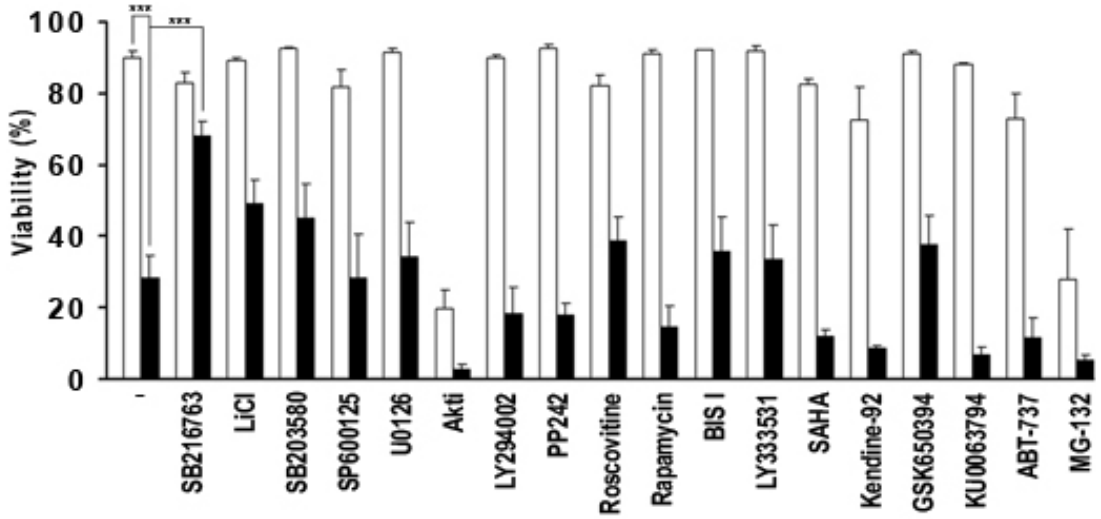

Figure 28. Effect of GSK3 inhibition on GC-induced apoptosis. Jurkat GR wt cells were untreated or pre-incubated for 30 minutes with inhibitors (opened bars) and/or treated with 10 nM dexamethasone for 24 hours (filled bars). Cell viability was analyzed by phosphatidylserine exposure. Data corresponds to the mean ± SEM of at least three representative experiments. ***p<0.001.

Inhibitor	Doses	Target
SB216763	10 μM	GSK3
LiCl	10 mM	GSK3
SB203580	10 μM	P38
SP600125	10 μM	JNK
U0126	10 μM	MEK
Akt inhibitor VIII (Akti)	10 μM	Akt
LY294002	20 μM	PI3K
PP242	50 nM	mTOR
Roscovitine	10 μM	CDKs
Rapamycin	10 nM	mTOR
BIS I	50 nM	PKC
LY333531	50 nM	PKCβ
SAHA	0.5 μM	HDACs
Kendine-92	0.5 μM	HDACs
GSK650394	1 μM	SGK1
KU0063794	5 μM	mTOR
ABT-737	5 μM	BCL-2 and BCL-XL
MG-132	1 μM	Proteasome

Table 10. Inhibitors used for cell viability analysis.

It has been previously reported that the decrease of MCL-1 protein is necessary to induce apoptosis (Nijhawan et al., 2003) and its phosphorylation by GSK3 leads to its ubiquitinylation and degradation (Maurer et al., 2006). According to this, pro-survival protein MCL-1 was downregulated after 24 hours of dexamethasone treatment and this downregulation was also blocked by GSK3 inhibition (Fig. 29A-B). To further understand the role of GSK3 over GC-induced apoptosis, we examined the activation of caspases under GSK3 inhibition. For this purpose we analyzed caspase-9 activation, determined by the appearance of the intermediate cleavage product of 37 kDa, and pro-caspase-3 disappearance as a parameter of caspase activation. Dexamethasone treatment clearly induced caspase-9 and caspase-3 activation. We observed that SB216763 treatment partially prevented caspase-3 and caspase-9 activation contributing to the blockade of dexamethasone-induced cell death (Fig. 29A).

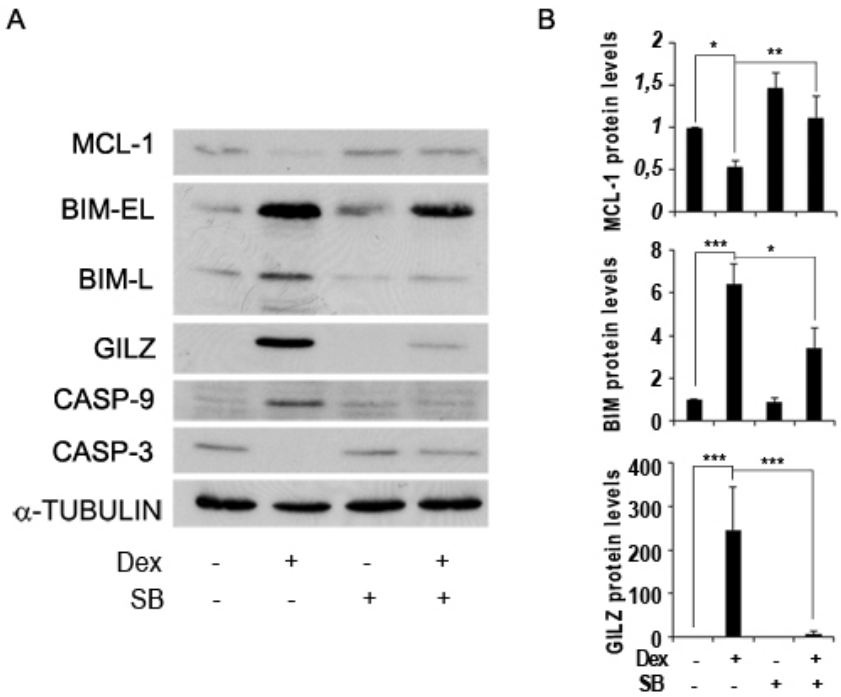

Figure 29. Effect of GSK3 inhibition on GC-regulated proteins. (A) Jurkat GR wt cells were untreated or pre-incubated for 30 minutes with 10 μM SB216763 (SB) in the absence or presence of 10 nM dexamethasone (Dex) and harvested at 24 hours. Analysis of MCL-1, BIM-EL, BIM-L, GILZ, caspase-9 and pro-caspase 3 protein levels were analyzed by Western Blot. α-TUBULIN was used as a loading control. **(B)** MCL-1, BIM-EL and GILZ were quantified by densitometric analysis and corrected by α-TUBULIN levels by using ImageJ software (NIH). Mean ± SEM of at least three independent experiments. *p<0.05, *p<0.01, ***p<0.001.

2.2. GSK3 inhibition alters GR-mediated gene expression at the transcriptional level in Jurkat GR wt cells

We previously saw that the mRNA expression of some BCL-2 family members was altered after 24 hours of treatment with dexamethasone (Fig. 24). In order to analyze early effects of GCs over transcription we examined the effect of dexamethasone treatment for 90 minutes by performing RT-MLPA in Jurkat GR wt cells. Dexamethasone significantly induced the expression of *BIM* (Fig. 30), which has been suggested to be critical for regulating the switch from survival to apoptosis (Akiyama et al., 2009). Additionally, a significant increase in mRNA levels was also observed for the anti-apoptotic gene *HIAP1*, another GC-induced gene (Webster et al., 2002) (Rogatsky et al., 2003). Other genes significantly modulated by dexamethasone treatment were the pro-apoptotic gene *BMF* and *DR6*, a member of the TNF receptor family, but their expression levels were very low comparing to those of *BIM* and *HIAP1*.

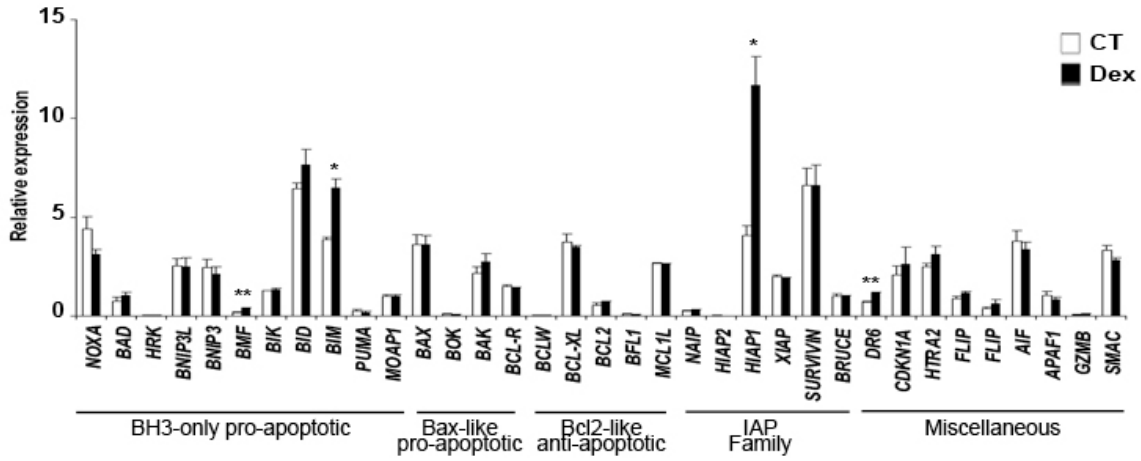

Figure 30. RT-MLPA analysis of Jurkat GR wt cells treated with dexamethasone. RT-MLPA gene expression profile induced by glucocorticoids. Jurkat GR wt cells were untreated or treated with 10 nM dexamethasone (Dex) for 90 minutes. Cells were lysed and the expression of apoptotic-related genes of the BCL-2 family, IAP family and other genes implicated in apoptosis was analyzed by RT-MLPA as described in Materials and methods. The mRNA levels of all the genes were normalized with respect to those of *GUS*. These results are shown as the mean ± SEM of at least three independent experiments. *$p<0.05$ and **$p<0.01$ versus untreated cells.

To further evaluate the role of GSK3 in early GC-induced transcriptional modulation, we examined the effect of SB216763 in the transcriptional induction of GC target genes following dexamethasone treatment by RT-qPCR. We decided to analyze *BIM* and *HIAP1*, which were both induced by dexamethasone as observed by RT-MLPA. We also analyzed

GILZ, as it is a direct target of the GR. RT-qPCR showed that dexamethasone treatment significantly induced *BIM, GILZ* and *HIAP1* mRNA levels in Jurkat GR wt. Pretreatment with SB216763 significantly reduced their induction in response to dexamethasone (Fig. 31). These results for *BIM* and *HIAP1* were confirmed by RT-MLPA analysis (Fig. 32).

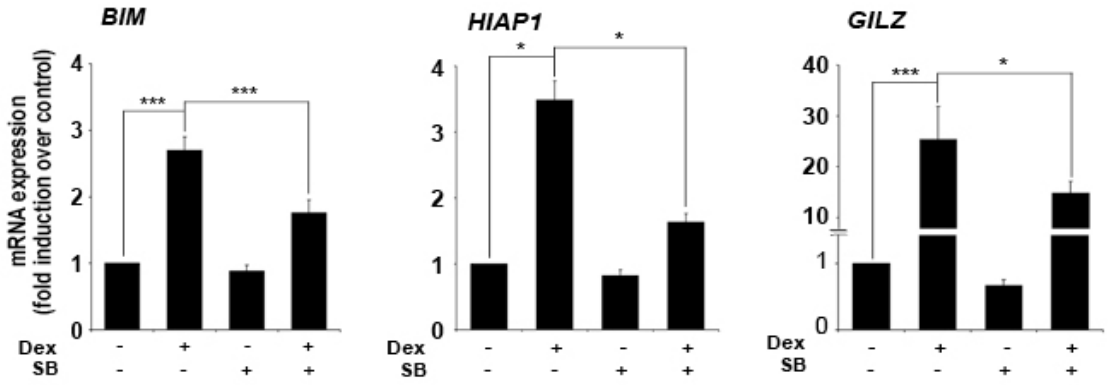

Figure 31. Effect of GSK3 inhibition over GC-induced gene expression. Jurkat GR wt cells were untreated or pre-incubated with 10 μM SB216763 (SB) in the absence or presence of 10 nM dexamethasone (Dex) and harvested at 90 minutes. *BIM*, *HIAP1* and *GILZ* mRNAs were measured by RT-qPCR. The mRNA levels of all genes were normalized with respect to those of *GUS*. These results are shown as the mean ± SEM of at least three independent experiments. *p<0.05, ***p<0.001.

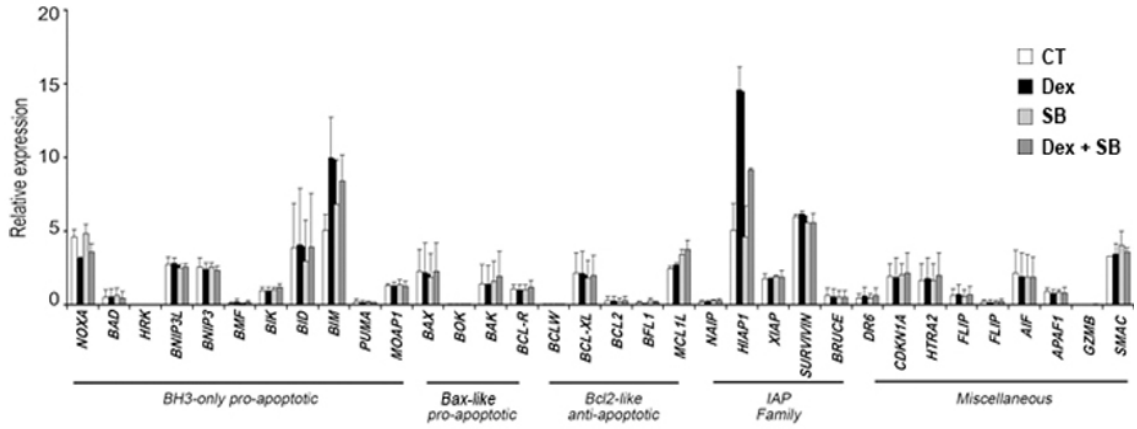

Figure 32. Analysis of the effect of GSK3 inhibition over GC-induced gene expression by RT-MLPA. Jurkat GR wt cells were untreated or pre-incubated with 10 μM SB216763 (SB) in the absence or presence of 10 nM dexamethasone (Dex) and harvested at 90 minutes. The expression of apoptotic-related genes of the BCL-2 family, IAP family and other genes implicated in apoptosis process was analyzed by RT-MLPA as described in Materials and methods. The mRNA levels of all the genes were normalized with respect to those of *GUS*. The results are shown as the mean ± SD of two independent experiments.

To confirm the role of GSK3 in GC-induced gene expression we analyzed *GILZ* mRNA levels in cell lines from different origin. *GILZ* mRNA expression was significantly induced

in response to dexamethasone in MC3T3 mouse pre-osteoblast, MCF-7 human breast adenocarcinoma and BxPC-3 human pancreatic cell lines (Fig. 33). SB216763 significantly reverted GC-dependent *GILZ* mRNA induction in the three cell lines. These results show that the role of GSK3 in the GC-dependent transcriptional induction of *GILZ* is species and cell-type independent.

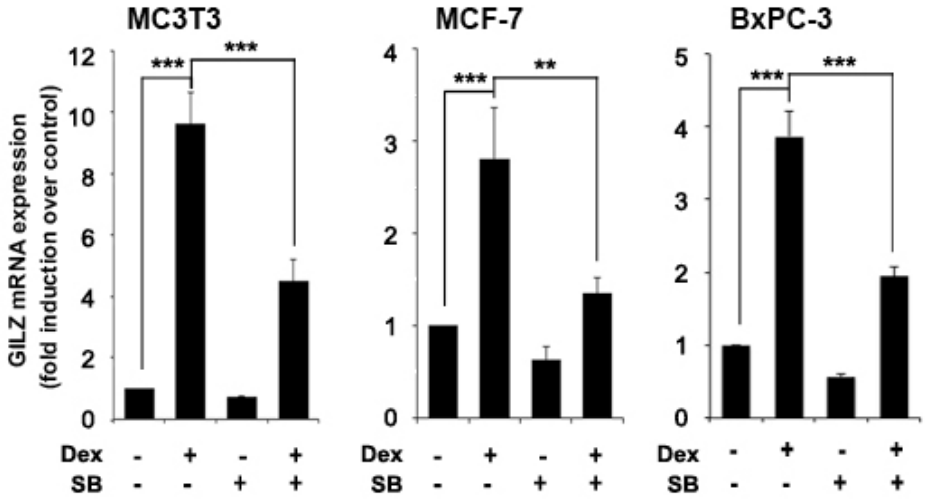

Figure 33. GSK3 is important for GC-dependent transcriptional induction of *GILZ*. MC3T3, MCF-7 and BxPC-3 cells were untreated or pre-incubated with 10 μM SB216763 (SB) in the absence or presence of 10 nM, 8nM and 4 μM dexamethasone (Dex), respectively, and harvested at 90 minutes. *GILZ* mRNA levels were measured by RT-qPCR. mRNA levels were normalized with respect to those of *GUS* in human cell lines or *GAPDH* in MC3T3. Mean ± SEM of at least three independent experiments. **p<0.01, ***p<0.001.

2.2.1 GSK3 inhibition does not affect GC-mediated transrepression in Jurkat GR wt cells

The GR is not only known for its ability to directly induce gene expression, but also for its transrepression capacity. For this reason we wanted to determine if GSK3 inhibition had any effect over the transrepression capacity of the GR. We analyzed the mRNA expression levels of *BCL-3* and *MYC*, two genes that are repressed in the presence of GCs (Zhou et al., 2000) (Reddy et al., 2009). RT-qPCR showed that dexamethasone treatment significantly repressed *BCL-3* and *MYC* mRNA levels and pretreatment with SB216763 had no effect over GC-dependent repression of these genes (Fig. 34). These results confirm that the transactivation and transrepression activities of the GR are regulated by independent mechanisms.

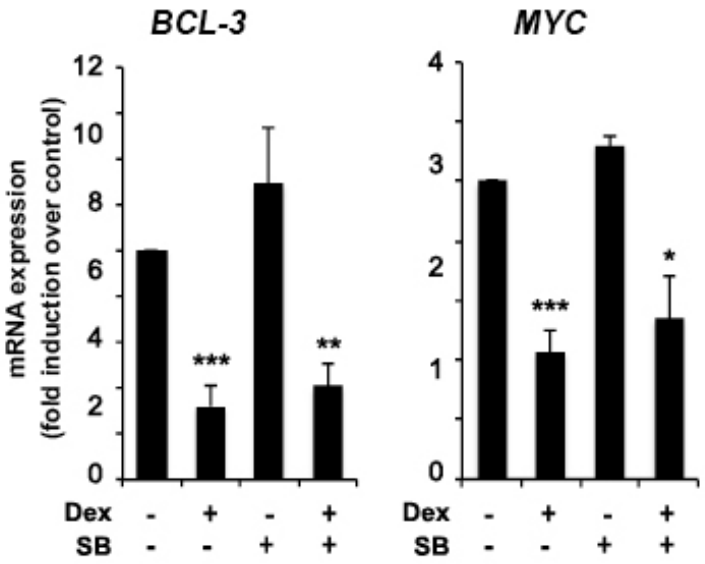

Figure 34. Effect of GSK3 inhibition over GR mediated transrepression. Jurkat GR wt cells were untreated or pre-incubated with 10 μM SB216763 (SB) in the absence or presence of 10 nM dexamethasone (Dex) and harvested at 90 minutes. *BCL3* and *MYC* mRNAs were measured by RT-qPCR. The mRNA levels of all genes were normalized with respect to those of *GUS*. These results are shown as the mean ± SEM of at least three independent experiments. *p<0.05, **p<0.01, ***p<0.001 versus untreated cells.

2.2.2. Akt and HDACs participate in *BIM* and *GILZ* transcriptional regulation in Jurkat GR wt cells

Besides GSK3 inhibitor, we also analyzed the effect of Akt and HDAC inhibitors on GC-dependent gene induction of *BIM* and *GILZ* in Jurkat GR wt cells. It was previously suggested that the PI3K/Akt pathway plays a role in controlling *GILZ* regulation (Grugan et al., 2008). Additionally, previous studies have demonstrated in CLL cells that HDAC inhibitors regulate *BIM* at the transcriptional level (Inoue et al., 2007) (Perez-Perarnau et al., 2011). Akt inhibitor Akti did not affect *BIM* gene expression either alone or in combination with dexamethasone in Jurkat GR wt cells (Fig. 35A). In the case of *GILZ*, Akti *per se* was capable of inducing its transcriptional induction (Fig. 35B) (Grugan et al., 2008). Moreover, *GILZ* mRNA expression was dramatically upregulated when Akti inhibitor was combined with dexamethasone (Grugan et al., 2008). As previously described in primary acute lymphoblastic leukemia cells (Bachmann et al., 2010), the HDAC inhibitor SAHA basally induced *BIM* mRNA expression, although the addition of dexamethasone did not enhance this effect (Fig. 35A). Interestingly, pre-incubation with SAHA significantly reverted GC-dependent *GILZ* mRNA induction, but did not affect its basal

levels (Fig. 35B). These results support the idea that Akt and HDACs have a role on *BIM* and *GILZ* transcriptional regulation in Jurkat GR wt cells. Nevertheless, SAHA was capable of reverting GC-dependent gene induction of *GILZ*, but not of *BIM*.

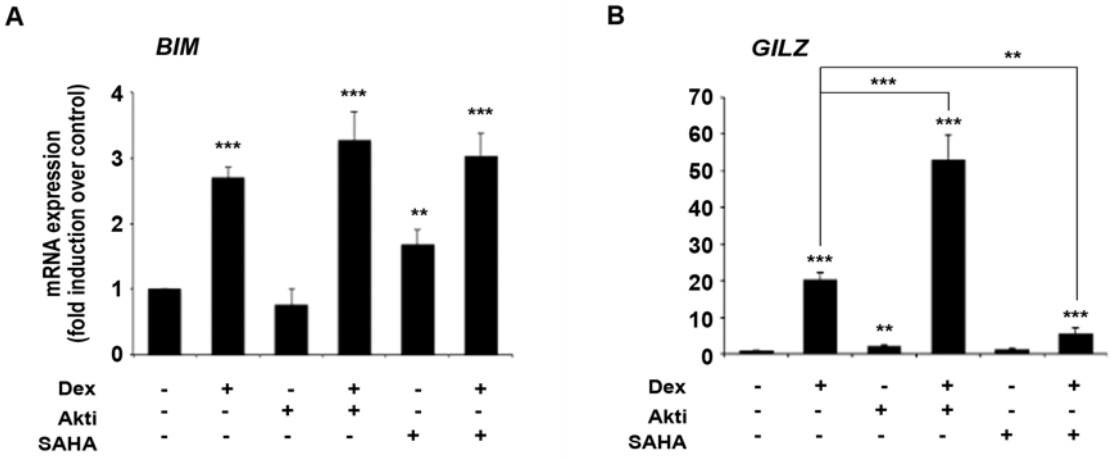

Figure 35. Effect of Akti and SAHA over GC-induced expression. Jurkat GR wt cells were untreated or pre-incubated with 10 μM Akti or 0,5 μM SAHA for 30 minutes followed by 10 nM dexamethasone (Dex) for 90 minutes. **(A)** *BIM* and **(B)** *GILZ* mRNAs were measured by RT-qPCR. The mRNA levels of all genes were normalized with respect to those of *GUS*. These results are shown as the mean ± SEM of at least three independent experiments. **p<0.01, ***p<0.001 versus untreated cells.

2.2.3. GSK3 activity is important for GR transcriptional function in Jurkat GR wt cells

To further analyze the involvement of GSK3 in GC-induced gene expression we examined the ability of the GR to regulate artificial GC-responsive gene promoter constructs in SB216763-treated Jurkat GR wt cells. As expected, cells treated with dexamethasone showed a significant increment in luciferase expression of a synthetic GRE promoter construct composed of two GREs (MMTV-Luc) (Fig. 36A) (Drouin et al., 1993). This was also the case of the p1940-Luc reporter construct that contains 1940 bp of the GILZ promoter (Fig. 36B) (Asselin-Labat et al., 2005). Pre-treatment of cells with SB216763 significantly decreased the response to GCs as compared to cells treated with dexamethasone alone (Fig. 36A-B), specially in the case of MMTV-Luc, confirming the effect of GSK3 inhibition on dexamethasonse-induced GR transcriptional activity. Pre-treatment with the less specific GSK3 inhibitor LiCl did not affect MMTV-Luc response to dexamethasone (Fig. 36A). These results indicate that GSK3 activity is an important determinant in the GR transcriptional response to GCs.

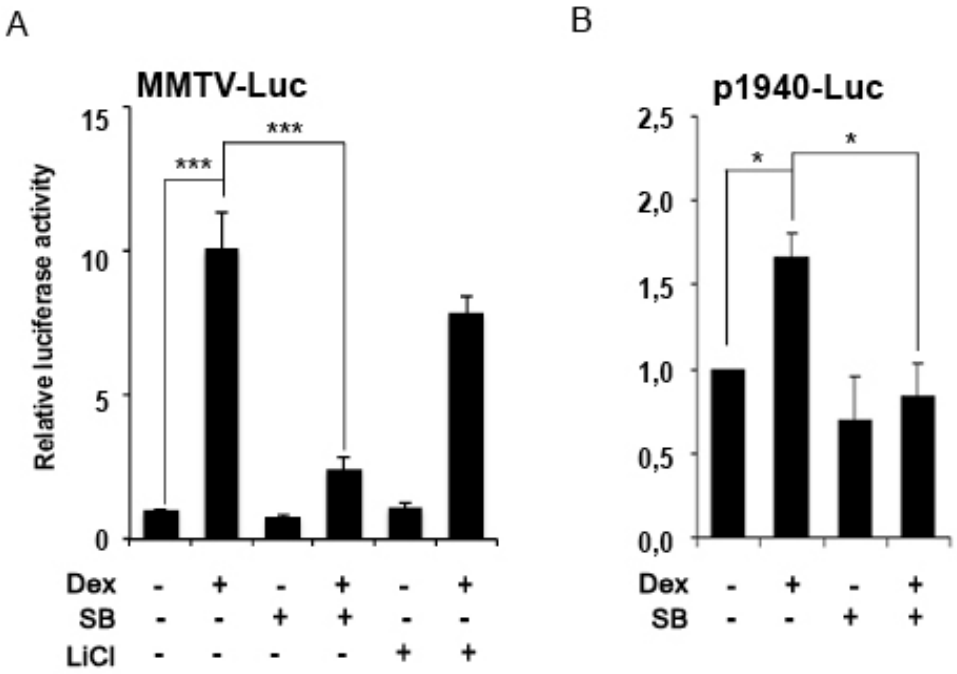

Figure 36. GSK3 is important for GR transcriptional function. Jurkat GR wt cells were transfected with MMTV-Luc **(A)** or p1940-Luc **(B)** vectors. 24 hours after transfection cells were untreated or pre-incubated with 10 μM SB216763 (SB) or 10mM LiCl for 30 minutes, followed by treatment with 10 nM dexamethasone (Dex) for another 4 hours. Luciferase activity was measured and expressed relative to untreated cells basal activity. Mean ± SEM of at least three independent experiments. *p<0.05, ***p<0.001.

2.3. GSK3 inhibition does not affect GR-mediated gene expression at the transcriptional level in Jurkat LS7 cells

To further analyze the role of GSK3 over GR-dependent gene induction we studied the effect of SB216763 in Jurkat LS7 cells, which harbor the LS7 GR mutant that exhibits minimal transactivation potential. As we previously observed, GCs induced less cell death in Jurkat LS7 cells than in Jurkat GR wt cells (Fig. 21 and 37). Pretreatment with SB216763 slightly reverted cell death in Jurkat LS7 cells but less than in Jurkat GR wt cells (Fig. 37). As expected, the mRNA levels of the GC-direct target gene *GILZ* were less induced in Jurkat LS7 cells when compared to Jurkat GR wt cells (Fig. 38A). This suggests that at least a small part of *GILZ* mRNA induction is independent of GR transcriptional activity. Besides, *BIM* and *HIAP1* mRNA levels were also induced in response to GCs in Jurkat LS7 cells (Fig. 38B-C). Both *BIM* and *HIAP1* mRNA induction was always lower in Jurkat LS7 cells when compared to Jurkat GR wt cells. These results suggest that *BIM* and *HIAP1* are regulated by mechanisms that are both dependent and independent of the GR transcriptional activity. Surprisingly, the inhibition of GSK3 had no effect over GC-

dependent induction of *GILZ*, *BIM* and *HIAP1* in Jurkat LS7 cells (Fig. 38A-B and C). This effect suggests that GSK3 inhibition is able to affect GC-mediated transcriptional regulation when it is dependent of a functional GR transactivation activity.

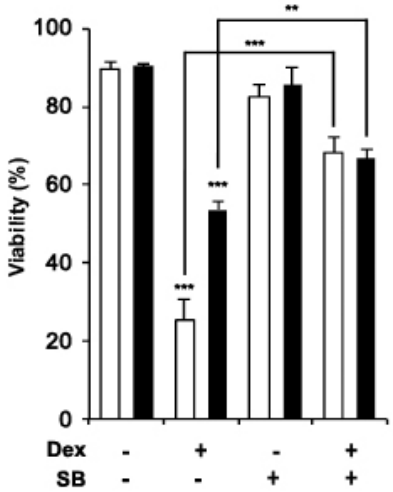

Figure 37. Effect of GSK3 inhibition over GC-induced apoptosis in Jurkat LS7 cells compared to Jurkat GR wt cells. Jurkat GR wt cells (opened bars) and LS7 cells (filled bars) were untreated or pre-incubated for 30 minutes with SB216763 (SB) 10 μM in the absence or presence of 10 nM dexamethasone (Dex) for 24 hours. Cell viability was analyzed by phosphatidylserine exposure. Data corresponds to the mean ± SEM of at least three representative experiments. **p<0.01, ***p<0.001 versus untreated cells.

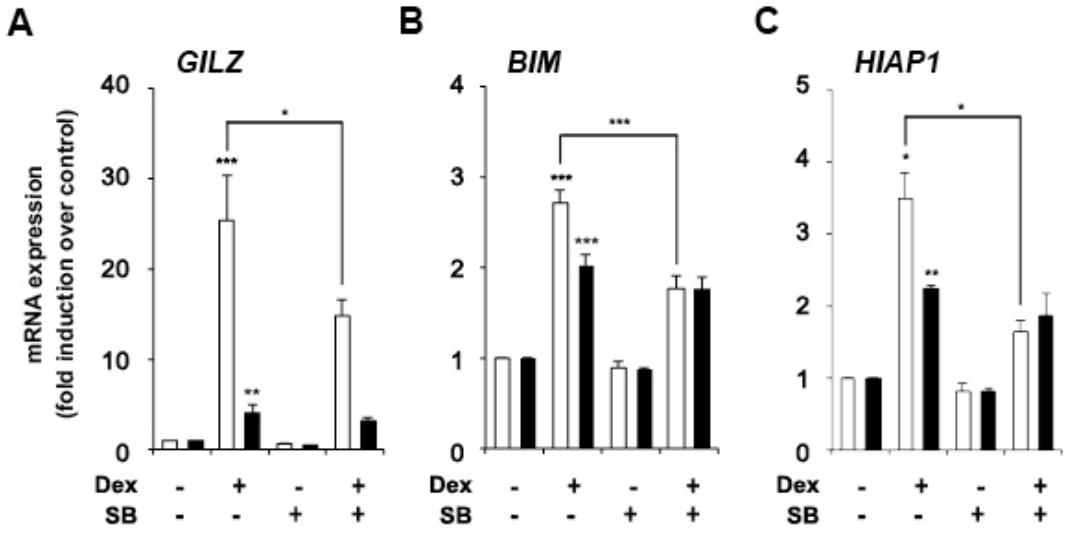

Figure 38. Effect of GSK3 inhibition over GR mediated gene expression in Jurkat LS7 cells compared to Jurkat GR wt cells. Jurkat GR wt cells (opened bars) and LS7 cells (filled bars) were untreated or pre-incubated for 30 minutes with SB216763 (SB) 10 μM in the absence or presence of 10 nM dexamethasone (Dex). After 90 minutes of dexamethasone treatment **(A)** *GILZ*, **(B)** *BIM* and **(C)** *HIAP1* mRNAs were measured by RT-qPCR. The mRNA levels of all genes were normalized with respect to those of *GUS*. These results are shown as the mean ± SEM of at least three independent experiments. *p<0.05, **p<0.01, ***p<0.001 versus untreated cells.

2.4. GSK3 inhibition affects GR and RNA polymerase II recruitment to the *GILZ* gene promoter

In order to establish the mechanism for GSK3 mediated GR transcriptional regulation, Jurkat GR wt cells were stimulated with dexamethasone for 2 hours, and *GILZ* promoter occupancy was evaluated by chromatin immunoprecipitation (ChIP) analysis. Using previously described primers (Chen et al., 2006) we observed a significant increase in the binding of the GR to the *GILZ* promoter (Fig. 39A), as well as increased binding of RNA polymerase II to the *GILZ* Transcription Starting Site (TSS) (Fig. 39B) in dexamethasone treated cells. Pre-treatment with SB216763 in combination with dexamethasone significantly reduced GR (41,27% less) and RNA polymerase II (42,44% less) binding to the *GILZ* promoter. Taken together, our results show that GC-dependent transcriptional activation by the GR requires a functional GSK3 signaling.

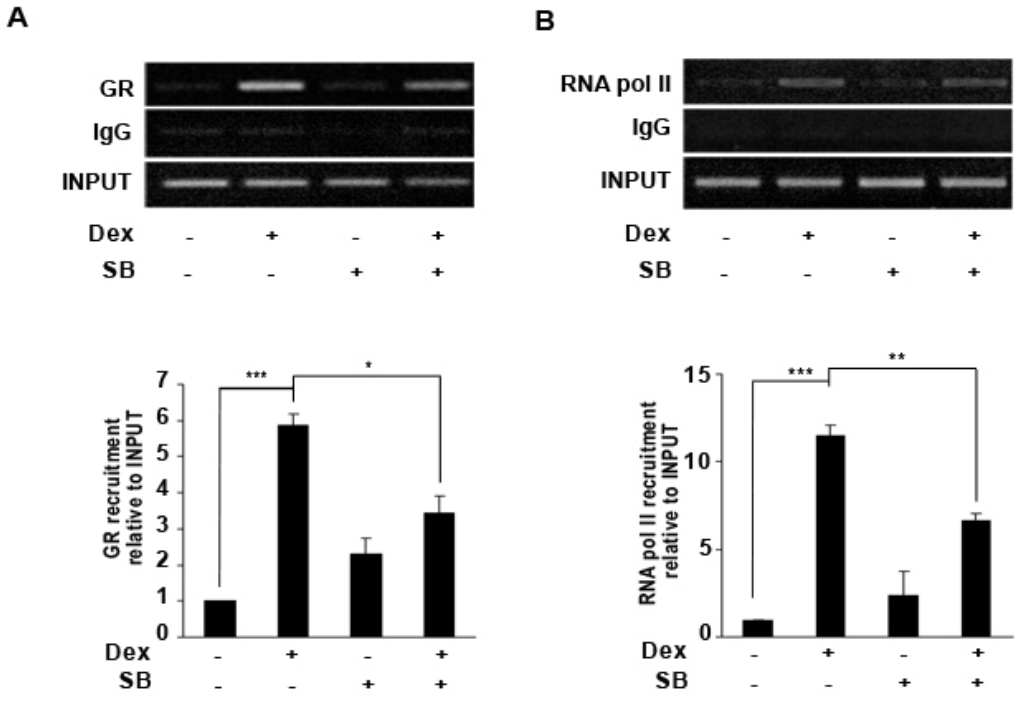

Figure 39. Recruitment of GR and RNA polymerase II to the *GILZ* promoter is affected by GSK3 inhibition. Jurkat GR wt cells were untreated or pre-incubated with 10 μM SB216763 (SB) and treated with 10 nM dexamethasone (Dex) for 2 hours. Chromatin Immunoprecipitation analysis was performed by incubating DNA-protein complexes with antibodies against **(A)** GR or **(B)** RNApol II and IgG as a negative control relative to the INPUT signal (Upper panel). Primers specific for the *GILZ* promoter used for PCR analysis were described in Materials and methods. Bars represent average values from densitometric analysis of the bands obtained in 4 separate experiments using ImageJ software (NIH) (Lower panel). Mean ± SEM of three independent experiments. *p<0.05, *p<0.01, ***p<0.001.

2.5. GSK3β gene silencing suppresses GC-stimulated gene expression in HeLa cells

GSK3 inhibitors do not distinguish between the two GSK3 isoforms. For this reason we evaluated the individual roles of GSK3α and GSK3β on GR-mediated transcriptional induction by gene silencing analysis. Due to low transfection efficiencies, we were unable to completely silence GSK3 gene expression in Jurkat cells. For this reason, we decided to perform GSK3α and GSK3β knockdown in HeLa cells. These cells have a functional GR but do not undergo apoptosis in response to GC treatment (Mann and Cidlowski, 2001). Relative mRNA levels and protein expression levels of GSK3α and GSK3β isoforms were determined after 72 hours of siRNA by performing RT-qPCR and Western Blot analysis. Transfection of HeLa cells with siRNAs for either GSK3α or GSK3β isoforms resulted in the knockdown of their respective transcripts (Fig. 40A) and proteins (Fig. 40B). Antibodies recognizing both isoforms and one of the two isoforms were used for GSK3α or GSK3β detection. As a control, mRNA and protein levels of the GSK3 isoforms were unaffected after transfection with scramble siRNA (Fig. 40A-B).

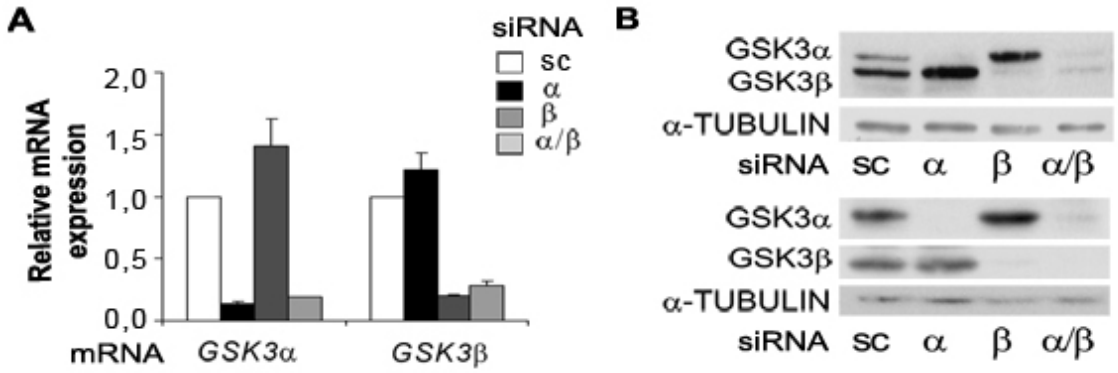

Figure 40. Genetic knockdown of GSK3α and GSK3β by siRNA. HeLa cells were transfected with GSK3 isoform-specific siRNAs. **(A)** mRNA levels were measured by RT-qPCR after the knockdown of the specific gene. The mRNA levels of both genes were normalized with respect to those of *GUS*. These results are shown as the mean ± SEM of at least three independent experiments. **(B)** Protein expression levels of GSK3α and β isoforms were analyzed by Western Blot with three different antibodies: GSK3α/β (StressGen Biotechnologies) (Fig. 40B upper panel) or GSK3α (Cell Signaling) and GSK3 β (Cell Signaling) (Fig. 40B lower panel). α-TUBULIN was used as loading control.

We first analyzed the effect of silencing GSK3α, GSK3β and GSK3α/β over *GILZ* mRNA expression levels in HeLa cells. GSK3α silencing had no effect on basal or GC-induced mRNA expression levels of endogenous *GILZ* (Fig. 41A). Interestingly, GSK3β and GSK3α/β silencing resulted in a significant decrease in basal *GILZ* mRNA levels and

reverted the transcriptional effects of dexamethasone treatment. We analyzed the effect of GSK3α/β silencing on GR-mediated transcription by using the GC-inducible promoter construct MMTV-Luc and luciferase activity was determined 4 hours after dexamethasone addition (Fig. 41B). As it was previously described, the basal transcription of the GRE reporter construct was induced by GSK3 silencing (Liang and Chuang, 2006) and the degree of basal activation of MMTV-Luc was similar between GSK3α and GSK3β silencing. Interestingly, GSK3β but not the GSK3α knockdown significantly decreased dexamethasone-stimulated MMTV-Luc promoter activity. The downregulation of both GSK3 isoforms decreased dexamethasone-stimulated MMTV-Luc luciferase activity to the same extent than GSK3β silencing alone. As expected, the scramble siRNA had no effect over the *GILZ* endogenous mRNA levels and MMTV-Luc reporter luciferase induction in response to GCs.

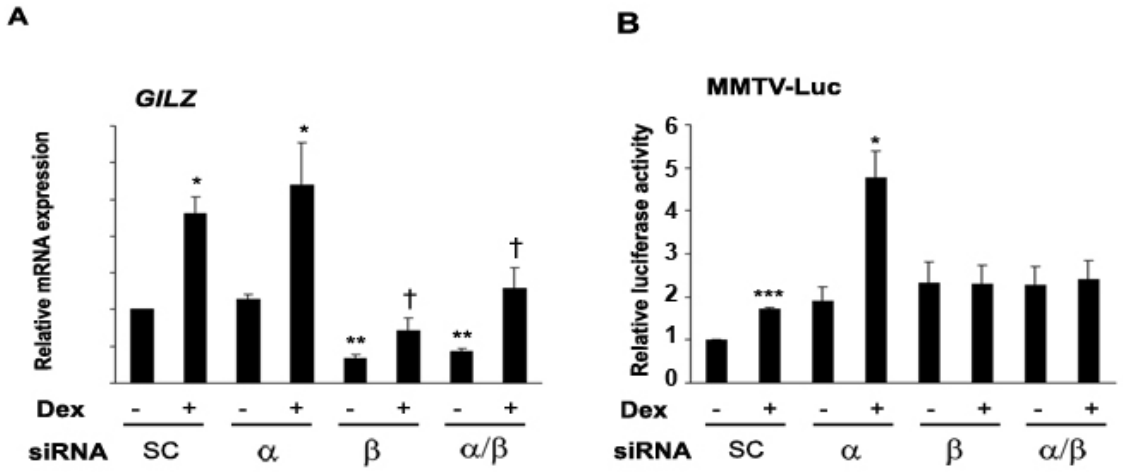

Figure 41. Genetic knockdown of GSK3β by siRNA results in disruption of GC-stimulated gene expression in HeLa cells. HeLa cells were transfected with isoform-specific siRNAs for 72 hours. **(A)** Effect of genetic disruption of GSK3α, GSK3β or both isoforms, on basal and GC-induced *GILZ* mRNA levels in HeLa cells after 4 hours of 100 nM dexamethasone (Dex) treatment. mRNA levels were normalized with respect to those of *GUS*. Mean ± SEM of 4 independent experiments. **(B)** Effect of genetic disruption of GSK3 on basal and dexamethasone induced GR activity measured by MMTV-Luc luciferase reporter assay in HeLa cells. Cells were co-transfected with MMTV-Luc and β-galactosidase (internal control) constructs after 48 hours of siRNA. 24 hours later cells were exposed to 100 nM dexamethasone for 4 hours. The normalized values are relative to the scramble siRNA untreated control. Mean ± SEM of 5 independent experiments. *p<0.05, **p<0.01, ***p<0.001 of dexamethasone treated cells compared to scramble untreated cells and **+** p<0.05 compared to scramble dexamethasone treated cells.

We further used RT-MLPA to analyze changes in response to GSK3α/β silencing in HeLa cells (Fig. 42A). *BMF*, *BCL-XL*, *MCL-1*, and *HIAP1* were significantly induced by dexamethasone (Fig. 42B). GSK3β or GSK3α/β silencing resulted in downregulation of GC-dependent *BMF*, *BCL-XL* and *MCL-1* mRNA induction. *HIAP1* was still induced by dexamethasone treatment even in the absence of GSK3α, GSK3β or both.

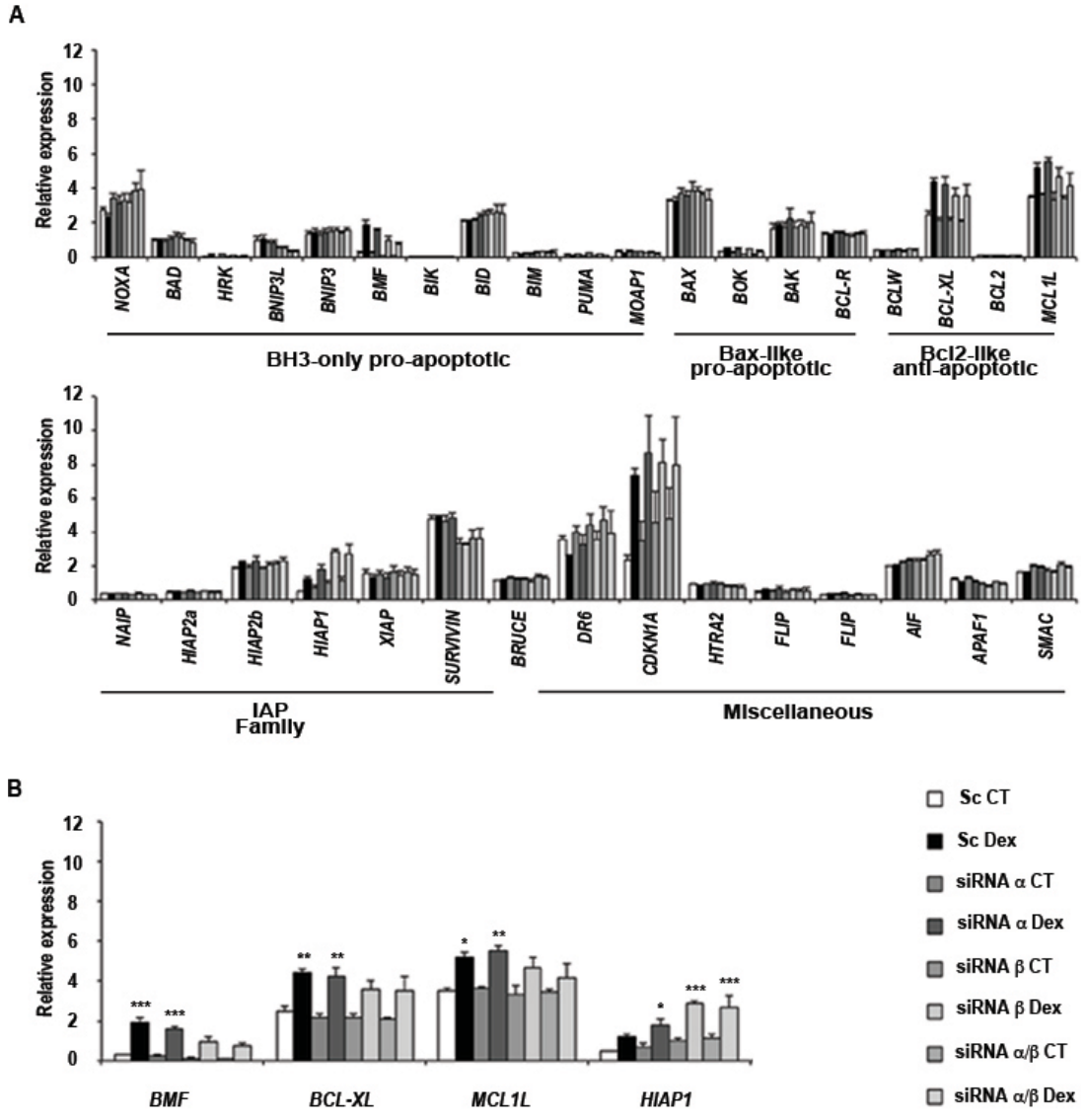

Figure 42. RT-MLPA analysis of GSK3α, GSK3β and GSK3α/β silenced HeLa cells. Cells were transfected with scramble or GSK3 isoform-specific siRNAs (α, β or α/β). 72 hours later cells were untreated (CT) or treated with 100 nM dexamethasone (Dex) for 4 hours. **(A)** Cells were lysed and the expression of apoptotic-related genes of the BCL-2 family, IAP family and other genes implicated in apoptosis process was analyzed by RT-MLPA as described in Materials and methods. The mRNA levels of all the genes were normalized with respect to those of *PARN*. **(B)** Genes significantly modulated by dexamethasone treatment are shown. The results are shown as the mean ± SEM of three independent experiments. *p<0.05, **p<0.01, ***p<0.001 compared to scramble untreated cells.

2.6. GR transcriptional function is impaired in GSK3β null MEFs

To further confirm our results obtained in GSK3 knockdown experiments in HeLa cells, we used WT, and GSK3α or β null MEFs to analyze endogenous *GILZ* mRNA induction in response to GC treatment. In accordance with our previous results in HeLa cells, we found that MEFs deficient for GSK3β expression did not induce *GILZ* mRNA levels in response to dexamethasone treatment, while wt and GSK3α null MEFs were able to significantly induce *GILZ* mRNA upon GC treatment (Fig. 43A). To further confirm our results, we transfected MEFs with the MMTV-Luc promoter construct. GSK3β null MEFs did not induce MMTV-Luc promoter activity in response to dexamethasone, while wt and GSK3α null MEFs significantly induced luciferase activity in response to GCs (Fig. 43B).

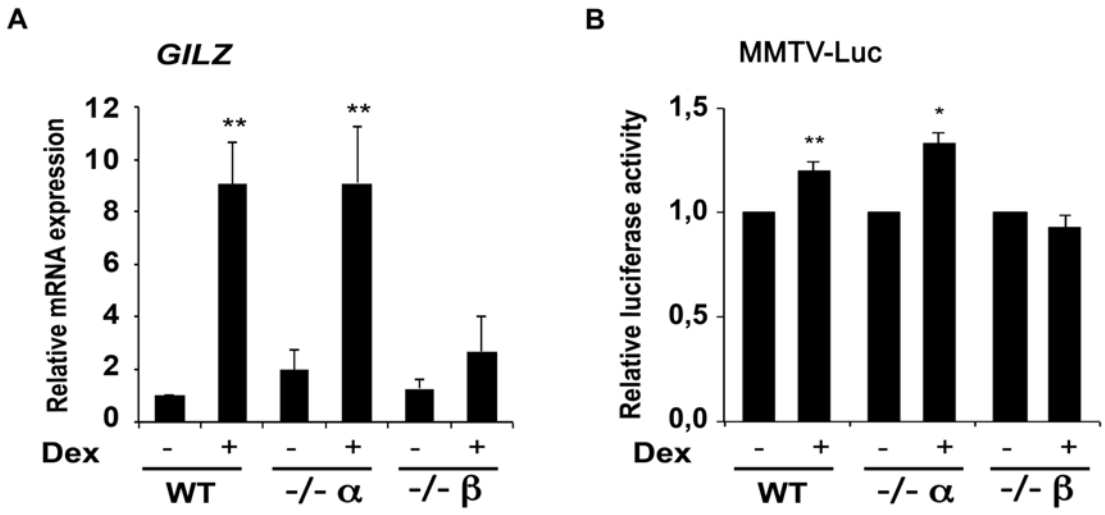

Figure 43. GR transcriptional activity is impaired in GSK3β null MEFs. (A) Wt, GSK3α and β null MEFs were untreated or treated with 100 nM dexamethasone for 4 hours. *GILZ* mRNA levels were measured by RT-qPCR and normalized with respect to *GAPDH*. Mean ± SEM of 4 independent experiments. **p<0.01 of dexamethasone treated cells compared to WT untreated cells. **(B)** MEFs were transfected with MMTV-Luc reporter and were treated with 100 nM dexamethasone (Dex) for 4 hours. Luciferase activity was measured. The normalized values are relative to the untreated control. Mean ± SEM of at least three independent experiments. *p<0.05, **p<0.01 compared to untreated cells.

On the other hand, even though there were differences in basal gene expression between MEF cell lines, RT-MLPA analysis showed no significant changes in MEF cells gene expression profile in response to GCs (Fig. 44). It is important to note that MEF cells do not undergo apoptosis under GC treatment, but instead GCs have shown to inhibit cell growth in this type of cells (Roca et al., 2003). If we had analyzed the growth control gene

expression profile we probably would have seen differences in gene expression in response to dexamethasone treatment.

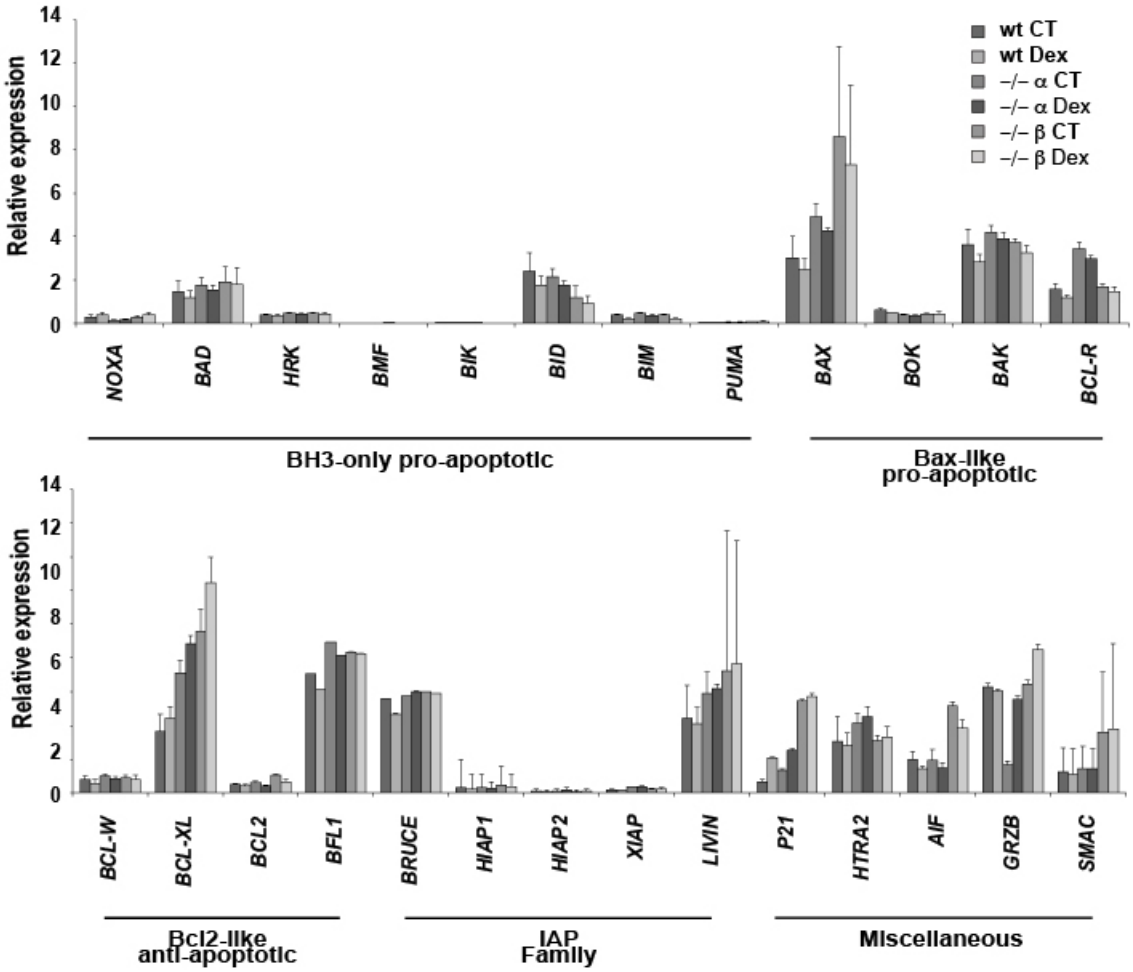

Figure 44. RT-MLPA analysis of wt, GSK3α-/- or GSK3β-/- MEFs. Cells were untreated (CT) and treated with 100 nM dexamethasone (Dex) for 4 hours. Cells were lysed and the expression of apoptotic-related genes of the BCL-2 family, IAP family and other genes implicated in apoptosis process was analyzed by RT-MLPA as described in Materials and methods. The mRNA levels of all the genes were normalized with respect to those of *TBP*. These results are shown as the mean ± SEM of three independent experiments.

Altogether, our results show that GSK3β activity, but not GSK3α, is required for GR-mediated transcriptional activity.

2.7. GSK3 inhibition affects GR cellular distribution in response to GCs

GSK3 inhibition has been previously demonstrated to affect Androgen Receptor (AR)-dependent transcriptional activity by causing a rapid nuclear export of endogenous AR

(Mazor et al., 2004) (Rinnab et al., 2008) (Schutz et al., 2010). GSK3 inhibition also affects Estrogen Receptor (ER) transcriptional activity (Medunjanin et al., 2005) (Grisouard and Mayer, 2009). To examine the role of GSK3 in the regulation of GR subcellular localization we analyzed cytosolic and membrane (which contains nuclei and mitochondrion) fractions from Jurkat GR wt cells treated with dexamethasone. In non-stimulated cells, the GR was detected mostly in the cytosol, while dexamethasone treatment induced its translocation to the nucleus (Fig. 45A). Dexamethasone-dependent GR nuclear protein localization was significantly reduced when cells were pretreated with SB216763 (Fig. 45A-B). GSK3α and GSK3β levels were mainly observed in the cytoplasm and the nucleus respectively, although under SB216763 treatment GSK3α levels where reduced in the nucleus. Additionally, there was an increase in β-CATENIN protein levels in the membrane fraction when cells were treated with SB216763, confirming GSK3 inhibition.

We wanted to determine if the partial reduction in GR nuclear translocation by SB216763 in dexamethasone treated cells was a result of a chromosome region maintenance 1 (CRM1)-dependent export, as CRM1 exportin has been suggested to play an important role in the early nuclear export of the GR (Itoh et al., 2002). For this purpose, nuclear translocation experiments were performed in the presence of leptomycin B (LMB), which blocks specifically the CRM1-dependent nuclear export (Kudo et al., 1999). A significant increase in nuclear GR localization was observed when cells were treated with LMB, suggesting that there might be a CRM1-dependent nuclear export of the GR in response to GSK3 inhibition (Fig 45A-B).

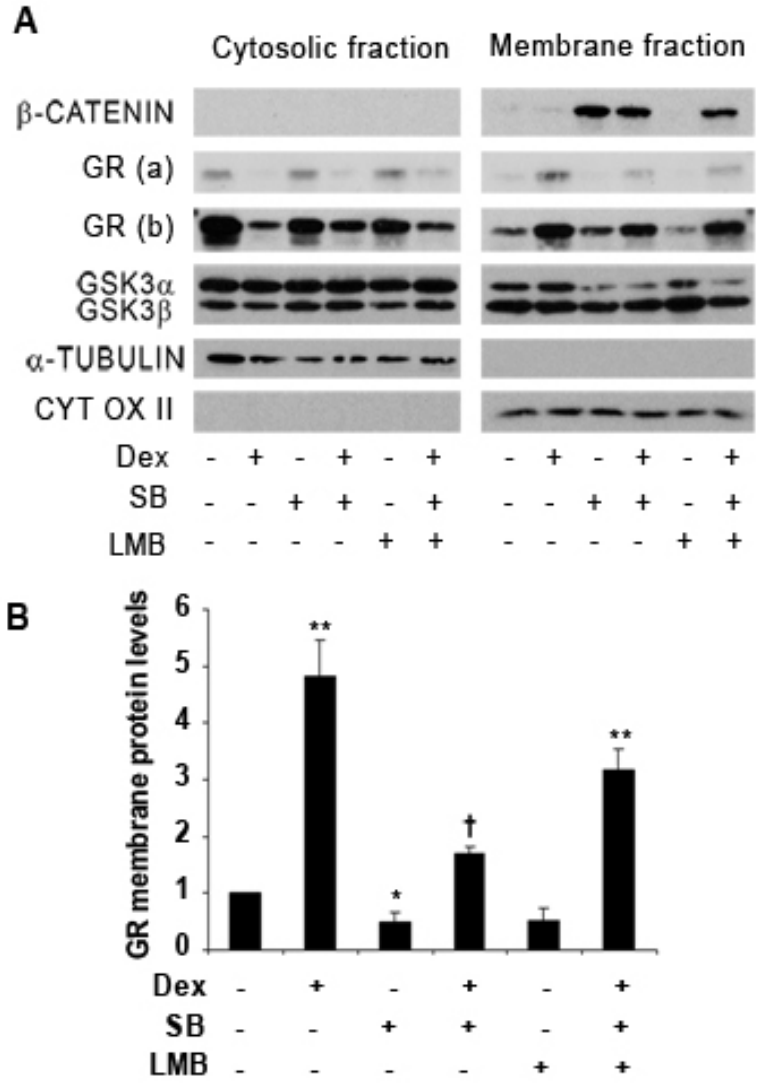

Figure 45. Subcellular localization of the GR in Jurkat GR wt cells treated with dexamethasone, SB216763 and leptomycin B. (A) Jurkat GR wt cells were treated or not with 1 nM leptomycin B (LMB). Thirty minutes later, cells were treated or not with 10 μM SB216763 (SB) prior to treatment with 10 nM dexamethasone (Dex). Three hours later, we lysed the cells to obtain cytoplasmic and membrane fractions as described in Materials and methods. GSK3α/β, GR ((a) less exposed, (b) more exposed) and β-CATENIN were detected by Western blotting. α-TUBULIN and CYTOCHROME OXIDASE II (CYT OX II) were analyzed as a control for cytosolic and membrane extracts, respectively. **(B)** Values obtained from membrane fractions were subjected to band densitometric analysis using ImageJ software (NIH). GR protein nuclear levels where quantified and normalized by the CYTOCHROME OXIDASE II protein levels. The graph shows the mean value ± SEM of 4 experiments expressed as the fold induction compared to untreated cells. *$p<0.05$, **$p<0.01$ of dexamethasone (Dex) treated cells compared to untreated cells and **+** $p<0.05$ compared to dexamethasone treated cells.

We further confirmed the subcellular localization of the GR through immunofluorescent staining visualized by confocal microscopy. In control Jurkat GR wt cells specific GR staining was mainly observed in the cytoplasm (Fig. 46) and treatment with dexamethasone for 2 hours induced GR nuclear translocation. Interestingly, cells pre-incubated with SB216763 in combination with dexamethasone presented a decrease in the GR protein levels in the nucleus compared with dexamethasone treatment alone. Moreover, SB216763 *per se* led to a slight increase in GR expression levels. Altogether, these results indicate that short-term GSK3 inhibition is able to affect GR protein localization by decreasing early GR nuclear levels in dexamethasone-treated Jurkat GR wt cells finally affecting GC-stimulated gene expression.

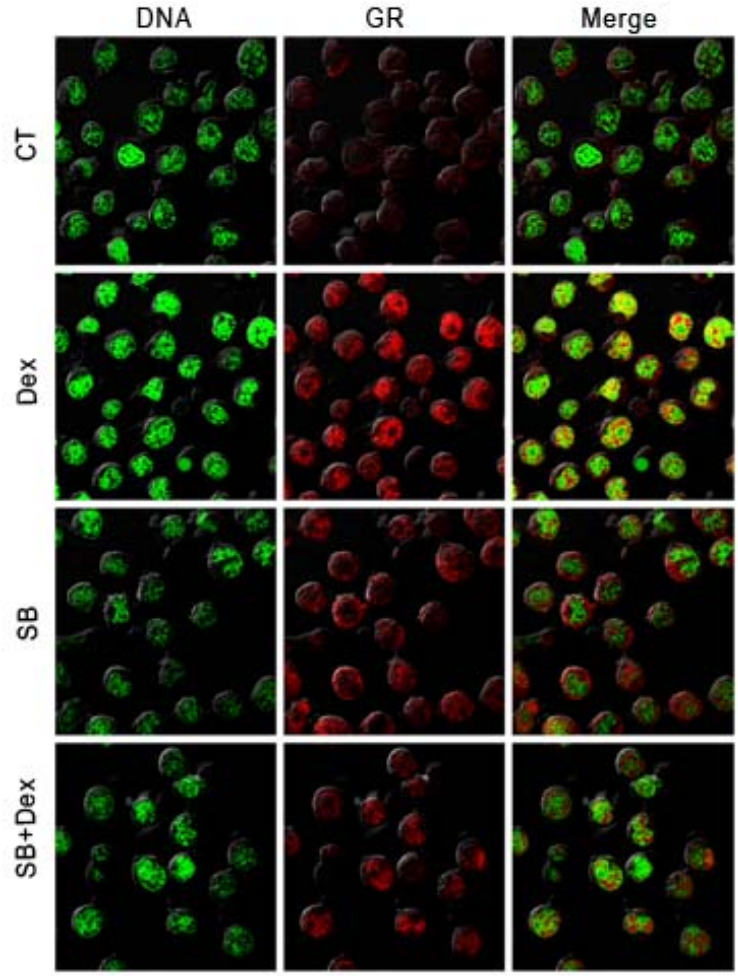

Figure 46. Immunofluorescent staining of the GR in Jurkat GR wt cells. Cells were pre-treated or not with 10 μM SB216763 (SB) prior to treatment with 10 nM dexamethasone (Dex) for 2 hours. Yoyo-1 iodide (green) stains nuclear DNA (DNA) and Alexa Fluor 647 (red) stains GR (GR). Merged images are shown for comparison. This is a representative experiment of 3 that were performed.

Next, we analyzed the effect of long-term silencing of GSK3α and GSK3β isoforms over the GR subcellular distribution induced by dexamethasone using isoform specific knockdown in HeLa cells. We determined GR subcellular distribution by analyzing cytoplasmic and nuclear fractions. Surprisingly, treatment with dexamethasone always resulted in GR translocation to the nucleus even when GSK3α, GSK3β, or GSK3α/β were silenced (Fig. 47). This was also observed through immunofluorescent staining visualized by confocal microscopy (Fig. 48). Moreover, depletion of GSK3β, or GSK3α/β proteins by siRNA led to an increase in general GR expression levels (Fig. 48).

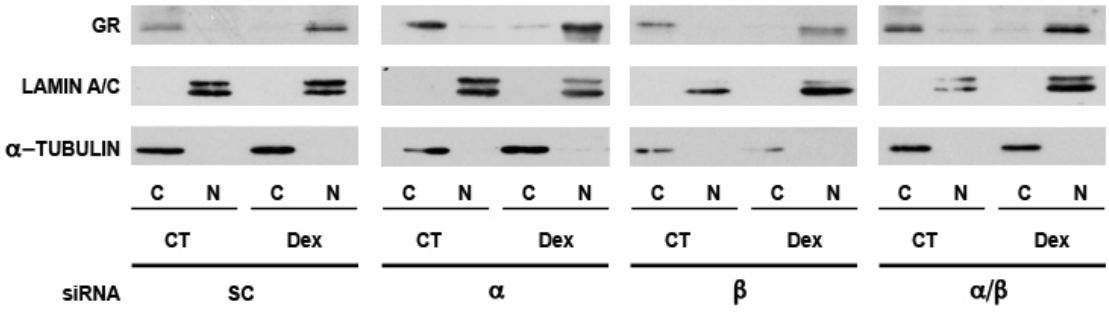

Figure 47. Subcellular localization of the GR using isoform specific knockdown in HeLa cells treated with dexamethasone. HeLa cells were transfected with GSK3 isoform-specific siRNAs. Cells were untreated (CT) or treated with 100 nM dexamethasone (Dex). Three hours later, we lysed the cells to obtain cytoplasmic and nuclear fractions as described in Materials and methods. GR was detected by Western blot. α-TUBULIN and LAMIN A/C were analyzed as a control for cytosolic (C) and nuclear (N) extracts respectively.

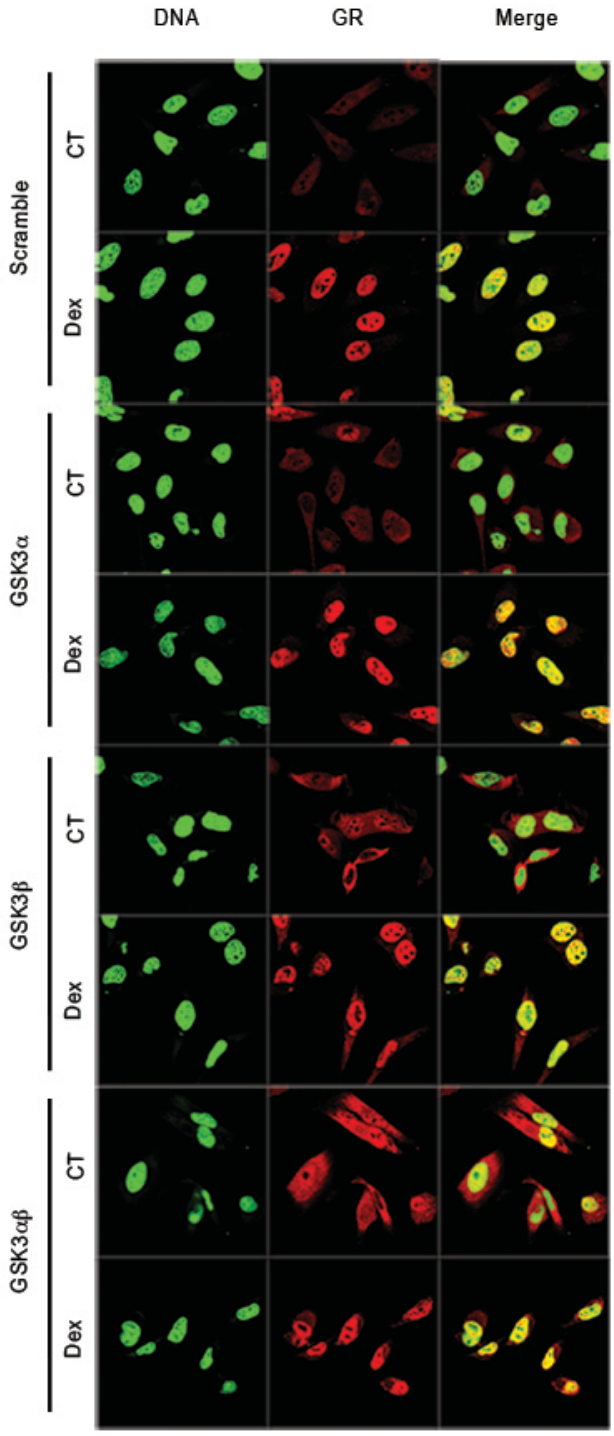

Figure 48. Immunofluorescent staining of the GR in HeLa cells. HeLa cells were transfected with GSK3 isoform-specific siRNAs for 72 hours. Cells were untreated or treated with 100 nM dexamethasone (Dex) for 3 hours. Yoyo-1 iodide (green) stains nuclear DNA (DNA) and Alexa Fluor 647 (red) stains GR (GR). Merged images are shown for comparison. This is a representative experiment of 3 that were performed.

2.8. GSK3 inhibition alters transcriptional activity of GR phosphorylation mutants

Besides phosphorylation of human GR at Ser404, GSK3β has also been described to phosphorylate rat GR at Thr171 (Rogatsky et al., 1998). As Jurkat GR wt cells harbor a rat GR, we mutated both Thr171 and Ser424 (corresponding to human Ser404 (Galliher-Beckley and Cidlowski, 2009)) residues in the rat GR in order to analyze mutant transactivation capacity under GSK3 inhibition. Both residues were replaced for Alanine making them unphosphorylatable by GSK3, which is a Serine/Threonine kinase. Figure 49 shows the two known residues phosphorylated by GSK3 and the changes made in the rat GR and the alignment with the human GR sequence. Note that Thr171 is not present in the human GR sequence.

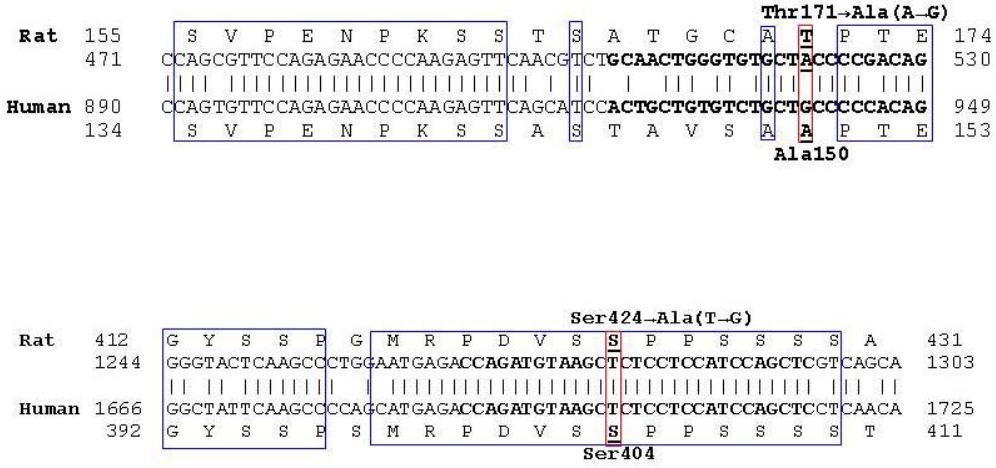

Figure 49. Phosphorylation sites of the GR by GSK3β. Schematic representation of the two known residues of rat GR that are phosphorylated by GSK3β, Thr171 and Ser424. The localization of each phosphorylation site of the rat and human receptor are shown. The framed sequences indicate the amino acids conserved between the two species. The nucleotide changes made by site directed mutagenesis to alter amino acid sequence are indicated.

GR wt and GR mutants were expressed in the Jurkat parental cell line, which harbor a function-impairing point mutation (R477H) in one of their GR alleles that causes GC resistance (Riml et al., 2004). We used the GC-inducible promoter MMTV-Luc to evaluate the effect of GSK3 inhibition over the GC-induced transactivation activity of single and double mutants. Cells were treated with dexamethasone for 4 hours in the presence or absence of SB216763. According to previous results in Jurkat GR wt cells, pre-treatment of Jurkat cells with SB216763 significantly inhibits GR wt hormone-dependent transcriptional

activity (Fig. 50A). As previously observed, the parental cell line that was not transfected with a GR was not able to induce MMTV-Luc luciferase activity in response to GCs. Interestingly, the GR mutants (T171A, S424A, and double mutant) responded to dexamethasone to the same extent as GR wt and SB216763 reverted dexamethasone-induced transactivation activity of all wt and mutant GRs (Fig.50A). These results were also observed at longer incubation times (Fig. 50B) where we observed higher luciferase inductions in response to GCs. At longer incubation times, GSK3 inhibition was equally able to inhibit GC-induced transactivation activity of GR wt and GR mutants.

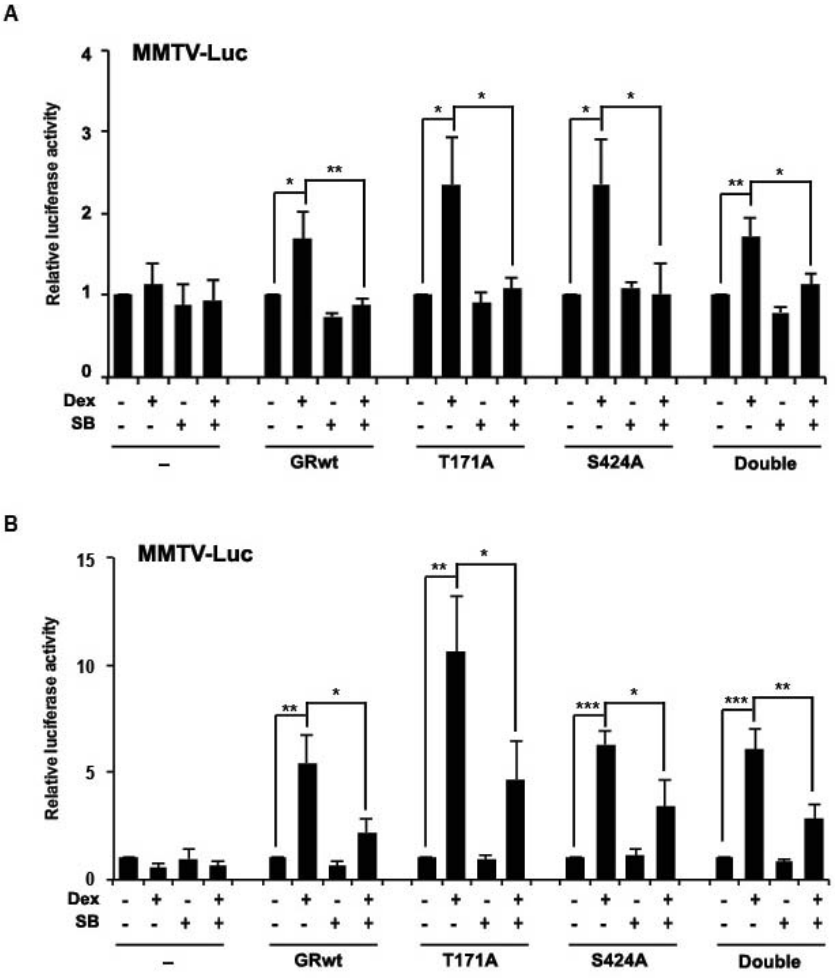

Figure 50. GSK3 inhibition affects GC-induced transcriptional activity of GR mutants. Jurkat parental cells were transfected with MMTV-Luc alone or in combination with GR wt, T171A, S424A or double mutant of the rat GR. 24 hours later cells were untreated or pre-incubated with 10 μM SB216763 (SB) for 30 minutes followed by treatment with 10 nM dexamethasone (Dex) for another **(A)** 4 hours and **(B)** 24 hours. Luciferase activity was measured and expressed relative to untreated cells basal activity. Mean ± SEM of at least three independent experiments. *p<0.05, **p<0.01, and ***p<0.001.

RT-qPCR showed that GR wt and GR mutants were equally able to induce endogenous *GILZ* mRNA levels in response to dexamethasone treatment. Pre-treatment with SB216763 significantly reduced GC-dependent *GILZ* mRNA induction by all the GR constructions (Fig. 51). Note that the parental cell line was able to slightly induced *GILZ* mRNA expression (Fig. 51), but not MMTV-Luc luciferase activity (Fig. 50) as previously described (Riml et al., 2004). *GILZ* mRNA induction in parental cell line was equally reverted by SB216763 treatment.

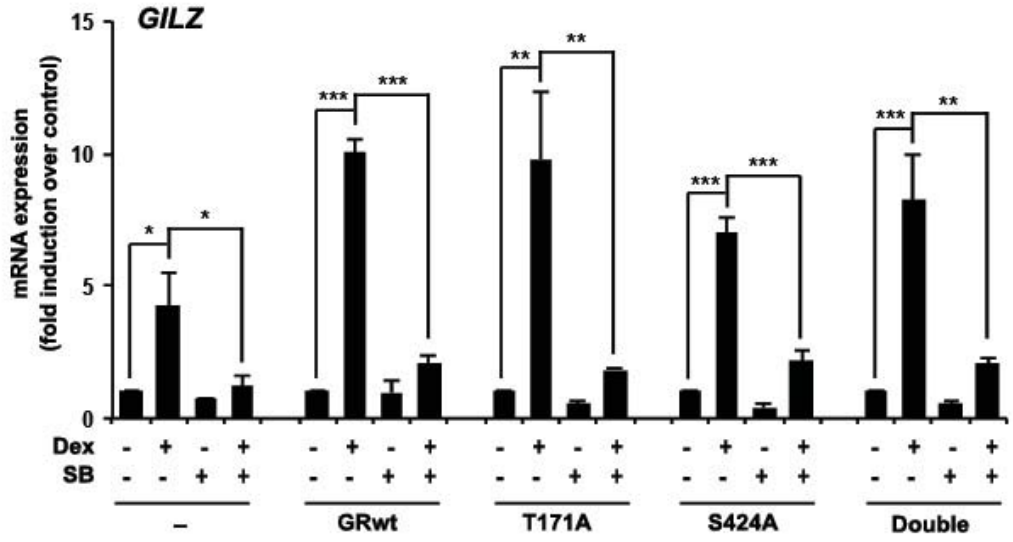

Figure 51. GSK3 inhibition affects *GILZ* mRNA induction by GR mutants. Jurkat parental cells were non-transfected or transfected with GR wt, T171A, S424A and Double mutant. 24 hours later cells were untreated or pre-incubated with 10 μM SB216763 (SB) in the absence or presence of dexamethasone (Dex) and harvested at 4 hours. *GILZ* mRNA levels were measured by RT-qPCR. mRNA levels were normalized with respect to those of *GUS*. Mean ± SEM of at least three independent experiments. *p<0.05, **p<0.01, and ***p<0.001.

Altogether, these results suggest that there is an additional mechanism, not involving phosphorylation of these residues, by which GSK3 regulates GR transcriptional activity.

3. Role of GSK3 in glucocorticoid-induced apoptosis in CLL cells

3.1. GSK3 inhibition affects GC-induced apoptosis in CLL cells

Glucocorticoids are used in the therapy of lymphoid malignancies because of their remarkable ability to induce apoptosis (Gokbuget and Hoelzer, 2006) (Pui and Evans, 2006). We wanted to study the effect of GSK3 inhibition over GC-induced apoptosis in a primary leukemia model. For this reason, we performed *ex vivo* assays in lymphocytes from patients with Chronic Lymphocytic Leukemia (CLL). Our group has been studying GC-induced apoptosis in CLL cells for a long time (Bellosillo et al., 1997) (Barragan et al., 2002) (Iglesias-Serret et al., 2007). As it was previously described by our group, dexamethasone significantly induced cell death of CLL cells (Fig. 52) (Bellosillo et al., 1997).

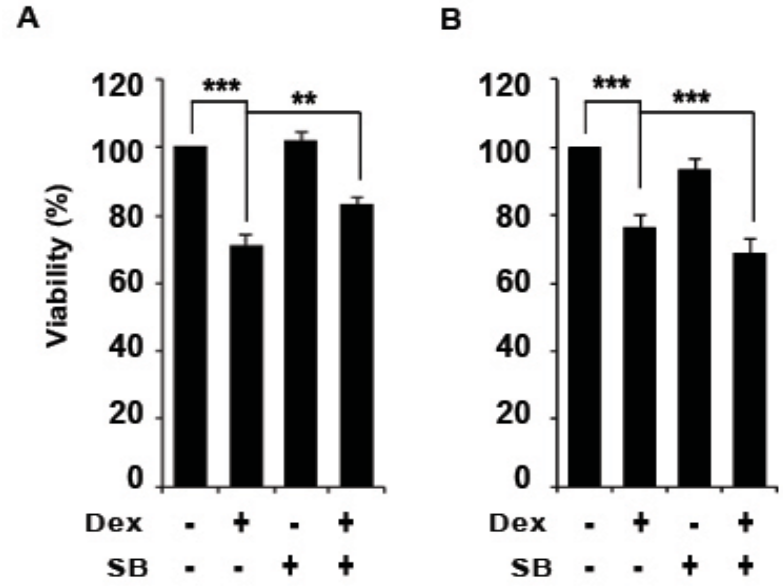

Figure 52. GSK3 inhibition affects GC-induced apoptosis in CLL cells. Cells from CLL patients (n = 29) were untreated or pre-incubated for 30 minutes with 10 μM SB216763 (SB) and treated with 10 μM dexamethasone (Dex) for 24 hours. Cell viability was analyzed by phosphatidylserine exposure. **(A)** Cell death was reverted by SB216763 in 19 of 29 samples and **(B)** in 10 out of 29 samples analyzed SB216763 did not revert GC-induced cell death. Viability is expressed as the percentage of annexin APC negative treated cells related to untreated cells. Data are shown as the mean value ± SEM. **p<0.01, ***p<0.001.

Contradictory results have been described about the use of the GSK3 inhibitor SB216763 in CLL cells. Previous studies described that treatment with SB216763 enhances survival of CLL lymphocytes *ex vivo* (Lu et al., 2004), while smaller doses leaded to apoptosis induction (Ougolkov et al., 2007). Our results showed that pre-treatment with GSK3 inhibitor SB216763 significantly decreased dexamethasone-induced apoptosis by 11,87%

in 19 of the 29 samples from patients analyzed (Fig. 52A and Table 11). On the other hand, this cell death was not reverted in 10 of the 29 samples from patients analyzed (Fig. 52B and Table 11).

Patient	CT	Dex	SB	Dex + SB
1*	55,04	28,05	57,71	48,45
2*	80,44	56,19	84,27	64,24
3*	75,91	65,55	75,51	68,22
4*	70,83	37,95	65,86	57,71
5*	38,76	18,05	44,50	31,27
6*	74,60	53,42	71,23	58,19
7*	41,82	29,37	55,43	32,63
8*	65,26	40,29	66,25	48,43
9*	62,48	46,21	69,14	48,03
10*	64,59	55,87	59,28	58,17
11*	90,83	83,94	94,73	91,31
12*	72,08	53,65	77,99	63,88
13*	78,22	50,24	77,15	60,10
14*	67,81	44,56	62,75	51,36
15*	71,21	56,20	77,81	61,02
16*	71,40	46,87	61,90	51,94
17*	71,12	58,50	65,94	64,66
18*	84,53	70,59	80,27	76,59
19*	42,05	28,85	45,43	31,03
20	66,09	46,19	60,54	36,90
21	56,68	40,55	59,14	33,53
22	40,38	35,80	35,42	28,88
23	43,09	34,50	45,76	36,02
24	52,34	27,41	43,18	28,28
25	56,82	34,65	48,07	29,02
26	63,54	53,06	60,63	46,23
27	50,26	42,38	54,58	42,68
28	78,31	68,47	65,27	66,70
29	75,68	62,73	68,96	54,04

Table 11. Viability of CLL samples. CLL cells were untreated (CT) or pre-incubated with 10 μM SB216763 (SB) and treated with 10 μM dexamethasone (Dex) for 24 hours. Viability was measured as described in Materials and methods and it is expressed as the percentage of annexin APC negative cells. * Patients where GC-induced apoptosis was reverted by GSK3 inhibition.

3.2. GSK3 inhibition affects GC-dependent gene induction in CLL cells

We next analyzed the effect of GSK3 inhibition on GC-dependent *BIM* and *GILZ* mRNA induction in CLL samples. The mRNA levels of these two genes were significantly induced in response to dexamethasone treatment and were diminished by GSK3 inhibition in six samples analyzed where SB216763 reverted cell death (Fig. 53A). In 5 samples where SB216763 did not revert cell death the mRNA levels of *BIM* and *GILZ* were also induced by dexamethasone treatment (Fig. 53B). In this case, only *GILZ* mRNA levels were reverted by GSK3 inhibition. Regarding *BIM*, pre-incubation with SB216763 combined with dexamethasone treatment significantly induced its mRNA levels when compared to dexamethasone alone.

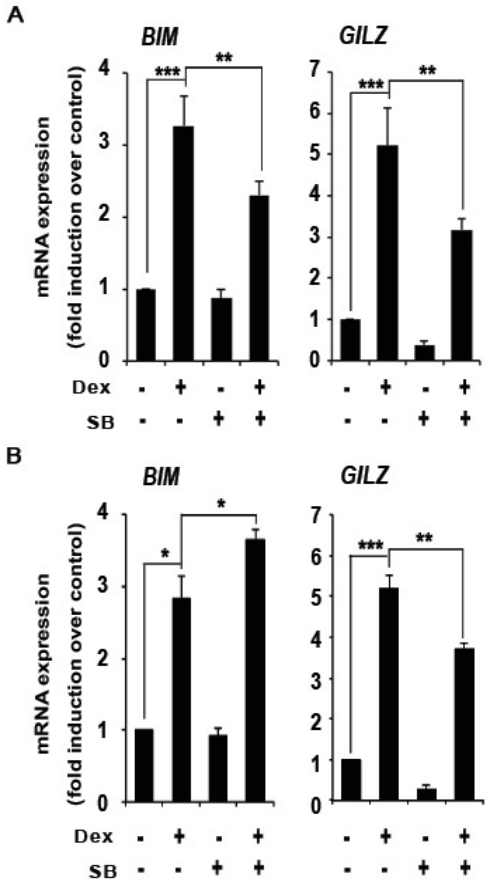

Figure 53. GSK3 inhibition affects GC-induced gene expression in CLL cells. CLL cells were untreated or pre-incubated with 10 μM SB216763 (SB) in the presence or absence of 10 nM dexamethasone (Dex) for 24 hours. *BIM* and *GILZ* mRNA levels of **(A)** 6 samples where SB216763 reverted cell death and **(B)** 5 samples where SB216763 did not revert cell death were measured by RT-qPCR. The mRNA levels of both genes were normalized with respect to those of *GUS*. Data are shown as the mean value ± SEM. *p<0.05, **p<0.01, ***p<0.001.

3.3. GSK3 inhibition affects GC-dependent protein induction in CLL cells

We analyzed GILZ and BIM protein levels in random samples, independently of their response to GSK3 inhibition, from the 29 analyzed for cell viability. Figure 54 shows 3 representative patients, in which GILZ and BIM protein levels were induced in response to GCs and reverted by GSK3 inhibition. When we performed densitometric analysis of all the patient samples analyzed there was a significant reversion in GC induced expression levels of BIM and GILZ (Fig. 55A), which could be also observed when analyzing the patients where GSK3 inhibition reverted GC-induced apoptosis (Fig. 55B). On the other hand, in the patient samples where GSK3 inhibition did not revert GC-induced apoptosis there was a significant reversion of BIM protein expression levels, but in the case of GILZ, even though there was a clear tendency to reversion, it was not significant (Fig. 55C).

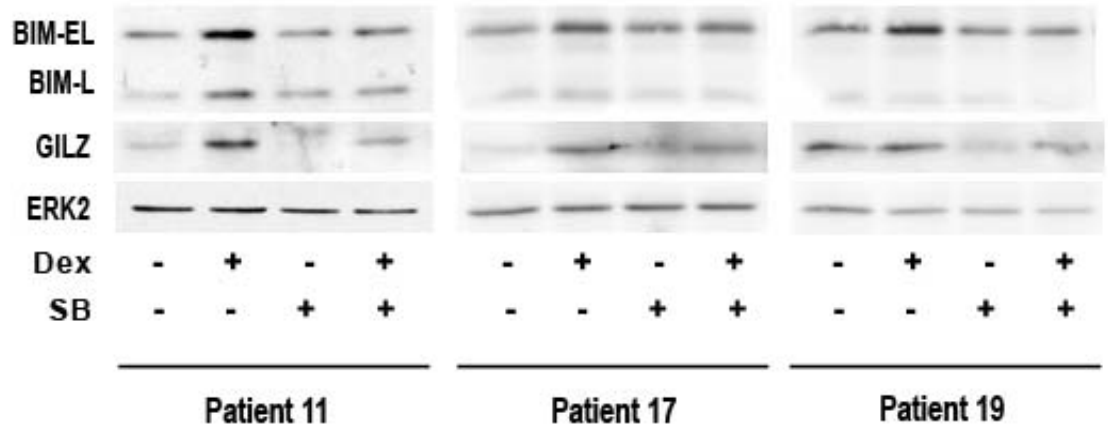

Figure 54. GSK3 inhibition reverts BIM and GILZ protein levels in CLL cells. CLL cells were untreated or pre-incubated with 10 μM SB216763 (SB) in the presence or absence of 10 nM dexamethasone (Dex) for 24 h. BIM-EL, BIM-L and GILZ protein levels were analyzed by Western Blot. These are three representative patients of the samples analyzed. ERK2 was used to normalize protein levels.

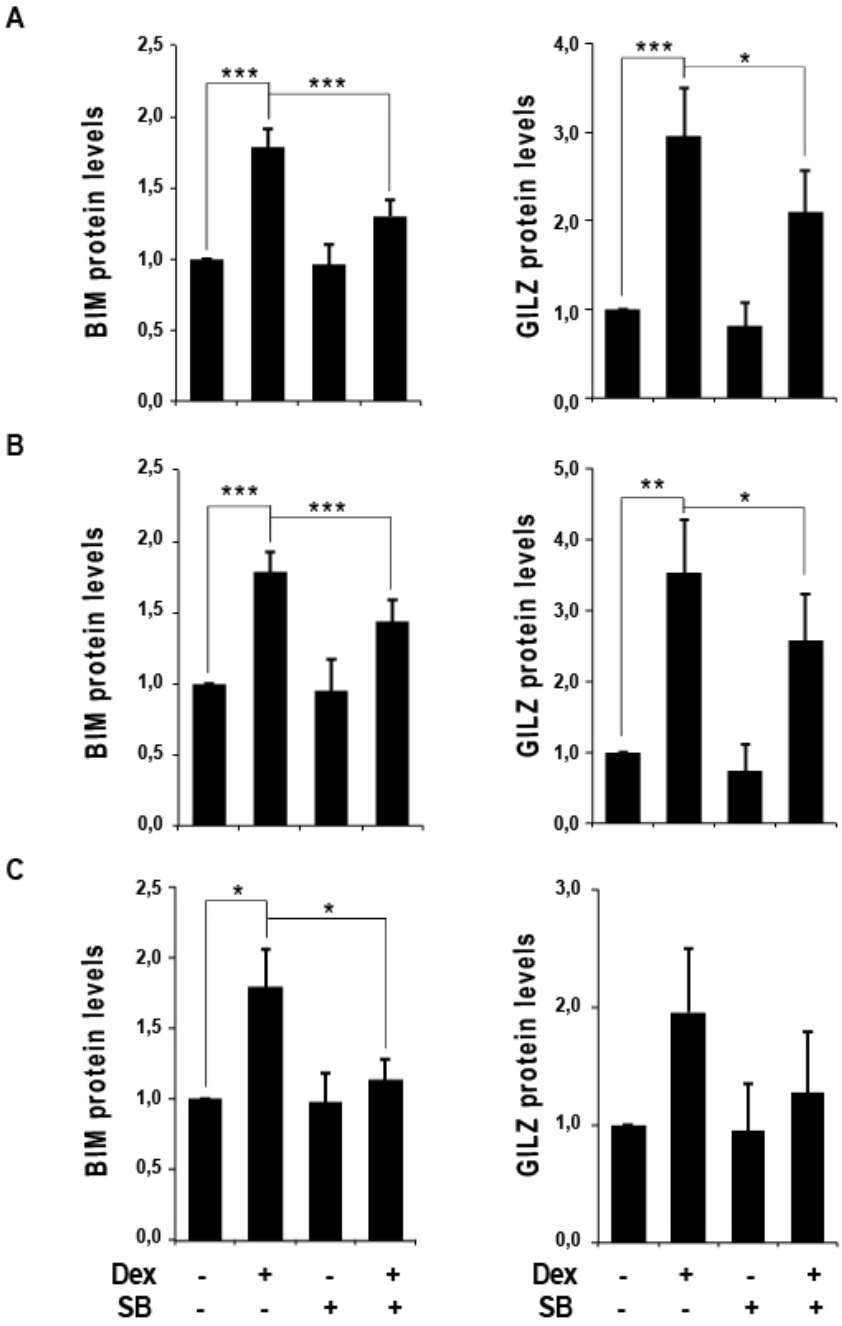

Figure 55. GSK3 inhibition affects GC-induced BIM and GILZ protein levels in CLL cells. BIM and GILZ protein levels from Western Blots from CLL patients were quantified by densitometric analysis and corrected by ERK2 levels by using ImageJ software (NIH). Results are represented as the mean ± SEM of **(A)** all the patients analyzed (BIM: 14 and GILZ: 11), **(B)** patients where GSK3 inhibition reverted GC-induced apoptosis (BIM: 6 and GILZ: 4), and **(C)** patients where GSK3 inhibition did not revert GC-induced apoptosis (BIM: 8 and GILZ: 7).

Collectively, these data indicate that GSK3 inhibition reduces sensitivity to GC-induced apoptosis in CLL cells and impairs GC-dependent gene and protein induction.

V. General discussion and future perspectives

Role of GSK3 on GC-mediated signaling and GR transcriptional regulation.

Effect of GCs in apoptosis induction

GCs are steroidal ligands for the GR, a ligand-activated transcription factor. In addition to their developmental and homeostatic roles, GCs also regulate the functions of the immune system (Glass and Ogawa, 2006) (Chinenov and Rogatsky, 2007) (Beck et al., 2009). For this reason, GCs are the first line of treatment in several inflammatory diseases (Glass and Saijo, 2010). Furthermore, GCs induce apoptosis in different cell types including leukemia cells, in a complex process regulated by multiple signaling pathways that alter gene expression profiles through GR-mediated transactivation and transrepression (Kfir-Erenfeld et al., 2010). Our group previously described that GCs induce apoptosis in CLL cells (Bellosillo et al., 1997) through a mechanism that regulates the pro-apoptotic BCL-2 family member BIM at the transcriptional and protein level (Iglesias-Serret et al., 2007).

Unfortunately, CLL cells are not easy to transfect making them an unsuitable model for molecular analysis. In order to analyze GC-mediated signaling at the molecular level, we used three Jurkat T-ALL cell lines harboring different types of GR. The Jurkat parental cell line carries one wt and one mutated GR allele. This function-impairing point mutation (R477H) affects transactivation, transrepression, but not ligand binding or translocation of the GR (Riml et al., 2004). As expected, this cell line was completely resistant to GC-induced apoptosis. We used the Jurkat GR wt cell line, which is stably transfected with a wt rat GR expression vector (Helmberg et al., 1995), suffered GC-induced apoptosis after dexamethasone treatment. Additionally, we used the Jurkat LS7 cell line, which expresses the LS7 mutant that contains two adjacent amino acid mutations in the second half of the second zinc finger (Helmberg et al., 1995). The LS7 GR mutant was previously reported to have little or no transactivating potential, while retaining transrepression capacity. These cells were also sensitive to GC-induced apoptosis, although to a less extent than Jurkat GR wt cells.

When we analyzed the mRNA expression profile of the BCL-2 family members and other apoptosis related genes in Jurkat cell lines we observed that in both Jurkat GR wt and LS7 cell lines, dexamethasone induced the mRNA levels of two well known GC-induced genes, *BIM* (Wang et al., 2003) (Zhang and Insel, 2004) and *HIAP1* (Webster et al., 2002)

(Rogatsky et al., 2003). These results show that the induction of these genes is independent of the transactivation capacity of the GR as the LS7 mutant is aunable to transactivate target genes. GCs equally induced BIM protein expression. We analyzed MCL-1 protein expression levels, as its overexpression is known to be important for cancer cells to evade cell death (Quinn et al., 2011) by sequestering BAX- or BAK-activating BH3-only proteins BIM and BID (Maurer et al., 2006). MCL-1 expression levels were downregulated in Jurkat GR wt and LS7 cell lines in the presence of dexamethasone. These results where BIM is induced and MCL-1 is downregulated confirm the importance of the balance between pro-apoptotic and anti-apoptotic BCL-2 family members in the regulation and determination of cell death or survival (Kelly and Strasser, 2011). As expected, in the parental cell line dexamethasone treatment did not induce changes in the mRNA expression profile or the protein expression of BIM and MCL-1. Besides analyzing the apoptotic profile in Jurkat cell lines we also analyzed the transcriptional regulation of *GILZ*, a direct GR-target gene (Beaulieu and Morand, 2011), and *BIM*, a gene regulated independently of GR direct binding to DNA (Molitoris et al., 2011) (Heidari et al., 2012), in Jurkat GR wt cells. We confirmed that ongoing transcription but not translation is required for the GC-dependent induction of *GILZ* and *BIM* in Jurkat GR wt cells. Both genes were shown to be primary GC targets, as opposed to those regulated by another glucocorticoid-inducible factor that would require *de novo* protein synthesis.

Role of GSK3 in GC-induced apoptosis

Previous studies have shown the involvement of different protein kinases in GC-mechanism of action (Galliher-Beckley et al., 2008). It has been previously described that in the absence of a ligand, GSK3α is bound to the GR and exposure to GCs or GSK3 inhibitor lead to the disruption of this interaction (Spokoini et al., 2010). It has also been described that the GR associates with GSK3β in the presence of dexamethasone but not with GSK3α (Galliher-Beckley et al., 2008). Consistent with previous studies in other cell lines, we observed a critical role for GSK3 in GC-dependent cell death (Nuutinen et al., 2009) (Spokoini et al., 2010). Inhibition of GSK3 by the specific inhibitor SB216763 significantly reverted GC-induced apoptosis in Jurkat GR wt cells. In Jurkat LS7 cells there was a less pronounced inhibitory effect of GSK3 inhibition over GC-induced apoptosis. The anti-apoptotic protein MCL-1 contains a conserved consensus site for GSK3 phosphorylation, which targets it for ubiquitin-dependent degradation (Maurer et al., 2006).

In Jurkat GR wt cells we observed that GC-dependent downregulation of MCL-1 protein levels and caspase activation was prevented by GSK3 inhibition. In accordance with a previous study, GSK3 inhibition reverted dexamethasone-induced upregulation of BIM (Nuutinen et al., 2009). Interestingly, this was also the case of GC-dependent GILZ protein induction, which was significantly reverted by GSK3 inhibition. To the best of our knowledge, there are no previous studies demonstrating that GSK3 is important in the GC-dependent upregulation of GILZ.

Role of GSK3 in GR-mediated transcriptional regulation

Pharmacological inhibition of GSK3 resulted in a reduced induction of *BIM*, *HIAP1* and *GILZ* endogenous mRNA levels in response to GCs in Jurkat GR wt cells. This effect over *GILZ* mRNA levels was confirmed in several cell lines form different species and tissue origin, ruling out cell type specific effects. GSK3 inhibition by SB216763, but not by LiCl, resulted in the reduced induction of GC-responsive promoter constructs. In Jurkat LS7 cells dexamethasone induced *BIM* and *HIAP1* mRNA levels, but to a less extent than in Jurkat GR wt cells. *GILZ* was only slightly induced in Jurkat LS7 cells as it is a GR-direct target gene and in agreement with the low transactivating potential of the LS7 mutant. Interestingly, there was no reversion in GC-induced mRNA levels of target genes in response to GSK3 inhibition in this cell line.

ChIP assays in Jurkat GR wt cells showed that GSK3 inhibition reduced GR and RNA polymerase II recruitment to the *GILZ* promoter after dexamethasone treatment. These results indicate that GC-dependent transcriptional activation requires a functional GSK3 signaling and show for the first time that GSK3 could be required by the GR for its activation as a transcription factor and for RNA polymerase II recruitment. These results are in the line with previous studies in which GSK3 inhibition represses other steroid receptors transcriptional activity in various cell types (Liao et al., 2004) (Mazor et al., 2004) (Medunjanin et al., 2005) (Grisouard and Mayer, 2009).

In contrast to transcriptional activation there are mechanisms by which the GR can transrepress gene expression. Transrepression typically involves indirect association (tethering) of the receptor with target genes rather than direct sequence-specific DNA

binding (Glass and Saijo, 2010). For example, GCs can interact with and inhibit AP1 and NF-κB family members, suppressing the expression of their target genes (De Bosscher et al., 2003). We wanted to determine if GSK3 inhibition is able to affect GC-induced transcriptional transrepression. We analyzed *MYC* and *BCL-3*, two genes that are transrepressed by GCs and whose promoters harbor AP1 and NF-κB binding sites (Duyao et al., 1990) (Ge et al., 2003) (Iavarone et al., 2003) (Vartanian et al., 2011) (Wang et al., 2011). As expected, these genes were significantly repressed by dexamethasone treatment in Jurkat GR wt cells. Interestingly, pretreatment with SB216763 had no significant effect over the GC-induced transrepression of these genes. These results suggest that GSK3 inhibition can affect GC-induced transactivation but not transrepression. These findings are of clinical interest, as several side effects of GC therapy are thought to be predominantly mediated via transactivation (Glass and Saijo, 2010). Thus, approaches, like GSK3 inhibition, that preferentially do not affect transrepression and suppress transactivation activity of the GR could result in fewer undesirable effects of therapy.

Interaction networks between the GR and different signaling pathways

Signaling pathways including protein kinase networks are known to regulate glucocorticoid-induced apoptosis (Kfir-Erenfeld et al., 2010). We observed that pre-incubation with protein kinase inhibitors, HDAC inhibitors, BCL-2 inhibitor, and proteasome inhibitor could not prevent apoptosis induction by dexamethasone.

We further analyzed the effect of SAHA over GC induced gene expression, as our group has recently demonstrated in CLL cells that BIM regulation is one of the most critical molecular events explaining the apoptotic effect of the HDAC inhibitors Kendine 92 and SAHA (Perez-Perarnau et al., 2011). HDAC inhibitors are promising chemotherapeutic agents that exert a range of antitumor activities through gene regulation, cell cycle arrest and apoptosis. In the case of SAHA, *BIM* upregulation is mediated by E2F recruitment to its promoter (Zhao et al., 2005). On the other hand, *GILZ* has been previously described to be dramatically upregulated when PI3K and Akt inhibitors were combined with dexamethasone (Grugan et al., 2008). In order to see if Akti inhibitor could shed a light on GC-mediated transcriptional regulation we analyzed its effect over *BIM* and *GILZ* mRNA induction in response to dexamethasone. We confirmed the previously described positive effect of SAHA over basal *BIM* mRNA expression (Bachmann et al., 2010). Nevertheless,

SAHA had no effect over GC-induced *BIM* mRNA levels. Interestingly, SAHA clearly reverted *GILZ* induction by GCs. Even though, acetylation of histones is thought to allow the transcriptional machinery to function (Hong et al., 1993), it was previously demonstrated that HDAC inhibitors are able to repress GC-induced MMTV-Luc transcriptional activity (Mulholland et al., 2003). This happens through chromatin remodeling independent mechanisms suggesting that the primary target of HDAC inhibition at the MMTV promoter is a nonhistone protein that is involved in an essential step of basal transcription. It is likely that the mechanism by which HDAC inhibition represses GC-dependent induction of *GILZ* mRNA levels is similar to the mechanism by which it represses MMTV-Luc activity.

As previously described, Akt inhibition affected basal levels and potentiated dexamethasone-induced *GILZ* mRNA expression (Grugan et al., 2008) probably through FOXO3 binding to the *GILZ* promoter (Asselin-Labat et al., 2004). As previously described by our group for CLL cells (de Frias et al., 2009), Akt inhibition had no effect over *BIM* mRNA levels in Jurkat GR wt cells. These data confirm a role for Akt in *GILZ* transcriptional regulation and of HDACs in the transcriptional regulation of *BIM* and *GILZ*.

Analysis of GSK3 isoforms and their implication in GR regulation

Furthermore, we analyzed which was the GSK3 isoform involved in the regulation of GR transcriptional activation in response to GCs. As inhibitors do not distinguish between the two isoforms, we performed isoform specific gene silencing analysis. As it was previously described, GSK3α and GSK3β silencing in HeLa cells, resulted in the activation of a GRE-promoter construct at a basal level (Liang and Chuang, 2006). Interestingly, only GSK3β silencing effectively reverted GC-dependent transcriptional activation. Knockdown of GSK3β and double knockdown of α and β isoforms reduced both basal and GC-induced mRNA expression of endogenous *GILZ*. This reversion in transcriptional activation was not observed after GSK3α silencing, indicating that GSK3β is the isoform that regulates basal and GC-induced gene transcription.

RT-MLPA analysis in HeLa cells revealed differences in apoptosis mRNA expression profile when compared to Jurkat GR wt cells. These results are coherent with the fact that

HeLa cells do not undergo apoptosis in response to dexamethasone (Mann and Cidlowski, 2001). We demonstrated that GSK3β and α/β silencing in HeLa cells resulted in the reduction of GC-dependent induction of *BMF*, *BCL-XL* and *MCL-1*, previously described GC-regulates genes (Scoltock et al., 2007) (Ploner et al., 2008) (Lynch et al., 2010) (Xu et al., 2011). Nevertheless, *HIAP1* was induced by dexamethasone even when GSK3β was silenced, suggesting a different mechanism of GC-dependent induction.

Moreover, we confirmed our results obtained from isoform silencing analysis in WT, GSK3α and GSK3β null MEF cells. Dexamethasone significantly induced *GILZ* mRNA levels and MMTV-Luc promoter construct luciferase activity in WT and GSK3α null MEF cells. Interestingly, GSK3β null MEF cells were significantly unable to induce *GILZ* mRNA levels and MMTV-Luc promoter construct luciferase activity in response to dexamethasone treatment.

GSK3 affects GR cellular distribution

The balance between nuclear import and export determines the subcellular localization of the GR. The mechanisms of nuclear transport have been extensively studied and even though the mechanism responsible for the nuclear import of steroid receptors is well documented, the mechanisms of GR export are still largely unknown (Vandevyver et al., 2011). It has been suggested that CRM1 plays an important role in the early nuclear export of the GR (Itoh et al., 2002). However, contradictory results have been reported on whether GR nuclear export is CRM1-dependent (Carrigan et al., 2007) or CRM1-independent (Liu and DeFranco, 2000) (Kumar et al., 2006). Our results demonstrate that short-term pharmacological inhibition of GSK3 activity in combination with dexamethasone treatment in Jurkat GR wt cells targets the GR for a rapid export from the nucleus. This nuclear export could collaborate in part with the observed down-regulation of early GR transcriptional activity. This was also described for the androgen receptor (AR) in prostate cancer cell lines, where GSK3 inhibition reverted AR-dependent transcriptional activity and caused a rapid nuclear export of endogenous AR (Rinnab et al., 2008) (Schutz et al., 2010). Interestingly, we observed that SB216763-induced nuclear export was partially inhibited by Leptomycin B, an inhibitor of CRM1-dependent export, suggesting there might be a CRM1-dependent nuclear export of the GR in response to GSK3 inhibition at

short incubation times (3 hours). However, other participating export mechanisms like Ca^{2+}-dependent Calreticulin-based mechanism cannot be completely ruled out (Holaska et al., 2002) (Kumar et al., 2004) (Beck et al., 2011).

One would expect that if GSK3β silencing in HeLa cells was responsible for the downregulation of GR transcriptional activity, we would obtain the same enhanced GR nuclear export observed in Jurkat GR wt cells, at least when both isoforms were silenced in HeLa cells at longer times. Nonetheless, dexamethasone treatment always resulted in GR translocation to the nucleus even after GSK3α, GSK3β and GSK3α/β were silenced, when analyzed by cytoplasm and nuclear fractionation. Interestingly, we observed by immunofluorescent staining in GSK3β silenced cells that there were higher basal GR expression levels and presence of the GR in the nucleus in response to GC treatment. This effect was not observed when it was analyzed by western blot. This is probably due to the fact that in western blots we were only analyzing GRα levels by focusing in the 94 kDa isoform. On the other side, in the immunofluorescent analysis, we were indiscriminately seeing all GR isoforms recognized by the antibody. Further GR isoform-specific cell fractioning analysis could help to better understand GSK3β silencing effects over each one of these isoforms. The increase in GR expression levels in GSK3β silenced cells is in agreement with previously described phosphorylation of Ser404 by GSK3β. This phosphorylation seems to be important for GR turnover by favoring GR protein export from the nucleus and downregulation by proteasome degradation (Galliher-Beckley et al., 2008). It is important to note that short pre-incubation times with SB216763 in Jurkat GR wt cells gives little time frame for changes to occur in the expression levels of GSK3 targets. When we used siRNAs to silence GSK3 isoforms there was 72 hours of GSK3 inhibition, which may significantly affect expression levels of GSK3 target proteins. For this reason, further analysis with longer incubation times should be performed in Jurkat GR wt cells in order to analyze more profoundly the effect of GSK3 inhibition over GR expression levels.

It was previously described that GSK3 phosphorylates the rat GR at Thr171 and that GSK3 overexpression inhibits GR transcriptional activity through this phosphorylation (Rogatsky et al., 1998). This phosphorylation site is not present in the human GR sequence, indicating that GSK3 mediated regulation of this residue is likely species-specific (Galliher-Beckley and Cidlowski, 2009). We wanted to know if GSK3-mediated GR phosphorylation

status affects the GR transcriptional function. For this reason we tested the effect of Thr171 and Ser424 (human Ser404) mutations, the two sites known to be phosphorylated by GSK3 on the rat GR, over GC-dependent transcriptional activation of the MMTV-Luc reporter construct and endogenous *GILZ* mRNA levels. Our results with rat GR mutants of these residues phosphorylated by GSK3 in Jurkat parental cells show that these mutations do not abrogate the ability of the GR to translocate to the nucleus and transactivate a GRE containing reporter construct. In the same line, all the mutants were able to induce endogenous *GILZ* mRNA levels. Surprisingly, GSK3 inhibition reverted the induction of luciferase activity of MMTV-Luc reporter construct and endogenous *GILZ* mRNA levels mediated by all mutants. These results indicate that there could be an additional mechanism, not involving the phosphorylation of these residues, by which GSK3 regulates GR transcriptional activity. Interestingly, the Jurkat parental cell line was able to slightly induce *GILZ* mRNA expression levels, but the MMTV-Luc reporter construct was not induced by dexamethasone treatment in these cells. The effect over the MMTV-Luc reposrter construct could be due to the previously described function-impairing point mutation (R477H) of Jurkat parental cell lines, which impairs GR transactivation and transrepression. These results are unclear, even though it was previously described (Riml et al., 2004) and they might be reflecting promoter specific differences or effects that are independent of the GR transcriptional activity over the *GILZ* promoter (Kfir-Erenfeld et al., 2010). Our results indicate that GSK3 isoforms regulate GR cellular response by using different mechanisms besides GSK3 mediated phosphorylation of the GR.

Role of GSK3 in GC-induced apoptosis in CLL cells

In order to elucidate the role of GSK3 in a more physiological context and model, we performed experiments with primary lymphocyte cells of CLL patients. We evaluated the effect of GSK3 inhibition over GC-induced apoptosis. SB216763 pre-treatment reverted GC-induced cell death in 19 of 29 samples and augmented it in 10 of 29 samples analyzed. Additionally, GC dependent *BIM* and *GILZ* mRNA levels were reverted in the patients analyzed where GSK3 inhibition reverted GC-dependent cell death. In the samples from patients where SB216763 increased GC-induced apoptosis, only *GILZ* mRNA levels were reverted by GSK3 inhibition. In these samples *BIM* mRNA levels were significantly induced when compared to dexamethasone treatment alone. These results may be

reflecting differences among patients, as CLL patients may harbor different genetic alterations that determine the response to GC-treatment. The fact that *GILZ* mRNA levels were always reverted suggests that GSK3 inhibition affects GR-transcriptional activity in CLL cells. Nevertheless, in the case of *BIM* its expression was always in accordance with the apoptotic outcome, suggesting that there are additional factors playing a role in its GC-dependent induction. Additionally, GC-dependent BIM and GILZ protein induction was reverted by GSK3 inhibition in most of the samples analyzed.

In summary, our results demonstrate that GSK3β is involved on GC-dependent gene transcriptional induction through the regulation of GR and RNA polymerase II recruitment to target gene sequences and by affecting GR protein subcellular localization. Our results suggest that GSK3 plays an important role in regulating GC mechanism of action. The fact that this regulation is exerted independently of known phosphorylation sites of the GR by GSK3β raises the possibility that other GR-GSK3β interactions could exist and have not been explored. One hypothesis would be that GSK3β could have a structural role making part of transcription complexes. This hypothesis is highly probable, as there is growing evidence on chromatin-associated protein kinases that regulate gene expression. Previous studies in yeast have shown that kinases translocate to the nucleus and associate with the promoter of genes to regulate expression (Pascual-Ahuir et al., 2006) (Pokholok et al., 2006). These chromatin-tethered kinases have been shown to make part of transcription complexes, as well as phosphorylating their target proteins (Edmunds and Mahadevan, 2006) (de Nadal and Posas, 2010). p38 is recruited to the chromatin of muscle-specific genes and targets the SWI-SNF chromatin remodeling complex (Simone et al., 2004). It has also been described that phosphorylated ERK can accumulate in the nucleus and with RUNX2 it specifically associates with osteoblast-specific genes inducing their expression (Li et al., 2010). Moreover, PKC-theta physically associates with the regulatory regions of inducible immune response genes in human T cells (Sutcliffe et al., 2011). This data indicates that further studies on the mechanism of GR-dependent transcriptional regulation by GSK3 are necessary for better understanding how this kinase affects GR transactivating potential.

Our results show that GSK3 plays an important role in regulating GC mechanism of action, suggesting that keeping GSK3 in an active state could improve GC therapy.

Therefore, additional analyses of the involvement of GSK3 activity in GC treatment of lymphoma and leukemia malignancies may help gain insight into the molecular basis of these disorders.

VI. Conclusions

- *BIM* and *GILZ* are GC-induced early genes in Jurkat GR wt cells, as ongoing transcription but not translation is required for their GC-dependent induction.
- GSK3 inhibition reverts GC-induced apoptosis in Jurkat GR wt cells by preventing GC-dependent MCL-1 downregulation and caspase-3 and -9 activation.
- GSK3 inhibition results in the reduction of GC-induced protein and mRNA expression in Jurkat GR wt and HeLa cells and does not affect GC-induced transrepression in Jurkat GR wt cells.
- In HeLa cells where GSK3β has been silenced and in GSK3β null MEF cells there is a reduction of the GC-induced mRNA expression and GR-dependent reporter gene activity.
- GSK3 inhibition impairs dexamethasone-mediated binding of the GR and RNA polymerase II to endogenous *GILZ* promoter in Jurkat GR wt cells by a mechanism that affects GR protein localization by decreasing early GR nuclear levels.
- GSK3 regulates rat GR transcriptional activity through a mechanism not involving phosphorylation of known GSK3β phosphorylation sites, serine 424 and threonine 171.
- In CLL primary cells GSK3 inhibition results in the reduction of GC-induced apoptosis and impairs GC-induced protein and mRNA levels of *BIM* and *GILZ* in most of the samples analyzed.

VII. References

A

- Abrams, M.T., Robertson, N.M., Yoon, K., and Wickstrom, E. (2004). Inhibition of glucocorticoid-induced apoptosis by targeting the major splice variants of BIM mRNA with small interfering RNA and short hairpin RNA. J. Biol. Chem. *279,* 55809-55817.
- Adams, J.M., and Cory, S. (2007). The Bcl-2 apoptotic switch in cancer development and therapy. Oncogene *26,* 1324-1337.
- Akgul, C., Moulding, D.A., and Edwards, S.W. (2004). Alternative splicing of Bcl-2-related genes: functional consequences and potential therapeutic applications. Cell Mol. Life Sci. *61,* 2189-2199.
- Akiyama, T., Dass, C.R., and Choong, P.F. (2009). Bim-targeted cancer therapy: a link between drug action and underlying molecular changes. Mol. Cancer. Ther. *8,* 3173-3180.
- Aouacheria, A., Brunet, F., and Gouy, M. (2005). Phylogenomics of life-or-death switches in multicellular animals: Bcl-2, BH3-Only, and BNip families of apoptotic regulators. Mol. Biol. Evol. *22,* 2395-2416.
- Asselin-Labat, M.L., Biola-Vidamment, A., Kerbrat, S., Lombes, M., Bertoglio, J., and Pallardy, M. (2005). FoxO3 mediates antagonistic effects of glucocorticoids and interleukin-2 on glucocorticoid-induced leucine zipper expression. Mol. Endocrinol. *19,* 1752-1764.
- Asselin-Labat, M.L., David, M., Biola-Vidamment, A., Lecoeuche, D., Zennaro, M.C., Bertoglio, J., and Pallardy, M. (2004). GILZ, a new target for the transcription factor FoxO3, protects T lymphocytes from interleukin-2 withdrawal-induced apoptosis. Blood *104,* 215-223.
- Ayroldi, E., Migliorati, G., Bruscoli, S., Marchetti, C., Zollo, O., Cannarile, L., D'Adamio, F., and Riccardi, C. (2001). Modulation of T-cell activation by the glucocorticoid-induced leucine zipper factor via inhibition of nuclear factor kappaB. Blood *98,* 743-753.
- Azoulay-Alfaguter, I., Yaffe, Y., Licht-Murava, A., Urbanska, M., Jaworski, J., Pietrokovski, S., Hirschberg, K., and Eldar-Finkelman, H. (2011). Distinct molecular regulation of glycogen synthase kinase-3alpha isozyme controlled by its N-terminal region: functional role in calcium/calpain signaling. J. Biol. Chem. *286,* 13470-13480.

B

- Bachmann, P.S., Piazza, R.G., Janes, M.E., Wong, N.C., Davies, C., Mogavero, A., Bhadri, V.A., Szymanska, B., Geninson, G., Magistroni, V.*, et al.* (2010). Epigenetic silencing of BIM in glucocorticoid poor-responsive pediatric acute lymphoblastic leukemia, and its reversal by histone deacetylase inhibition. Blood *116,* 3013-3022.
- Barragan, M., Bellosillo, B., Campas, C., Colomer, D., Pons, G., and Gil, J. (2002). Involvement of protein kinase C and phosphatidylinositol 3-kinase pathways in the survival of B-cell chronic lymphocytic leukemia cells.*99,* 2969-2976.
- Beaulieu, E., and Morand, E.F. (2011). Role of GILZ in immune regulation, glucocorticoid actions and rheumatoid arthritis. Nat. Rev. Rheumatol. *7,* 340-348.
- Beck, I.M., De Bosscher, K., and Haegeman, G. (2011). Glucocorticoid receptor mutants: man-made tools for functional research. Trends Endocrinol. Metab. *22,* 295-310.
- Beck, I.M., Vanden Berghe, W., Vermeulen, L., Yamamoto, K.R., Haegeman, G., and De Bosscher, K. (2009). Crosstalk in inflammation: the interplay of glucocorticoid receptor-based mechanisms and kinases and phosphatases. Endocr. Rev. *30,* 830-882.
- Bellosillo, B., Dalmau, M., Colomer, D., and Gil, J. (1997). Involvement of CED-3/ICE proteases in the apoptosis of B-chronic lymphocytic leukemia cells. Blood *89,* 3378-3384.
- Bertrand, M.J., Milutinovic, S., Dickson, K.M., Ho, W.C., Boudreault, A., Durkin, J., Gillard, J.W., Jaquith, J.B., Morris, S.J., and Barker, P.A. (2008). cIAP1 and cIAP2 facilitate cancer cell survival by functioning as E3 ligases that promote RIP1 ubiquitination. Mol. Cell *30,* 689-700.
- Beurel, E., and Jope, R.S. (2006). The paradoxical pro- and anti-apoptotic actions of GSK3 in the intrinsic and extrinsic apoptosis signaling pathways. Prog. Neurobiol. *79,* 173-189.
- Bouillet, P., Metcalf, D., Huang, D.C., Tarlinton, D.M., Kay, T.W., Kontgen, F., Adams, J.M., and Strasser, A. (1999). Proapoptotic Bcl-2 relative Bim required for certain apoptotic responses, leukocyte homeostasis, and to preclude autoimmunity. Science *286,* 1735-1738.
- Bratton, S.B., and Salvesen, G.S. (2010). Regulation of the Apaf-1-caspase-9 apoptosome. J. Cell. Sci. *123,* 3209-3214.

- Bruna, A., Nicolas, M., Munoz, A., Kyriakis, J.M., and Caelles, C. (2003). Glucocorticoid receptor-JNK interaction mediates inhibition of the JNK pathway by glucocorticoids. EMBO J. *22,* 6035-6044.
- Burz, C., Berindan-Neagoe, I., Balacescu, O., and Irimie, A. (2009). Apoptosis in cancer: key molecular signaling pathways and therapy targets. Acta Oncol. *48,* 811-821.

C

- Carrigan, A., Walther, R.F., Salem, H.A., Wu, D., Atlas, E., Lefebvre, Y.A., and Hache, R.J. (2007). An active nuclear retention signal in the glucocorticoid receptor functions as a strong inducer of transcriptional activation. J. Biol. Chem. *282,* 10963-10971.
- Cartron, P.F., Gallenne, T., Bougras, G., Gautier, F., Manero, F., Vusio, P., Meflah, K., Vallette, F.M., and Juin, P. (2004). The first alpha helix of Bax plays a necessary role in its ligand-induced activation by the BH3-only proteins Bid and PUMA. Mol. Cell *16,* 807-818.
- Certo, M., Del Gaizo Moore, V., Nishino, M., Wei, G., Korsmeyer, S., Armstrong, S.A., and Letai, A. (2006). Mitochondria primed by death signals determine cellular addiction to antiapoptotic BCL-2 family members. Cancer. Cell. *9,* 351-365.
- Chakravarti, D., LaMorte, V.J., Nelson, M.C., Nakajima, T., Schulman, I.G., Juguilon, H., Montminy, M., and Evans, R.M. (1996). Role of CBP/P300 in nuclear receptor signalling. Nature *383,* 99-103.
- Chandra, J., Gilbreath, J., Freireich, E.J., Kliche, K.O., Andreeff, M., Keating, M., and McConkey, D.J. (1997). Protease activation is required for glucocorticoid-induced apoptosis in chronic lymphocytic leukemic lymphocytes. Blood *90,* 3673-3681.
- Chen, J., and McMillan, N.A. (2008). Molecular basis of pathogenesis, prognosis and therapy in chronic lymphocytic leukaemia. Cancer. Biol. Ther. *7,* 174-179.
- Chen, L., Willis, S.N., Wei, A., Smith, B.J., Fletcher, J.I., Hinds, M.G., Colman, P.M., Day, C.L., Adams, J.M., and Huang, D.C. (2005). Differential targeting of prosurvival Bcl-2 proteins by their BH3-only ligands allows complementary apoptotic function. Mol. Cell *17,* 393-403.
- Chen, W., Rogatsky, I., and Garabedian, M.J. (2006). MED14 and MED1 differentially regulate target-specific gene activation by the glucocorticoid receptor. Mol. Endocrinol. *20,* 560-572.

- Chinenov, Y., and Rogatsky, I. (2007). Glucocorticoids and the innate immune system: crosstalk with the toll-like receptor signaling network. Mol. Cell. Endocrinol. *275,* 30-42.
- Chiorazzi, N., Rai, K.R., and Ferrarini, M. (2005). Chronic lymphocytic leukemia. N. Engl. J. Med. *352,* 804-815.
- Chipuk, J.E., Moldoveanu, T., Llambi, F., Parsons, M.J., and Green, D.R. (2010). The BCL-2 family reunion. Mol. Cell *37,* 299-310.
- Chu, Z.L., McKinsey, T.A., Liu, L., Gentry, J.J., Malim, M.H., and Ballard, D.W. (1997). Suppression of tumor necrosis factor-induced cell death by inhibitor of apoptosis c-IAP2 is under NF-kappaB control. Proc. Natl. Acad. Sci. U. S. A. *94,* 10057-10062.
- Collins, R.J., Verschuer, L.A., Harmon, B.V., Prentice, R.L., Pope, J.H., and Kerr, J.F. (1989). Spontaneous programmed death (apoptosis) of B-chronic lymphocytic leukaemia cells following their culture in vitro. Br. J. Haematol. *71,* 343-350.
- Coll-Mulet, L. (2007). Doctoral Thesis.
- Cote-Velez, A., Perez-Martinez, L., Charli, J.L., and Joseph-Bravo, P. (2008). The PKC and ERK/MAPK pathways regulate glucocorticoid action on TRH transcription. Neurochem. Res. *33,* 1582-1591.

D

- D'Adamio, F., Zollo, O., Moraca, R., Ayroldi, E., Bruscoli, S., Bartoli, A., Cannarile, L., Migliorati, G., and Riccardi, C. (1997). A new dexamethasone-induced gene of the leucine zipper family protects T lymphocytes from TCR/CD3-activated cell death. Immunity *7,* 803-812.
- Dameshek, W. (1967). Chronic lymphocytic leukemia--an accumulative disease of immunolgically incompetent lymphocytes. Blood *29,* Suppl:566-84.
- Danial, N.N., and Korsmeyer, S.J. (2004). Cell death: critical control points. Cell *116,* 205-219.
- De Bosscher, K., Vanden Berghe, W., and Haegeman, G. (2003). The interplay between the glucocorticoid receptor and nuclear factor-kappaB or activator protein-1: molecular mechanisms for gene repression. Endocr. Rev. *24,* 488-522.

- de Frias, M., Iglesias-Serret, D., Cosialls, A.M., Coll-Mulet, L., Santidrian, A.F., Gonzalez-Girones, D.M., de la Banda, E., Pons, G., and Gil, J. (2009). Akt inhibitors induce apoptosis in chronic lymphocytic leukemia cells. Haematologica *94,* 1698-1707.
- de Nadal, E., and Posas, F. (2010). Multilayered control of gene expression by stress-activated protein kinases. EMBO J. *29,* 4-13.
- Decker, T., Hipp, S., Ringshausen, I., Bogner, C., Oelsner, M., Schneller, F., and Peschel, C. (2003). Rapamycin-induced G1 arrest in cycling B-CLL cells is associated with reduced expression of cyclin D3, cyclin E, cyclin A, and survivin. Blood *101,* 278-285.
- Deveraux, Q.L., Takahashi, R., Salvesen, G.S., and Reed, J.C. (1997). X-linked IAP is a direct inhibitor of cell-death proteases. Nature *388,* 300-304.
- Diehl, J.A., Cheng, M., Roussel, M.F., and Sherr, C.J. (1998). Glycogen synthase kinase-3beta regulates cyclin D1 proteolysis and subcellular localization. Genes Dev. *12,* 3499-3511
- Dighiero, G., and Hamblin, T.J. (2008). Chronic lymphocytic leukaemia. Lancet *371,* 1017-1029.
- Drouin, J., Sun, Y.L., Chamberland, M., Gauthier, Y., De Lean, A., Nemer, M., and Schmidt, T.J. (1993). Novel glucocorticoid receptor complex with DNA element of the hormone-repressed POMC gene. EMBO J. *12,* 145-156.
- Duyao, M.P., Buckler, A.J., and Sonenshein, G.E. (1990). Interaction of an NF-kappa B-like factor with a site upstream of the c-myc promoter. Proc. Natl. Acad. Sci. U. S. A. *87,* 4727-4731.

E

- Eckelman, B.P., and Salvesen, G.S. (2006). The human anti-apoptotic proteins cIAP1 and cIAP2 bind but do not inhibit caspases. J. Biol. Chem. *281,* 3254-3260.
- Edmunds, J.W., and Mahadevan, L.C. (2006). Cell signaling. Protein kinases seek close encounters with active genes. Science *313,* 449-451.
- Eldering, E., Spek, C.A., Aberson, H.L., Grummels, A., Derks, I.A., de Vos, A.F., McElgunn, C.J., and Schouten, J.P. (2003). Expression profiling via novel multiplex assay allows rapid assessment of gene regulation in defined signalling pathways.*31,* e153.

F

- Fischer, U., Janicke, R.U., and Schulze-Osthoff, K. (2003). Many cuts to ruin: a comprehensive update of caspase substrates. Cell Death Differ. *10,* 76-100.
- Force, T., and Woodgett, J.R. (2009). Unique and overlapping functions of GSK-3 isoforms in cell differentiation and proliferation and cardiovascular development. J. Biol. Chem. *284,* 9643-9647.
- Forde, J.E., and Dale, T.C. (2007). Glycogen synthase kinase 3: a key regulator of cellular fate.*64,* 1930-1944.
- Freedman, L.P., and Luisi, B.F. (1993). On the mechanism of DNA binding by nuclear hormone receptors: a structural and functional perspective. J. Cell. Biochem. *51,* 140-150.
- Fuentes-Prior, P., and Salvesen, G.S. (2004). The protein structures that shape caspase activity, specificity, activation and inhibition. Biochem. J. *384,* 201-232.
- Fulda, S., and Debatin, K.M. (2006). Extrinsic versus intrinsic apoptosis pathways in anticancer chemotherapy. Oncogene *25,* 4798-4811.

G

- Galliher-Beckley, A.J., Williams, J.G., Collins, J.B., and Cidlowski, J.A. (2008). Glycogen synthase kinase 3beta-mediated serine phosphorylation of the human glucocorticoid receptor redirects gene expression profiles.*28,* 7309-7322.
- Galliher-Beckley, A.J., and Cidlowski, J.A. (2009). Emerging roles of glucocorticoid receptor phosphorylation in modulating glucocorticoid hormone action in health and disease. IUBMB Life *61,* 979-986.
- Galliher-Beckley, A.J., Williams, J.G., and Cidlowski, J.A. (2011). Ligand-independent phosphorylation of the glucocorticoid receptor integrates cellular stress pathways with nuclear receptor signaling. Mol. Cell. Biol. *31,* 4663-4675.
- Galton, D.A. (1966). The pathogenesis of chronic lymphocytic leukemia. Can. Med. Assoc. J. *94,* 1005-1010.
- Garlatti, M., Daheshia, M., Slater, E., Bouguet, J., Hanoune, J., Beato, M., and Barouki, R. (1994). A functional glucocorticoid-responsive unit composed of two overlapping inactive receptor-binding sites: evidence for formation of a receptor tetramer. Mol. Cell. Biol. *14,* 8007-8017.

- Ge, B., Li, O., Wilder, P., Rizzino, A., and McKeithan, T.W. (2003). NF-kappa B regulates BCL3 transcription in T lymphocytes through an intronic enhancer. J. Immunol. *171,* 4210-4218.
- Gentile, M., Mauro, F.R., Guarini, A., and Foa, R. (2005). New developments in the diagnosis, prognosis and treatment of chronic lymphocytic leukemia. Curr. Opin. Oncol. *17,* 597-604.
- Gilley, J., Coffer, P.J., and Ham, J. (2003). FOXO transcription factors directly activate bim gene expression and promote apoptosis in sympathetic neurons. J. Cell Biol. *162,* 613-622.
- Glass, C.K., and Ogawa, S. (2006). Combinatorial roles of nuclear receptors in inflammation and immunity. Nat. Rev. Immunol. *6,* 44-55.
- Glass, C.K., and Saijo, K. (2010). Nuclear receptor transrepression pathways that regulate inflammation in macrophages and T cells. Nat. Rev. Immunol. *10,* 365-376.
- Gokbuget, N., and Hoelzer, D. (2006). Treatment of adult acute lymphoblastic leukemia. Hematology Am. Soc. Hematol. Educ. Program. 133-141.
- Gribben, J.G. (2010). How I treat CLL up front. Blood *115,* 187-197.
- Gribben, J.G. (2008). Molecular profiling in CLL. Hematology Am. Soc. Hematol. Educ. Program. 444-449.
- Grisouard, J., and Mayer, D. (2009). Specific involvement of glycogen synthase kinase-3 in the function and activity of sex steroid hormone receptors reveals the complexity of their regulation. J. Steroid Biochem. Mol. Biol. *117,* 87-92.
- Grugan, K.D., Ma, C., Singhal, S., Krett, N.L., and Rosen, S.T. (2008). Dual regulation of glucocorticoid-induced leucine zipper (GILZ) by the glucocorticoid receptor and the PI3-kinase/AKT pathways in multiple myeloma. J. Steroid Biochem. Mol. Biol. *110,* 244-254.

H

- Hallek, M., Cheson, B.D., Catovsky, D., Caligaris-Cappio, F., Dighiero, G., Dohner, H., Hillmen, P., Keating, M.J., Montserrat, E., Rai, K.R., and Kipps, T.J. International Workshop on Chronic Lymphocytic Leukemia. (2008). Guidelines for the diagnosis and treatment of chronic lymphocytic leukemia: a report from the International

Workshop on Chronic Lymphocytic Leukemia updating the National Cancer Institute-Working Group 1996 guidelines. Blood *111,* 5446-5456.

- Hanahan, D., and Weinberg, R.A. (2011). Hallmarks of cancer: the next generation. Cell *144,* 646-674.
- Heidari, N., Miller, A.V., Hicks, M.A., Marking, C.B., and Harada, H. (2012). Glucocorticoid-mediated BIM induction and apoptosis are regulated by Runx2 and c-Jun in leukemia cells. Cell. Death Dis. *3,* e349.
- Heitzer, M.D., Wolf, I.M., Sanchez, E.R., Witchel, S.F., and DeFranco, D.B. (2007). Glucocorticoid receptor physiology. Rev. Endocr Metab. Disord. *8,* 321-330.
- Helmberg, A., Auphan, N., Caelles, C., and Karin, M. (1995). Glucocorticoid-induced apoptosis of human leukemic cells is caused by the repressive function of the glucocorticoid receptor.*14,* 452-460.
- Herr, I., Gassler, N., Friess, H., and Buchler, M.W. (2007). Regulation of differential pro- and anti-apoptotic signaling by glucocorticoids. Apoptosis *12,* 271-291.
- Hinds, M.G., Norton, R.S., Vaux, D.L., and Day, C.L. (1999). Solution structure of a baculoviral inhibitor of apoptosis (IAP) repeat. Nat. Struct. Biol. *6,* 648-651.
- Hoeflich, K.P., Luo, J., Rubie, E.A., Tsao, M.S., Jin, O., and Woodgett, J.R. (2000). Requirement for glycogen synthase kinase-3beta in cell survival and NF-kappaB activation.*406,* 86-90.
- Holaska, J.M., Black, B.E., Love, D.C., Hanover, J.A., Leszyk, J., and Paschal, B.M. (2001). Calreticulin Is a receptor for nuclear export. J. Cell Biol. *152,* 127-140.
- Holaska, J.M., Black, B.E., Rastinejad, F., and Paschal, B.M. (2002). Ca2+-dependent nuclear export mediated by calreticulin. Mol. Cell. Biol. *22,* 6286-6297.
- Hollenberg, S.M., Weinberger, C., Ong, E.S., Cerelli, G., Oro, A., Lebo, R., Thompson, E.B., Rosenfeld, M.G., and Evans, R.M. (1985). Primary structure and expression of a functional human glucocorticoid receptor cDNA. Nature *318,* 635-641.
- Hong, L., Schroth, G.P., Matthews, H.R., Yau, P., and Bradbury, E.M. (1993). Studies of the DNA binding properties of histone H4 amino terminus. Thermal denaturation studies reveal that acetylation markedly reduces the binding constant of the H4 "tail" to DNA. J. Biol. Chem. *268,* 305-314.

- Hongisto, V., Smeds, N., Brecht, S., Herdegen, T., Courtney, M.J., and Coffey, E.T. (2003). Lithium blocks the c-Jun stress response and protects neurons via its action on glycogen synthase kinase 3. Mol. Cell. Biol. *23,* 6027-6036.
- Hotchkiss, R.S., Strasser, A., McDunn, J.E., and Swanson, P.E. (2009). Cell death. N. Engl. J. Med. *361,* 1570-1583.
- Hughes, K., Nikolakaki, E., Plyte, S.E., Totty, N.F., and Woodgett, J.R. (1993). Modulation of the glycogen synthase kinase-3 family by tyrosine phosphorylation. EMBO J. *12,* 803-808.

I

- Iavarone, C., Catania, A., Marinissen, M.J., Visconti, R., Acunzo, M., Tarantino, C., Carlomagno, M.S., Bruni, C.B., Gutkind, J.S., and Chiariello, M. (2003). The platelet-derived growth factor controls c-myc expression through a JNK- and AP-1-dependent signaling pathway. J. Biol. Chem. *278,* 50024-50030.
- Iglesias-Serret, D., de Frias, M., Santidrian, A.F., Coll-Mulet, L., Cosialls, A.M., Barragan, M., Domingo, A., Gil, J., and Pons, G. (2007). Regulation of the proapoptotic BH3-only protein BIM by glucocorticoids, survival signals and proteasome in chronic lymphocytic leukemia cells.*21,* 281-287.
- Inoue, S., Riley, J., Gant, T.W., Dyer, M.J., and Cohen, G.M. (2007). Apoptosis induced by histone deacetylase inhibitors in leukemic cells is mediated by Bim and Noxa. Leukemia *21,* 1773-1782.
- Ismaili, N., and Garabedian, M.J. (2004). Modulation of glucocorticoid receptor function via phosphorylation. Ann. N. Y. Acad. Sci. *1024,* 86-101.
- Itoh, M., Adachi, M., Yasui, H., Takekawa, M., Tanaka, H., and Imai, K. (2002). Nuclear export of glucocorticoid receptor is enhanced by c-Jun N-terminal kinase-mediated phosphorylation. Mol. Endocrinol. *16,* 2382-2392.

J

- Jenkins, B.D., Pullen, C.B., and Darimont, B.D. (2001). Novel glucocorticoid receptor coactivator effector mechanisms. Trends Endocrinol. Metab. *12,* 122-126.

- Jiang, Z., Zheng, X., Lytle, R.A., Higashikubo, R., and Rich, K.M. (2004). Lovastatin-induced up-regulation of the BH3-only protein, Bim, and cell death in glioblastoma cells. J. Neurochem. *89,* 168-178.
- Jun, C.D., Hoon-Ryu, Um, J.Y., Kim, T.Y., Kim, J.M., Kang, S.S., Kim, H.M., and Chung, H.T. (1994). Involvement of protein kinase C in the inhibition of nitric oxide production from murine microglial cells by glucocorticoid. Biochem. Biophys. Res. Commun. *199,* 633-638.

K

- Kajita, K., Ishizuka, T., Miura, A., Kanoh, Y., Ishizawa, M., Kimura, M., Muto, N., and Yasuda, K. (2001). Glucocorticoid-induced insulin resistance associates with activation of protein kinase C isoforms. Cell. Signal. *13,* 169-175.
- Kelly, P.N., and Strasser, A. (2011). The role of Bcl-2 and its pro-survival relatives in tumourigenesis and cancer therapy. Cell Death Differ. *18,* 1414-1424.
- Kerr, J.F., Wyllie, A.H., and Currie, A.R. (1972). Apoptosis: a basic biological phenomenon with wide-ranging implications in tissue kinetics. Br. J. Cancer *26,* 239-257.
- Kfir-Erenfeld, S., Sionov, R.V., Spokoini, R., Cohen, O., and Yefenof, E. (2010). Protein kinase networks regulating glucocorticoid-induced apoptosis of hematopoietic cancer cells: fundamental aspects and practical considerations.*51,* 1968-2005.
- Kim, H., Rafiuddin-Shah, M., Tu, H.C., Jeffers, J.R., Zambetti, G.P., Hsieh, J.J., and Cheng, E.H. (2006). Hierarchical regulation of mitochondrion-dependent apoptosis by BCL-2 subfamilies. Nat. Cell Biol. *8,* 1348-1358.
- Krueger, A., Baumann, S., Krammer, P.H., and Kirchhoff, S. (2001). FLICE-inhibitory proteins: regulators of death receptor-mediated apoptosis. Mol. Cell. Biol. *21,* 8247-8254.
- Kudo, N., Matsumori, N., Taoka, H., Fujiwara, D., Schreiner, E.P., Wolff, B., Yoshida, M., and Horinouchi, S. (1999). Leptomycin B inactivates CRM1/exportin 1 by covalent modification at a cysteine residue in the central conserved region. Proc. Natl. Acad. Sci. U. S. A. *96,* 9112-9117.

- Kuida, K., Haydar, T.F., Kuan, C.Y., Gu, Y., Taya, C., Karasuyama, H., Su, M.S., Rakic, P., and Flavell, R.A. (1998). Reduced apoptosis and cytochrome c-mediated caspase activation in mice lacking caspase 9. Cell *94,* 325-337.
- Kumar, R., and Thompson, E.B. (2005). Gene regulation by the glucocorticoid receptor: structure:function relationship. J. Steroid Biochem. Mol. Biol. *94,* 383-394.
- Kumar, S., Chaturvedi, N.K., Nishi, M., Kawata, M., and Tyagi, R.K. (2004). Shuttling components of nuclear import machinery involved in nuclear translocation of steroid receptors exit nucleus via exportin-1/CRM-1* independent pathway. Biochim. Biophys. Acta *1691,* 73-77.
- Kumar, S., Saradhi, M., Chaturvedi, N.K., and Tyagi, R.K. (2006). Intracellular localization and nucleocytoplasmic trafficking of steroid receptors: an overview. Mol. Cell. Endocrinol. *246,* 147-156.
- Kuwana, T., Bouchier-Hayes, L., Chipuk, J.E., Bonzon, C., Sullivan, B.A., Green, D.R., and Newmeyer, D.D. (2005). BH3 domains of BH3-only proteins differentially regulate Bax-mediated mitochondrial membrane permeabilization both directly and indirectly. Mol. Cell *17,* 525-535.

L

- Latre de Late, P., Pepin, A., Assaf-Vandecasteele, H., Espinasse, C., Nicolas, V., Asselin-Labat, M.L., Bertoglio, J., Pallardy, M., and Biola-Vidamment, A. (2010). Glucocorticoid-induced leucine zipper (GILZ) promotes the nuclear exclusion of FOXO3 in a Crm1-dependent manner. J. Biol. Chem. *285,* 5594-5605.
- Leist, M., and Jaattela, M. (2001). Four deaths and a funeral: from caspases to alternative mechanisms. Nat. Rev. Mol. Cell Biol. *2,* 589-598.
- Leo, C., and Chen, J.D. (2000). The SRC family of nuclear receptor coactivators. Gene *245,* 1-11.
- Letai, A., Bassik, M.C., Walensky, L.D., Sorcinelli, M.D., Weiler, S., and Korsmeyer, S.J. (2002). Distinct BH3 domains either sensitize or activate mitochondrial apoptosis, serving as prototype cancer therapeutics. Cancer. Cell. *2,* 183-192.
- Li, K., Li, Y., Shelton, J.M., Richardson, J.A., Spencer, E., Chen, Z.J., Wang, X., and Williams, R.S. (2000). Cytochrome c deficiency causes embryonic lethality and attenuates stress-induced apoptosis. Cell *101,* 389-399.

- Li, Y., Ge, C., and Franceschi, R.T. (2010). Differentiation-dependent association of phosphorylated extracellular signal-regulated kinase with the chromatin of osteoblast-related genes. J. Bone Miner. Res. *25,* 154-163.
- Liang, M.H., and Chuang, D.M. (2006). Differential roles of glycogen synthase kinase-3 isoforms in the regulation of transcriptional activation.*281,* 30479-30484.
- Liao, X., Thrasher, J.B., Holzbeierlein, J., Stanley, S., and Li, B. (2004). Glycogen synthase kinase-3beta activity is required for androgen-stimulated gene expression in prostate cancer.*145,* 2941-2949.
- Liao, X., Zhang, L., Thrasher, J.B., Du, J., and Li, B. (2003). Glycogen synthase kinase-3beta suppression eliminates tumor necrosis factor-related apoptosis-inducing ligand resistance in prostate cancer. Mol. Cancer. Ther. *2,* 1215-1222.
- Linseman, D.A., Butts, B.D., Precht, T.A., Phelps, R.A., Le, S.S., Laessig, T.A., Bouchard, R.J., Florez-McClure, M.L., and Heidenreich, K.A. (2004). Glycogen synthase kinase-3beta phosphorylates Bax and promotes its mitochondrial localization during neuronal apoptosis. J. Neurosci. *24,* 9993-10002.
- Liu, J., and DeFranco, D.B. (2000). Protracted nuclear export of glucocorticoid receptor limits its turnover and does not require the exportin 1/CRM1-directed nuclear export pathway. Mol. Endocrinol. *14,* 40-51.
- Liu, X., Kim, C.N., Yang, J., Jemmerson, R., and Wang, X. (1996). Induction of apoptotic program in cell-free extracts: requirement for dATP and cytochrome c. Cell *86,* 147-157.
- Lonard, D.M., and O'Malley, B.W. (2005). Expanding functional diversity of the coactivators. Trends Biochem. Sci. *30,* 126-132.
- Lopez-Royuela, N., Balsas, P., Galan-Malo, P., Anel, A., Marzo, I., and Naval, J. (2010). Bim is the key mediator of glucocorticoid-induced apoptosis and of its potentiation by rapamycin in human myeloma cells. Biochim. Biophys. Acta *1803,* 311-322.
- Lu, D., Zhao, Y., Tawatao, R., Cottam, H.B., Sen, M., Leoni, L.M., Kipps, T.J., Corr, M., and Carson, D.A. (2004). Activation of the Wnt signaling pathway in chronic lymphocytic leukemia. Proc. Natl. Acad. Sci. U. S. A. *101,* 3118-3123.

- Lu, J., Quearry, B., and Harada, H. (2006). p38-MAP kinase activation followed by BIM induction is essential for glucocorticoid-induced apoptosis in lymphoblastic leukemia cells.*580,* 3539-3544.
- Lynch, J.T., Rajendran, R., Xenaki, G., Berrou, I., Demonacos, C., and Krstic-Demonacos, M. (2010). The role of glucocorticoid receptor phosphorylation in Mcl-1 and NOXA gene expression. Mol. Cancer. *9,* 38.

M

- Maddali, K.K., Korzick, D.H., Turk, J.R., and Bowles, D.K. (2005). Isoform-specific modulation of coronary artery PKC by glucocorticoids. Vascul Pharmacol. *42,* 153-162.
- Mahoney, D.J., Cheung, H.H., Mrad, R.L., Plenchette, S., Simard, C., Enwere, E., Arora, V., Mak, T.W., Lacasse, E.C., Waring, J., and Korneluk, R.G. (2008). Both cIAP1 and cIAP2 regulate TNFalpha-mediated NF-kappaB activation. Proc. Natl. Acad. Sci. U. S. A. *105,* 11778-11783.
- Malavasi, F., Deaglio, S., Damle, R., Cutrona, G., Ferrarini, M., and Chiorazzi, N. (2011). CD38 and chronic lymphocytic leukemia: a decade later. Blood *118,* 3470-3478.
- Malkoski, S.P., and Dorin, R.I. (1999). Composite glucocorticoid regulation at a functionally defined negative glucocorticoid response element of the human corticotropin-releasing hormone gene. Mol. Endocrinol. *13,* 1629-1644.
- Mann, C.L., and Cidlowski, J.A. (2001). Glucocorticoids regulate plasma membrane potential during rat thymocyte apoptosis in vivo and in vitro. Endocrinology *142,* 421-429.
- Matsui, H., Shinjyo, T., and Inaba, T. (2005). Structure of the human Bim gene and its transcriptional regulation in Baf-3, interleukin-3-dependent hematopoietic cells. Mol. Biol. Rep. *32,* 79-85.
- Maurer, U., Charvet, C., Wagman, A.S., Dejardin, E., and Green, D.R. (2006). Glycogen synthase kinase-3 regulates mitochondrial outer membrane permeabilization and apoptosis by destabilization of MCL-1.*21,* 749-760.

- Mazor, M., Kawano, Y., Zhu, H., Waxman, J., and Kypta, R.M. (2004). Inhibition of glycogen synthase kinase-3 represses androgen receptor activity and prostate cancer cell growth. Oncogene *23,* 7882-7892.
- McConkey, D.J., Aguilar-Santelises, M., Hartzell, P., Eriksson, I., Mellstedt, H., Orrenius, S., and Jondal, M. (1991). Induction of DNA fragmentation in chronic B-lymphocytic leukemia cells. J. Immunol. *146,* 1072-1076.
- McKenna, N.J., and O'Malley, B.W. (2002). Minireview: nuclear receptor coactivators--an update. Endocrinology *143,* 2461-2465.
- McKenna, N.J., and O'Malley, B.W. (2001). Nuclear receptors, coregulators, ligands, and selective receptor modulators: making sense of the patchwork quilt. Ann. N. Y. Acad. Sci. *949,* 3-5.
- McNally, J.G., Muller, W.G., Walker, D., Wolford, R., and Hager, G.L. (2000). The glucocorticoid receptor: rapid exchange with regulatory sites in living cells. Science *287,* 1262-1265.
- Medina, M., and Wandosell, F. (2011). Deconstructing GSK-3: The Fine Regulation of Its Activity. Int. J. Alzheimers Dis. *2011,* 479249.
- Medunjanin, S., Hermani, A., De Servi, B., Grisouard, J., Rincke, G., and Mayer, D. (2005). Glycogen synthase kinase-3 interacts with and phosphorylates estrogen receptor alpha and is involved in the regulation of receptor activity. J. Biol. Chem. *280,* 33006-33014.
- Meier, P., and Vousden, K.H. (2007). Lucifer's labyrinth--ten years of path finding in cell death. Mol. Cell *28,* 746-754.
- Melarangi, T., Zhuang, J., Lin, K., Rockliffe, N., Bosanquet, A.G., Oates, M., Slupsky, J.R., and Pettitt, A.R. (2012). Glucocorticoid resistance in chronic lymphocytic leukaemia is associated with a failure of upregulated Bim/Bcl-2 complexes to activate Bax and Bak. Cell. Death Dis. *3,* e372.
- Meyer, T., Gustafsson, J.A., and Carlstedt-Duke, J. (1997). Glucocorticoid-dependent transcriptional repression of the osteocalcin gene by competitive binding at the TATA box. DNA Cell Biol. *16,* 919-927.
- Molitoris, J.K., McColl, K.S., and Distelhorst, C.W. (2011). Glucocorticoid-mediated repression of the oncogenic microRNA cluster miR-17~92 contributes to the induction of Bim and initiation of apoptosis. Mol. Endocrinol. *25,* 409-420.

- Montserrat, E., and Rozman, C. (1995). Chronic lymphocytic leukemia: present status. Ann. Oncol. *6,* 219-235.
- Muchmore, S.W., Sattler, M., Liang, H., Meadows, R.P., Harlan, J.E., Yoon, H.S., Nettesheim, D., Chang, B.S., Thompson, C.B., Wong, S.L., Ng, S.L., and Fesik, S.W. (1996). X-ray and NMR structure of human Bcl-xL, an inhibitor of programmed cell death. Nature *381,* 335-341.
- Mulholland, N.M., Soeth, E., and Smith, C.L. (2003). Inhibition of MMTV transcription by HDAC inhibitors occurs independent of changes in chromatin remodeling and increased histone acetylation. Oncogene *22,* 4807-4818.

N

- Nguyen, C.H., and Watts, V.J. (2006). Dexamethasone-induced Ras protein 1 negatively regulates protein kinase C delta: implications for adenylyl cyclase 2 signaling. Mol. Pharmacol. *69,* 1763-1771.
- Nijhawan, D., Fang, M., Traer, E., Zhong, Q., Gao, W., Du, F., and Wang, X. (2003). Elimination of Mcl-1 is required for the initiation of apoptosis following ultraviolet irradiation. Genes Dev. *17,* 1475-1486.
- Nogami, H., Hiraoka, Y., Matsubara, M., Nonobe, E., Harigaya, T., Katayama, M., Hemmi, N., Kobayashi, S., Mogi, K., Aiso, S., Kawamura, K., and Hisano, S. (2002). A composite hormone response element regulates transcription of the rat GHRH receptor gene. Endocrinology *143,* 1318-1326.
- Nuutinen, U., Postila, V., Matto, M., Eeva, J., Ropponen, A., Eray, M., Riikonen, P., and Pelkonen, J. (2006). Inhibition of PI3-kinase-Akt pathway enhances dexamethasone-induced apoptosis in a human follicular lymphoma cell line. Exp. Cell Res. *312,* 322-330.
- Nuutinen, U., Ropponen, A., Suoranta, S., Eeva, J., Eray, M., Pellinen, R., Wahlfors, J., and Pelkonen, J. (2009). Dexamethasone-induced apoptosis and up-regulation of Bim is dependent on glycogen synthase kinase-3.*33,* 1714-1717.

O

- Oakley, R.H., and Cidlowski, J.A. (2011). Cellular processing of the glucocorticoid receptor gene and protein: new mechanisms for generating tissue-specific actions of glucocorticoids.*286,* 3177-3184.
- Oscier, D., Fegan, C., Hillmen, P., Illidge, T., Johnson, S., Maguire, P., Matutes, E., Milligan, D., and Guidelines Working Group of the UK CLL Forum. British Committee for Standards in Haematology. (2004). Guidelines on the diagnosis and management of chronic lymphocytic leukaemia. Br. J. Haematol. *125,* 294-317.
- Ougolkov, A.V., Bone, N.D., Fernandez-Zapico, M.E., Kay, N.E., and Billadeau, D.D. (2007). Inhibition of glycogen synthase kinase-3 activity leads to epigenetic silencing of nuclear factor kappaB target genes and induction of apoptosis in chronic lymphocytic leukemia B cells. Blood *110,* 735-742.

P

- Packham, G., and Stevenson, F.K. (2005). Bodyguards and assassins: Bcl-2 family proteins and apoptosis control in chronic lymphocytic leukaemia. Immunology *114,* 441-449.
- Pap, M., and Cooper, G.M. (2002). Role of translation initiation factor 2B in control of cell survival by the phosphatidylinositol 3-kinase/Akt/glycogen synthase kinase 3beta signaling pathway. Mol. Cell. Biol. *22,* 578-586.
- Pascual-Ahuir, A., Struhl, K., and Proft, M. (2006). Genome-wide location analysis of the stress-activated MAP kinase Hog1 in yeast. Methods *40,* 272-278.
- Pearl, L.H., and Barford, D. (2002). Regulation of protein kinases in insulin, growth factor and Wnt signalling. Curr. Opin. Struct. Biol. *12,* 761-767.
- Pekarsky, Y., Zanesi, N., and Croce, C.M. (2010). Molecular basis of CLL. Semin. Cancer Biol. *20,* 370-376.
- Perez-Perarnau, A., Coll-Mulet, L., Rubio-Patino, C., Iglesias-Serret, D., Cosialls, A.M., Gonzalez-Girones, D.M., de Frias, M., de Sevilla, A.F., de la Banda, E., Pons, G., and Gil, J. (2011). Analysis of apoptosis regulatory genes altered by histone deacetylase inhibitors in chronic lymphocytic leukemia cells. Epigenetics *6,* 1228-1235.

- Pique, M., Barragan, M., Dalmau, M., Bellosillo, B., Pons, G., and Gil, J. (2000). Aspirin induces apoptosis through mitochondrial cytochrome c release. FEBS Lett. *480,* 193-196.
- Ploner, C., Rainer, J., Niederegger, H., Eduardoff, M., Villunger, A., Geley, S., and Kofler, R. (2008). The BCL2 rheostat in glucocorticoid-induced apoptosis of acute lymphoblastic leukemia. Leukemia *22,* 370-377.
- Pokholok, D.K., Zeitlinger, J., Hannett, N.M., Reynolds, D.B., and Young, R.A. (2006). Activated signal transduction kinases frequently occupy target genes. Science *313,* 533-536.
- Pop, C., Timmer, J., Sperandio, S., and Salvesen, G.S. (2006). The apoptosome activates caspase-9 by dimerization. Mol. Cell *22,* 269-275.
- Pradelli, L.A., Beneteau, M., and Ricci, J.E. (2010). Mitochondrial control of caspase-dependent and -independent cell death. Cell Mol. Life Sci. *67,* 1589-1597.
- Pui, C.H., and Evans, W.E. (2006). Treatment of acute lymphoblastic leukemia. N. Engl. J. Med. *354,* 166-178.

Q

- Qiong, Z., Ruofan, H., Xiaohua, L., Xinli, Z., Jingwei, J., and Zhaohui, C. (2010). Role of dephosphorylation of FOXO1 on apoptosis induced by wortmannin for non-Hodgkin's lymphoma cells. Mol. Biol. Rep. *37,* 2397-2402.
- Quinn, B.A., Dash, R., Azab, B., Sarkar, S., Das, S.K., Kumar, S., Oyesanya, R.A., Dasgupta, S., Dent, P., Grant, S.*, et al.* (2011). Targeting Mcl-1 for the therapy of cancer. Expert Opin. Investig. Drugs *20,* 1397-1411.

R

- Rambal, A.A., Panaguiton, Z.L., Kramer, L., Grant, S., and Harada, H. (2009). MEK inhibitors potentiate dexamethasone lethality in acute lymphoblastic leukemia cells through the pro-apoptotic molecule BIM. Leukemia *23,* 1744-1754.
- Rayasam, G.V., Tulasi, V.K., Sodhi, R., Davis, J.A., and Ray, A. (2009). Glycogen synthase kinase 3: more than a namesake. Br. J. Pharmacol. *156,* 885-898.

- Reddy, T.E., Pauli, F., Sprouse, R.O., Neff, N.F., Newberry, K.M., Garabedian, M.J., and Myers, R.M. (2009). Genomic determination of the glucocorticoid response reveals unexpected mechanisms of gene regulation. Genome Res. *19,* 2163-2171.
- Renshaw, S.A., Dempsey, C.E., Barnes, F.A., Bagstaff, S.M., Dower, S.K., Bingle, C.D., and Whyte, M.K. (2004). Three novel Bid proteins generated by alternative splicing of the human Bid gene. J. Biol. Chem. *279,* 2846-2855.
- Riml, S., Schmidt, S., Ausserlechner, M.J., Geley, S., and Kofler, R. (2004). Glucocorticoid receptor heterozygosity combined with lack of receptor auto-induction causes glucocorticoid resistance in Jurkat acute lymphoblastic leukemia cells. Cell Death Differ. *11 Suppl 1,* S65-72.
- Rinnab, L., Schutz, S.V., Diesch, J., Schmid, E., Kufer, R., Hautmann, R.E., Spindler, K.D., and Cronauer, M.V. (2008). Inhibition of glycogen synthase kinase-3 in androgen-responsive prostate cancer cell lines: are GSK inhibitors therapeutically useful? Neoplasia *10,* 624-634.
- Roca, R., Kypta, R.M., and Vivanco, M.M. (2003). Loss of p16INK4a results in increased glucocorticoid receptor activity during fibrosarcoma development. Proc. Natl. Acad. Sci. U. S. A. *100,* 3113-3118.
- Rogatsky, I., Waase, C.L., and Garabedian, M.J. (1998). Phosphorylation and inhibition of rat glucocorticoid receptor transcriptional activation by glycogen synthase kinase-3 (GSK-3). Species-specific differences between human and rat glucocorticoid receptor signaling as revealed through GSK-3 phosphorylation.*273,* 14315-14321.
- Rogatsky, I., Wang, J.C., Derynck, M.K., Nonaka, D.F., Khodabakhsh, D.B., Haqq, C.M., Darimont, B.D., Garabedian, M.J., and Yamamoto, K.R. (2003). Target-specific utilization of transcriptional regulatory surfaces by the glucocorticoid receptor. Proc. Natl. Acad. Sci. U. S. A. *100,* 13845-13850.
- Roig, M.B., Roset, R., Ortet, L., Balsiger, N.A., Anfosso, A., Cabellos, L., Garrido, M., Alameda, F., Brady, H.J., and Gil-Gomez, G. (2009). Identification of a novel cyclin required for the intrinsic apoptosis pathway in lymphoid cells. Cell Death Differ. *16,* 230-243.
- Rothe, M., Pan, M.G., Henzel, W.J., Ayres, T.M., and Goeddel, D.V. (1995). The TNFR2-TRAF signaling complex contains two novel proteins related to baculoviral inhibitor of apoptosis proteins. Cell *83,* 1243-1252.

- Rubio-Patino, C., Palmeri, C.M., Perez-Perarnau, A., Cosialls, A.M., Moncunill-Massaguer, C., Gonzalez-Girones, D.M., Pons-Hernandez, L., Lopez, J.M., Ventura, F., Gil, J., Pons, G., and Iglesias-Serret, D. (2012). Glycogen synthase kinase-3beta is involved in ligand-dependent activation of transcription and cellular localization of the glucocorticoid receptor. Mol. Endocrinol. *26,* 1508-1520.

S

- Santoro, M.M., Samuel, T., Mitchell, T., Reed, J.C., and Stainier, D.Y. (2007). Birc2 (cIap1) regulates endothelial cell integrity and blood vessel homeostasis. Nat. Genet. *39,* 1397-1402.
- Sattler, M., Liang, H., Nettesheim, D., Meadows, R.P., Harlan, J.E., Eberstadt, M., Yoon, H.S., Shuker, S.B., Chang, B.S., Minn, A.J., Thompson, C.B., and Fesik, S.W. (1997). Structure of Bcl-xL-Bak peptide complex: recognition between regulators of apoptosis. Science *275,* 983-986.
- Schlette, E., Medeiros, L.J., Keating, M., and Lai, R. (2003). CD79b expression in chronic lymphocytic leukemia. Association with trisomy 12 and atypical immunophenotype. Arch. Pathol. Lab. Med. *127,* 561-566.
- Schulz, M., Eggert, M., Baniahmad, A., Dostert, A., Heinzel, T., and Renkawitz, R. (2002). RU486-induced glucocorticoid receptor agonism is controlled by the receptor N terminus and by corepressor binding. J. Biol. Chem. *277,* 26238-26243.
- Schutz, S.V., Cronauer, M.V., and Rinnab, L. (2010). Inhibition of glycogen synthase kinase-3beta promotes nuclear export of the androgen receptor through a CRM1-dependent mechanism in prostate cancer cell lines. J. Cell. Biochem. *109,* 1192-1200.
- Scoltock, A.B., Heimlich, G., and Cidlowski, J.A. (2007). Glucocorticoids inhibit the apoptotic actions of UV-C but not Fas ligand in hepatoma cells: direct evidence for a critical role of Bcl-xL. Cell Death Differ. *14,* 840-850.
- Shanafelt, T.D., Kay, N.E., Jenkins, G., Call, T.G., Zent, C.S., Jelinek, D.F., Morice, W.G., Boysen, J., Zakko, L., Schwager, S., Slager, S.L., and Hanson, C.A. (2009). B-cell count and survival: differentiating chronic lymphocytic leukemia from monoclonal B-cell lymphocytosis based on clinical outcome. Blood *113,* 4188-4196.

- Shu, H.B., Takeuchi, M., and Goeddel, D.V. (1996). The tumor necrosis factor receptor 2 signal transducers TRAF2 and c-IAP1 are components of the tumor necrosis factor receptor 1 signaling complex. Proc. Natl. Acad. Sci. U. S. A. *93,* 13973-13978.
- Simone, C., Forcales, S.V., Hill, D.A., Imbalzano, A.N., Latella, L., and Puri, P.L. (2004). p38 pathway targets SWI-SNF chromatin-remodeling complex to muscle-specific loci. Nat. Genet. *36,* 738-743.
- Song, L., Zhou, T., and Jope, R.S. (2004). Lithium facilitates apoptotic signaling induced by activation of the Fas death domain-containing receptor. BMC Neurosci. *5,* 20.
- Spitaler, M., and Cantrell, D.A. (2004). Protein kinase C and beyond. Nat. Immunol. *5,* 785-790.
- Spokoini, R., Kfir-Erenfeld, S., Yefenof, E., and Sionov, R.V. (2010). Glycogen synthase kinase-3 plays a central role in mediating glucocorticoid-induced apoptosis.*24,* 1136-1150.
- Srinivasula, S.M., and Ashwell, J.D. (2008). IAPs: what's in a name? Mol. Cell *30,* 123-135.
- Stahn, C., and Buttgereit, F. (2008). Genomic and nongenomic effects of glucocorticoids. Nat. Clin. Pract. Rheumatol. *4,* 525-533.
- Stavreva, D.A., Muller, W.G., Hager, G.L., Smith, C.L., and McNally, J.G. (2004). Rapid glucocorticoid receptor exchange at a promoter is coupled to transcription and regulated by chaperones and proteasomes. Mol. Cell. Biol. *24,* 2682-2697.
- Strasser, A. (2005). The role of BH3-only proteins in the immune system. Nat. Rev. Immunol. *5,* 189-200.
- Sun, C., Cai, M., Gunasekera, A.H., Meadows, R.P., Wang, H., Chen, J., Zhang, H., Wu, W., Xu, N., Ng, S.C., and Fesik, S.W. (1999). NMR structure and mutagenesis of the inhibitor-of-apoptosis protein XIAP. Nature *401,* 818-822.
- Sun, M., Meares, G., Song, L., and Jope, R.S. (2009). XIAP associates with GSK3 and inhibits the promotion of intrinsic apoptotic signaling by GSK3. Cell. Signal. *21,* 1857-1865.

- Sutcliffe, E.L., Bunting, K.L., He, Y.Q., Li, J., Phetsouphanh, C., Seddiki, N., Zafar, A., Hindmarsh, E.J., Parish, C.R., Kelleher, A.D.*, et al.* (2011). Chromatin-associated protein kinase C-theta regulates an inducible gene expression program and microRNAs in human T lymphocytes. Mol. Cell *41,* 704-719.
- Sutherland, C. (2011). What Are the bona fide GSK3 Substrates? Int. J. Alzheimers Dis. *2011,* 505607.
- Szapary, D., Huang, Y., and Simons, S.S.,Jr. (1999). Opposing effects of corepressor and coactivators in determining the dose-response curve of agonists, and residual agonist activity of antagonists, for glucocorticoid receptor-regulated gene expression. Mol. Endocrinol. *13,* 2108-2121.

T

- Tait, S.W., and Green, D.R. (2010). Mitochondria and cell death: outer membrane permeabilization and beyond. Nat. Rev. Mol. Cell Biol. *11,* 621-632.
- Taylor, R.C., Cullen, S.P., and Martin, S.J. (2008). Apoptosis: controlled demolition at the cellular level. Nat. Rev. Mol. Cell Biol. *9,* 231-241.
- Thornberry, N.A., and Lazebnik, Y. (1998). Caspases: enemies within. Science *281,* 1312-1316.
- Thornton, P.D., Matutes, E., Bosanquet, A.G., Lakhani, A.K., Grech, H., Ropner, J.E., Joshi, R., Mackie, P.H., Douglas, I.D., Bowcock, S.J., and Catovsky, D. (2003). High dose methylprednisolone can induce remissions in CLL patients with p53 abnormalities. Ann. Hematol. *82,* 759-765.
- Tighe, A., Ray-Sinha, A., Staples, O.D., and Taylor, S.S. (2007). GSK-3 inhibitors induce chromosome instability. BMC Cell Biol. *8,* 34.
- Timmer, J.C., and Salvesen, G.S. (2007). Caspase substrates. Cell Death Differ. *14,* 66-72.
- Truss, M., and Beato, M. (1993). Steroid hormone receptors: interaction with deoxyribonucleic acid and transcription factors. Endocr. Rev. *14,* 459-479.

V

- Van Cruchten, S., and Van Den Broeck, W. (2002). Morphological and biochemical aspects of apoptosis, oncosis and necrosis. Anat. Histol. Embryol. *31,* 214-223.

- Vandevyver, S., Dejager, L., and Libert, C. (2011). On the Trail of the Glucocorticoid Receptor: Into the Nucleus and Back. Traffic
- Vangestel, C., Van de Wiele, C., Mees, G., and Peeters, M. (2009). Forcing cancer cells to commit suicide. Cancer Biother. Radiopharm. *24,* 395-407.
- Varfolomeev, E., Blankenship, J.W., Wayson, S.M., Fedorova, A.V., Kayagaki, N., Garg, P., Zobel, K., Dynek, J.N., Elliott, L.O., Wallweber, H.J., *et al.* (2007). IAP antagonists induce autoubiquitination of c-IAPs, NF-kappaB activation, and TNFalpha-dependent apoptosis. Cell *131,* 669-681.
- Vartanian, R., Masri, J., Martin, J., Cloninger, C., Holmes, B., Artinian, N., Funk, A., Ruegg, T., and Gera, J. (2011). AP-1 regulates cyclin D1 and c-MYC transcription in an AKT-dependent manner in response to mTOR inhibition: role of AIP4/Itch-mediated JUNB degradation. Mol. Cancer. Res. *9,* 115-130.
- Vaux, D.L., and Strasser, A. (1996). The molecular biology of apoptosis. Proc. Natl. Acad. Sci. U. S. A. *93,* 2239-2244.
- Veis, D.J., Sorenson, C.M., Shutter, J.R., and Korsmeyer, S.J. (1993). Bcl-2-deficient mice demonstrate fulminant lymphoid apoptosis, polycystic kidneys, and hypopigmented hair. Cell *75,* 229-240.
- Vince, J.E., Wong, W.W., Khan, N., Feltham, R., Chau, D., Ahmed, A.U., Benetatos, C.A., Chunduru, S.K., Condon, S.M., McKinlay, M., *et al.* (2007). IAP antagonists target cIAP1 to induce TNFalpha-dependent apoptosis. Cell *131,* 682-693.

W

- Wang, C.Y., Mayo, M.W., Korneluk, R.G., Goeddel, D.V., and Baldwin, A.S.,Jr. (1998). NF-kappaB antiapoptosis: induction of TRAF1 and TRAF2 and c-IAP1 and c-IAP2 to suppress caspase-8 activation. Science *281,* 1680-1683.
- Wang, H., Song, W., Hu, T., Zhang, N., Miao, S., Zong, S., and Wang, L. (2011). Fank1 interacts with Jab1 and regulates cell apoptosis via the AP-1 pathway. Cell Mol. Life Sci. *68,* 2129-2139.
- Wang, Z., Chen, W., Kono, E., Dang, T., and Garabedian, M.J. (2007). Modulation of glucocorticoid receptor phosphorylation and transcriptional activity by a C-terminal-associated protein phosphatase. Mol. Endocrinol. *21,* 625-634.

- Wang, Z., Malone, M.H., He, H., McColl, K.S., and Distelhorst, C.W. (2003). Microarray analysis uncovers the induction of the proapoptotic BH3-only protein Bim in multiple models of glucocorticoid-induced apoptosis.*278,* 23861-23867.
- Watson, P.J., Fairall, L., and Schwabe, J.W. (2012). Nuclear hormone receptor co-repressors: structure and function. Mol. Cell. Endocrinol. *348,* 440-449.
- Webster, J.C., Huber, R.M., Hanson, R.L., Collier, P.M., Haws, T.F., Mills, J.K., Burn, T.C., and Allegretto, E.A. (2002). Dexamethasone and tumor necrosis factor-alpha act together to induce the cellular inhibitor of apoptosis-2 gene and prevent apoptosis in a variety of cell types. Endocrinology *143,* 3866-3874.
- Willis, S.N., and Adams, J.M. (2005). Life in the balance: how BH3-only proteins induce apoptosis. Curr. Opin. Cell Biol. *17,* 617-625.
- Willis, S.N., Fletcher, J.I., Kaufmann, T., van Delft, M.F., Chen, L., Czabotar, P.E., Ierino, H., Lee, E.F., Fairlie, W.D., Bouillet, P.*, et al.* (2007). Apoptosis initiated when BH3 ligands engage multiple Bcl-2 homologs, not Bax or Bak. Science *315,* 856-859.
- Woodgett, J.R. (1990). Molecular cloning and expression of glycogen synthase kinase-3/factor A.*9,* 2431-2438.

X

- Xu, B., Strom, J., and Chen, Q.M. (2011). Dexamethasone induces transcriptional activation of Bcl-xL gene and inhibits cardiac injury by myocardial ischemia. Eur. J. Pharmacol. *668,* 194-200.

Y

- Yano, T., Ito, K., Fukamachi, H., Chi, X.Z., Wee, H.J., Inoue, K., Ida, H., Bouillet, P., Strasser, A., Bae, S.C., and Ito, Y. (2006). The RUNX3 tumor suppressor upregulates Bim in gastric epithelial cells undergoing transforming growth factor beta-induced apoptosis. Mol. Cell. Biol. *26,* 4474-4488.
- Yoshida, H., Kong, Y.Y., Yoshida, R., Elia, A.J., Hakem, A., Hakem, R., Penninger, J.M., and Mak, T.W. (1998). Apaf1 is required for mitochondrial pathways of apoptosis and brain development. Cell *94,* 739-750.
- Youle, R.J., and Strasser, A. (2008). The BCL-2 protein family: opposing activities that mediate cell death. Nat. Rev. Mol. Cell Biol. *9,* 47-59.

Z

- Zambon, A.C., Wilderman, A., Ho, A., and Insel, P.A. (2011). Increased expression of the pro-apoptotic protein BIM, a mechanism for cAMP/protein kinase A (PKA)-induced apoptosis of immature T cells. J. Biol. Chem. *286,* 33260-33267.
- Zhang, L., and Insel, P.A. (2004). The pro-apoptotic protein Bim is a convergence point for cAMP/protein kinase A- and glucocorticoid-promoted apoptosis of lymphoid cells. J. Biol. Chem. *279,* 20858-20865.
- Zhao, Y., Tan, J., Zhuang, L., Jiang, X., Liu, E.T., and Yu, Q. (2005). Inhibitors of histone deacetylases target the Rb-E2F1 pathway for apoptosis induction through activation of proapoptotic protein Bim. Proc. Natl. Acad. Sci. U. S. A. *102,* 16090-16095.
- Zhou, F., Medh, R.D., and Thompson, E.B. (2000). Glucocorticoid mediated transcriptional repression of c-myc in apoptotic human leukemic CEM cells. J. Steroid Biochem. Mol. Biol. *73,* 195-202.
- Zhou, J., and Cidlowski, J.A. (2005). The human glucocorticoid receptor: one gene, multiple proteins and diverse responses. Steroids *70,* 407-417.

VIII. Resumen en castellano

Introducción

Apoptosis

La apoptosis es un proceso de muerte celular programada altamente conservado en la evolución (Kerr et al., 1972). En células de mamíferos, la apoptosis se produce a través de dos vías moleculares distintas. La vía extrínseca de la apoptosis recibe señales a través de la unión de proteínas extracelulares que sirven como ligandos de muerte a los receptores de muerte con la posterior activación de las caspasas. Por otro lado, la vía intrínseca o mitocondrial es activada por eventos intracelulares y depende de la liberación de factores pro-apoptóticos de la mitocondria. Los miembros anti-apoptóticos de la familia de BCL-2 preservan la integridad de la membrana mitocondrial externa, mientras que los miembros pro-apoptóticos promueven su permeabilización. La permeabilización de la membrana mitocondrial externa (MOMP) permite la liberación al citosol de proteínas mitocondriales tales como el citocromo c, lo que conduce a la activación de las caspasas, un paso esencial en la ejecución de la apoptosis. Otras proteínas pro-apoptóticas liberadas por la mitocondrias son EndoG, AIF, Omi/HtrA2 y Smac/DIABLO (Pradelli et al., 2010).

Glucocorticoides

Los glucocorticoides (GCs) son hormonas esteroidales que regulan procesos esenciales como el crecimiento, el desarrollo, el metabolismo, la supervivencia, la diferenciación, la proliferación y la apoptosis. Son comúnmente utilizados en el tratamiento de enfermedades hematopoyéticas como las leucemias, debido a su capacidad de inducir apoptosis en células cancerosas y a su actividad antiinflamatoria e inmunosupresora (Kfir-Erenfeld et al., 2010). La mayoría de los efectos de los GCs están mediados a través del receptor de glucocorticoides (GR), un miembro de la superfamilia de receptores esteroidales.

Después de que el ligando se une al GR, éste sufre un cambio conformacional que lleva a su homodimerización (Stahn and Buttgereit, 2008). El dímero del GR se transloca al núcleo para regular la expresión génica por medio de su unión a los elementos de respuesta a GCs (GREs). Al unirse a los GREs, el GR sufre un cambio conformacional que le permite reclutar coactivadores y corepresores y complejos de remodelación de la cromatina, influenciando la actividad de la RNA polimerasa II y modulando la transcripción génica por medio de transactivación o transrepresión (Beck et al., 2011).

Regulación del GR por la GSK3

La GSK3 es una Serina/Treonina quinasa que fue inicialmente identificada como reguladora de la síntesis de glicógeno dependiente de insulina, pero se ha demostrado que es una quinasa multifuncional relacionada con el metabolismo celular, la transducción de señales, el crecimiento, la diferenciación, y la muerte celular (Forde and Dale, 2007). Existen dos isoformas de la GSK3 y estas son la GSK3α y la GSK3β. La GSK3 actúa sobre una gran variedad de substratos, incluyendo la glicógeno sintasa, Tau, c-Myc, β-Catenina, MCL-1 y la ciclina D. Esta quinasa facilita la vía intrínseca e inhibe la vía extrínseca de la apoptosis (Beurel and Jope, 2006)

Previamente se ha descrito la fosforilación del GR humano por la GSK3β en la serina 404 de manera dependiente de hormona y esta fosforilación es importante para la estabilidad de la proteína, regulando la expresión génica (Galliher-Beckley et al., 2008). Por otro lado, la GSK3β fosforila al GR de rata en la treonina 171. Adicionalmente, se ha descrito que en ausencia de ligando, la GSK3α se encuentra unida al GR (Spokoini et al., 2010). Por último, se ha descrito que el GR interactúa con la GSK3β en presencia de GCs (Galliher-Beckley et al., 2008).

Leucemia Linfocítica Crónica

La Leucemia Linfocítica Crónica (LLC) es la leucemia mas común en países occidentales, representando aproximadamente el 30% de las leucemias, un 90% de las leucemias linfoides crónicas y un 7% de los linfomas no-Hodkin (Montserrat and Rozman, 1995). La LLC es una patología caracterizada por la expansión monoclonal de linfocitos B de pequeño tamaño y con apariencia madura aunque funcionalmente inmaduros (Chiorazzi et al., 2005). La LLC se manifiesta por linfocitosis absoluta permanente en sangre periférica, acompañada de infiltración linfocitaria en médula ósea y tejidos linfáticos (Dighiero and Hamblin, 2008). Actualmente se considera que la LLC es una enfermedad causada por una apoptosis inapropiada, ya que las células circulantes de LLC no proliferan y se encuentran paradas en la fase G_0/G_1 del ciclo celular (Decker et al., 2003).

Los GCs son potentes inductores de la apoptosis en células de LLC, a través de un mecanismo dependiente de caspasas (McConkey et al., 1991) (Chandra et al., 1997).

También se sabe que los GCs regulan la inducción de BIM a nivel de proteína y ARNm en células de LLC (Iglesias-Serret et al., 2007). Sin embargo, el mecanismo de la apoptosis inducida por GCs en la LLC sigue siendo desconocido. A pesar de que el efecto pro-apoptótico de los GCs en células de LLC se conoce hace muchos años, su uso se limita a menudo a su actividad inmunosupresora con el fin de controlar fenómenos autoinmunes. Los GCs son de interés en el tratamiento de la LLC, debido a que pueden inducir apoptosis de manera independiente de p53 y los defectos en p53 están fuertemente asociados a la quimioresistencia (Thornton et al., 2003).

Objetivos

1. Analizar el efecto de los GCs en células Jurkat parentales, GR wt y LS7.

2. Analizar el papel de la actividad de la GSK3 en la vía de señalización mediada por GCs.

3. Estudiar el papel de la actividad de la GSK3 en la apoptosis inducida por GCs en células de LLC.

Resultados

1. Análisis del efecto de los GCs en células Jurkat Parentales, GR wt y LS7.

La dexametasona induce apoptosis en células Jurkat GR wt y LS7.

Nuestro grupo tiene una amplia experiencia en el estudio de los miembros de la familia de BCL-2 y su regulación en la apoptosis inducida por diferentes drogas, como los GCs, en células de LLC. Las células primarias de pacientes con LLC son difíciles de transfectar de manera exitosa sin afectar la viabilidad celular. Por esta razón, utilizamos una línea Jurkat parental (PT) que expresa un GR no funcional (Riml et al., 2004). Este GR tiene una mutación de pérdida de función en uno de los alelos (R477H). Esta mutación afecta la capacidad transactivadora y transrepresora del GR, pero no su unión al ligando o su translocación al núcleo. Estas células PT se transfectaron de manera estable con el GR de rata bajo el control del promotor de la β-actina para asegurar su expresión constante (Jurkat GR wt) y con el mutante LS7 (Jurkat LS7) (Helmberg et al., 1995). Este mutante tiene dos mutaciones cerca del dominio de unión al ADN del GR (Fig. 20) y por lo tanto presenta un

potencial transactivador muy bajo o nulo, mientras que conserva su potencial transrepresor. Después de tratar estas células con dexametasona durante 24 horas observamos que la línea Jurkat PT fueron resistentes al tratamiento con GCs, mientras que las líneas Jurkat GR wt y LS7 fueron sensibles a la dexametasona (Fig.21). La línea Jurkat GR wt fue más sensible al tratamiento con GCs que las células Jurkat LS7, probablemente debido a que su receptor mantiene su capacidad transactivadora de genes.

Efecto de la dexametasona sobre la expresión génica en células Jurkat PT, GR wt y LS7.

Para confirmar la especificidad de nuestro modelo, la actividad del GR se midió utilizando una construcción MMTV-Luc en células Jurkat GR wt y LS7. Esta construcción reportera tiene dos sitios de unión consensus para el GR o GREs (Drouin et al., 1993). De acuerdo con estudios previos (Helmberg et al., 1995) el GR wt indujo la actividad luciferasa del MMTV-Luc y el mutante LS7 mostró un potencial de transactivación mínimo (Fig. 22).

Estas líneas celulares se utilizaron para analizar el efecto de los GCs sobre la expresión de la proteína pro-apoptótica BIM. La dexametasona indujo la expresión de las tres isoformas de BIM (BIM-EL, BIM-L y BIM-S) de manera dosis dependiente en células Jurkat GR wt y LS7 (Fig. 23). También analizamos el efecto de los GCs sobre la expresión de la proteína anti-apoptótica MCL-1 y observamos que los niveles de ésta disminuyen en ambas líneas celulares, facilitando la muerte celular por apoptosis. Al analizar por RT-MLPA los niveles de mensajero de los miembros de la familia de BCL-2 y otros genes relacionados con la apoptosis observamos que las células Jurkat PT no sufrieron ningún cambio a nivel transcripcional en respuesta al tratamiento con dexametasona. Las líneas Jurkat GR wt y LS7 mostraron perfiles de expresión parecidos, al inducirse tanto *BIM* como *HLAP1* en respuesta a los GCs en ambas líneas (Fig. 24).

***BIM* y *GILZ* son genes de inducción temprana por GCs.**

Analizamos a tiempos cortos a *GILZ* como un gen regulado por el GR y a *BIM* como un gen que no tiene GREs en su promotor. Se trataron las células Jurkat GR wt con dexametasona por 1 hora y se analizaron los niveles de ARNm de los dos genes. *BIM* y *GILZ* se indujeron de manera significativa (Fig. 25) en respuesta al tratamiento con GCs. Pre-incubamos las células con un inhibidor de la síntesis proteica, la cicloheximida (CHX),

o con un inhibidor de la transcripción, la actinomicina D (Act D). La inducción transcripcional de *BIM* (Fig. 25A) y *GILZ* (Fig. 25B) en respuesta al tratamiento con dexametasona es independiente de síntesis proteica, pero dependiente de transcripción ya que el tratamiento con Act D abolió la respuesta hormonal.

Análisis de la actividad transcripcional de diferentes construcciones del promotor de *BIM* en respuesta a los GCs.

Buscando analizar la inducción transcripcional de *BIM* en respuesta al tratamiento con GCs, utilizamos 4 construcciones diferentes del promotor de *BIM* (Fig. 26). BIM#1 contiene 874 pb por encima del sitio de inicio de transcripción del promotor humano de *BIM*. BIM#2 contiene el intrón 1 insertado entre la secuencia del promotor/exon1 humano y el gen de la luciferasa. BIM#3 contiene 3.3 kb por encima del sitio de inicio de transcripción del promotor humano de *BIM*. BIM#4 contiene 2.5 kb por encima del sitio de inicio de transcripción, el exón 1, el primer intrón y la región no codificante del exón 2 del promotor de rata de *BIM*. Esta última construcción tiene mutados dos sitios de unión de FOXOs. Transfectamos las células Jurkat GR wt con estas construcciones y tratamos con dexametasona durante 24 horas (Fig. 27). En ninguno de los cuatro casos observamos actividad luciferasa en respuesta al tratamiento con dexametasona, wortmanina o cAMP, otros inductores de *BIM* (Jiang et al., 2004) (Zhang and Insel, 2004) (Zambon et al., 2011). Solo la lovastatina fue capaz de inducir la actividad luciferasa de BIM#4.

2. Análisis del papel de la actividad de la GSK3 en la vía de señalización mediada por GCs.

La apoptosis inducida por la dexametasona es revertida por la inhibición de la GSK3.

Quisimos analizar las posibles vías de señalización relacionadas con la apoptosis inducida por GCs. Analizamos el efecto de diferentes inhibidores de quinasas, de HDACs, de BCL-2 y del proteasoma sobre la viabilidad celular de células Jurkat GR wt (Table 10). Como era de esperar, el tratamiento con dexametasona por 24 horas produjo una disminución significativa de la viabilidad celular (Fig. 28). Sólo el SB216763, un inhibidor de la GSK3, revirtió significativamente la muerte inducida por GCs. Esto sugiere un papel importante de la GSK3 en la vías de señalización de la apoptosis inducida por GCs. La inhibición de la

GSK3 revirtió significativamente la inducción de BIM y GILZ a nivel de proteína (Fig. 29). Estos resultados establecieron por primera vez que *GILZ*, un gen regulado por GCs, requiere la actividad de la GSK3 para su inducción proteica dependiente de GCs. La inhibición de la GSK3 también revirtió la disminución en los niveles proteicos de MCL-1 causada por los GCs (Fig. 29). Además de esto, revirtió la inducción de las caspasas-9 y -3, contribuyendo al bloqueo de la muerte inducida por el tratamiento con dexametasona (Fig. 29).

La inhibición de la GSK3 altera la expresión génica mediada por GCs a nivel transcripcional en células Jurkat GR wt.

Se analizó el perfil de RT-MLPA de las células Jurkat GR wt a tiempos cortos de tratamiento (90 minutos) con GCs en células Jurkat GR wt (Fig. 30). El tratamiento con dexametasona indujo significativamente la expresión de *BIM* y *HIAP1*. Utilizamos al SB216763 para evaluar el papel de la GSK3 en la regulación transcripcional temprana por los GCs. Por medio de RT-q PCR observamos que la inhibición de la GSK3 revirtió la inducción transcripcional de *BIM*, *GILZ* y *HIAP1* en repuesta a los GCs (Fig. 31). Los efectos sobre *BIM* y *HIAP1* se confirmaron por medio de la técnica RT-MLPA (Fig. 32). Este efecto sobre los niveles de ARNm de *GILZ* fueron confirmados en otras líneas celulares de origen distinto (Fig. 33). El SB216763 no tuvo ningún efecto sobre la transrepresión mediada por GCs en células Jurkat GR wt, tal como se observó con *BCL-3* y *MYC*, dos genes que son transreprimidos en repuesta al tratamiento con dexametasona (Fig. 34).

Adicionalmente, analizamos el efecto de la inhibición de Akt y de las HDACs en la regulación transcripcional de BIM y GILZ. Nuestros resultados apoyan la idea de que Akt y las HDACs cumplen un papel importante en la regulación transcripcional de estos dos genes. La inhibición de Akt potenció la inducción de *GILZ* en respuesta a los GCs sin afectar los niveles de *BIM* (Fig. 35A). La inhibición de las HDACs con SAHA afectó los niveles basales de *BIM* (Fig. 35A) y fue capaz de revertir la inducción transcripcional dependiente de GCs de *GILZ* (Fig. 35B).

La inhibición de la GSK3 fue capaz de revertir la actividad luciferasa del MMTV-Luc inducida por GCs (Fig. 36A). Éste fue también el caso de la construcción p1940-Luc del

promotor de *GILZ* (Fig. 36B). Estos resultados sugieren que la actividad de la GSK3 puede ser importante para determinar la respuesta transcripcional del GR al tratamiento con GCs.

La inhibición de la GSK3 no altera la expresión génica mediada por GCs a nivel transcripcional en células Jurkat LS7.

Las células Jurkat LS7 respondieron de manera diferente a la inhibición de la GSK3 en comparación con las células Jurkat GR wt. Estas células mueren menos que las Jurkat GR wt en presencia de GCs y el SB216763 revirtió la apoptosis pero en menor porcentaje (Fig. 37). *GILZ* se indujo muy poco en estas células de acuerdo con la poca capacidad transactivadora del mutante LS7 (Fig. 38A). *BIM* y *HIAP1* también se indujeron transcripcionalmente en respuesta a los GCs, pero menos que en las Jurkat GR wt (Fig. 38B-C). La inhibición de la GSK3 no tuvo ningún efecto sobre la inducción transcripcional de *GILZ*, *BIM* y *HIAP1*. Este efecto sugiere que la inhibición de la GSK3 la regulación transcripcional mediada por GCs cuando ésta depende de la actividad transactivadora del GR.

La inhibición de la GSK3 afecta el reclutamiento del GR y la RNA polimerasa II al promotor de *GILZ*.

Quisimos determinar el mecanismo mediante el cual la GSK3 regula al GR. Tratamos las células Jurkat GR wt con dexametasona por 2 horas y evaluamos la ocupación del promotor de *GILZ* por medio de la técnica de inmunoprecipitación de la cromatina (ChIP). Observamos un aumento significativo en el reclutamiento del GR (Fig. 39A) y la RNA polimerasa II (Fig. 39B) al promotor de *GILZ* en respuesta al tratamiento con dexametasona. La inhibición de la GSK3 con el SB216763 redujo significativamente la unión de estas dos proteínas al promotor de *GILZ*. Esto demuestra que la activación transcripcional dependiente de GCs del GR requiere que la vía de la GSK3 esté activa.

La silenciación génica de la GSK3β suprime la expresión génica estimulada por GCs.

Debido a que los inhibidores de la GSK3 no distinguen entre sus dos isoformas, analizamos el efecto de la silenciación de la GSK3α y la GSK3β en la regulación transcripcional mediada por GCs. Transfectamos células HeLa con siRNAs para las dos

isoformas de la GSK3 (Fig. 40) y observamos que el silenciamiento de la GSK3β o de GSK3α/β resultó en una disminución significativa de los niveles basales de *GILZ* y de su inducción en respuesta al tratamiento con dexametasona (Fig. 41A). Otros genes inducidos por GCs siguieron el mismo comportamiento, tales como *BMF*, *MCL-1* y *BCL-XL* (Fig. 42). Este no fue el caso de *HIAP1*. En el caso de la construcción MMTV-Luc la inhibición de las dos isoformas de la GSK3 produjo un incremento de la actividad luciferasa basal (Fig. 42B). Sin embargo, el silenciamiento de la GSK3β o de GSK3α/β resultó en la inhibición de la actividad luciferasa inducida por GCs.

La función transcripcional del GR está bloqueada en MEFs deficientes para la GSK3β

De acuerdo con los resultados obtenidos en células HeLa, las células MEF deficientes para la GSK3β no indujeron los niveles de ARNm de *GILZ* en respuesta al tratamiento con GCs, a diferencia de las células WT o deficientes para la GSK3α que sí lo hicieron (Fig. 43A). Éste fue también el caso de la construcción MMTV-Luc donde los MEFs deficientes para la GSK3β no indujeron la actividad luciferasa de esta construcción (Fig. 43B). Debido a que las células MEF no mueren por apoptosis, no se observaron cambios en el perfil de RT-MLPA de estas células, aunque sí se observaron diferencias en los niveles basales de expresión génica entre las líneas celulares (Fig. 44). Estos resultados sugieren que la GSK3β, pero no la GSK3α, es necesaria para la actividad transcripcional mediada por el GR.

La inhibición de la GSK3 afecta la distribución celular del GR en respuesta a GCs.

Analizamos el papel de la GSK3 en la regulación de la localización subcelular del GR en las células Jurkat GR wt por medio de la técnica de fraccionamiento celular (Fig. 45 A-B). El GR se mostró principalmente citoplasmático en células sin estimular y el tratamiento con dexametasona indujo su translocación al núcleo. La localización del GR se redujo significativamente cuando las células eran pre-incubadas con SB216763. Este resultado se confirmó por inmunocitoquímica (Fig. 46). Este efecto sobre la localización del GR fue parcialmente inhibido por la pre-incubación con leptomicina B (LMB), tal y como se observó por medio de la técnica de fraccionamiento celular (Fig. 45A-B). Estos resultados sugieren un posible mecanismo de exporte nuclear del GR dependiente de CRM1 en

respuesta a la inhibición de la GSK3. Estos resultados también indican que la inhibición de la GSK3 a tiempos cortos es capaz de afectar la localización del GR, disminuyendo sus niveles nucleares en células tratadas con dexametasona. En el caso de las células HeLa, el tratamiento con GCs siempre resultó en la translocación del GR al núcleo incluso cuando la GSK3β o GSK3α/β estaban silenciadas (Fig. 47-48). Adicionalmente, la silenciación de la GSK3β o GSK3α/β, resultó en un aumento en los niveles de expresión del GR (Fig. 48).

La inhibición de la GSK3 altera la actividad transcripcional de los mutantes de fosforilación del GR.

Analizamos la actividad transcripcional de los mutantes para los residuos descritos que son fosforilados por la GSK3. Estos son mutantes de la treonina 171 y la serina 424 del receptor de rata. Ambos aminoácidos fueron substituidos por alanina, de manera que no pudieran ser fosforilados por la GSK3 (Fig. 49). Tanto la construcción WT como las mutantes fueron expresadas en células Jurkat PT y evaluamos la actividad luciferasa de la construcción MMTV-Luc (Fig. 50) y la inducción de *GILZ* a nivel endógeno (Fig. 51). Ambos se indujeron en respuesta al tratamiento con dexametasona y ambos fueron revertidos por el SB216763 en las células transfectadas con todas las construcciones. Estos resultados sugieren que existe un mecanismo adicional que no implica la fosforilación de estos residuos, por medio del cual la GSK3 regula la actividad transcripcional del GR.

3. Estudio del papel de la GSK3 en la apoptosis inducida por GCs en células de LLC

La inhibición de la GSK3 afecta la apoptosis inducida por GCs y la inducción proteica y génica dependiente de GCs en células de LLC.

Quisimos estudiar el efecto de la inhibición de la GSK3 sobre la apoptosis inducida por GCs en células de pacientes con LLC. Estas células murieron por apoptosis en respuesta al tratamiento con dexametasona y la pre-incubación con SB216763 redujo significativamente el porcentaje de muerte en la mayoría de las muestras analizadas (Fig. 52A and Table 11). En estas muestras la inhibición de la GSK3 también revirtió la inducción transcripcional de *BIM* y *GILZ* (Fig. 53A). En aquellas muestras en las que no se observó reversión de la muerte celular por la inhibición de la GSK3 (Fig. 52B and Table 11) tampoco se observó reversión en los niveles de ARNm de *BIM* en respuesta a GCs (Fig. 53B). En el caso de

GILZ, sí se observó reversión en sus niveles de ARNm en respuesta a la inhibición de la GSK3 en estas muestras (Fig. 53). A nivel de proteína tanto BIM como GILZ se indujeron en respuesta al tratamiento con GCs y se observó reversión con el SB216763 en la mayoría de las muestras analizadas (Fig. 54).

Discusión

Los GCs inducen apoptosis en diferentes tipos celulares, incluyendo células de leucemia, en un proceso regulado por múltiples vías de señalización que alteran el perfil de expresión génica a través de la transactivación y la transrepresión mediada por el GR (Kfir-Erenfeld et al., 2010). Nuestro grupo demostró previamente que los GCs inducen apoptosis en las células de LLC (Bellosillo et al., 1997) por medio de un mecanismo que regula la proteína pro-apoptótica BIM a nivel proteico y transcripcional (Iglesias-Serret et al., 2007). Sin embargo, las células primarias de LLC son difíciles de transfectar sin afectar la viabilidad celular, por lo que utilizamos tres líneas celulares Jurkat. La línea PT expresa un receptor no funcional del GR. Esto es debido a una mutación de pérdida de función (R477H) en uno de los alelos del GR (Riml et al., 2004). Esta línea fue totalmente resistente al tratamiento con GCs. La línea PT se transfectó de manera estable con el GR de rata bajo el control del promotor de la β-actina para asegurar su expresión constante (Jurkat GR wt) y con el mutante LS7 (Jurkat LS7) (Helmberg et al., 1995). Este GR tiene dos mutaciones cerca del DBD (Fig. 20) y por lo tanto tiene un potencial transactivador muy bajo o nulo, mientras que conserva su potencial transrepresor. Estas dos líneas fueron sensibles al tratamiento con GCs. Adicionalmente, confirmamos que *BIM* y *GILZ* son genes de inducción temprana por GCs, ya que su inducción es independiente de síntesis proteica y dependiente de transcripción.

En esta tesis se demuestra que la GSK3 regula la actividad transcripcional del GR afectando su localización y su reclutamiento a promotores de genes diana, afectando su expresión. Se observó un papel crítico para la GSK3 en la muerte celular dependiente de GCs ya que su inhibición con el inhibidor específico SB216763 revirtió la apoptosis inducida por GCs de manera consistente con estudios previos (Nuutinen et al., 2009) (Sun et al., 2009) (Spokoini et al., 2010). MCL-1 contiene un sitio consenso conservado de fosforilación por la GSK3, que regula su degradación por la vía del proteasoma (Maurer et al., 2006). Hemos observado que la inhibición de MCL-1 dependiente de GCs fue revertida

por la inhibición de la GSK3. Esto fue acompañado por la inhibición de la activación de la caspasa-9 y -3 y por la reducción de la inducción de BIM (Nuutinen et al., 2009) y de GILZ. A nuestro conocimiento, no existen estudios previos que demuestren la participación de la GSK3 en la regulación de la inducción dependiente de GCs de GILZ. También se evaluó el efecto de la inhibición de la GSK3 sobre la apoptosis inducida por GCs en células primarias de LLC. El pre-tratamiento con SB216763 revertió la muerte celular inducida por GCs en la mayoría de los pacientes analizados. Además, la inducción de proteína y ARNm dependiente de GC de BIM y GILZ fue revertida por la inhibición de la GSK3 en la mayoría de las muestras analizadas.

La inhibición farmacológica de la GSK3 resultó en una inducción reducida de los niveles de ARNm de *BIM*, *GILZ* y *HLAP1* y de construcciones sensibles a los GCs en células Jurkat GR wt. Este efecto sobre los niveles de ARNm endógeno de *GILZ* se confirmó en varias líneas celulares de origen diferente. En las células Jurkat LS7 la dexametasona indujo los niveles de ARNm de *BIM* y *HLAP1*, pero en menor porcentaje que en las Jurkat GR wt. *GILZ* se indujo levemente en las Jurkat LS7 debido a la baja capacidad transactivadora de genes de este GR. La pre-incubación con SB216763 no tuvo ningún efecto sobre la inducción de los genes de respuesta a GCs en estas células. Esto sugiere que el SB216763 tiene un efecto sobre la capacidad transactivadora del GR.

Los ensayos de ChIP mostraron que la inhibición de la GSK3 reduce el reclutamiento del GR y la ARN polimerasa II al promotor de GILZ después del tratamiento con dexametasona. Estos resultados indican que la activación transcripcional dependiente de GCs requiere una señalización funcional de la GSK3 y muestra por primera vez que la GSK3 podría ser requerida por el GR para su activación como un factor de transcripción y para el reclutamiento de la RNA polimerasa II. Adicionalmente, demostramos que la inhibición de la GSK3 no afecta la transrepresión mediada por GCs.

El presente estudio demuestra que la GSK3β es la isoforma involucrada en la regulación de la activación transcripcional del GR en respuesta a los GCs. El silenciamiento de la GSK3α y la GSK3β en células HeLa resultó en la activación del MMTV-Luc a nivel basal, pero sólo el silenciamiento de la GSK3ß fue eficaz en la reversión de su activación transcripcional dependiente de GCs. El silenciamiento de la GSK3β y de las dos isoformas

de la GSK3 redujo la expresión tanto basal como inducida por GCs del ARNm de *GILZ*. El silenciamiento de la GSK3β y de la las dos isoformas de la GSK3 produjo una reversión en la inducción de genes dependiente de GCs. Sin embargo, la *HIAP1* fue inducida por el tratamiento con dexametasona, incluso cuando la GSK3β fue silenciada. Además, las células MEF deficientes para la GSK3β fueron incapaces de inducir los niveles de ARNm de *GILZ* y la actividad luciferasa de la construcción promotora MMTV-Luc en respuesta al tratamiento con dexametasona.

Demostramos que la inhibición de la GSK3 en combinación con los GCs en células Jurkat GR wt causa una exportación rápida del GR del núcleo, causando una bajada en su actividad transcripcional temprana. La exportación nuclear inducido por el SB216763 fue parcialmente inhibida por el tratamiento con LMB, lo que sugiere que podría haber una exportación nuclear del GR dependiente de CRM1 en respuesta a la inhibición de la GSK3.

Se demostró que el silenciamiento de la GSK3β y de la GSK3α/β en células HeLa resulta en la reducción de la inducción dependiente de GCs de *BMF*, *BCL-XL* y *MCL-1*, genes previamente descritos como diana de GCs (Scoltock et al., 2007) (Ploner et al., 2008) (Lynch et al., 2010) (Xu et al., 2011). Sin embargo, observamos que en estas condiciones el tratamiento con GCs siempre llevó a una acumulación de GR en el núcleo y un aumento en los niveles de expresión del GR en respuesta al tratamiento con GCs. El aumento en los niveles de expresión del GR en respuesta al silenciamiento de la GSK3β está de acuerdo con la fosforilación de la serina 404 por la GSK3β, que previamente había sido descrita y que favorece la regulación negativa de la proteína del GR por medio de su degradación proteasomal (Galliher-Beckley et al., 2008).

La GSK3 también fosforila la Thr171 del GR de rata (Rogatsky et al., 1998). Este sitio de fosforilación no está presente en la secuencia humana del GR, lo cual indica que la regulación de este residuo por la GSK3 es específica de la especie (Galliher-Beckley and Cidlowski, 2009). Nuestros resultados con mutantes del GR de rata de los residuos que son fosforilados por la GSK3 muestran que estas mutaciones no anulan la capacidad del GR de trasladarse al núcleo y transactivar genes diana. Todos los mutantes fueron capaces de inducir los niveles endógenos de ARNm de *GILZ*. La inhibición de la GSK3 revirtió la inducción de la actividad luciferasa de la construcción reportera MMTV-Luc y del ARNm

de *GILZ* en todos los mutantes. Estos resultados indican que podría existir un mecanismo adicional, que no implica la fosforilación de estos residuos, por medio del cual la GSK3 regula la actividad transcripcional del GR. La línea celular Jurkat PT fue capaz de inducir ligeramente los niveles de expresión de ARNm de *GILZ*, mientras que fue incapaz de inducir la actividad lucifera de la construcción MMTV-Luc. Estos resultados no están claros, aunque se han descrito previamente (Riml et al., 2004) y pueden ser el reflejo de las diferencias específicas de promotor o de efectos que son independientes de la actividad transcripcional del GR sobre el promotor de *GILZ* (Kfir-Erenfeld et al., 2010).

Se ha descrito previamente que, en ausencia de ligando, la GSK3α está unida al GR y que la exposición a los GCs o al inhibidor de la GSK3 inhibe esta interacción (Spokoini et al., 2010). También se ha descrito que el GR se asocia con la GSK3β en presencia de dexametasona, pero no con la GSK3α (Galliher-Beckley et al., 2008). Nuestros resultados indican que las isoformas de la GSK3 regulan la respuesta celular del GR por medio de diferentes mecanismos, además de la fosforilación del GR mediada por la GSK3.

En resumen, el presente estudio demuestra la participación de la GSK3β en la inducción transcripcional de genes por GCs a través de la regulación del reclutamiento del GR y la ARN polimerasa II a genes diana y afectando la localización subcelular de la proteína del GR.

Conclusiones

- *BIM* y *GILZ* son genes de inducción temprana por GCs en células Jurkat GR wt, ya que su inducción es independiente de síntesis proteica e independiente de transcripción.
- La inhibición de la GSK3 revirte la apoptosis inducida por GCs en células Jurkat GR wt por medio de la prevención de la disminución regulada de MCL-1 y la activación de las caspasas-9 y -3 dependientes de GCs.
- La inhibición de la GSK3 resulta en la reducción de la expresión proteica y de ARNm inducida por GCs en células Jurkat GR wt y HeLa y no afecta la transrepresión inducida por GCs en células Jurkat GR wt.

- En células HeLa donde la GSK3β ha sido silenciada y en MEFs deficientes para la GSK3β hay una reducción en la expresión de ARNm inducida por GCs y de la actividad reportera de construcciones de respuesta a GCs.
- La inhibición de la GSK3 perjudica la unión dependiente de GCs del GR y la RNA polimerasa II al promotor endógeno de *GILZ* en células Jurkat GR wt por medio de un mecanismo que afecta la localización de la proteína del GR y que disminuye los niveles nucleares tempranos del GR.
- La GSK3 regula la actividad transcripcional del GR de rata por medio de un mecanismo que no incluye la fosforilación de residuos descritos como fosforilables por la GSK3, como la serina 424 y la treonina 171.
- En células primarias de LLC la inhibición de la GSK3 resulta en la reducción de la apoptosis inducida por GCs y perjudica la inducción mediada por GCs de la proteína y el ARNm de *BIM* y *GILZ* en la mayoría de las muestras analizadas.

IX. Abbreviations

Act D: actinomycin D
AF-1: activation function-1
AF-2: activation function-2
Akti: Akt inhibitor VIII
APAF-1: apoptotic protease-activating factor-1
APC: allophycocyanin
AR: androgen receptor
ATCC: American Type Culture Collection
BAK: BCL-2 antagonis/killer-1
BAX: BCL-2 associated X protein
BCA: bicinchoninic acid
BCL-2: B-cell lymphoma-2
BCL-XL: BCL-2-related gene
BFK: BCL-2-family kin
BH: BCL-2 homology
BIR: baculoviral IAP repeat
BIRC: baculoviral IAP repeat-containing
Bis I: bisindolylmaleimide I
BOK: BCL-2 related ovarian killer
CARD: caspase-recruitment domain
Caspases: cysteine-dependent-aspartate-directed proteases
CBP: CREB-binding protein
CC: coiled-coil
CDKs: cyclin-dependent kinases
cFLIP: FLICE inhibitory protein
ChIP: Chromatin inmunoprecipitation
CLL: Chronic Lymphocytic Leukemia
CREB: Cyclic AMP response element binding protein
CRM1: chromosome-region maintenance 1
CRT: calreticulin
CHX: Cycloheximide
DBD: DNA-binding domain
DED: death effector domain
Dex: dexamethasone
DISC: Death-Inducing Signaling Complex
DR: death receptors
DMSO: dimethyl sulfoxide
ER: estrogen receptor
FBS: fetal bovine serum
FCR: combination of fludarabine, cyclophosphamide and rituximab
GCs: Glucocorticoids
GILZ: Glucocorticoid-induced Leucine Zipper
GR: glucocorticoid receptor
GREs: glucocorticoid response elements
GSK3: glycogen synthase kinase-3
GUS: β-glucoronidase
H: hinge región
HDACs: histone deacetylases
HIAPs: human inhibitors of apoptosis

HSF1: Heat shock factor 1
HSP: Heat shock protein
IAPs: inhibitors of apoptosis
IP: Immunoprecipitation
LiCl: Lithium chloride
LB: Luria Bertani
LBD: ligand-binding domain
LMB: leptomycin B
LRR: leaucine repeats
LZ: leucine zipper
MAPKs: mitogen activated protein kinases
MCL-1: myeloid cell leukemia 1
MEFs: Mouse embryonic fibroblasts
MOMP: Mitochondrial outer membrane permeabilization
MR: mineralocorticoid receptor
nGREs: negative GREs
NCoR: nuclear receptor corepressor
NES: Nuclear export signal
NFAT: nuclear factor of activated T cells
NLS: nuclear localization signals
NOD: Nucleotide-binding and oligomerization domain
NPC: nuclear pore complex
NTD: N-terminal transactivation domain
PBS: phosphate saline buffer
PE: phycoerythrin
PI3K: phosphatydilinositol-3-kinase
PKB: protein kinase B
PKC: protein kinase C
PR: progesterone receptor
PT: parental
RING: Really Interesting New Gene
RNA pol II: RNA polymerase II
RT-qPCR: Reverse Transcriptase quantitative PCR
RT-MLPA: Reverse Transcriptase Multiplex Ligation-dependent Probe Amplification
SAHA: Suberoylanilide hydroxamic acid
SB: SB216763
SD: standard deviation
SEM: standard error of the mean
SGK-1: serum and GC-regulated kinase-1
SMRT: silencing mediator or retinoid and thyroid receptors
SRCs: steroid receptor coactivators
STAT6: signal transducer and activator of transcription 6
tBID: truncated BID
TBP: TATA box-binding protein
TBS: tris buffered saline
TRAIL: TNF-related apoptosis-inducing ligand
TSC: tuberous sclerosis complex
TSS: Transcription Starting Site
UBC: ubiquitin-conjugating

WB: Western Blot
Wort: Wortmannin

X. Publications

Glycogen Synthase Kinase-3β Is Involved in Ligand-Dependent Activation of Transcription and Cellular Localization of the Glucocorticoid Receptor

Camila Rubio-Patiño, Claudia M. Palmeri, Alba Pérez-Perarnau, Ana M. Cosialls, Cristina Moncunill-Massaguer, Diana M. González-Gironès, Lluís Pons-Hernández, José M. López, Francesc Ventura, Joan Gil, Gabriel Pons,* and Daniel Iglesias-Serret*

Departament de Ciències Fisiològiques II (C.R.-P., C.M.P., A.P.-P., A.M.C., C.M.-M., D.M.G.-G., L.P.-H., F.V., J.G., G.P., D.I.-S.), Institut d'Investigació Biomèdica de Bellvitge, Universitat de Barcelona, L'Hospitalet de Llobregat, E-08907 Barcelona, Spain; and Department de Bioquímica i Biología Molecular, Unitat de Bioquímica, Institut de Neurociències (J.M.L.), Facultat de Medicina, Universitat Autònoma de Barcelona, E-08193 Cerdanyola del Vallès, Barcelona, Spain

Glucocorticoids (GC) induce cell cycle arrest and apoptosis in different cell types and therefore are widely used to treat a variety of diseases including autoimmune disorders and cancer. This effect is mediated by the GC receptor (GR), a ligand-activated transcription factor that translocates into the nucleus where it modulates transcription of target genes in a promoter-specific manner. Glycogen synthase kinase-3 (GSK3) regulates GR response by genomic and nongenomic mechanisms, although the specific role of each isoform is not well defined. We used GSK3 pharmacological inhibitors and isoform-specific small interfering RNA to evaluate the role of GSK3 in the genomic regulation induced by GC. GSK3 inhibition resulted in the reduction of GC-induced mRNA expression of GC-induced genes such as *BIM*, *HIAP1*, and *GILZ*. Knockdown of GSK3β but not GSK3α reduced endogenous *GILZ* induction in response to dexamethasone and GR-dependent reporter gene activity. Chromatin immunoprecipitation experiments revealed that GSK3 inhibition impaired the dexamethasone-mediated binding of GR and RNA polymerase II to endogenous *GILZ* promoter. These results indicate that GSK3β is important for GR transactivation activity and that GSK3β inhibition suppresses GC-stimulated gene expression. Furthermore, we show that genomic regulation by the GR is independent of known GSK3β phosphorylation sites. We propose that GC-dependent transcriptional activation requires functional GSK3β signaling and that altered GSK3β activity influences cell response to GC. **(*Molecular Endocrinology* 26: 1508–1520, 2012)**

NURSA Molecule Pages[†]: Nuclear Receptors: GR.

Glucocorticoids (GC) are steroid hormones that regulate essential biological processes, including growth, development, metabolism, survival, differentiation, proliferation, and apoptosis in a large variety of cell types and are commonly used in the treatment of various inflammatory diseases and cancer. Specifically, GC are currently being used in the treatment of hematopoietic malignancies such as chronic lymphocytic leukemia (CLL), T-acute lymphoblastic leukemia, multiple myeloma, and non-Hodgkin's lymphoma due to their abil-

ISSN Print 0888-8809 ISSN Online 1944-9917
Printed in U.S.A.

doi: 10.1210/me.2011-1366 Received December 16, 2011. Accepted June 12, 2012.
First Published Online July 6, 2012

* D.I.-S. and G.P. contributed equally to this work.

[†] Annotations provided by Nuclear Receptor Signaling Atlas (NURSA) Bioinformatics Resource. Molecule Pages can be accessed on the NURSA website at www.nursa.org.

Abbreviations: AR, Androgen receptor; ChIP, chromatin immunoprecipitation; CLL, chronic lymphocytic leukemia; CRM1, chromosome region maintenance 1; GC, glucocorticoids; GR, GC receptor; GRE, GC response elements; GSK3, glycogen synthase kinase-3; LMB, leptomycin B; MEF, mouse embryonic fibroblast; RT-MLPA, reverse transcriptase multiplex ligation-dependent probe amplification; RT-qPCR, reverse transcriptase quantitative PCR; siRNA, small interfering RNA; WT, wild type.

ity to induce intrinsic caspase-dependent apoptosis in these cell types (1).

Most of the actions of GC are mediated through the GC receptor (GR), a member of the steroid receptor superfamily (2). The unliganded GR resides primarily in the cytoplasm in an inactive state as part of a large heat-shock protein heterocomplex that includes various chaperone proteins, such as heat-shock protein 90 (3). Upon GC binding, the GR undergoes a conformational change that results in its dissociation from the cytoplasmic chaperone multiprotein complex and unmasking of the nuclear localization signal, leading to its translocation to the nucleus. Once in the nucleus, the dimerized GR binds GC response elements (GRE), usually located in the promoter of GR-regulated genes, resulting in gene transactivation or transrepression (4).

It has been shown that the modulation of the GR phosphorylation cycle by phosphatases maintains steady-state receptor phosphorylation at a low basal level in the absence of ligand, and GC-dependent GR phosphorylation affects GR target gene expression (5). Previous studies have highlighted the involvement of different protein kinases in GC-mediated effects (6). Recently, a protein kinase screening in lymphoid cells showed that glycogen synthase kinase-3 (GSK3) has a role in GC-induced apoptosis (7). Pharmacological inhibition of GSK3 blocked GC-induced apoptosis in different hematopoietic cell lines (7), and attenuated GC-induced up-regulation of BIM (8), a Bcl-2 homology domain-3-only protein involved in GC-induced apoptosis in leukemia cells (9–11).

GSK3 is a serine/threonine protein kinase highly conserved from yeast to mammals (12–14). It was initially identified as a key regulator of insulin-dependent glycogen synthesis, but it has been demonstrated that GSK3 is a multifunctional kinase involved in cellular metabolism, signaling transduction, growth, differentiation, and cell fate determination (13). There are two homologous mammalian GSK3 isoforms encoded by different genes, *GSK3α* and *GSK3β*. They share 98% identity within their catalytic domain, but N- and C-terminal sequences diverge, making them structurally similar but not functionally identical (13, 15).

GSK3 demonstrates a preference for prephosphorylated (primed) substrates by different priming kinases (12–14). GSK3β phosphorylates different substrates, including glycogen synthase, and transcription factors such as c-myc, β-catenin, and Tau-microtubule-associated protein (12). There is a hormone-dependent GR phosphorylation on human serine 404 (Ser404) by GSK3β, which plays an important role in GR protein stability and regulates GR-dependent gene expression (6). Additionally, GSK3β-mediated phosphorylation of rat GR threonine 171 (Thr171) has been described (16). Different interactions between GSK3 and the GR have been previously described. In the absence of a ligand, GSK3α is bound to the GR, and exposure to GC leads to its dissociation from the GR (7). Moreover, it has been described that the GR associates with GSK3β in the presence of dexamethasone but not with GSK3α (6). Thus, it seems that GSK3 isoforms regulate GR cellular response by using different mechanisms.

In the present study, we have used pharmacological inhibitors and GSK3 isoform-specific small interfering RNA (siRNA) to analyze the role of GSK3 isoforms in the regulation of GR-mediated transcriptional activation.

Materials and Methods

CLL samples and cell isolation

Blood samples from CLL patients were obtained from the Hospital de Bellvitge, L'Hospitalet de Llobregat, Spain. CLL was diagnosed according to standard clinical and laboratory criteria. Written informed consent was obtained from all patients in accordance with the Hospital de Bellvitge Ethical Committee. Peripheral blood mononuclear cells were isolated by centrifugation on a Ficoll-Hypaque (Seromed, Berlin, Germany) gradient. Human lymphocytes were cultured immediately after thawing or isolation at a concentration of $0.5–3 \times 10^6$ cells/ml in RPMI 1640 culture medium (Biological Industries) supplemented with 10% heat-inactivated fetal bovine serum (Biological Industries, Kibbutz Beit Haemek, Israel), 2 mM L-glutamine, 100 U/ml penicillin, and 100 μg/ml streptomycin at 37 C in a humidified atmosphere containing 5% carbon dioxide.

Cell culture

Jurkat GR wild-type (WT) cells, derived from a parental cell line of Jurkat T-acute lymphoblastic leukemia cells harboring a nonfunctional GR were generated by expressing the rat GR under control of the β-actin promoter (17, 18). These cells were kindly provided by Dr. Carme Caelles (Institute for Research in Biomedicine, Universitat de Barcelona, Barcelona, Spain). Parental Jurkat, Jurkat GR WT, and BxPC-3 cells were grown in RPMI 1640 medium (Biological Industries), 2 mM L-glutamine, 100 μg/ml penicillin, and 100 mg/ml streptomycin at 37 C in a humidified atmosphere at 5% carbon dioxide. WT, GSK3$\alpha^{-/-}$, and GSK3$\beta^{-/-}$ mouse embryonic fibroblast (MEF) cells were kindly given by Dr. J. Woodgett (Samuel Lunenfeld Research Institute, Toronto, Canada). HeLa, MC3T3, and MCF-7 cells and WT, GSK3$\alpha^{-/-}$, and GSK3$\beta^{-/-}$ MEF cells were maintained in DMEM (Biological Industries) containing 10% fetal bovine serum (Biological Industries).

Plasmids and reagents

Dexamethasone and SB216763 were purchased from Sigma-Aldrich (St. Louis, MO). Akt inhibitor VIII, SB203580, U0126, LY294002, bisindolylmaleimide I, and rapamycin were purchased from Calbiochem (La Jolla, CA). SP600125, GSK650394, and KU0063794 were from Tocris Bioscience

(Bristol, UK). Lithium chloride (LiCl), PP242, and MG-132 were from Sigma-Aldrich, and LY333531 from Enzo Life Sciences. ABT-737 was purchased from Selleck Chemicals LLC (Houston, TX). Roscovitine was kindly provided by Dr. Jacint Boix (Universitat de Lleida, Lleida, Spain). Suberoylanilide hydroxamic acid (vorinostat, Zolinza) was obtained from Cayman Chemical (Ann Arbor, MI) and Kendine-92 (5-diaryl-1H-pyrrole-2-carboxamide derivates) was generously provided by Dr. Fernando Cossío (Universidad del Pais Vasco, Bilbao, Spain). Annexin V allophycocyanin was purchased from eBiosciences (San Diego, CA). MMTV-Luc reporter plasmid containing two consensus GRE was kindly provided by Dr. Carme Caelles (Institute for Research in Biomedicine, Universitat de Barcelona), and p-1940Luc (19) was a kind gift of Dr. Marc Pallardy (Institut National de la Santé et de la Recherche Médicale Unité 461, Université de Paris, Paris, France).

Analysis of apoptosis and cell viability by flow cytometry

Cell viability was determined by measuring phosphatidylserine exposure and membrane integrity. This was determined by annexin V APC staining and a flow cytometric analysis using the FACSCalibur and the CellQuest software (Becton Dickinson, San Jose, CA). Cell viability was measured as the percentage of annexin V APC-negative cell population, and it is expressed as the percentage of nonapoptotic cells. In total, 2.5×10^5 cells were incubated for 24 h with the indicated factors. Cells were washed and incubated with 150 μl annexin-binding buffer and 1.5 μl annexin V APC for 15 min in the dark. Cells were then analyzed by flow cytometry.

Western blot analysis and antibodies

Cells were lysed with Laemmli sample buffer, and Western blot analysis was performed as described previously (20) using the following antibodies: MCL-1 (Santa Cruz Biotechnology, Santa Cruz, CA), BIM (Cell Signaling Technology, Danvers, MA), GILZ (Santa Cruz), cleaved caspase-9 (Cell Signaling), pro-caspase-3 (BD Biosciences, San Jose, CA), β-catenin (BD Biosciences), GR (H-300) (Santa Cruz), GSK3α/β (StressGen Biotechnologies), cytochrome oxidase subunit II (Molecular Probes Inc., Eugene, OR), α-tubulin (Oncogene Research Products), and ERK2 (Upstate Biotechnology, Lake Placid, NY). Antibody binding was detected by using a secondary antibody conjugated to horseradish peroxidase and the enhanced chemiluminescence detection system (Amersham, Piscataway, NJ).

Reverse transcriptase multiplex ligation-dependent probe amplification (RT-MLPA)

Total RNA was isolated from Jurkat GR WT cells using the RNeasy Micro Kit (QIAGEN, Hilden, Germany) according to the manufacturer's protocol. RNA content was analyzed by RT-MLPA using SALSA MLPA kit R011-C1 apoptosis mRNA from MRC-Holland (Amsterdam, Netherlands) for the simultaneous detection of 38 mRNA molecules (21). In brief, RNA samples (200 ng total RNA) were first reverse transcribed using a gene-specific probe mix. The resulting cDNA was annealed overnight at 60 C to the MLPA probe mix. Annealed oligonucleotides were ligated by adding Ligase-65 (MRC-Holland) and incubated at 54 C for 15 min. Ligation products were amplified by PCR (35 cycles of 30 sec at 95 C, 30 sec at 60 C, and 1 min at 72 C) with one unlabeled and one FAM-labeled primer. The final PCR fragments amplified were separated by capillary electrophoresis on a 48-capillary ABI-Prism 3730 Genetic Analyzer (Applied Biosystems, Foster City, CA). Peak area and height were measured using GeneScan version 3.0 analysis software (Applied Biosystems). The sum of all peak data was set at 100% to normalize for fluctuations in total signal among samples, and individual peaks were calculated relative to the 100% value. The mRNA levels of all the genes were standardized to those of β-glucoronidase (*GUS*) for Jurkat cells and *PARN* for HeLa cells.

Reverse transcriptase quantitative PCR (RT-qPCR) analysis

Total RNA was isolated from cells using the RNeasy Micro Kit (QIAGEN) according to the manufacturer's protocol. Two micrograms of total RNA were reverse-transcribed using a Ready-To-Go You-Prime First-Strand Beads Kit (GE Healthcare, Buckinghamshire, UK) and Random Hexamers (Applied Biosystems). Quantitative PCR were carried out using ABI Prism 7900 HT Fast Real-Time PCR System, and designed human TaqMan assays (Applied Biosystems) were used to quantify gene expression of *BIM* (Hs00197982_m1), *GILZ* (Hs00608272_m1), *GILZ* (Mm00726417_s1), and *HIAP1* (HS00154109_m1) according to the manufacturer's guidelines. The housekeeping gene *GUS* (Hs99999908_m1) or *GAPDH* (Mm99999915_g1) was used as a control for RNA quality and used for normalization. PCR data were captured and analyzed using the Sequence Detector software (SDS version 2.2.2; Applied Biosystems).

Transient transfection and reporter assays

Jurkat GR WT were transiently transfected using Neon transfection system (Invitrogen, Carlsbad, CA). Jurkat GR WT cells (1×10^6) were resuspended in 100 μl Neon resuspension buffer R. For each electroporation, cells and 10 μg plasmid DNA were aliquoted into a sterile microcentrifuge tube. A Neon tip was inserted into the Neon pipette and the cell-DNA mixture was aspirated into the tip avoiding air bubbles. The Neon pipette was then inserted into the Neon tube containing 3 ml Neon electrolytic buffer E in the Neon pipette station. Cells were pulsed three times with a voltage of 1350 V and a width of 10 msec. After the pulse, cells were quickly transferred into a culture plate containing complete medium. After 24 h, cells were split before reaching confluence and treated with dexamethasone and/or SB216763 for 4 h. HeLa cells were transiently transfected with 2 μg plasmid DNA using Lipofectamine 2000 (Invitrogen). Luciferase activity was quantified using the luciferase assay system (Promega, Madison, WI). Luciferase values were normalized by protein quantification for Jurkat GR WT and Jurkat parental cells and with the luminescent β-galactosidase kit II for HeLa cells.

Chromatin immunoprecipitation (ChIP) assays

Jurkat GR WT cells (20×10^6) were treated with 10 μM SB216763 and/or 10 nM dexamethasone for 2 h. ChIP assays were performed using the ChIP assay kit (Upstate) following the manufacturer's instructions. ChIP assays were performed using an antibody against rabbit IgG (Upstate) as a negative control.

Recruitment of GR (H-300) (Santa Cruz) and RNA polymerase II (Upstate) are relative to the input signal. We used previously described *GILZ*-specific primers (22), which amplify a portion containing a GRE and another containing the transcription starting site. Densitometric scanning and quantification of the intensities in PCR bands were carried out using Image J version 1.44o software-based analysis (National Institute of Health, Bethesda, MD).

siRNA transfection

HeLa cells were transfected with commercially available scramble siRNA, anti-GSK3α, anti-GSK3β. or both siRNA (Invitrogen) at a concentration of 200 nM using Lipofectamine 2000 transfection reagent (Invitrogen). After 48 h, cell populations at a density of 50–60% in six-well plates were transfected with 1–2 μg MMTV-Luc plasmid DNA, after the formation of lipid-DNA complexes for 20 min at room temperature in OptiMEM I medium (GIBCO, Paisley, UK). Complexes were added directly to growing cells in DMEM and incubated for 4–6 h followed by washing with PBS buffer and addition of fresh DMEM. Cells were used in experiments 72 h after siRNA transfection.

Cellular fractionation

Jurkat GR WT cells (5×10^6) were harvested, washed once with ice-cold PBS, and gently lysed for 30 sec in 80 μl ice-cold lysis buffer [250 mM sucrose, 1 mM EDTA, 0.05% digitonin, 25 mM Tris (pH 6.8), 1 mM dithiothreitol, 1 μg/ml leupeptin, 1 μg/ml pepstatin, 1 μg/ml aprotinin, 1 mM benzamidine, and 0.1 mM phenylmethylsulfonyl fluoride]. Lysates were centrifuged at 12,000 $\times$ *g* for 3 min to obtain the supernatants (cytosolic extracts free of mitochondria) and the pellets (membrane fraction that contains nuclei and mitochondria), as described previously (23). Supernatants (50 μg) and pellet lysates (40 μg) were separated by SDS-PAGE.

Confocal laser scanning microscopy

Jurkat GR WT cells were collected after treatment with 10 μM SB216763 and/or 10 nM dexamethasone for 2 h, resuspended in PBS, and incubated at room temperature for 30–60 min over poly-L-lysine-coated coverslips (0.01% solution; Sigma-Aldrich). HeLa cells were grown on sterilized glass coverslips and then treated with 100 nM dexamethasone for 3 h. Coverslips containing attached cells were fixed with 4% paraformaldehyde, permeabilized with 0.25% Triton X-100 in PBS, and incubated for 1 h in 5% PBS-BSA to block nonspecific binding. Slides were incubated overnight at 4 C in a humidified chamber with rabbit polyclonal anti-GR (H-300) (1/100) primary antibody (Santa Cruz). Afterward, the slides were washed three times with PBS and further incubated with Alexa Fluor 647 antirabbit secondary antibody (1/500; Invitrogen) for 1 h. Nuclei were stained with YOYO-1 iodide (Invitrogen). To validate the specificity of the immunostaining, controls were performed by applying the same protocol but replacing primary antibody with 5% PBS-BSA. Images were then obtained with a spectral confocal microscope (TCS-SL; Leica Microsystems, Wetzlar, Germany) using a Plan-Apochromat $\times$63/1.4 numeric aperture immersion oil objective (Leica Microsystems). We used a HeNe laser at 633 nm (Lasos Inc., Jena, Germany) and pinhole of 114.54 μm for Alexa Fluor 647 GR staining and argon laser at 488 nm and pinhole of 114.54 μm for YOYO-1 nuclear staining. Images were captured using the accompanying image processing software from Cytovision (Leica Microsystems).

Reporter plasmids pSGF-T171A-Luc, pSGF-S424A-Luc, and double mutant

The mutants pSGF-T171A-Luc (with Thr171 mutated to Ala), pSGF-S424A-Luc (with Ser424 mutated to Ala), and double mutant (with Thr171 and Ser424 mutated to Ala) were generated by PCR using the rat GR DNA as a template and the QuikChange site-directed mutagenesis kit (Stratagene, La Jolla, CA) according to the manufacturer's instructions. The primers used for generating the mutations were the following: for Thr171 mutation, forward, 5′-GCAACTGGGTGTGCTGCCCCGACAGAGAA-3′, and reverse, 5′-TTCTCTGTCGGGGCAGCACACCCAGTTGC-3′; and for Ser424, forward, 5′-CCAGATGTAAGCGCTCCTCCATCCAGCTC-3′, and reverse, 5′-GAGCTGGATGGAGGAGCGCTTACATCTGG-3′. The mutated nucleotide is underlined. All plasmids and mutagenesis products were verified by DNA sequencing with the following primers: forward, 5′-CCTACAGCTCCTGGGCAACGTGCTGGTTA-3′; reverse, 5′-CGAGTCAGTGAGCGAGGAAGCGGAAGAGT-3′; forward, 5′-TCTCAGCAGCAGGATCAGAA-3′; and reverse, 5′-GCTGGATGGAGGAGAGCTTA-3′.

Statistical analysis

Results are shown as the mean $\pm$ SEM of values obtained in three or more independent experiments. Data were analyzed using SPSS version 11.0 software package. The paired Student's *t* test was used to compare the differences between paired samples. ANOVA-Tukey was used to compare the differences between treatments. Differences were considered significant at P values < 0.05.

Results

Dexamethasone-induced apoptosis is reverted by GSK3 inhibition

To study the protein kinases involved in GC-induced apoptosis, we examined cell viability upon treatment with dexamethasone in combination with different protein kinase inhibitors. We used the T cell leukemia-derived Jurkat cell line, which was stably transfected with a rat GR expression vector under the control of the β-actin promoter to ensure constant GR protein expression (Jurkat GR WT) (17). Exposure to dexamethasone resulted in a loss of viability of Jurkat GR WT cells at 24 h (Fig. 1A). Previous reports showed cell death induction upon GC treatment in primary CLL cells and other leukemic cells (7, 11, 24). Preincubation with the selective GSK3 inhibitor SB216763 significantly decreased this effect, in agreement with a recent observation where the pharmacological inhibition of GSK3 reduced GC-induced apoptosis in hematopoietic cell lines (7). Other protein kinase inhibitors, histone deacetylase inhibitors, Bcl-2 inhibitor, and

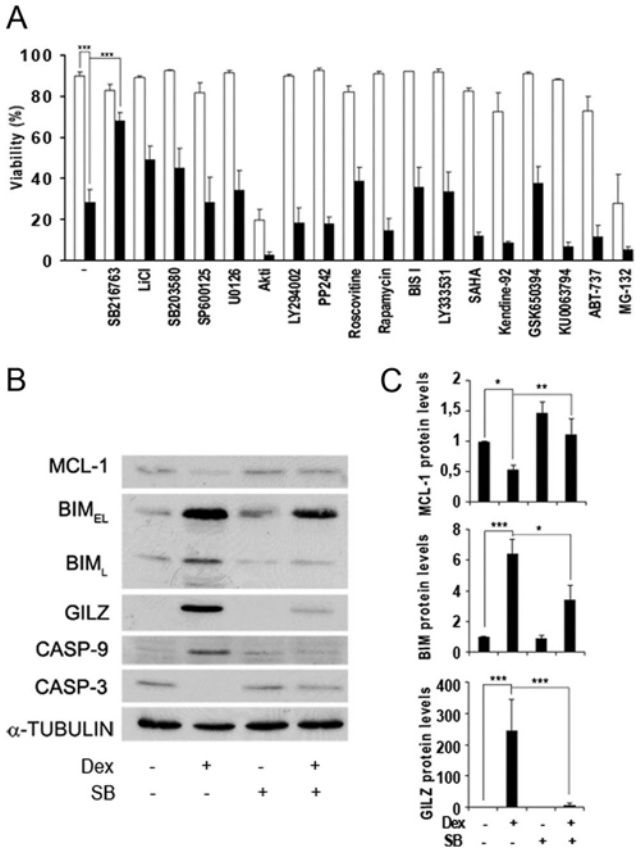

FIG. 1. Effect of GSK3 inhibition on GC-induced apoptosis. A, Jurkat GR WT cells were preincubated for 30 min with different protein kinases, HDAC, and proteasome inhibitors (*white bars*) and treated with 10 nM dexamethasone for 24 h (*black bars*). Cell viability was analyzed by phosphatidylserine exposure. Data correspond to the mean ± SEM of at least three representative experiments. Concentrations of inhibitors used were 10 μM SB216763, 10 mM LiCl, 10 μM SB203580, 10 μM SP600125, 10 μM U0126, 10 μM Akt inhibitor VIII (Akti), 20 μM LY294002, 50 nM PP242, 10 μM roscovitine, 10 nM rapamycin, 50 nM bisindolylmaleimide I (BIS I), 50 nM LY333531, 0.5 μM suberoylanilide hydroxamic acid (SAHA), 0.5 μM Kendine-92, 1 μM GSK650394, 5 μM KU0063794, 5 μM ABT-737, and 1 μM MG132. B, Jurkat GR WT cells were preincubated for 30 min with 10 μM SB216763 (SB) in the absence or presence of 10 nM dexamethasone (Dex) and harvested at 24 h. Analysis of MCL-1, BIM$_{EL}$ (extra large), BIM$_L$ (large), GILZ, caspase-9 (CASP-9), and pro-caspase 3 (CASP-3) protein levels were analyzed by Western blot. α-Tubulin was used as loading control. C) MCL-1, BIM$_{EL}$ and GILZ were quantified by densitometric analysis and corrected by α-tubulin levels by using ImageJ software (National Institutes of Health). Mean ± SEM of at least three independent experiments. *, $P < 0.05$; **, $P < 0.01$; ***, $P < 0.001$.

proteasome inhibitor could not prevent apoptosis induction, including the less specific inhibitor of GSK3, lithium chloride (LiCl) (Fig. 1A). This suggests that GSK3 plays a major role in GC-mediated apoptotic signaling pathways in leukemic cells.

We next examined the effect of SB216763 treatment on the expression of GC-induced proteins BIM and GILZ, two well-known targets of GC (9, 10, 25). Western blot analysis revealed that the expression of these proteins was induced by dexamethasone treatment, and preincubation with SB216763 reduced this up-regulation (Fig. 1, B and C). These data establish for the first time that *GILZ*, a GR direct target gene, requires GSK3 activity for its GC-dependent protein induction. Furthermore, prosurvival protein MCL-1 was down-regulated after 24 h of dexamethasone treatment, and this down-regulation was also diminished by GSK3 inhibition (Fig. 1, B and C). Next, we examined the activation of caspases. For this purpose, we analyzed caspase-9 activation, determined by the appearance of the intermediate cleavage product of 37 kDa and pro-caspase-3 disappearance as a parameter of caspase activation. We observed that SB216763 treatment prevented caspase-3 and caspase-9 activation (Fig. 1B), contributing to the blockade of dexamethasone-induced cell death (Fig. 1A).

GSK3 inhibition alters GR-mediated gene expression at the transcriptional level

We first examined the effect of dexamethasone treatment for 90 min on the mRNA expression of the *BCL-2* family members and other genes involved in the control of apoptosis by performing RT-MLPA. Dexamethasone significantly induced the expression of *BIM* (Fig. 2A), which has been suggested to be critical for regulating the switch from survival to apoptosis (9, 11). Additionally, an increase in mRNA levels was also observed for the antiapoptotic gene *HIAP1*, another GC-induced gene (26, 27). Other genes modulated by dexamethasone treatment were the proapoptotic gene *BMF* and *DR6*, a member of the TNF receptor family, but their expression levels were low compared with that of *BIM* and *HIAP1*. To evaluate the role of GSK3 in GC-induced transcriptional modulation, we examined the effect of SB216763 in the transcriptional induction of GC target genes after dexamethasone treatment. RT-qPCR showed that dexamethasone treatment significantly induced *BIM*, *GILZ*, and *HIAP1* mRNA levels, and pretreatment with SB216763 significantly reduced their induction in response to dexamethasone (Fig. 2B). These results were confirmed by RT-MLPA analysis (Supplemental Fig. 1, published on The Endocrine Society's Journals Online web site at http://mend.endojournals.org).

To further characterize the involvement of GSK3 in GC-induced gene expression, we examined the ability of the GR to regulate artificial GC-responsive gene promoter constructs in SB216763-treated Jurkat cells. As expected, cells treated with dexamethasone showed a significant increment in luciferase expression of a synthetic GRE promoter construct composed of two GRE (MMTV-Luc) (Fig. 3A) (28) and the p1940-Luc GILZ reporter construct (Fig. 3B) (29). Pretreatment of cells

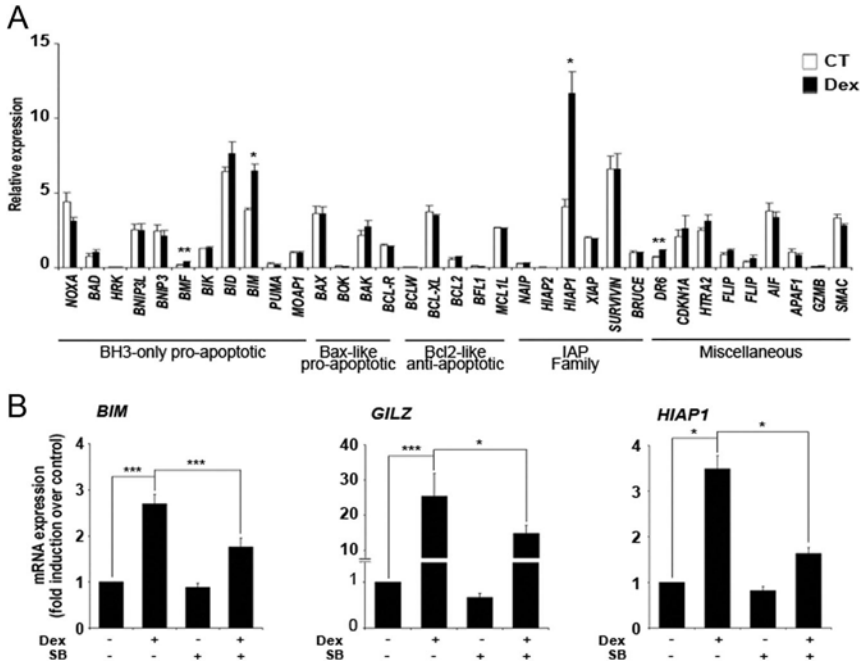

FIG. 2. GR ability to regulate GC-induced gene expression is affected by GSK3 inhibition. A, RT-MLPA gene expression profile induced by GC. Jurkat GR WT cells were untreated [control (CT)] or treated with 10 nM dexamethasone (Dex) for 90 min. Cells were lysed and the expression of apoptotic-related genes of the Bcl-2 family, IAP (inhibitors of apoptosis) family, and other genes implicated in apoptosis was analyzed by RT-MLPA as described in *Materials and Methods*. The mRNA levels of all the genes were normalized with respect to those of *GUS*. B, Jurkat GR WT cells were preincubated with 10 μM SB216763 (SB) in the absence or presence of 10 nM dexamethasone (Dex) and harvested at 90 min. *BIM*, *GILZ*, and *HIAP1* mRNA were measured by RT-qPCR. The mRNA levels of all genes were normalized with respect to those of *GUS*. These results are shown as the mean ± SEM of at least three independent experiments. *, $P < 0.05$; **, $P < 0.01$; ***, $P < 0.001$ *vs.* untreated cells.

with SB216763 significantly decreased the response to GC as compared with cells treated with dexamethasone alone, especially in the case of MMTV-Luc, confirming the role of GSK3 on dexamethasone-induced GR transcriptional activity.

Moreover, we analyzed *GILZ* mRNA levels in different cell types. *GILZ* expression was also induced by GC treatment in MC3T3 mouse preosteoblast, MCF-7 human breast adenocarcinoma, and BxPC-3 human pancreatic adenocarcinoma cell lines and significantly reverted by SB216763 pretreatment (Fig. 3C). These results indicate that GSK3 is an important determinant in the GR transcriptional response to GC in a species- and cell type-independent manner.

GSK3 inhibition affects GC-induced apoptosis and GC-dependent gene induction in CLL cells

GC are used in the therapy of lymphoid malignancies because of their remarkable ability to induce apoptosis (30, 31). To study the effect of GSK3 inhibition over GC-induced apoptosis in a primary leukemia model, we employed B lymphocytes from patients with CLL. As we described previously, dexamethasone significantly induced cell death of CLL cells (24). Moreover, pretreatment with GSK3 inhibitor SB216763 significantly decreased dexamethasone-induced apoptosis by 11.87% in 19 of the 29 patients analyzed (Fig. 4A). Supplemental Table 1 shows the viability of the full cohort of patients analyzed. We next analyzed the effect of GSK3 inhibition on GC-dependent GILZ and BIM induction. mRNA levels were induced in response to dexamethasone treatment and reverted by GSK3 inhibition in the six patients analyzed (Fig. 4B). GILZ and BIM protein levels were also induced in response to GC and reverted by GSK3 inhibition in nine of 12 samples for GILZ and 11 of 13 samples for BIM (Fig. 4C). Collectively, these data indicate that GSK3 inhibition reduces sensitivity to GC-induced apoptosis in CLL cells and impairs GC-dependent gene and protein induction.

GSK3 inhibition affects GR and RNA polymerase II recruitment to the *GILZ* gene promoter

To establish the mechanism for GSK3-mediated GR transcriptional regulation, Jurkat GR WT cells were stimulated with dexamethasone for 2 h, and *GILZ* promoter occupancy was evaluated by ChIP analysis. Using previously described primers (22), we observed a significant increase in binding of the GR to the *GILZ* promoter (Fig. 5A) as well as increased binding of RNA polymerase II to the *GILZ* transcription start site (Fig. 5B) in dexamethasone-treated cells. Pretreatment with SB216763 significantly reduced GR and RNA polymerase II binding to the *GILZ* promoter induced by dexamethasone. Taken together, our results show that GC-dependent transcriptional activation requires a functional GSK3 signaling.

GSK3β gene silencing suppresses GC-stimulated gene expression

GSK3 inhibitors do not distinguish between the two GSK3 isoforms, so we next evaluated the individual roles of GSK3α and GSK3β on GR-mediated transcriptional activation by gene silencing analysis. Because we were unable to completely silence *GSK3* gene expression in Jurkat cells, we performed *GSK3α* and *GSK3β* knockdown in HeLa cells. Relative mRNA levels and protein expression levels of GSK3α and GSK3β were determined

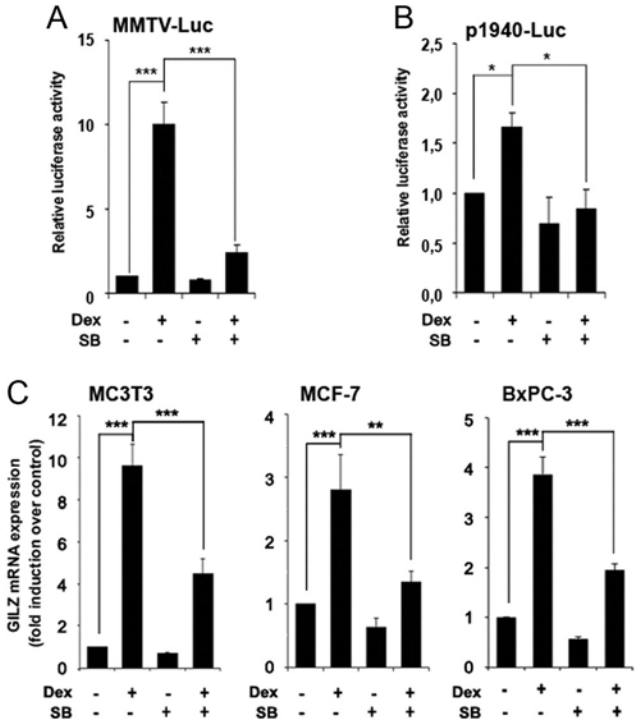

FIG. 3. GSK3 is important for GR transcriptional function. A and B, Jurkat GR WT cells were transfected with MMTV-Luc (A) or p1940-Luc (B) vectors. At 24 h after transfection, cells were preincubated with 10 μM SB216763 (SB) for 30 min, followed by treatment with 10 nM dexamethasone (Dex) for another 4 h. Luciferase activity was measured and expressed relative to basal activity of untreated cells. C, MC3T3, MCF-7, and BxPC-3 cells were preincubated with 10 μM SB216763 (SB) in the absence or presence of 10 nM, 8 nM, and 4 μM dexamethasone (Dex), respectively, and harvested at 90 min. *GILZ* mRNA levels were measured by RT-qPCR. mRNA levels were normalized with respect to those of *GUS* in human cell lines or *GAPDH* in MC3T3. Mean ± SEM of at least three independent experiments. *, $P < 0.05$; **, $P < 0.01$; ***, $P < 0.001$.

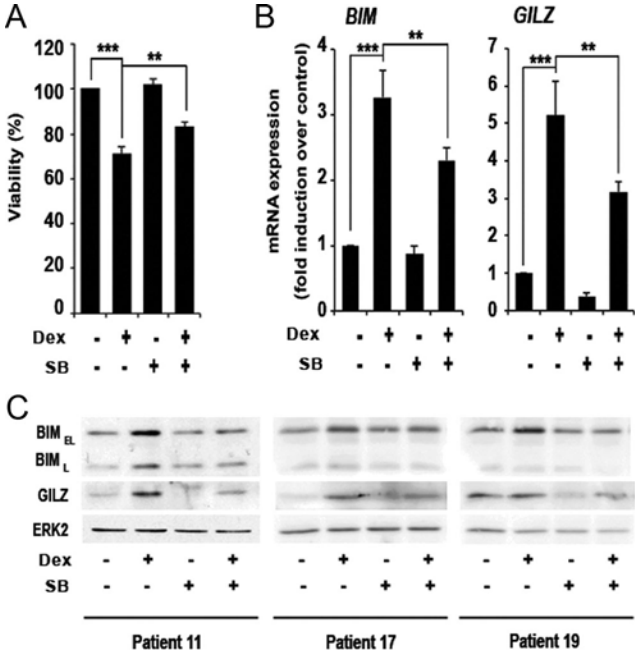

FIG. 4. GSK3 inhibition affects GC-induced apoptosis and gene expression in CLL cells. Cells from CLL patients were preincubated for 30 min with 10 μM SB216763 (SB) and treated with 10 μM dexamethasone (Dex) for 24 h. A, Cell viability of the 19 patient samples in which SB216763 decreased GC-induced apoptosis was analyzed by phosphatidylserine exposure. Viability is expressed as the percentage of annexin APC-negative treated cells relative to untreated cells. B, *BIM* and *GILZ* mRNA levels of six patients were measured by RT-qPCR. The mRNA levels of both genes were normalized with respect to those of *GUS*. Data are shown as the mean value ± SEM. *, $P < 0.05$; **, $P < 0.01$; ***$P < 0.001$. C, BIM_{EL}, BIM_L, and GILZ protein levels were analyzed by Western blot. These are three representative patients of at least 12 that were analyzed. ERK2 was used to normalize protein levels.

after 72 h of siRNA by performing RT-qPCR and Western blot, respectively. Transfection of HeLa cells with siRNA for either GSK3α or GSK3β resulted in knockdown of their respective transcripts and proteins, whereas mRNA and protein levels of the GSK3 isoforms were unaffected after transfection with scramble siRNA (Fig. 6A and Supplemental Fig. 2).

Next, we analyzed the effect of silencing GSK3α, GSK3β, or both isoforms over *GILZ* mRNA levels in HeLa cells. Depletion of GSK3α had no effect on basal or GC-induced mRNA expression levels of *GILZ* (Fig. 6B). Interestingly, GSK3β and GSK3α/β silencing resulted in a significant decrease in basal *GILZ* mRNA levels and attenuated the effects of dexamethasone treatment. We next investigated the effect of GSK3α/β silencing on GR-mediated transcription using the GC-inducible promoter MMTV-Luc. Luciferase activity was determined 4 h after dexamethasone addition (Fig. 6C). As it was previously described, basal transcription of GRE reporter was induced by GSK3 silencing (32). The degree of basal activation of MMTV-Luc was similar between GSK3α and GSK3β siRNA. Interestingly, GSK3β but not the GSK3α knockdown significantly decreased dexamethasone-stimulated MMTV-Luc promoter activity. The down-regulation of both GSK3 isoforms decreased dexamethasone-stimulated MMTV-Luc luciferase activity to the same extent as GSK3β silencing alone. As expected, the scramble siRNA had no effect over the MMTV-Luc reporter luciferase induction in response to dexamethasone.

We also used RT-MLPA to analyze changes in response to GSK3α/β silencing in HeLa cells (Supplemental Fig. 3). Apoptosis mRNA expression profile was quite different from Jurkat GR WT cells, because HeLa cells do not undergo apoptosis in response to dexamethasone treatment. Only *BMF*, *MCL-1*, *BCL-XL*, and *HIAP1* were significantly induced by dexamethasone. GSK3β or GSK3α/β silencing resulted in down-regulation of GC-dependent *BMF*, *BCL-XL*, and *MCL-1* mRNA induction, whereas *HIAP1* was still induced by dexamethasone treatment.

To further confirm our results obtained in GSK3 knockdown experiments in HeLa cells, we used WT and

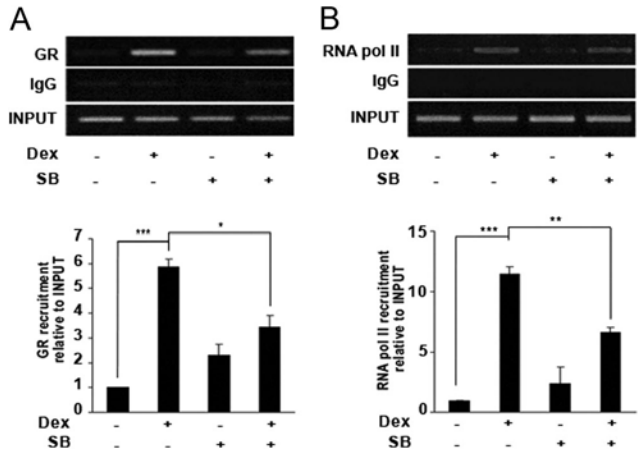

FIG. 5. Recruitment of GR and RNA polymerase II to the *GILZ* gene is affected by GSK3 inhibition. Jurkat GR WT cells were preincubated with 10 μM SB216763 (SB) and treated with 10 nM dexamethasone (Dex) for 2 h. ChIP analysis was performed by incubating DNA-protein complexes with antibodies against GR (A) or RNA polymerase II (RNA pol II) (B) and IgG as a negative control relative to the input signal. Primers specific for the *GILZ* promoter used for PCR analysis were described in *Materials and Methods*. *Bars* represent average values from densitometric analysis of the bands obtained in four separate experiments using ImageJ software (National Institutes of Health). Mean ± SEM of at least three independent experiments. *, $P < 0.05$; **, $P < 0.01$; ***, $P < 0.001$.

GSK3α- or GSK3β-null MEF cells to analyze endogenous *GILZ* mRNA induction (Fig. 6D) in response to GC treatment. Moreover, we found that MEF cells deficient for GSK3β expression did not induce *GILZ* mRNA levels in response to dexamethasone, whereas WT and GSK3α-null MEF cells were able to significantly induce *GILZ* mRNA upon GC treatment. Additionally, we showed that MEF cells deficient for GSK3β did not exhibit dexamethasone-induced luciferase activity, whereas WT and GSK3α-null MEF cells significantly induced MMTV-Luc promoter activity in response to dexamethasone (Supplemental Fig. 4). On the other hand, RT-MLPA analysis showed no significant changes in MEF cells gene expression profile in response to GC, even though there were differences in basal gene expression between cell lines (Supplemental Fig. 5). Together, these results show that GSK3β activity, but not GSK3α, is required for the transcriptional GR-mediated activity.

GSK3 inhibition affects GR cellular distribution in response to GC

To examine the role of GSK3 in the regulation of GR subcellular localization, we analyzed cytosolic and membrane (which contains nuclei and mitochondria) fractions from Jurkat GR WT cells. In nonstimulated cells, the GR was detected mostly in the cytosolic fractions, whereas dexamethasone treatment induced its translocation to the membrane fractions (Fig. 7A). Dexamethasone-dependent GR nuclear protein localization was significantly reduced by SB216763 (Fig. 7, A and B). GSK3α and GSK3β levels were mainly observed in the cytoplasm and the nucleus, respectively. Under SB216763 treatment, GSK3α levels were reduced in the nucleus, and there was an increase in β-catenin protein levels in the membrane fraction, confirming GSK3 inhibition.

Taking into account that chromosome region maintenance 1 (CRM1) exportin has been suggested to play a pivotal role in the early nuclear export of the GR (33), we wanted to determine whether the partial reduction of the GR nuclear translocation by SB216763 in dexamethasone-treated cells is a result of a CRM1-dependent export. For this purpose, nuclear translocation experiments were performed in the presence of leptomycin B (LMB), which blocks specifically the CRM1-dependent nuclear export. A significant increase in nuclear GR localization was observed when cells were treated with LMB, suggesting that there might be a CRM1-dependent nuclear export of the GR in response to GSK3 inhibition (Fig. 7, A and B).

We further confirmed the subcellular localization of the GR through immunofluorescent staining visualized by confocal microscopy. In control Jurkat GR WT cells, specific staining of GR was mainly observed in the cytoplasmic compartment (Fig. 7C). As expected, treatment with dexamethasone for 2 h induced GR translocation to the nuclear compartment predominantly to regions where euchromatin was present. Interestingly, when cells were preincubated with SB216763 in combination with dexamethasone, a decrease in the GR protein levels in the nucleus was observed compared with dexamethasone treatment alone. Altogether, these results indicate that GSK3 inhibition is able to affect GR protein localization and decreases early GR nuclear levels in dexamethasone-treated Jurkat GR WT cells, affecting GC-stimulated gene expression.

Next, we analyzed the contribution of GSK3α and GSK3β to GR subcellular distribution induced by dexamethasone using isoform-specific knockdown in HeLa cells. Treatment with dexamethasone always resulted in GR translocation to the nucleus even when GSK3β or GSK3α/β was silenced. Moreover, depletion of GSK3β or GSK3α/β proteins by siRNA led to an increase in general GR expression levels (Supplemental Fig. 6). These results are also in agreement with a previous report where mutation of human Ser404 (a residue phosphorylated by GSK3β) leads to the inability of the GR to exit the nucleus, making it inaccessible to the proteasome degradation machinery (6).

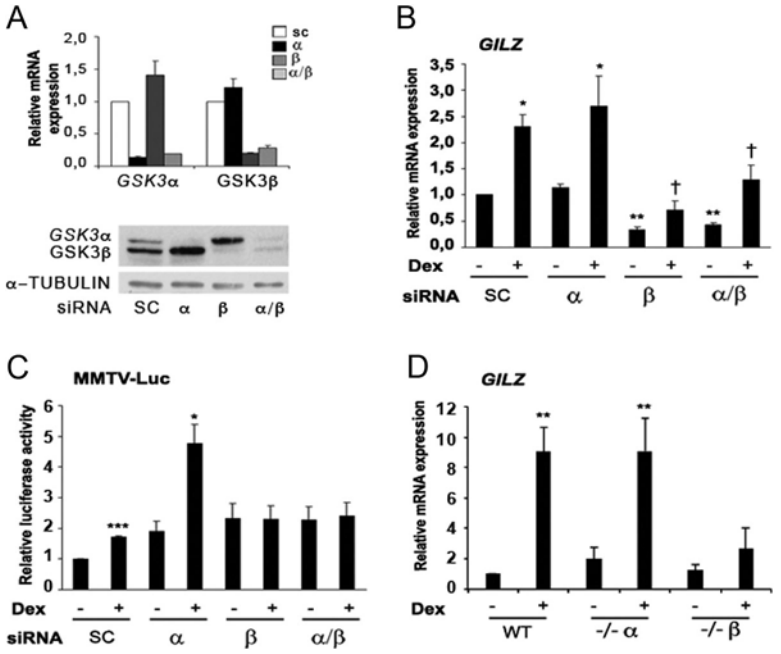

FIG. 6. Genetic knockdown of *GSK3β* by siRNA results in disruption of GC-stimulated gene expression. A, HeLa cells were transfected with GSK3 isoform-specific siRNA. mRNA and protein expression levels are shown of *GSK3α* and *GSK3β* isoforms after their knockdown of the specific gene. The mRNA levels of both genes were normalized with respect to those of *GUS*. B, Effect of genetic disruption of GSK3 isoforms α, β, or both on basal and dexamethasone (Dex)-induced *GILZ* mRNA levels in HeLa cells. Mean ± SEM of four independent experiments. C, Effect of genetic disruption of GSK3 on basal and dexamethasone (Dex)-induced GR activity measured by MMTV-Luc luciferase reporter assay in HeLa cells. Cells were cotransfected with MMTV-Luc and β-galactosidase (internal control) constructs. The cells were then exposed to 100 nM dexamethasone for 4 h. The normalized values are relative to the scrambled siRNA untreated control. Mean ± SEM of five independent experiments. D, WT and *GSK3α*- and *GSK3β*-null MEF cells were treated with 100 nM dexamethasone for 4 h. *GILZ* mRNA was measured by RT-qPCR and normalized with respect to *GAPDH*. Mean ± SEM of four independent experiments. *, $P < 0.05$; **, $P < 0.01$; ***, $P < 0.001$ of dexamethasone-treated cells compared with untreated cells; †, $P < 0.05$ compared with treated cells.

GSK3 inhibition alters transcriptional activity of GR phosphorylation mutants

Besides phosphorylation of human GR at Ser404, GSK3β has been described to phosphorylate rat GR at Thr171 (16). Because Jurkat GR WT cells harbor a rat GR, we mutated both Thr171 and Ser424 (corresponding to human Ser404) (34) residues in the rat GR to analyze mutant transactivation capacity under GSK3 inhibition (Supplemental Fig. 7). WT and GR mutants were expressed in the Jurkat parental cell line, which harbor a function-impairing point mutation (R477H) in one of their GR alleles that causes GC resistance (18). We used the GC-inducible promoter MMTV-Luc to evaluate the effect of SB216763 over the dexamethasone-induced transactivation activity of single and double mutants. According to previous results in Jurkat GR WT cells, pretreatment of Jurkat cells with SB216763 significantly inhibits GR WT hormone-dependent transcriptional activity (Fig. 8A). Interestingly, the GR mutants (T171A, S424A, and double mutant) responded to dexamethasone to the same extent as GR WT, and SB216763 reverted dexamethasone-induced transactivation activity of all mutants (Fig. 8A). These results were also observed at longer incubation times (Supplemental Fig. 8).

RT-qPCR showed that GR WT and GR mutants were equally able to induce endogenous *GILZ* mRNA levels in response to dexamethasone treatment. Pretreatment with SB216763 significantly reduced GC-dependent *GILZ* mRNA induction by all the GR constructions (Fig. 8B). Note that parental Jurkat cells slightly induced *GILZ* mRNA expression (Fig. 8B) but not MMTV-Luc luciferase activity (Fig. 8A) as previously described (18). This mRNA induction was also reverted by SB216763 treatment. These results suggest that there is an additional mechanism, not involving phosphorylation of these residues, by which GSK3 regulates GR transcriptional activity.

Discussion

GC induce apoptosis in different cell types including leukemia cells in a complex process regulated by multiple signaling pathways that alter gene expression profiles through GR-mediated transactivation and transrepression (1). In this report, we demonstrate that GSK3 regulates GR transcriptional activity by affecting GR protein localization, recruitment to target gene promoters, and changes in target gene expression in different cell types. We observed a critical role for GSK3 in GC-dependent cell death because inhibition of GSK3 by the specific GSK3 inhibitor SB216763 reverted GC-induced apoptosis, consistent with previous studies (7, 8, 35). The antiapoptotic Bcl-2 family member protein MCL-1 contains a conserved consensus site for GSK3 phosphorylation, which targets it for ubiquitin-dependent degradation (36). We observed that GC-dependent down-regulation of MCL-1 protein was prevented by GSK3 inhibition. This was accompanied by the reduction of dexamethasone-induced up-regulation of BIM (8) and GILZ protein levels. To the best of our knowledge, there are no previous

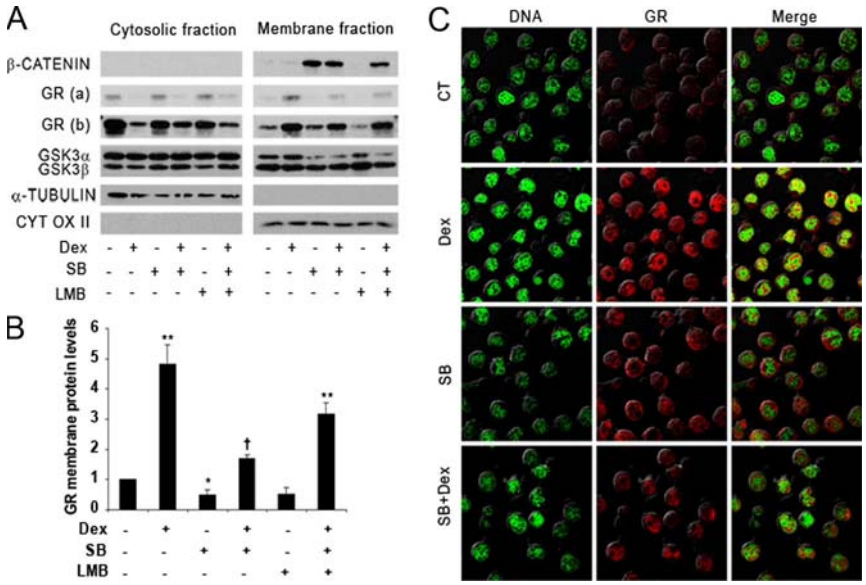

FIG. 7. Subcellular localization of GR in Jurkat GR WT cells treated with dexamethasone, SB216763, and LMB. A, Jurkat GR WT cells were treated or not with 1 nM LMB. Thirty minutes later, cells were treated or not with 10 μM SB216763 (SB) before treatment with 10 nM dexamethasone (Dex). Three hours later, we lysed the cells to obtain cytoplasmic and membrane fractions as described in *Materials and Methods*. GSK3α/β, GR [(a), less exposed; (b), more exposed] and β-catenin were detected by Western blotting. α-Tubulin and cytochrome oxidase II (CYT OX II) were analyzed as a control for cytosolic and membrane extracts, respectively. B, Values obtained from membrane fractions were subjected to band densitometry using ImageJ software. GR protein nuclear levels were quantified and normalized by the cytochrome oxidase II protein levels. The graph shows the mean value ± SEM of four experiments expressed as the fold induction compared with untreated cells. *, $P < 0.05$; **, $P < 0.01$ of dexamethasone (Dex)-treated cells compared with untreated cells; †, $P < 0.05$ compared with treated cells. C, Immunofluorescent staining of the GR in Jurkat GR WT cells. Cells were untreated (CT) or pretreated with 10 μM SB216763 (SB) and treated with 10 nM dexamethasone (Dex) for 2 h. YOYO-1 iodide (*green*) stains nuclear DNA, and Alexa Fluor 647 (*red*) stains GR. Merged images are shown for comparison. This is a representative experiment of three that were performed.

studies demonstrating the involvement of GSK3 in the GC-dependent up-regulation of GILZ. We also evaluated the effect of GSK3 inhibition over GC-induced apoptosis in primary CLL cells. SB216763 pretreatment reverted GC-induced cell death in 19 of 29 patients analyzed. It is important to note that CLL patients have different genetic alterations that determine response to treatment. Additionally, GC-dependent *BIM* and *GILZ* mRNA and protein induction was reverted by GSK3 inhibition. The effect over *GILZ* mRNA induction was confirmed in other cell types, ruling out cell-type-specific effects.

Pharmacological inhibition of GSK3 resulted in a reduced induction of *BIM*, *HIAP1*, and *GILZ* endogenous mRNA levels and GC-responsive promoter constructs in response to GC. These results suggested that the inhibitory effect of SB216763 on GC-stimulated promoter activity was due to an impairment of GR DNA binding. Interestingly, ChIP assays showed that GSK3 inhibition reduced GR and RNA polymerase II recruitment to the *GILZ* promoter after dexamethasone treatment. These results indicate that GC-dependent transcriptional activation requires functional GSK3 signaling and show for the first time that GSK3 could be required by the GR for its activation as a transcription factor and for RNA polymerase II recruitment. These results are in the line with previous studies in which GSK3 inhibition represses other steroid receptor transcriptional activity in various cell types (37–40).

The present study demonstrates that GSK3β is the isoform involved in the regulation of GR transcriptional activation in response to GC. GSK3α and GSK3β silencing in HeLa cells, resulted in the activation of a GRE-promoter construct at a basal level, but only GSK3β silencing was effective in reverting its GC-dependent transcriptional activation. Inhibition of GSK3β or double knockdown of α- and β-isoforms reduced both basal and GC-induced mRNA expression of endogenous *GILZ*. On the other hand, GSK3α silencing was unable to reduce any of them, indicating that GSK3β affects basal and GC-induced gene transcription. RT-MLPA analysis revealed differences in apoptosis expression profile when compared with Jurkat GR WT cells, because HeLa cells do not undergo apoptosis in response to dexamethasone (41). GSK3β and GSK3α/β silencing down-regulated GC-dependent gene induction. Nevertheless, *HIAP1* was induced by dexamethasone even when GSK3β was silenced, suggesting that it might be regulated by an indirect mechanism. Moreover, GSK3β-null MEF cells were significantly unable to induce *GILZ* mRNA levels and MMTV-Luc promoter construct luciferase activity in response to dexamethasone treatment.

Although the mechanism responsible for the nuclear import of steroid receptors is well documented, the mechanisms of GR export remain largely unknown (42). It has been suggested that CRM1 plays a pivotal role in the early nuclear export of the GR (33). However, contradictory results have been reported on whether GR nuclear export is CRM1 dependent (43) or CRM1 independent (44, 45). We demonstrate that the pharmacological inhibition of GSK3 activity in combination with dexamethasone treatment in Jurkat GR WT cells targets the activated GR for a rapid export from the nucleus, thereby down-regulating early GR transcriptional activity. A similar effect was de-

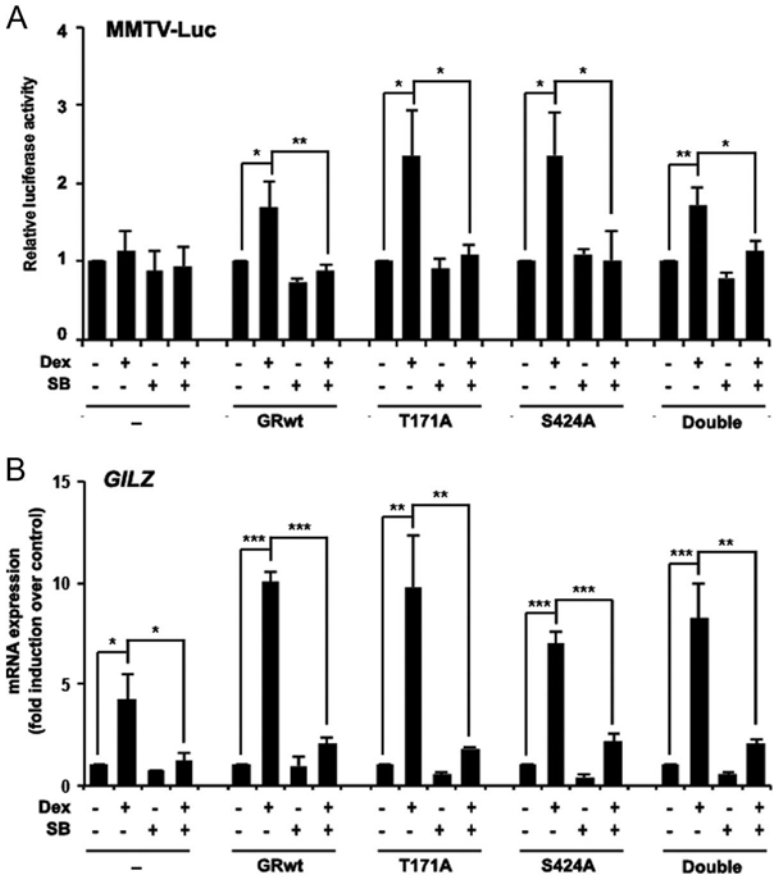

FIG. 8. GSK3 inhibition affects GC-induced transcriptional activity of GR mutants. A, Jurkat parental cells were transfected with MMTV-Luc alone or in combination with GR WT, T171A, S424A, or double mutant of the rat GR and preincubated with 10 μM SB216763 (SB) for 30 min followed by treatment with 10 nM dexamethasone (Dex) for another 4 h. Luciferase activity was measured and expressed relative to basal activity of untreated cells. B, Jurkat parental cells were nontransfected or transfected with GR WT, T171A, S424A, and double mutant, preincubated with 10 μM SB216763 in the absence or presence of dexamethasone, and harvested at 4 h. *GILZ* mRNA levels were measured by RT-qPCR. mRNA levels were normalized with respect to those of *GUS*. Mean ± SEM of at least three independent experiments. *, $P < 0.05$; ** $P < 0.01$; ***, $P < 0.001$.

scribed for the androgen receptor (AR) in prostate cancer cell lines, where GSK3 inhibitors attenuated AR-dependent transcriptional activity and caused a rapid nuclear export of endogenous AR (46, 47). SB216763-induced nuclear export was partially inhibited by LMB, suggesting there might be a CRM1-dependent nuclear export of the GR in response to GSK3 inhibition. However, other participating export mechanisms like Ca^{2+}-dependent calreticulin-based mechanism cannot be completely ruled out (4, 48, 49).

We demonstrate that GSK3β and GSK3α/β silencing in HeLa cells resulted in the reduction of GC-dependent induction of *BMF*, *BCL-XL*, and *MCL-1*, previously described GC-regulated genes (50–53). Nevertheless, we observed higher basal GR expression levels and presence of the GR in the nucleus in response to GC treatment in these cells. The increase in GR expression levels in GSK3β-silenced cells is in agreement with previously described phosphorylation of Ser404 by GSK3β, which favors GR protein down-regulation by proteasome degradation (6).

GSK3 also phosphorylates the rat GR at Thr171 (16). This phosphorylation site is not present in the human GR sequence, indicating that GSK3-mediated regulation of this residue is likely species specific (34). Our results with rat GR mutants of the residues that are phosphorylated by GSK3 show that these mutations do not abrogate the ability of the GR to translocate to the nucleus and transactivate a GRE-containing reporter construct. In the same line, all the mutants were able to induce endogenous *GILZ* mRNA levels. GSK3 inhibition reverted the induction of luciferase activity of MMTV-Luc reporter construct and endogenous *GILZ* mRNA of all mutants. These results indicate that there could be an additional mechanism, not involving the phosphorylation of these residues, by which GSK3 regulates GR transcriptional activity. The Jurkat parental cell line was able to slightly induce *GILZ* mRNA expression levels, whereas it was unable to induce MMTV-Luc reporter construct. These cells harbor a function-impairing point mutation (R477H) in one of their GR alleles (18). This mutation might cause GC resistance by impairing transactivation and transrepression without affecting GR ligand-dependent nuclear import. These results are unclear, even though it was previously described (18) and might be reflecting promoter-specific differences or nongenomic effects of GC over the *GILZ* promoter (1).

It has been previously described that in the absence of a ligand, GSK3α is bound to the GR, and exposure to GC or GSK3 inhibitor leads to the disruption of this interaction (7). It has also been described that the GR associates with GSK3β in the presence of dexamethasone but not with GSK3α (6). In the same line, our results indicate that GSK3 isoforms regulate GR cellular response by using different mechanisms besides GSK3-mediated phosphorylation of the GR.

In summary, the current study demonstrates the involvement of GSK3β on GC-dependent gene transcrip-

tional induction through the regulation of GR and RNA polymerase II recruitment to target gene sequences and by affecting GR protein subcellular localization. Our results suggest that GSK3 plays an important role in regulating GC mechanism of action, suggesting that keeping GSK3 in an active state could improve GC therapy. Therefore, additional analyses of the involvement of GSK3 activity in GC treatment of lymphoma and leukemia malignancies may help gain insight into the molecular basis of these disorders.

Acknowledgments

We thank Dr. Jose Luis Rosa, Edgardo Rodríguez-Carballo, and Miguel Peña-Rico for helpful discussions and suggestions. We also thank Adriana Forero for English language editing. Moreover, we thank the Scientific-Technical Services of the Unitat de Bellvitge at the Universitat de Barcelona for their technical support. We thank Dr. Carme Caelles for kindly providing Jurkat GR WT cells and MMTV-Luc construct and Dr. Marc Pallardy for providing p-1940-Luc construct. We also thank Dr. J. Woodgett for providing WT, GSK3$\alpha^{-/-}$, and GSK3$\beta^{-/-}$ MEF cells.

Address all correspondence and requests for reprints to: Gabriel Pons, Departament de Ciències Fisiològiques II, Universitat de Barcelona, Institut d'Investigació Biomèdica de Bellvitge, C/Feixa Llarga s/n, L'Hospitalet de Llobregat, E-08907 Barcelona, Spain. E-mail: gpons@ub.edu

This study was supported by grants from the Ministerio de Economía y Competitividad and FEDER (SAF2010-20519), the Instituto de Salud Carlos III (RTICC RD06/0020/0097), and the AGAUR-Generalitat de Catalunya (AGAUR- 2009SGR395). C.R.-P., A.P.-P., C.M.-M., and D.M.G.-G. are recipients of research fellowships from the Ministerio de Economía y Competitividad. D.I.-S. has a postdoctoral contract from Fundació Bosch i Gimpera.

Disclosure Summary: The authors have nothing to disclose.

References

1. **Kfir-Erenfeld S, Sionov RV, Spokoini R, Cohen O, Yefenof E** 2010 Protein kinase networks regulating glucocorticoid-induced apoptosis of hematopoietic cancer cells: fundamental aspects and practical considerations. Leuk Lymphoma 51:1968–2005
2. **Zhou J, Cidlowski JA** 2005 The human glucocorticoid receptor: one gene, multiple proteins and diverse responses. Steroids 70:407–417
3. **Oakley RH, Cidlowski JA** 2011 Cellular processing of the glucocorticoid receptor gene and protein: new mechanisms for generating tissue-specific actions of glucocorticoids. J Biol Chem 286:3177–3184
4. **Beck IM, De Bosscher K, Haegeman G** 2011 Glucocorticoid receptor mutants: man-made tools for functional research. Trends Endocrinol Metab 22:295–310
5. **Wang Z, Chen W, Kono E, Dang T, Garabedian MJ** 2007 Modulation of glucocorticoid receptor phosphorylation and transcriptional activity by a C-terminal-associated protein phosphatase. Mol Endocrinol 21:625–634
6. **Galliher-Beckley AJ, Williams JG, Collins JB, Cidlowski JA** 2008 Glycogen synthase kinase 3β-mediated serine phosphorylation of the human glucocorticoid receptor redirects gene expression profiles. Mol Cell Biol 28:7309–7322
7. **Spokoini R, Kfir-Erenfeld S, Yefenof E, Sionov RV** 2010 Glycogen synthase kinase-3 plays a central role in mediating glucocorticoid-induced apoptosis. Mol Endocrinol 24:1136–1150
8. **Nuutinen U, Ropponen A, Suoranta S, Eeva J, Eray M, Pellinen R, Wahlfors J, Pelkonen J** 2009 Dexamethasone-induced apoptosis and up-regulation of Bim is dependent on glycogen synthase kinase-3. Leuk Res 33:1714–1717
9. **Wang Z, Malone MH, He H, McColl KS, Distelhorst CW** 2003 Microarray analysis uncovers the induction of the proapoptotic BH3-only protein Bim in multiple models of glucocorticoid-induced apoptosis. J Biol Chem 278:23861–23867
10. **Zhang L, Insel PA** 2004 The pro-apoptotic protein Bim is a convergence point for cAMP/protein kinase A- and glucocorticoid-promoted apoptosis of lymphoid cells. J Biol Chem 279:20858–20865
11. **Iglesias-Serret D, de Frias M, Santidrián AF, Coll-Mulet L, Cosialls AM, Barragán M, Domingo A, Gil J, Pons G** 2007 Regulation of the proapoptotic BH3-only protein BIM by glucocorticoids, survival signals and proteasome in chronic lymphocytic leukemia cells. Leukemia 21:281–287
12. **Beurel E, Jope RS** 2006 The paradoxical pro- and anti-apoptotic actions of GSK3 in the intrinsic and extrinsic apoptosis signaling pathways. Prog Neurobiol 79:173–189
13. **Forde JE, Dale TC** 2007 Glycogen synthase kinase 3: a key regulator of cellular fate. Cell Mol Life Sci 64:1930–1944
14. **Rayasam GV, Tulasi VK, Sodhi R, Davis JA, Ray A** 2009 Glycogen synthase kinase 3: more than a namesake. Br J Pharmacol 156:885–898
15. **Woodgett JR** 1990 Molecular cloning and expression of glycogen synthase kinase-3/factor A. EMBO J 9:2431–2438
16. **Rogatsky I, Waase CL, Garabedian MJ** 1998 Phosphorylation and inhibition of rat glucocorticoid receptor transcriptional activation by glycogen synthase kinase-3 (GSK-3). Species-specific differences between human and rat glucocorticoid receptor signaling as revealed through GSK-3 phosphorylation. J Biol Chem 273:14315–14321
17. **Helmberg A, Auphan N, Caelles C, Karin M** 1995 Glucocorticoid-induced apoptosis of human leukemic cells is caused by the repressive function of the glucocorticoid receptor. EMBO J 14:452–460
18. **Riml S, Schmidt S, Ausserlechner MJ, Geley S, Kofler R** 2004 Glucocorticoid receptor heterozygosity combined with lack of receptor auto-induction causes glucocorticoid resistance in Jurkat acute lymphoblastic leukemia cells. Cell Death Differ 11(Suppl 1):S65–S72
19. **Asselin-Labat ML, David M, Biola-Vidamment A, Lecoeuche D, Zennaro MC, Bertoglio J, Pallardy M** 2004 GILZ, a new target for the transcription factor FoxO3, protects T lymphocytes from interleukin-2 withdrawal-induced apoptosis. Blood 104:215–223
20. **Barragán M, Bellosillo B, Campàs C, Colomer D, Pons G, Gil J** 2002 Involvement of protein kinase C and phosphatidylinositol 3-kinase pathways in the survival of B-cell chronic lymphocytic leukemia cells. Blood 99:2969–2976
21. **Eldering E, Spek CA, Aberson HL, Grummels A, Derks IA, de Vos AF, McElgunn CJ, Schouten JP** 2003 Expression profiling via novel multiplex assay allows rapid assessment of gene regulation in defined signalling pathways. Nucleic Acids Res 31:e153
22. **Chen W, Rogatsky I, Garabedian MJ** 2006 MED14 and MED1 differentially regulate target-specific gene activation by the glucocorticoid receptor. Mol Endocrinol 20:560–572
23. **Piqué M, Barragán M, Dalmau M, Bellosillo B, Pons G, Gil J** 2000 Aspirin induces apoptosis through mitochondrial cytochrome c release. FEBS Lett 480:193–196
24. **Bellosillo B, Dalmau M, Colomer D, Gil J** 1997 Involvement of

CED-3/ICE proteases in the apoptosis of B-chronic lymphocytic leukemia cells. Blood 89:3378–3384

25. **D'Adamio F, Zollo O, Moraca R, Ayroldi E, Bruscoli S, Bartoli A, Cannarile L, Migliorati G, Riccardi C** 1997 A new dexamethasone-induced gene of the leucine zipper family protects T lymphocytes from TCR/CD3-activated cell death. Immunity 7:803–812
26. **Webster JC, Huber RM, Hanson RL, Collier PM, Haws TF, Mills JK, Burn TC, Allegretto EA** 2002 Dexamethasone and tumor necrosis factor-α act together to induce the cellular inhibitor of apoptosis-2 gene and prevent apoptosis in a variety of cell types. Endocrinology 143:3866–3874
27. **Rogatsky I, Wang JC, Derynck MK, Nonaka DF, Khodabakhsh DB, Haqq CM, Darimont BD, Garabedian MJ, Yamamoto KR** 2003 Target-specific utilization of transcriptional regulatory surfaces by the glucocorticoid receptor. Proc Natl Acad Sci USA 100:13845–13850
28. **Drouin J, Sun YL, Chamberland M, Gauthier Y, De Léan A, Nemer M, Schmidt TJ** 1993 Novel glucocorticoid receptor complex with DNA element of the hormone-repressed POMC gene. EMBO J 12:145–156
29. **Asselin-Labat ML, Biola-Vidamment A, Kerbrat S, Lombès M, Bertoglio J, Pallardy M** 2005 FoxO3 mediates antagonistic effects of glucocorticoids and interleukin-2 on glucocorticoid-induced leucine zipper expression. Mol Endocrinol 19:1752–1764
30. **Gokbuget N, Hoelzer D** 2006 Treatment of adult acute lymphoblastic leukemia. Hematology Am Soc Hematol Educ Program 2006:133–141
31. **Pui CH, Evans WE** 2006 Treatment of acute lymphoblastic leukemia. N Engl J Med 354:166–178
32. **Liang MH, Chuang DM** 2006 Differential roles of glycogen synthase kinase-3 isoforms in the regulation of transcriptional activation. J Biol Chem 281:30479–30484
33. **Itoh M, Adachi M, Yasui H, Takekawa M, Tanaka H, Imai K** 2002 Nuclear export of glucocorticoid receptor is enhanced by c-Jun N-terminal kinase-mediated phosphorylation. Mol Endocrinol 16:2382–2392
34. **Galliher-Beckley AJ, Cidlowski JA** 2009 Emerging roles of glucocorticoid receptor phosphorylation in modulating glucocorticoid hormone action in health and disease. IUBMB Life 61:979–986
35. **Sun M, Meares G, Song L, Jope RS** 2009 XIAP associates with GSK3 and inhibits the promotion of intrinsic apoptotic signaling by GSK3. Cell Signal 21:1857–1865
36. **Maurer U, Charvet C, Wagman AS, Dejardin E, Green DR** 2006 Glycogen synthase kinase-3 regulates mitochondrial outer membrane permeabilization and apoptosis by destabilization of MCL-1. Mol Cell 21:749–760
37. **Liao X, Thrasher JB, Holzbeierlein J, Stanley S, Li B** 2004 Glycogen synthase kinase-3β activity is required for androgen-stimulated gene expression in prostate cancer. Endocrinology 145:2941–2949
38. **Mazor M, Kawano Y, Zhu H, Waxman J, Kypta RM** 2004 Inhibition of glycogen synthase kinase-3 represses androgen receptor activity and prostate cancer cell growth. Oncogene 23:7882–7892
39. **Medunjanin S, Hermani A, De Servi B, Grisouard J, Rincke G, Mayer D** 2005 Glycogen synthase kinase-3 interacts with and phosphorylates estrogen receptor α and is involved in the regulation of receptor activity. J Biol Chem 280:33006–33014
40. **Grisouard J, Mayer D** 2009 Specific involvement of glycogen synthase kinase-3 in the function and activity of sex steroid hormone receptors reveals the complexity of their regulation. J Steroid Biochem Mol Biol 117:87–92
41. **Mann CL, Cidlowski JA** 2001 Glucocorticoids regulate plasma membrane potential during rat thymocyte apoptosis *in vivo* and *in vitro*. Endocrinology 142:421–429
42. **Vandevyver S, Dejager L, Libert C** 2012 On the trail of the glucocorticoid receptor: into the nucleus and back. Traffic 13:364–374
43. **Carrigan A, Walther RF, Salem HA, Wu D, Atlas E, Lefebvre YA, Haché RJ** 2007 An active nuclear retention signal in the glucocorticoid receptor functions as a strong inducer of transcriptional activation. J Biol Chem 282:10963–10971
44. **Liu J, DeFranco DB** 2000 Protracted nuclear export of glucocorticoid receptor limits its turnover and does not require the exportin 1/CRM1-directed nuclear export pathway. Mol Endocrinol 14:40–51
45. **Kumar S, Saradhi M, Chaturvedi NK, Tyagi RK** 2006 Intracellular localization and nucleocytoplasmic trafficking of steroid receptors: an overview. Mol Cell Endocrinol 246:147–156
46. **Rinnab L, Schütz SV, Diesch J, Schmid E, Küfer R, Hautmann RE, Spindler KD, Cronauer MV** 2008 Inhibition of glycogen synthase kinase-3 in androgen-responsive prostate cancer cell lines: are GSK inhibitors therapeutically useful? Neoplasia 10:624–634
47. **Schütz SV, Cronauer MV, Rinnab L** 2010 Inhibition of glycogen synthase kinase-3β promotes nuclear export of the androgen receptor through a CRM1-dependent mechanism in prostate cancer cell lines. J Cell Biochem 109:1192–1200
48. **Holaska JM, Black BE, Rastinejad F, Paschal BM** 2002 Ca^{2+}-dependent nuclear export mediated by calreticulin. Mol Cell Biol 22:6286–6297
49. **Kumar S, Chaturvedi NK, Nishi M, Kawata M, Tyagi RK** 2004 Shuttling components of nuclear import machinery involved in nuclear translocation of steroid receptors exit nucleus via exportin-1/CRM-1* independent pathway. Biochim Biophys Acta 1691:73–77
50. **Ploner C, Rainer J, Niederegger H, Eduardoff M, Villunger A, Geley S, Kofler R** 2008 The BCL2 rheostat in glucocorticoid-induced apoptosis of acute lymphoblastic leukemia. Leukemia 22:370–377
51. **Scoltock AB, Heimlich G, Cidlowski JA** 2007 Glucocorticoids inhibit the apoptotic actions of UV-C but not Fas ligand in hepatoma cells: direct evidence for a critical role of Bcl-xL. Cell Death Differ 14:840–850
52. **Xu B, Strom J, Chen QM** 2011 Dexamethasone induces transcriptional activation of Bcl-xL gene and inhibits cardiac injury by myocardial ischemia. Eur J Pharmacol 668:194–200
53. **Lynch JT, Rajendran R, Xenaki G, Berrou I, Demonacos C, Krstic-Demonacos M** 2010 The role of glucocorticoid receptor phosphorylation in Mcl-1 and NOXA gene expression. Mol Cancer 9:38

SUPPLEMENTAL DATA

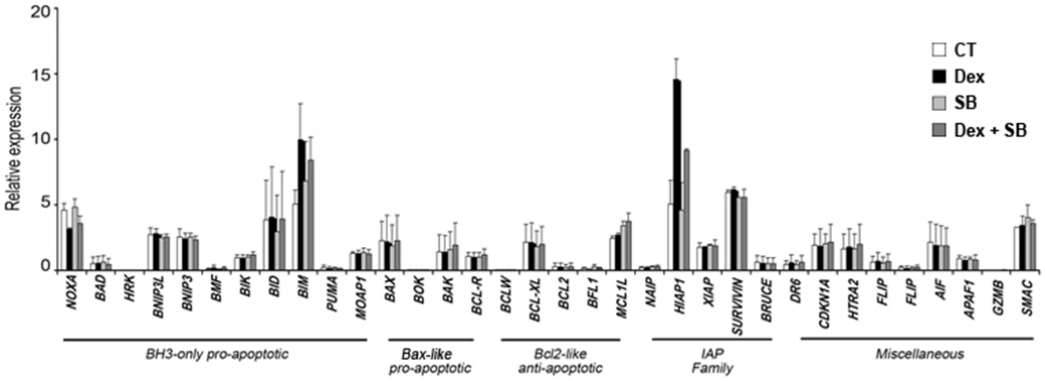

Supplemental Figure S1. RT-MLPA analysis of Jurkat GR wt cells. Jurkat GR wt cells were pre-incubated with 10 μM SB216763 (SB) for 30 minutes followed by 10 nM dexamethasone (Dex) for 90 minutes. Cells were lysed and the expression of apoptotic-related genes of the Bcl-2 family, IAP family and other genes implicated in apoptosis process was analyzed by RT-MLPA as described in Materials and methods. The mRNA levels of all the genes were normalized with respect to those of *GUS*. The results are shown as the mean of two independent experiments.

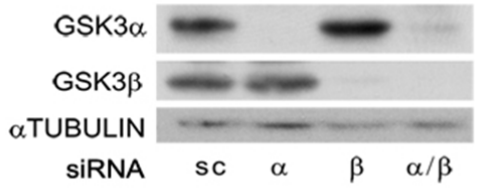

Supplemental Figure S2. Protein expression levels of GSK3α and β isoforms. This Western Blot confirms the genetic knockdown of the specified gene with different antibodies than the one used in Fig. 6A. Independent antibodies were used for each isoform. α-Tubulin was used to normalize protein levels.

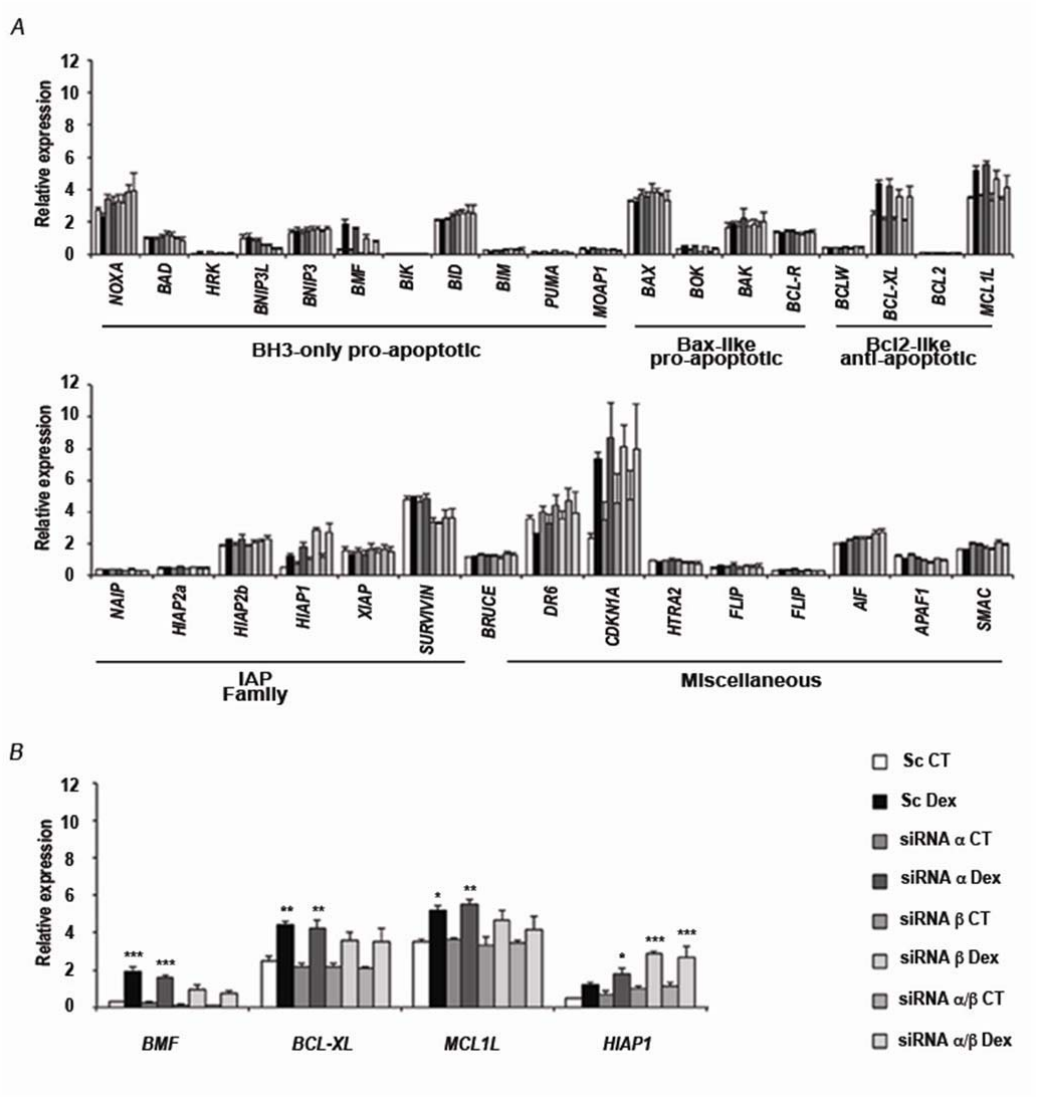

Supplemental Figure S3. RT-MLPA analysis of HeLa cells. Cells were transfected with scramble siRNA (SC) or GSK3 isoform-specific siRNAs (α, β or α/β). 72 hours later cells were untreated (CT) or treated with 100 nM dexamethasone (Dex) for 4 hours. **A)** Cells were lysed and the expression of apoptotic-related genes of the Bcl-2 family, IAP family and other genes implicated in apoptosis process was analyzed by RT-MLPA as described in Materials and methods. The mRNA levels of all the genes were normalized with respect to those of *PARN*. **B)** Genes significantly modulated by dexamethasone treatment are shown. The results are shown as the Mean ± SEM of three independent experiments. *p < 0.05, **p < 0.01, ***p<0.001 compared to wt untreated cells.

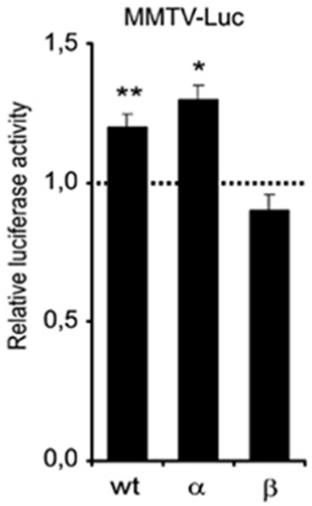

Supplemental Figure S4. MMTV-Luc luciferase activity in wt, GSK3α-/- or GSK3β-/- MEFs. Cells were transfected with MMTV-Luc reporter and were treated with 100 nM dexamethasone (Dex) for 4 hours. Luciferase activity was measured. The normalized values are relative to the untreated control (indicating basal level of MMTV-Luc activity, which is represented by dotted line. Mean ± SEM of at least three independent experiments. *$p < 0.05$, **$p < 0.01$, ***$p<0.001$ compared to wt untreated cells.

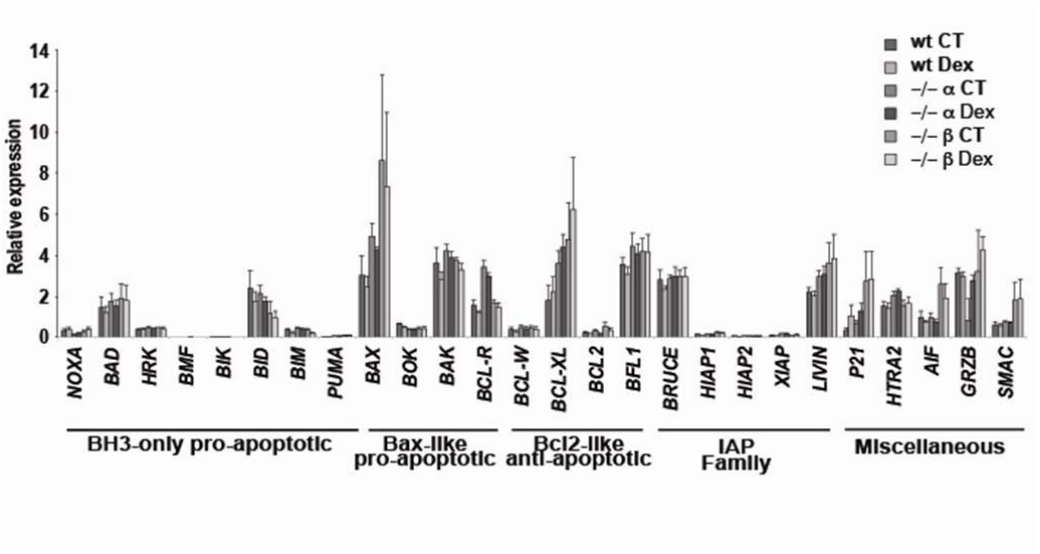

Supplementary Figure S5. RT-MLPA analysis of wt, GSK3α-/- or GSK3β-/- MEFs. Cells were untreated (CT) or treated with 100 nM dexamethasone (Dex) for 4 hours. Cells were lysed and the expression of apoptotic-related genes of the Bcl-2 family, IAP family and other genes implicated in apoptosis process was analyzed by RT-MLPA as described in Materials and methods of supplemental data. The mRNA levels of all the genes were normalized with respect to those of *TBP*.

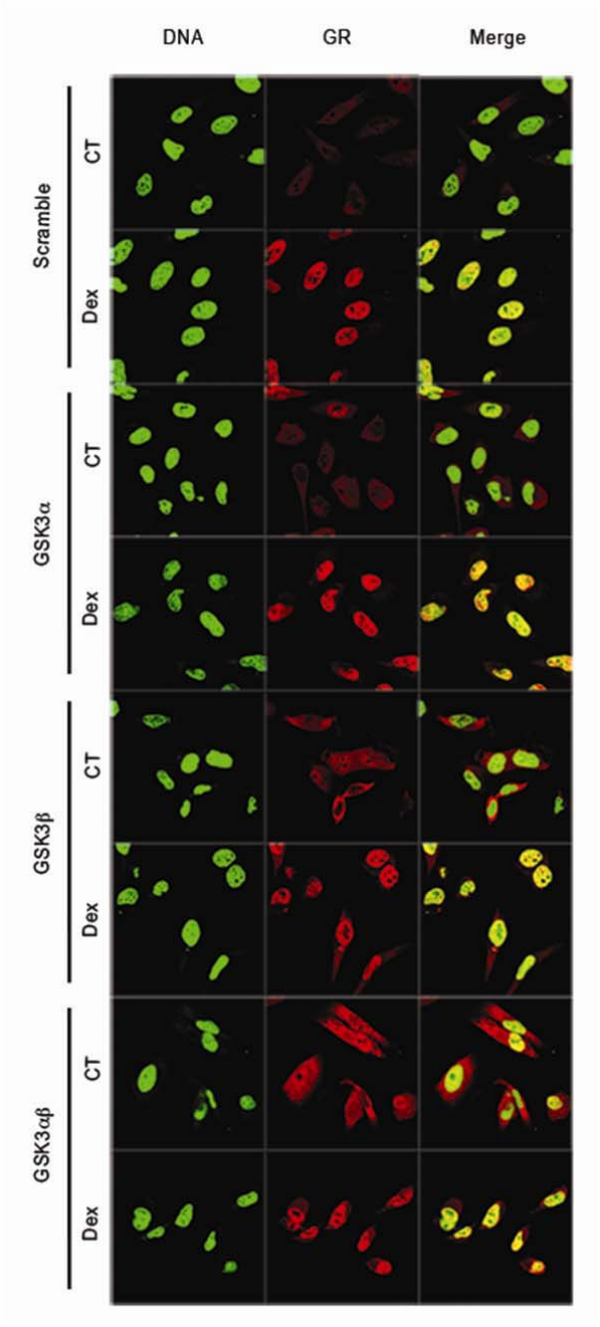

Supplemental Figure S6. Immunofluorescent staining of the GR in HeLa cells. HeLa cells were transfected with GSK3 isoform-specific siRNAs for 72 hours. Cells were treated with 100 nM dexamethasone (Dex) for 3 hours. Yoyo-1 iodide (green) stains nuclear DNA and Alexa Fluor 647 (red) stains GR. Merged images are shown for comparison. This is a representative experiment of 3 that were performed.

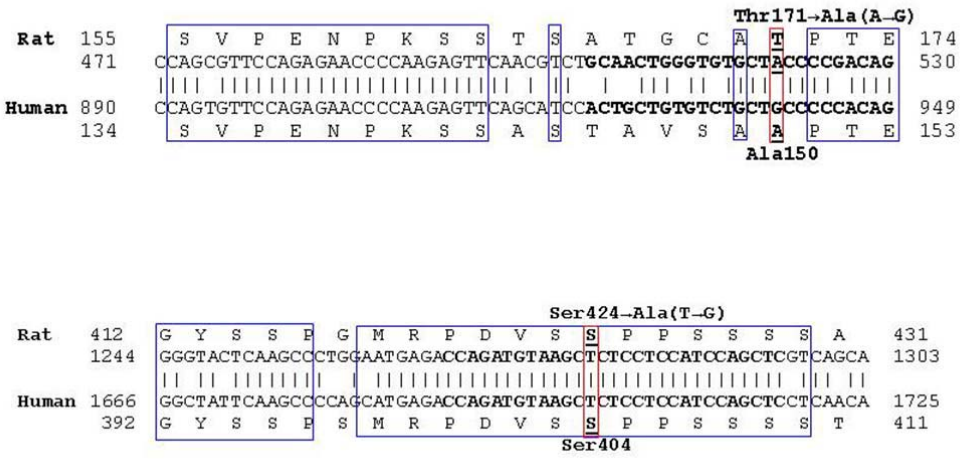

Supplemental Figure S7. Phosphorylation sites of the GR by GSK3. Schematic representation of the two known residues of rat GR phosphorylated by GSK3, Thr171 and Ser424. The localization of each phosphorylation site of the rat and human receptor are shown. The framed sequences indicate the amino acids conserved between the two species. The nucleotide changes made by site directed mutagenesis to alter amino acid sequence are indicated.

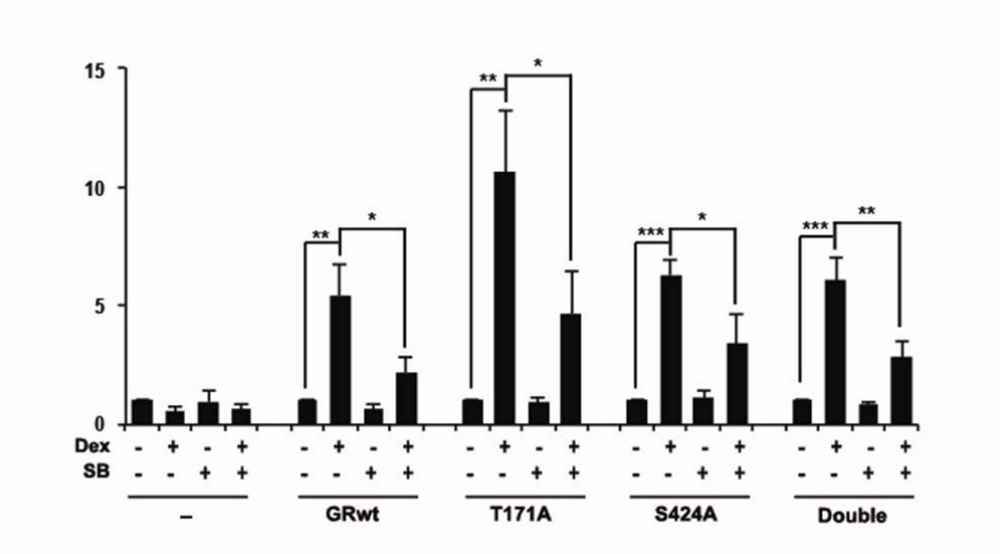

Supplemental Figure S8. GSK3 inhibition affects GC-induced transcriptional activity of rat GR mutants. Jurkat parental cells were transfected with MMTV-Luc reporter construct alone or co-transfected with GR wt, T171A, S424A or Double mutants. Cells were pre-incubated with 10 μM SB216763 (SB) for 30 minutes followed by treatment with 10 nM dexamethasone (Dex) for another 20 hours. Luciferase activity was measured and expressed relative to untreated cells basal activity. Mean ± SEM of at least three independent experiments. *$p < 0.05$, **$p < 0.01$ ***$p < 0.001$.

Patient	CT	Dex	SB	Dex + SB
1*	55,04	28,05	57,71	48,45
2*	80,44	56,19	84,27	64,24
3*	75,91	65,55	75,51	68,22
4*	70,83	37,95	65,86	57,71
5*	38,76	18,05	44,50	31,27
6*	74,60	53,42	71,23	58,19
7*	41,82	29,37	55,43	32,63
8*	65,26	40,29	66,25	48,43
9*	62,48	46,21	69,14	48,03
10*	64,59	55,87	59,28	58,17
11*	90,83	83,94	94,73	91,31
12*	72,08	53,65	77,99	63,88
13*	78,22	50,24	77,15	60,10
14*	67,81	44,56	62,75	51,36
15*	71,21	56,20	77,81	61,02
16*	71,40	46,87	61,90	51,94
17*	71,12	58,50	65,94	64,66
18*	84,53	70,59	80,27	76,59
19*	42,05	28,85	45,43	31,03
20	66,09	46,19	60,54	36,90
21	56,68	40,55	59,14	33,53
22	40,38	35,80	35,42	28,88
23	43,09	34,50	45,76	36,02
24	52,34	27,41	43,18	28,28
25	56,82	34,65	48,07	29,02
26	63,54	53,06	60,63	46,23
27	50,26	42,38	54,58	42,68
28	78,31	68,47	65,27	66,70
29	75,68	62,73	68,96	54,04

Supplemental Table S1. Viability of CLL samples. CLL cells were untreated (CT) or pre-incubated with 10 μM SB216763 (SB) and treated with 10 μM dexamethasone (Dex) for 24 hours. Viability was measured as described in Materials and methods and it is expressed as the percentage of annexin APC negative cells.

* Patients were GC-induced apoptosis was reverted by GSK3 inhibition.

SUPLEMENTAL MATERIALS AND METHODS

Reagents and antibodies

GSK3α and GSK3β (27C10) antibodies were from Cell Signaling.

RT-MLPA for mouse samples

RNA content of wt, GSK3α-/- or GSK3β-/- MEF cells were analyzed by RT-MLPA using SALSA KIT RM002-B1 Mouse Apoptosis mRNA from MRC-Holland. The mRNA levels of all these genes were standardized to those of *TBP*.